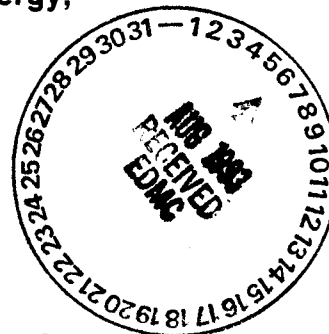# Effects of Long-Term Exposure to Elevated Temperature on the Mechanical Properties of Hanford Concrete

Construction Technology Laboratories, Portland Cement Association

APPROVED FOR
PUBLIC RELEASE
3-9-92

REFERENCE COPY

Rockwell International

Rockwell International

Rockwell Hanford Operations
Energy Systems Group
Richland, WA 99352

DISCLAIMER

INFORMATION RELEASE REQUEST

References:
WHC-CM-3-4

COMPLETE FOR ALL TYPES OF RELEASE

Purpose

[] Speech or Presentation
  [] Full Paper   (Check only one suffix)
  [] Summary
  [] Abstract
  [] Visual Aid
[] Speakers Bureau
[] Poster Session
[] Videotape

[X] Reference
[] Technical Report
[] Thesis or Dissertation
[] Manual
[] Brochure/Flier
[] Software/Database
[] Controlled Database
[] Other

New ID Number

Existing ID Number (include revision, volume, etc.)
RHO-C-54

If previously cleared, list ID number

Date Release Required
2-28-92

Title **Effects of Long-Term Exposure to Elevated Temperature on the Mechanical Properties of Hanford Concrete**

Unclassified Category
UC-

Impact Level

COMPLETE FOR SPEECH OR PRESENTATION
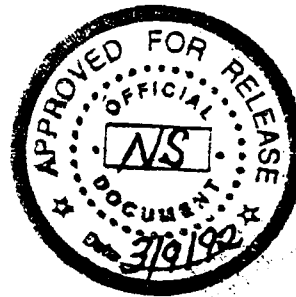
Title of Journal

Group or Society Sponsoring

Date(s) of Conference or Meeting

City/State

Will proceedings be published? [] Yes [] No
Will material be handed out? [] Yes [] No

Title of Conference or Meeting

CHECKLIST FOR SIGNATORIES

Review Required per WHC-CM-3-4	Yes	No	Reviewer Name (printed)	Signature	Date
Classification/Unclassified Controlled Nuclear Information	[X]	[]	D. L. BECKER	*A. L. Becker*	2/25/92
Patent - General Counsel	[X]	[]	S. M. Berglin	*signature*	3/4/92
Legal - General Counsel	[X]	[]	SW Berglin	*signature*	3/4/92
Applied Technology/Export Controlled Information or International Program	[]	[X]			
WHC Program	[]	[X]			
Communications	[]	[X]			
DOE-RL Program	[]	[X]			
Publication Services	[]	[X]			
Other Program	[]	[X]			
References Available to Intended Audience	[]	[X]			
Transmit to DOE-HQ/Office of Scientific and Technical Information	[]	[X]			

Information conforms to all applicable requirements. The above information is certified to be correct.

Author/Requestor (Printed/Signature)
L. D. Blackburn
L. D. Blackburn   Date 2-24-92

Responsible Manager (Printed/Signature) Date
WFBREHM *WFBrehm* 2-24-92

INFORMATION RELEASE ADMINISTRATION APPROVAL STAMP

Stamp is required before release. Release is contingent upon resolution of mandatory comments.

[Stamp: APPROVED FOR RELEASE OFFICIAL DOCUMENT NS 3/9/92]

Intended Audience

[] Internal [] Sponsor [X] External

Date Received 3/3/92 NS

EFFECTS OF LONG-TERM EXPOSURE TO ELEVATED TEMPERATURE ON THE MECHANICAL PROPERTIES OF HANFORD CONCRETE

Construction Technology Laboratories,
Portland Cement Association

October 1981

Title: EFFECTS OF LONG-TERM EXPOSURE TO ELEVATED TEMPERATURE ON THE MECHANICAL PROPERTIES OF HANFORD CONCRETE

Issue Approval:

_____   _____
Author   C. DeFigh-Price   Date   9-10-81

_____   _____
Issuing Manager   D. E. Braden   Date   9-11-81

_____   _____
Concurring Approval   R. C. Roal   Date   9/11/81

_____   _____
Program Representative   J. R. Wetch   Date   9/11/81

_____   _____
Program Office   I. E. Reep   Date   9/11-81

Rockwell International

**Rockwell Hanford Operations
Energy Systems Group**

CONTENTS

1.0 INTRODUCTION

A multiyear test program was conducted to determine the influence of long-term heating on the mechanical properties of concrete similar to that used in Hanford nuclear underground storage (UGS) tanks. The concrete was fabricated from basalt aggregates and American Society of Testing and Materials (ASTM) Designation C150 Type II portland cement. The following sections describe the background, purpose, and scope of the test program. The concrete testing program was conducted for the U.S. Department of Energy with funding from Rockwell Hanford Operations (Rockwell) Long-Term High-Level Defense Waste Program (AR-05-15-20).

1.1 BACKGROUND

This report describes results of a 5-year testing program to determine the effects of long-term exposure to elevated temperatures on the mechanical properties of concrete used in constructing Hanford radioactive UGS tanks. Tests were conducted to determine concrete moduli of elasticity, Poisson's ratios, splitting tensile strengths, and compressive strengths at ambient conditions and after being subjected to elevated temperatures for periods of up to 2 3/4 years. Tests were also conducted to determine the influences of specimen geometry, steam curing, and cyclically varying temperature on these same properties. Related test programs were run to measure concrete thermal expansion, thermal conductivity, and creep behavior at elevated temperatures. In addition, a petrographic examination was made of selected specimens after heating and testing.

Test specimens used in this program were cast at the Construction Technology Laboratories of the Portland Cement Association (CTL/PCA), using the same mix proportions that were specified for concrete in Hanford UGS tanks. Cements, aggregates, and admixtures came from the same sources as materials used in Hanford tank construction. The objective was to use test specimens that would match, as nearly as possible, the compositions and properties of the concretes used in Hanford UGS tanks in their original, "as-cast" condition.

By using concrete cast and tested under laboratory conditions, it was possible to study, in detail, the influences of elevated temperatures on selected properties. The effects of specific test temperatures (from ambient to 450°F), differing lengths of high-temperature exposure, steam curing, and cyclically varying temperatures were studied. Test variables also included concrete mix proportions, age, specimen geometry, and length of curing prior to heating.

Data from this test program were intended to provide the baseline information needed to characterize the mechanical behavior of Hanford concrete in situ when exposed to elevated temperatures for prolonged periods of time. However, only data from tests conducted on concrete cast at CTL/PCA are presented. No results of tests on concrete core materials from Hanford UGS tanks have been included in this report.

1.2 PURPOSE

The objective of this testing program was to determine the effects of long-term exposure to elevated temperatures on the physical/mechanical properties of concrete mixes used in Hanford radioactive UGS tanks. Information obtained from this study was needed for the purposes outlined below.

- The information was used to determine how much thermally induced degradation, if any, can be expected to have occurred in the concrete used in existing UGS tanks. Data will also help evaluate the adequacy of those tanks for continued waste storage.

- The information was also used to determine if there is any appreciable advantage to altering the temperature of waste storage solutions in existing tanks; whether it is desirable to use a cooler waste solution, or if a more concentrated, higher temperature solution can be contained with no decrease in expected tank life.

● It was used to aid in the selection of optimum solution temperatures and tank heating rates for any needed future waste tank designs. Data can also be used in the design and evaluation of concrete casks currently being proposed for long-term retrievable storage of solidified waste.

In addition, at the inception of the testing program, there was no published literature available on the long-term effects of elevated temperatures on concrete mechanical properties. This program has provided data that are generally applicable to the use of concrete at elevated temperatures for prolonged periods of time.

1.3 SCOPE

Information obtained from the test program related to the effects of prolonged exposure at elevated temperatures on physical/mechanical properties of concrete mixes used in constructing Hanford UGS tanks. Properties of major importance in evaluating the integrity of present tanks and designing future tanks are modulus of elasticity, Poisson's ratio, splitting tensile strength, and compressive strength. Variables that were considered as possibly affecting these properties are described in the following sections.

1.3.1 Mix Designs and Materials

Two concrete mix designs with nominal design compressive strengths of 3,000 psi and 4,500 psi were used in Hanford UGS tank construction. These mix designs are shown in Table 1-1. Test specimens in the present program were cast at CTL/PCA, using the same proportions as specified for tank construction. The raw materials used were identified as having come from the same sources as those used for tank construction; sand and gravel from the Hanford batch plant, and ASTM Designation C150 Type II portland cement from Lonestar Industries, Seattle, Washington.

TABLE 1-1. Hanford Concrete Mix Designs.

Batch Ingredients	Quantity (lb/yd^3)	
	3,000 psi Mix (3K)	4,500 psi Mix (4.5K)
Portland Cement, Type II	493	653
Aggregate	2,096	1,880
Sand	1,213	1,240
Water	271	286
Darex, 2% Solution	3 oz	4.50 oz
Air (Percent by volume)	5	5
Water:Cement Ratio	0.54	0.43

Those test specimens cast using the Hanford mix design for 3,000 psi concrete are identified in this report with the prefix 3K; those cast using the mix design for 4,500 psi concrete with the prefix 4.5K. A total of 16 batches of 3K conctete and 13 batches of 4.5K concrete were cast at CTL/PCA between April 1975 and October 1977. Detailed information on each batch may be found in Tables A-1 through A-29 in Appendix A.

Test specimens for strength and elastic property determinations were normally 6- by 12-in. cylinders. However, to determine if size of specimens influenced results, tests were also conducted on 3- by 6-in. cylinders, and 3-in. cubes cored and cut from 6- by 12-in. cylinders. Depending on its volume, each batch produced between 15 and 30 concrete test cylinders. One day after casting, cylinders were demolded and marked with a code that identified its mix design, batch number, and cylinder number. For example, 3K7-24 identifies the 24th cylinder from the seventh batch of concrete cast, using the mix design for 3,000 psi Hanford concrete. This code numbering system is used to reference all weight, dimension, and properties data in the appendices for each concrete cylinder tested in this program.

1.3.2 Curing

Concrete cylinders used for properties tests were continuously stored in a 100% relative humidity (RH) fog room, maintained at 70°F, until heated or tested. The minimum moist cure received prior to heating was 30 days. Most specimens used for high temperature tests were moist cured for 200 to 300 days prior to heating.

Cylinders that were tested in the unheated condition were moist cured for as long as 4 1/4 years. Test specimens used for nondestructive determination of elastic properties with the sonic method were continuously cured in the fog room and tested in the moist condition.

The effects of steam curing on Hanford concrete mechanical properties were also investigated using cylinders from a single batch of 3K concrete. Details of the accelerated curing regime used are described in the Test Descriptions section of this report.

1.3.3 Physical Properties

A number of physical properties were considered as potentially influencing Hanford concrete integrity at elevated temperatures, including concrete density, thermal expansion, and thermal conductivity. Concrete undergoes several physical and chemical changes when heated that are known to affect its mechanical behavior.

When heated above 212°F, unsealed concrete will lose its internal free moisture, causing loss in weight and shrinkage that can induce cracking. At higher temperatures, chemically combined water within the cement paste is released, causing further weight and volumetric losses.

In the region of 1,000° to 1,100°F, the mineral quartz undergoes a phase transformation from the α to β form that causes a discontinuous 2.4% volume increase in the crystal lattice.[1] Concrete containing large quantities of quartz-bearing aggregates have been found to suffer large strength losses in this temperature range. At temperatures of about 1,300°F, calcium carbonate in calcareous aggregates begins to decompose to calcium oxide and carbon dioxide, with accompanying shrinkage.[2]

These thermally induced changes in concrete physical and chemical properties also affect mechanical behavior. For this reason, tests were conducted to determine the influence of temperature on Hanford concrete thermal expansion and thermal properties, including conductivity, diffusivity, and specific heat.

In addition, petrographic and fractographic analyses were conducted on heated test specimens to determine the extent of any changes in concrete physical/chemical composition, soundness, and paste-aggregate bond strength caused by exposure to high temperatures.

It was reasonable to assume that examination of the microstructure of the concrete would aid in identification of damage mechanisms. Correlation of damage mechanisms to microstructural changes would strongly support the extrapolation of data to longer times by establishing specific chemical/structural changes in the concrete. This could identify whether the rate of a specific reaction causing damage was decreasing to a stable level with time or if it was continuously degrading the concrete.

1.3.4 Mechanical Properties

In the past, most research into the effects of elevated temperatures on the mechanical properties of concrete has focused on the type of exposure experienced during a fire. This usually involved tests of relatively short duration, typically 1 to 6 hours, where temperatures exceeded 1,000°F.

The use of concrete for structural applications in nuclear power plants, where temperatures on the order of 500°F would be experienced for prolonged periods, has prompted research into the effects of such conditions on concrete mechanical properties.[3,4,5] Those studies, reported in the literature, involved a wide range of testing techniques, specimen sizes and curing conditions, temperatures, rates of heating, durations of exposure, and other experimental variables.

Unfortunately, the diversity of test procedures often makes it difficult to compare results of different test programs and apply these data to the Hanford concrete mixes in situ. For example, because mass

concrete in a nuclear power plant is essentially sealed to prevent moisture loss on heating, much research has concentrated on investigating the effects of elevated temperatures on sealed concrete. However, the moisture in concrete in Hanford UGS tanks is not effectively sealed in, but is free to diffuse into the surrounding soil or atmosphere. Consequently, data obtained from elevated temperatures tests on sealed concrete will generally not be applicable to Hanford UGS tank concrete. Furthermore, tests described in the literature covered concrete exposed to elevated temperatures for, at most, a period of four months.

For those and other reasons, it was felt that a separate investigation was necessary to determine the effects of prolonged exposure to elevated temperatures on the mechanical properties of unsealed Hanford concrete mixes. To characterize the effects of elevated temperatures on concrete integrity, the following properties were studied:

- Modulus of elasticity
- Poisson's ratio
- Splitting tensile strength
- Compressive strength.

In addition, test programs were carried out to determine the effects of cyclically varying temperatures on these properties. Also, in an effort to relate data obtained from this study to those of other investigators, one test series was conducted to determine the variation in measured properties values caused by using specimens of different geometries. One test series also examined the long-term creep on Hanford concrete mixes at elevated temperatures.

In the following sections, a brief summary is given from published data on the influence of elevated temperatures on selected concrete properties. These short-term data are useful for two reasons. First, they give some indication of those concrete properties which are relatively more sensitive to temperature and can be anticipated to be seriously affected by long-term heat exposure. Second, these short-term data can serve as a basis by which influences of length of elevated temperature exposure can be measured.

1.3.4.1 <u>Modulus of Elasticity</u>. Typical results of moduli tests on unsealed concrete exposed to elevated temperatures for relatively short time periods are shown in Figure 1-1.[6] For carbonate and light-weight aggregate concrete, moduli values are seen to decrease smoothly from ambient to 1,200°F. The same is true for siliceous aggregate concrete from room temperature to about 900°F. Above this temperature, the modulus of elasticity drops off more sharply than carbonate or lightweight aggregate concrete. This discontinuity is believed to be caused by the alpha to beta phase transformation in the quartz-rich siliceous aggregate, with its accompanying disruptive volume increase.

At 450°F, the elasticity modulus of concrete averages only about 70% of values measured with unheated concrete.
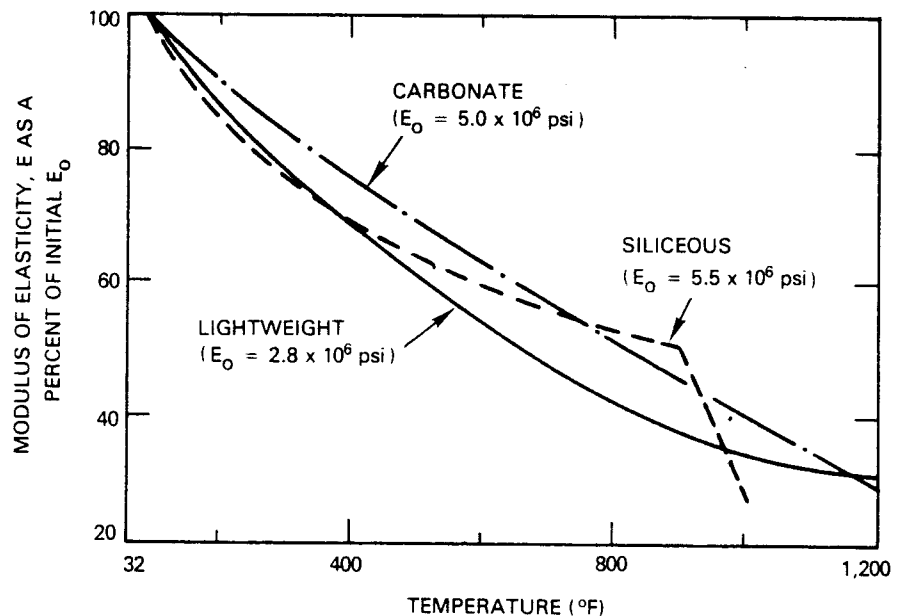
RCP8106-5

FIGURE 1-1. Modulus of Elasticity of Concrete at High Temperatures.

1.3.4.2 Poisson's Ratio. Several investigators have examined the influence of elevated temperatures on Poisson's ratio of concrete.[7,8]
In one study, there were indications that the magnitude of Poisson's ratio decreases with increasing temperature. However, results from all published test results contain large scatter. Overall, no general trend of the effect of temperature on Poisson's ratio of concrete has been established.

1.3.4.3 Compressive Strength. Abrams has shown that strength reductions due to heat exposure are influenced by the presence, or absence, of applied stresses on the concrete during heating, and on the type of aggregates used in the concrete.[6] This can be seen in Figures 1-2, 1-3, and 1-4. Here, tests were conducted on concrete with three types of aggregates: carbonate, siliceous, and lightweight aggregate concrete. Three test methods were employed to test each concrete type.
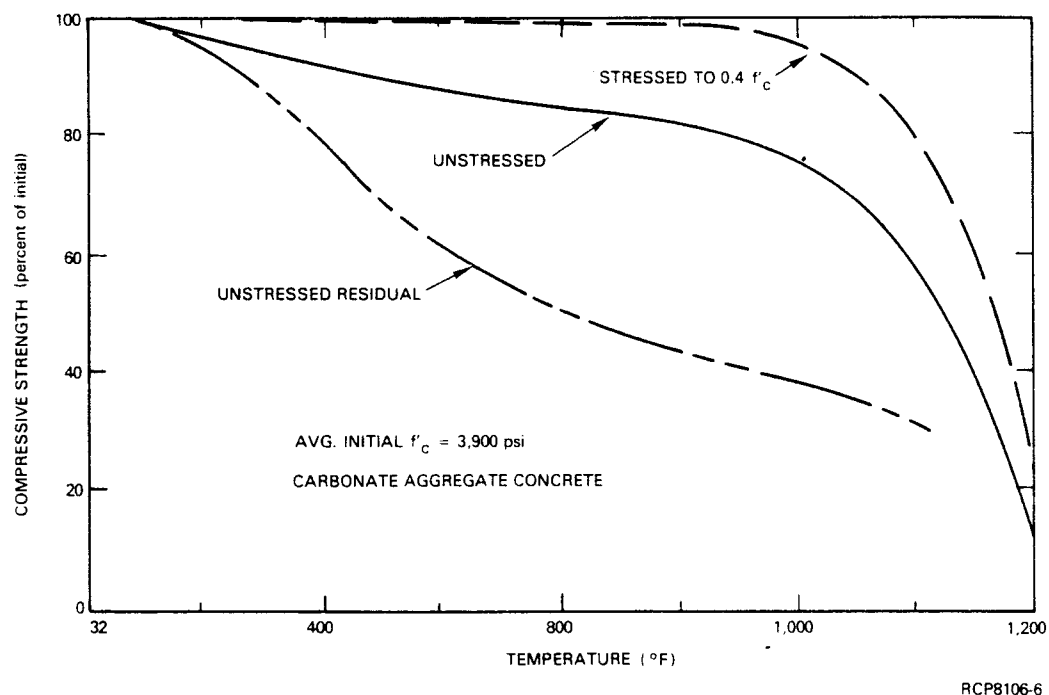
FIGURE 1-2. Compressive Strength of Carbonate Aggregate Concrete at High Temperatures and After Cooling.
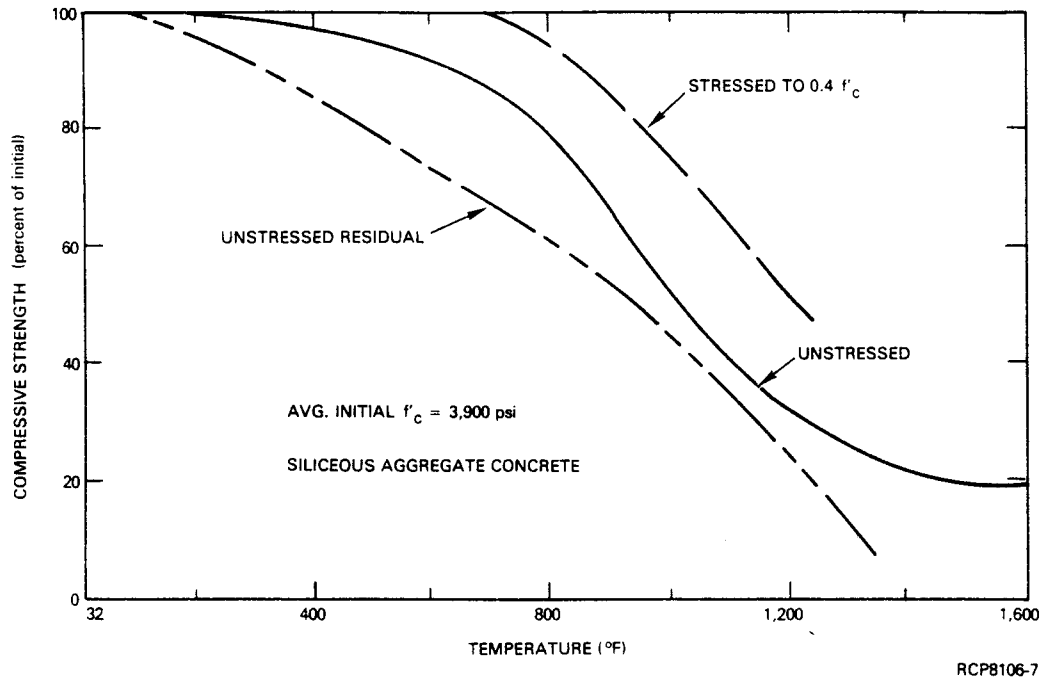
FIGURE 1-3. Compressive Strength of Siliceous Aggregate Concrete at High Temperatures and After Cooling.
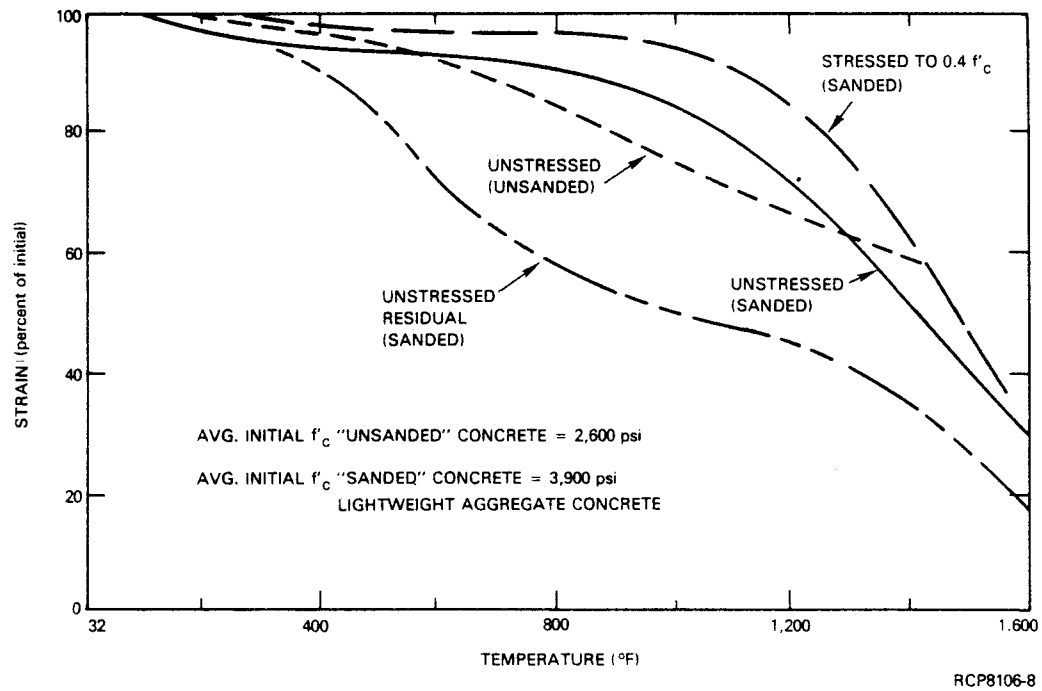
FIGURE 1-4. Compressive Strength of Sanded Lightweight Aggregate Concrete at High Temperatures and After Cooling.

Those curves labeled "unstressed" were heated to test temperature with no external load applied. Those curves identified as "Stressed to 0.4 f'$_c$" were heated with an externally applied load equal to 40% of the concrete's room temperature strength. In both cases, compressive strength tests were carried out at the elevated test temperature. Those curves marked "Unstressed Residual" were heated with no load applied, cooled to ambient, stored 6 days at 75% RH, and then tested in compression at room temperature.

The significant points are outlined below.

- Concrete made from different aggregates have different strength loss trends on heating. In particular, strength of siliceous aggregate concrete decreases more rapidly above 800°F than does carbonate or lightweight aggregate concrete.

- The presence of externally applied loads during heating tends to improve measured compressive strength at elevated temperatures, regardless of the type of aggregate used in the concrete.

- The worst case from a strength standpoint is when concrete is in the "unstressed residual" condition; i.e., room temperature testing after heating.

The above tests were conducted on unsealed concrete cylinders. On heating, moisture present within the concrete was free to evaporate to the surroundings. However, investigations by Lankard, et al, have shown that strength and elastic properties suffer relatively greater losses than described above when the concrete is sealed to prevent moisture loss.[3] From this it is clear that the movement of internal moisture is another factor affecting concrete mechanical behavior at high temperatures.

Further data on the mechanical behavior of concrete at elevated temperatures have been reported by Zoldners, Malhotra, and others.[9,10,11,12] However, the above data can be considered representative of most information published in this field.

1.3.4.4 Splitting Tensile Strength. Compared to compressive strength behavior, the influence of elevated temperatures on concrete tensile strength has received relatively little attention. Two reasons may account for this. First, at ambient conditions, the tensile strength is much lower than compressive strength of concrete, typically only about 10% of f'_c. In design of concrete structures, tensile stresses are assumed primarily by the steel reinforcement, not the concrete. For this reason, magnitude of compressive strength is considered as a more important design criterion than the tensile strength.

Also, because of its brittleness and relatively low resistance to tensile stress, it is difficult to determine concrete tensile strength directly by using a simple uniaxial tensile test method of the type commonly used for testing metals, plastics, etc. The two most common methods for measuring concrete's resistance to tensile forces are the flexure test, as described in ASTM Method of Test C293, and the split cylinder test, as described in ASTM Method of Test C496.[13,14]

In the split cylinder test, a compressive load is applied in a plane normal to the test cylinder's longitudinal axis. This produces corresponding tensile stresses in a direction perpendicular to the plane of the applied load. This is shown schematically in Figure 1-5(a). Because concrete's tensile strength is much lower than its compressive strength, the cylinder fractures in tension, usually in the manner shown in Figure 1-5(b). The strength determined by this method is called the splitting tensile strength.

Some investigations into the effects of elevated temperatures on concrete tensile strength have been conducted using both test methods.[15,16] A number of variables have been examined in these studies. From these, the strength-temperature relations reported by Thelandersson are typical. These results are shown graphically in Figure 1-6.

When these data are compared to the compressive strength data for siliceous aggregate concrete of Abrams, it can be seen that the loss trends are very similar.

APPLIED LOAD, P

TENSILE STRESS

(a)

COMPRESSIVE
STRESS

(b)

CRACK PRODUCED
BY TENSILE STRESS
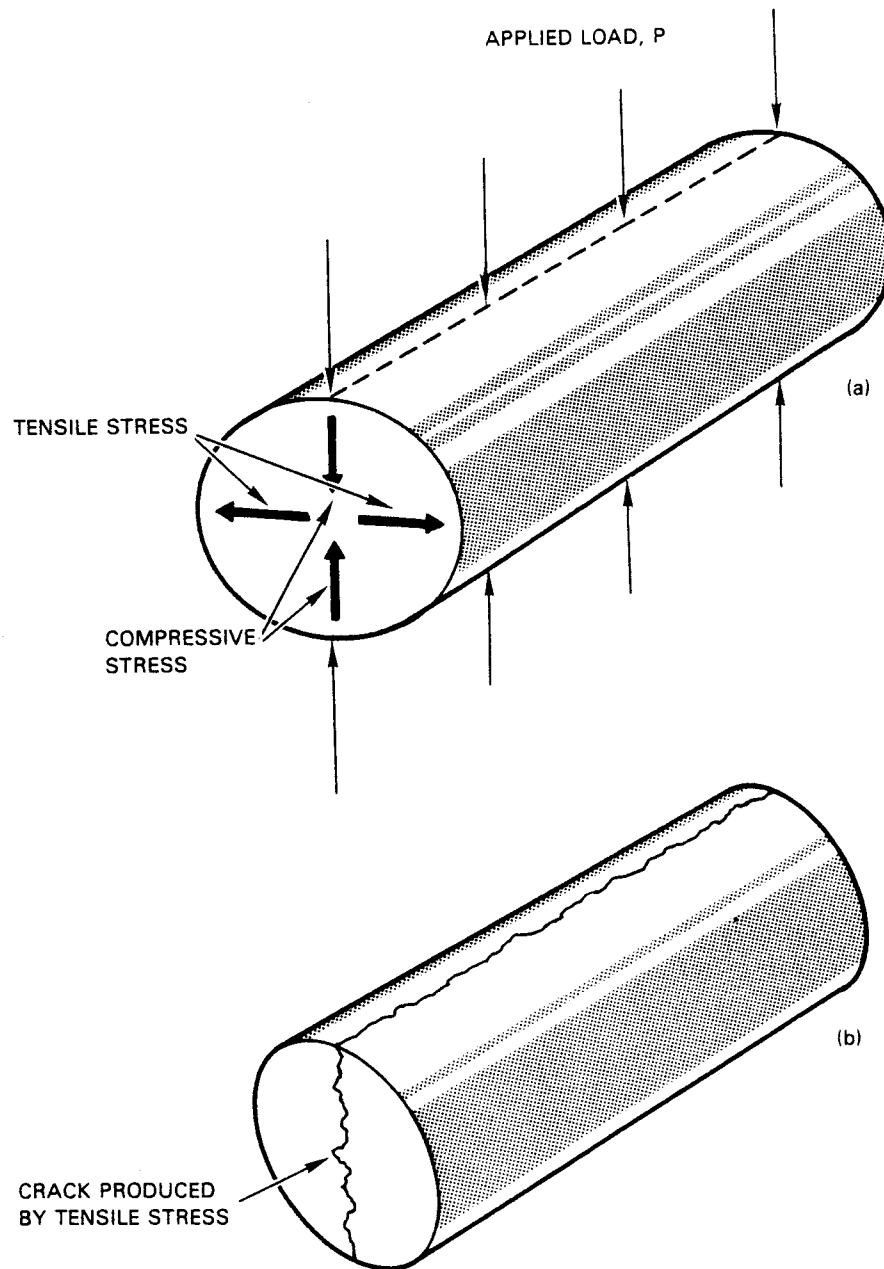
RCP8106-9

FIGURE 1-5. Split Cylinder Test.

SLOW HEATING
(~ 3.6°F/min)

RAPID HEATING
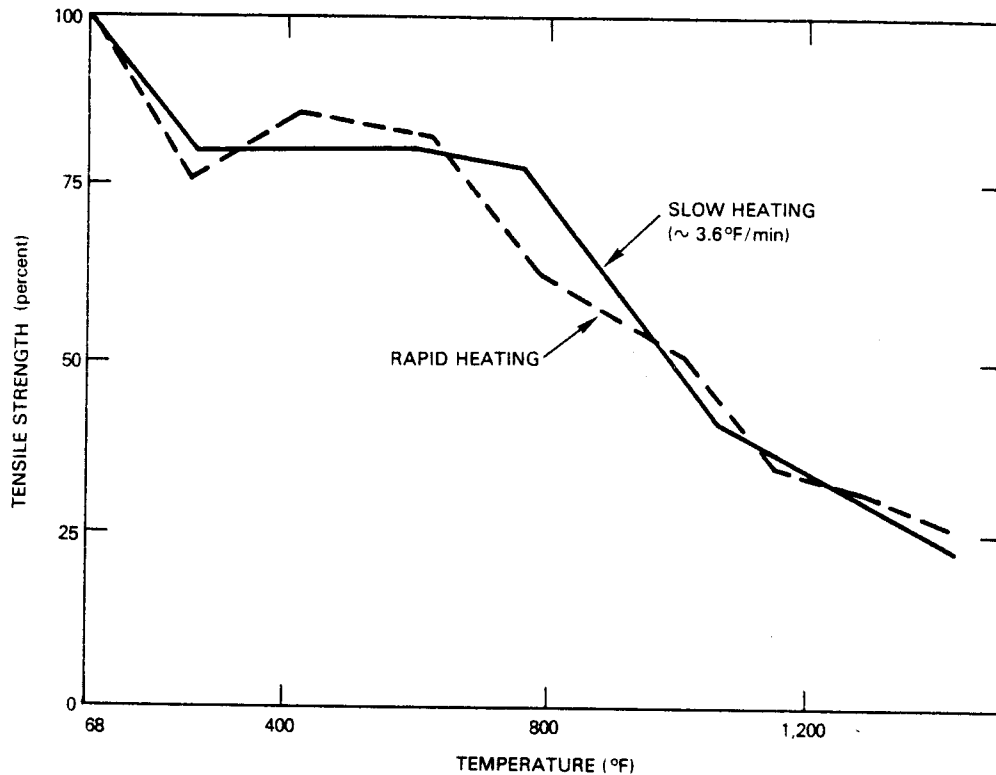
RCP8106-10

FIGURE 1-6. Split Tensile Strength From Thelandersson Data.

1.3.4.5 <u>Creep</u>. Time dependent deformation of concrete under load is referred to as creep. It is a phenomenon common to engineering materials, particularly at elevated temperatures. In the specific case of high service temperatures encountered in nuclear power plants, much experimental and analytical work has been conducted on concrete creep behavior.[12,17,18,19] Characterization of concrete creep behavior at elevated temperatures was considered as an important goal for analysis of long-term structural performance.

This has led to a number of sophisticated mathematical models of concrete creep behavior based on a fairly large amount of experimental data. Generally, trends indicate that the magnitude of creep strain increases with increased service temperature. This can be seen in the curves shown in Figure 1-7, from data reported by Schneider.[12]
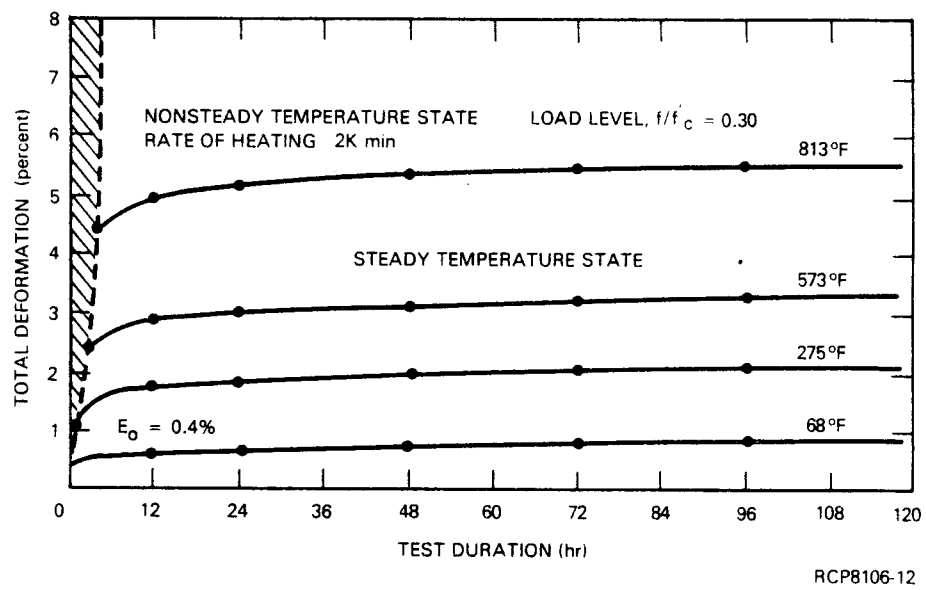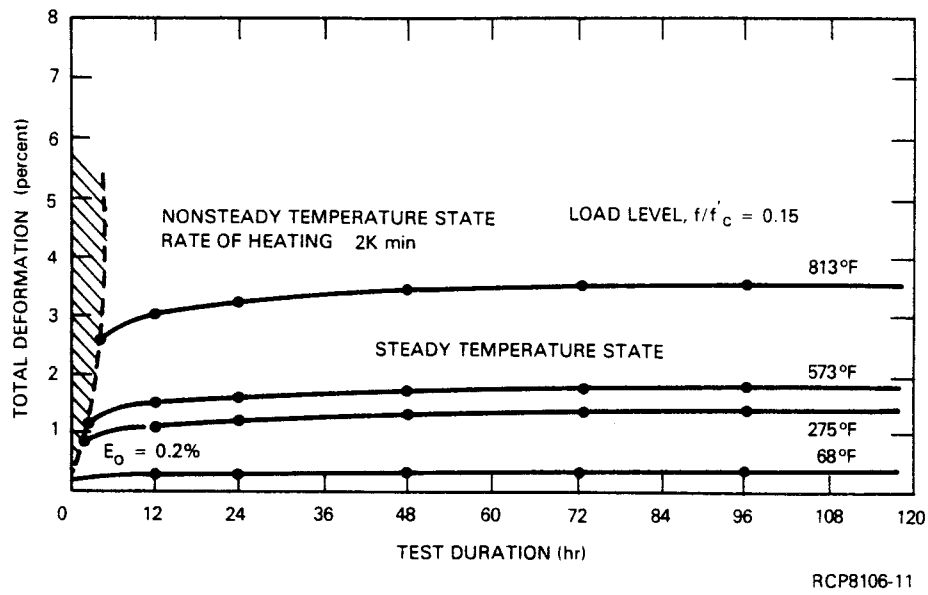
FIGURE 1-7.   Creep Curves from Schneider Data.

Further tests by Cruz,[20] Gillen,[21] Anderberg and Thelandersson,[22] and others have shown that creep at elevated temperatures is influenced by a number of factors, including concrete strength, type of aggregate, rate of heating, and migration of moisture within the concrete.

The purpose of examining high temperature creep in the current program was to provide sufficient data for determining if the behavior of Hanford concrete can be adequately modeled by existing mathematical expressions. It was not intended to be a detailed examination of the time dependent deformation of Hanford concrete, subject to a large number of test variables.

1.3.4.6. <u>Thermal Cycling</u>. In actual service, the Hanford UGS tanks are subjected to repeated exposure to elevated temperatures. Each time wastes are placed in a tank, temperatures increase, then gradually cool. Thus, the temperature in a tank is a cyclically varying function of time.

However, strength and properties data in this program were determined primarily from concrete at constant elevated temperatures. Therefore, it was necessary to determine if cyclically varying temperatures would produce more deleterious effects on concrete properties than exposure to constant high temperatures.

Effects of cyclically varying elevated temperatures on strength and elastic properties of concrete have been studied by a number of investigators.[4,15,23] Published test data indicate that at least four factors strongly influence the degree of deterioration of concrete mechanical properties under repeated temperature variations above ambient. These are outlined below.

- <u>Maximum Temperature Applied</u>. Temperatures above 400°F in particular may result in considerable strength loss . This is probably due to microcracking caused by volume changes as the cement matrix dehydrates.

- <u>Rate of Heating and Cooling</u>. Rapid heating and cooling tends to aggravate strength loss. This is true of most engineering materials.

- **Presence of Moisture.** Sealed concrete with no loss of moisture when heated suffers a greater strength reduction than concrete that loses moisture during heating.

- **Load Applied During Heating.** The application of a compressive load during all phases of heating tends to reduce strength loss.

A fifth factor influencing strength and elastic constants is number of temperature cycles. Studies have not been undertaken to determine the effect of a large number of thermal cycles (greater than 100) on strength and elastic properties of concrete. However, past investigations have shown that strength losses are usually most severe during the first few cycles. Thereafter, unless temperatures are above 400°F, continued cycling produces proportionately smaller changes in concrete properties.

In the present test program, the effect of temperature cycling on unsealed 6- by 12-in. Hanford concrete cylinders is examined. Rates of heating averaged 140°F per day to a maximum temperature of 350°F. Two heat cycle periods, one 14 days and the other 28, were studied for a maximum of 18 temperature cycles. In addition, the effects of temperature cycling on concrete thermal expansion behavior were also examined.

1.3.4.7 **Size Effects.** The fact that tests on similar materials fabricated into different specimen geometries yield different values for measured mechanical properties is well recognized. In some cases, "correction factors" have been experimentally determined to relate results from tests on specimens of varying dimensions to that obtained from a standard specimen geometry.

For example, specifications for testing compressive strength of concrete usually require a concrete test cylinder with a length/diameter (L/D) ratio of 2.0. In the case of cored concrete, it is not always possible to obtain a specimen with the desired L/D ratio. It has been established that concrete cylinders with an L/D ratio less than 2.0 yield higher compressive strengths than cylinders with an L/D equal to 2.0. Through experimental investigation, an empirical relation has been

developed to take into account this geometrical effect and to apply a correction which will reduce measured values to that obtained with an equivalent cylinder with an L/D exactly equal to 2.0.[24]

However, the general relations between test results obtained from specimens of different geometries are not known. Therefore, establishing high temperature behavior of concrete through data comparison from investigations that use different specimen geometries can be difficult.

Properties tests were conducted on Hanford concrete specimens of differing geometries to determine what influence concrete shape and size had on measured properties data. Knowledge of the "size effect" on test data will not only help relate results of the present study to other published data in this area, but will also provide a means of relating results of any future investigation into Hanford concrete high temperature properties to data from the current program.

2.0 TEST DESCRIPTIONS

The methods of determining concrete mechanical properties used in this study were, in general, derived from the relevant ASTM test standards. However, since most tests were conducted at elevated temperatures, it was necessary to alter equipment and procedures in order to maintain the desired test environment. The ASTM standards are referenced and changes are described in the following sections.

2.1 STRENGTH AND ELASTIC PROPERTIES TESTS

Compressive strength, splitting tensile strength, and elastic properties of Hanford concrete were determined on specimens heated for various lengths of time at 250°, 350°, and $450^{\circ}F$, as well as on unheated concrete of different ages.

Specimens used for room temperature tests were continuously moist cured in a 100% RH fog room. Prior to testing, cylinders were removed from the moist room for measurement of height, diameter, and weight. Elastic properties and strength determinations were made on unheated cylinders while in the moist condition.

Test cylinders for elevated temperature tests were subject to the following procedures. Height, diameter, and weight of test cylinders were measured prior to being placed in the oven for heating. This information is listed in Table B-1 in Appendix B. Cylinder lengths and diameters are the average of two or three measurements, as required by ASTM Designations C39,[25] C215,[26] C469,[27] and C496.[14]

Specimens tested at elevated temperatures were heated to test temperatures at a rate of 70° to $75^{\circ}F$ per day. Five temperature changes over the 24-hr period were made to obtain the 70° to $75^{\circ}F$ temperature rise. Required temperature variation limits of $\pm15^{\circ}F$ at $250^{\circ}F$ and $350^{\circ}F$, and $\pm20^{\circ}F$ at $450^{\circ}F$ were easily maintained. A continuous record of oven temperatures was maintained during the temperature rise and soak periods.

All specimens were transported from the oven to the test area in a well insulated container. Tests were performed as quickly as possible to prevent heat loss. Specimens not tested to destruction were returned to the oven in the insulated container.

2.1.1 Modulus of Elasticity and Poisson's Ratio Tests

Elastic constants of test cylinders were obtained using a dynamic and static method. A description of each method follows.

2.1.1.1 Sonic (Dynamic) Method. Moduli of elasticity and Poisson's ratios were obtained on specimens cured in the moist room at $70^{\circ}F$ by following the general provisions given in ASTM Designation C215.[26] The equipment consisted of a variable frequency audiooscillator, amplifiers, a driver unit, a pickup unit, and meter type and cathode ray oscilloscope indicators. Specimens were supported at the quarter points. The driving force was applied normal to the specimen surface near one end. Fundamental, transverse, and torsional frequencies were obtained. The driving force also was applied normal to the surface midway between the ends of the specimen. The fundamental transfer frequency can be obtained by driving the specimen by one end. Frequency determination required about 1 min. The test equipment with a test cylinder in place is shown in Figure 2-1.

2.1.1.2 Static Method. The provisions of ASTM Designation C469[27] were followed in determining the elastic constants by this method. A compressometer, fitted with differential transformers, was used to measure longitudinal and lateral strains. During elevated temperature tests, the transformers were protected with asbestos heat shields. A differential transformer was also used to indicate load. Outputs from the differential transformers were recorded on an X-Y-Y recorder. Thus, the stress longitudinal strain and stress lateral strain curves were obtained simultaneously during each loading of the specimens. Loading surfaces of the specimens used for determining the elastic constants were leveled.
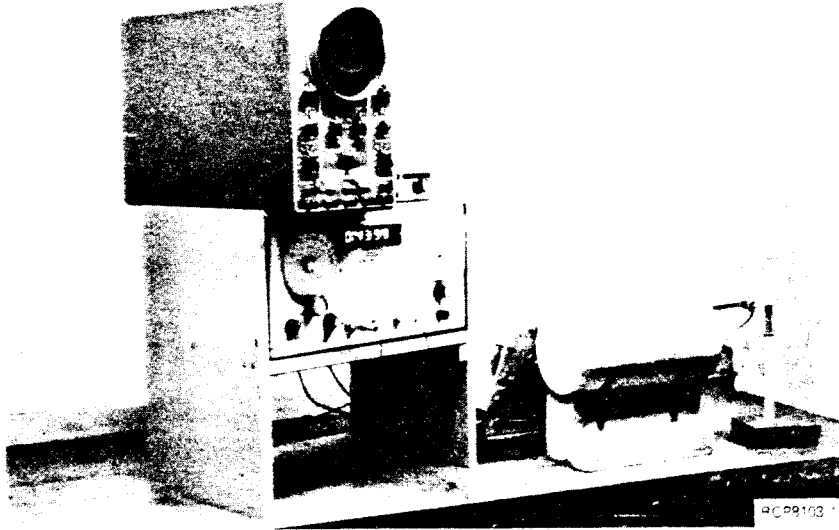
FIGURE 2-1. Sonic Test Method for Determining
Elastic Constants.

Specimens were loaded three or four times for the determination of elastic constants. The first loading was a seating loading, and the information obtained from it was not used. Elastic constants were calculated for subsequent loadings and averaged. Specimens were usually loaded to 40 or 50% of ultimate strength for obtaining elastic constants data. Typical stress/strain curves obtained during a loading are shown in Figure 2-2. Fitting the specimen with the compressometer, balancing the electrical circuits, and loading the specimen required from 10 to 15 min. A test cylinder subjected to the static load test for elastic constants determination is shown in Figure 2-3.

A smaller version of the compressometer described above was used for testing 3- by 6-in. cylinders and 3-in. cubes. Test procedures used for smaller specimens were identical to those used for testing 6- by 12-in. cylinders.
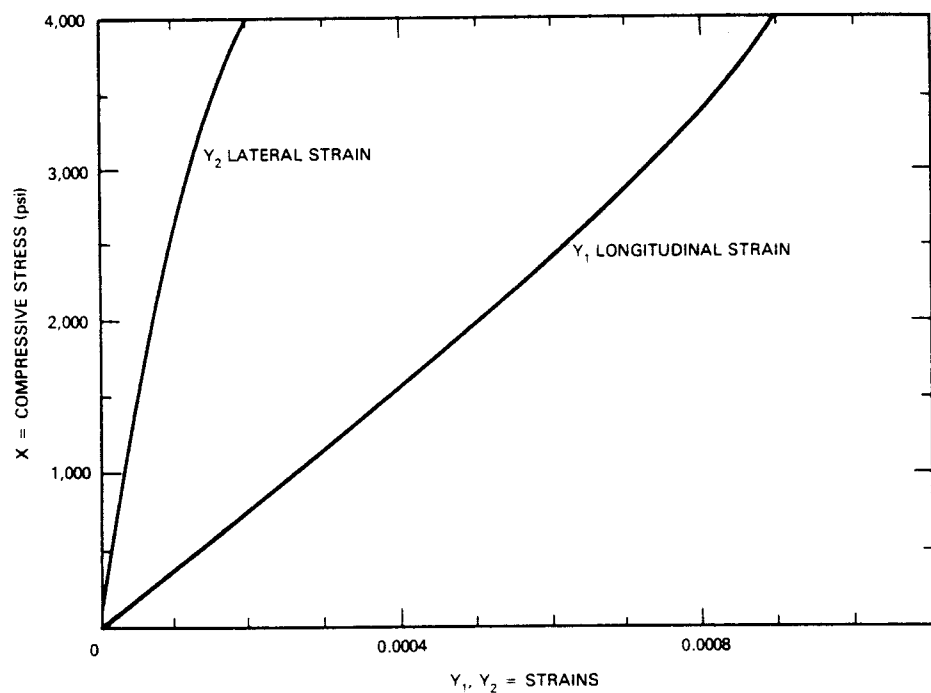
FIGURE 2-2. Stress/Strain Curves, Using X-Y-Y
Plotter for Static Test.
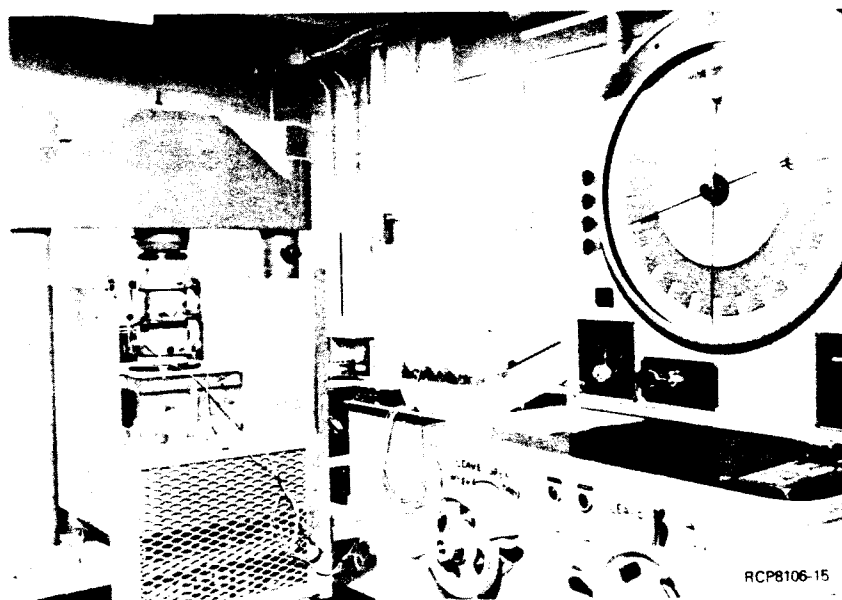
FIGURE 2-3. Static Test Method for Determining
Elastic Constants and Compressive Strength.

2.1.2 Compressive Strength Tests

Compressive strength at room and elevated temperatures was obtained by following the general guideline of ASTM Designation C39.[25] Loading surfaces of cylinders used to obtain cylinder strength were lapped plane and parallel. Elevated temperature strength determinations were made on cylinders that were also used for obtaining elastic constants by the static method. After the elastic constants were obtained, the cylinders were returned to the oven for at least 2 hr before being tested for compressive strength. The compressive strength test took about 5 min. Compressive strengths of 3- by 6-in. cylinders and 3-in. cubes were determined using the same test procedures used for 6- by 12-in. cylinder strength determinations.

2.1.3 Splitting Tensile Strength Tests

To determine splitting tensile strength, the provisions of ASTM Designation C496[14] were followed. At each test date, one of the two specimens of each mix design tested at elevated temperatures was used for determining elastic constants. Test specimens were removed from the fog room or oven, marked with diametral lines, positioned in the testing machine, and loaded to failure. The 1/8-in. thick plywood bearing-strips were not affected by the heat from the test specimens. The time required for this test procedure did not exceed 10 min. Splitting tensile strengths of 3- by 6-in. cylinders were determined by using the same apparatus and procedures as described above.

2.2 CREEP TESTS

Creep tests measure the time-dependent deformation of concrete under constant load. In the present study, creep of concrete cylinders was measured at 250° and $350^\circ F$ under a constant load of either 500 or 1,500 psi. Test apparatus and procedures used were similar to those described in ASTM Designation C512,[28] modified to enable tests to be run at temperatures above ambient.

2.2.1 Creep Test Specimens

Test specimens were six 6- by 12-in. concrete cylinders. Cylinders were cast at CTL/PCA in September 1977.

All specimens tested were selected from a single batch of concrete. Cylinders used were designated 4.5K11-14, 4.5K11-15, 4.5K11-17, 4.5K11-18, 4.5K11-22, and 4.5K11-24. The average compressive strength of cylinders moist cured 28 days was 6040 psi.

Specimens were stored continuously in a 100% RH fog room at 73°F until about 2 days prior to heating. Specimen ends were leveled to insure even distribution of compressive loads.

Brass gage points were affixed to the sides of cylinders at a distance of approximately 1 in. from each end, as shown in Figure 2-4. Deformation of cylinders was measured by the relative movement of these gage points. Gage length for strain measurements was thus 10 in.

SPECIMEN DIAMETER
6 in.

NOTE:
DEFORMATION OF SPECIMENS IS MEASURED BY MOVEMENTS OF A PAIR OF GAGE POINTS INITIALLY PLACED 10 in. APART ON THE SIDE OF THE CYLINDER.

SPECIMEN LENGTH
12 in.

GAGE LENGTH
10 in.
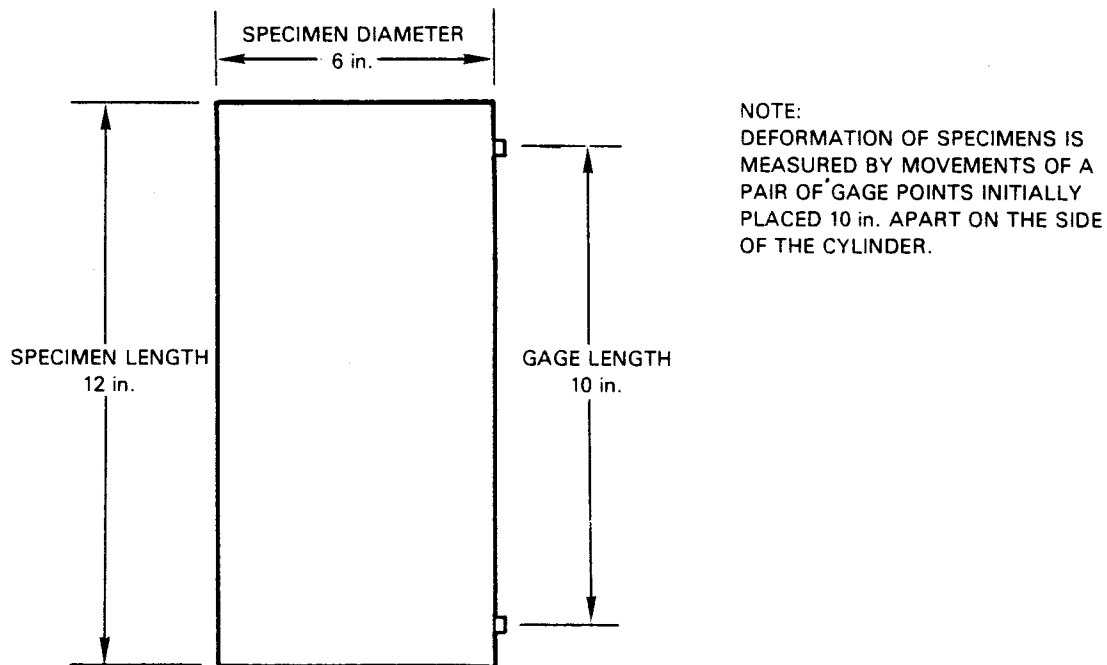
RCP8106-16

FIGURE 2-4. Schematic Diagram of Concrete Specimen Indicating Placement of Gage Points.

2.2.2 Creep Test Apparatus and Procedures

Three creep frames used in testing specimens were of the type described in ASTM Designation C512-66T,[28] each with a 5-cylinder capacity. Two specimens were tested on each frame; the remaining space on each frame was filled with uninstrumented cylinders.

Specimens were heated by furnaces designed and built in the Fire Research Laboratory division of the PCA. The furnaces encircle the creep frame, providing a heating zone 3 ft long. Specimens are shown in place in the furnaces in Figure 2-5.

Duplicate specimens were tested in one of three sets of load and temperature conditions; 1,500 psi at 250°F, 500 psi at 350°F, and 1,500 psi at 350°F. Load was applied to the specimens just prior to heating to test temperature.

Strain readings were taken daily during the first week the specimens were under load. Thereafter, the interval of readings was increased to weekly, later biweekly, then monthly.
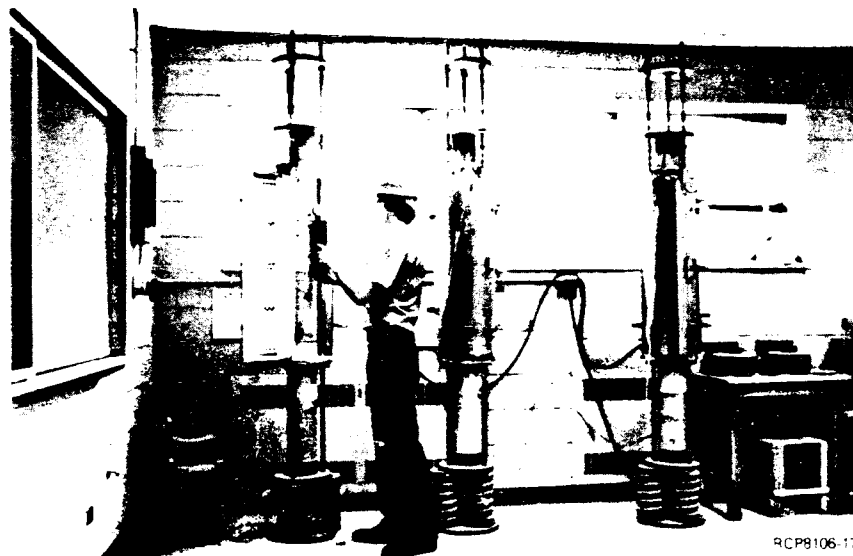
FIGURE 2-5. Creep Frames.

2.3 THERMAL EXPANSION TESTS

Equipment and test procedures used to determine the thermal expansion of concrete specimens are described in the following sections.

2.3.1 Thermal Expansion Test Specimens

Dilatometer specimens of Hanford concrete came from 6- by 12-in. cylinders, cast at the CTL/PCA in May 1975 and September 1977. Cylinders were cast using materials and mix designs similar to those in Hanford structures. All cylinders had been conditioned continuously in a fog room maintained at 100% RH and 73°F prior to removal and fabrication of dilatometer specimens in March 1978.

Cylinders 3K8-7, 3K9-18, 4.5K8-19, and 4.5K9-10 (cast in 1975), and 3K14-12 and 4.5K12-12 (cast in 1977), were used to obtain dilatometer specimens. Cylinders were cut into three 4- by 6-in. cylindrical sections. Next, 1/2-in. diameter cores were obtained from each cylindrical section with a diamond tipped core drill bit.

Ends of these cores were then cut with a precision saw to a length of about 3 in. Finally, core ends were leveled to provide 0.5-in. diameter by 3-in. long cylindrical dilatometer specimens. Cores were then stored at 50% RH and 73°F until tested in August/September 1978.

2.3.2 Thermal Expansion Test Apparatus and Procedures

Equipment and test procedures used to determine the thermal expansion of Hanford concrete are described in the following sections.

2.3.2.1 Thermal Expansion Test Apparatus. Thermal expansion of 0.5- by 3.0-in. cylinders was measured with a commercially manufactured dilatometer. This equipment consisted of an electric furnace, capable of heating specimens to 1,800°F, and instruments for measuring the resulting thermal strains. A schematic of the dilatometer system is shown in Figure 2-6.

·During testing, the specimens were contained in the closed end of a fused silica tube that extended into the furnace. The open end of the tube was fixed to the support base by a large bracket.

FUSED SILICA TUBE   THERMOCOUPLES

LINEAR VARIABLE
DIFFERENTIAL TRANSFORMER   FUSED SILICA ROD

DIAL GAGE   INVAR BAR

SLATE BASE   FURNACE   SPECIMEN
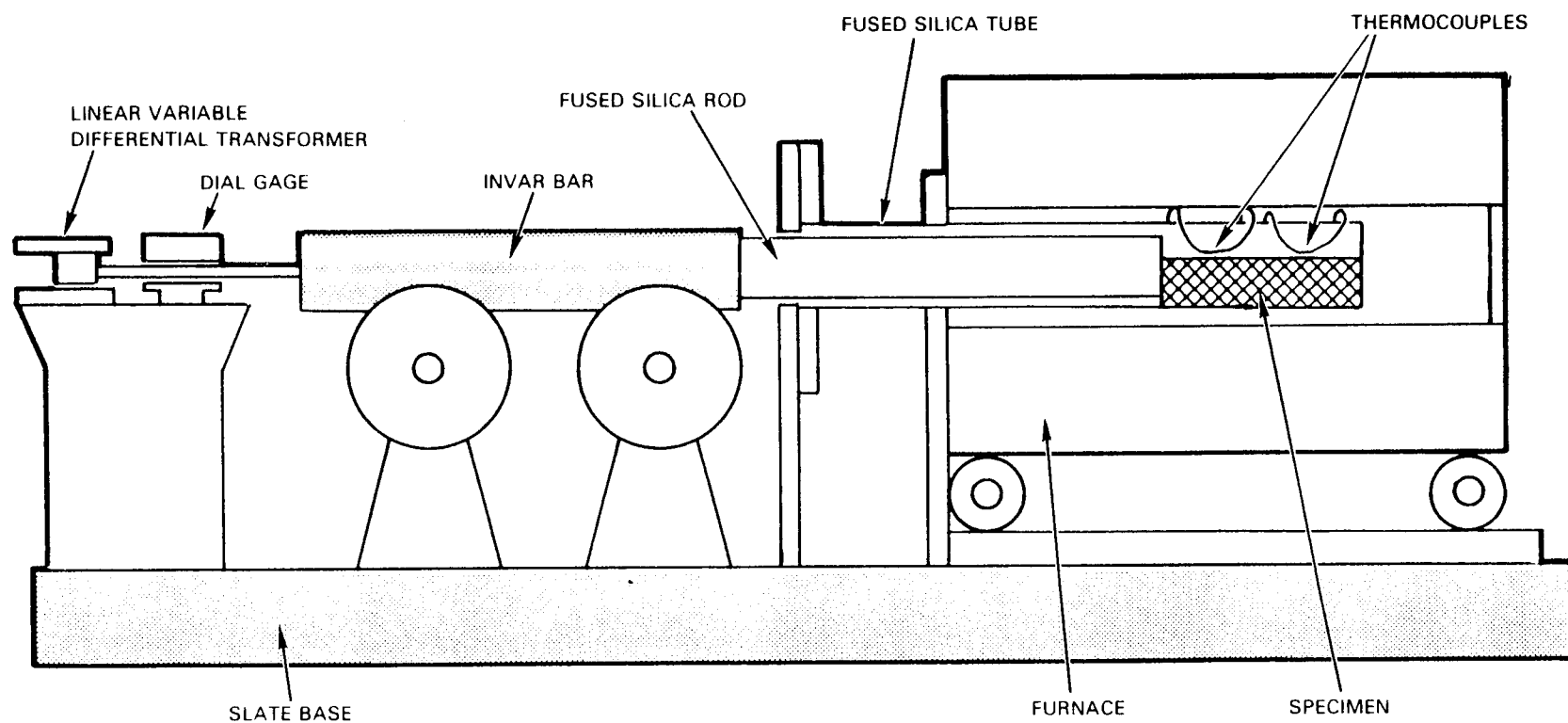
RCP8106-18

FIGURE 2-6.   Longitudinal Section of Dilatometer.

Thermally induced movement of the specimens was transferred through a fused silica rod attached to an Invar bar that rode on ball bearing pulleys. The end of the Invar bar rested against the plunger of a dial gage with a 0.0001-in. calibrated sensitivity. Pressure from the light spring of the dial gage kept the specimen in contact with the closed end of the fused silica tube.

The core of a linear variable differential transformer (LVDT) was mounted axially on the outer end of the dial gage plunger. Dial gage and LVDT housings were mounted on the base support of the assembly. The strain-measuring apparatus is shown in Figure 2-7. In addition to lightly loading the specimen, the dial gage was also used to calibrate the LVDT.

Length change measurements by the LVDT included a component measurement, caused by thermal expansion of the fused silica rod and tube used to contain the specimen. Expansion of fused silica components was only about 5% of the specimen length changes and data were corrected for this effect.

A commercial automatic instrument, actuated by one of the chromel-alumel thermocouples mounted inside the silica tube, controlled and recorded furnace atmosphere temperatures. This instrument was set to change temperature at a rate of $10^{\circ}F/min$.

Thermal expansion of specimens measured by the LVDT and temperature measured by a thermocouple were continuously recorded on an X-Y plotter. The assembled test equipment is shown in Figure 2-8.

2.3.2.2 <u>Thermal Expansion Test Procedures</u>. Specimens for thermal expansion testing were selected to avoid those with visible cracks, surface flaws, or air voids. Prior to testing, each specimen was weighed and measured. Weight and dimensions are listed in Table F-1 in Appendix F.

Test specimens were placed in the fused silica tube of the dilatometer and the fused silica rod seated against the end of the specimen. Temperature was increased with the electric furnace at a rate of $10^{\circ}F/min$. to $1,600^{\circ}F$. Temperature was then returned to ambient at a rate of $10^{\circ}F/min$. Thermal movement and temperature were recorded with the X-Y plotter throughout the heat cycle.
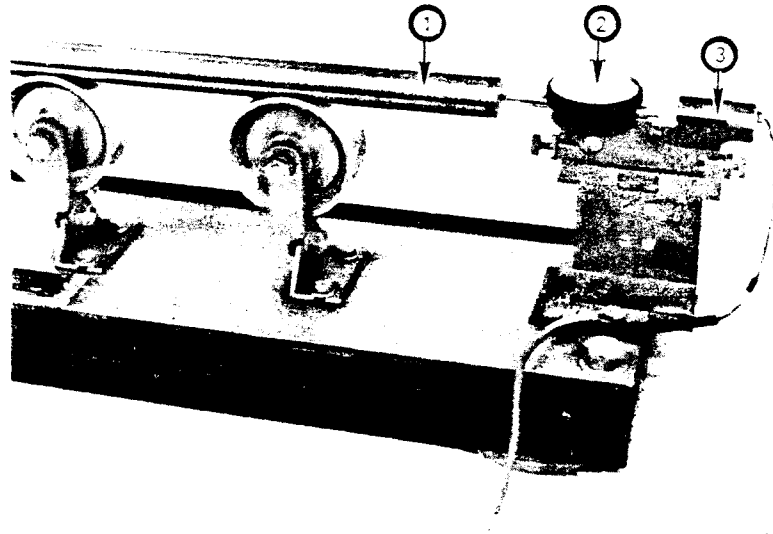
FIGURE 2-7. Dilatometer, A Strain Measuring Apparatus.

1. Invar Bar   2. Dial Gage   3. LVDT
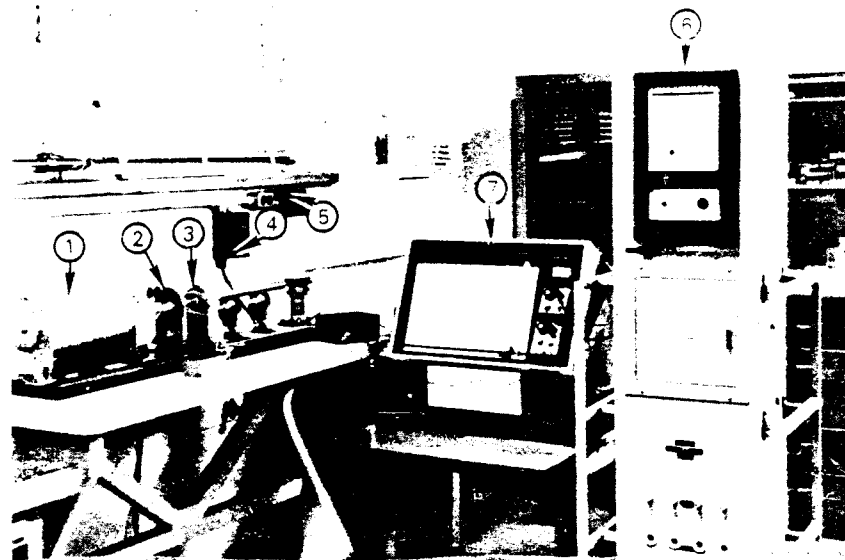
FIGURE 2-8. Dialatometer and Recorders.

1. Elecric Furnace   4. Invar Bar
2. Fused Silica Tube   5. Dial Gage and LVDT
3. Fused Silica Rod   6. Recorder-Controller Instrument
                          7. X-Y Recorder

After cooling, specimens were weighed to determine weight loss resulting from heating. Values are reported in Table F-1 in Appendix F.

2.4 THERMAL CYCLING TESTS

The influence of cyclically varying temperatures on the physical/ mechanical properties of Hanford concrete was determined in three related test programs. Two programs measured the effect of thermal cycling on concrete compressive strength and elastic properties for different cycling periods of 14- and 28-day cycles, respectively. A third program examined the influence of cyclic temperatures on concrete thermal expansion benavior.

2.4.1 Thermal Cycling Strength and Elastic Properties Tests

Two testing programs, used to determine effects of thermal cycling on concrete compressive strength and elastic properties, are described in the following sections.

2.4.1.1 Thermal Cycling Strength Test Specimens. Cylinders were cast at the PCA/CTL during September 1977. Four mix designs, designated Series 3K10, 3K14, 4.5K10 and 4.5K12, were selected for thermal cycling tests. Mix designs for each batch of 6- by 12-in. test cylinders are given in Tables A-1 through A-29 in Appendix A.

Test cylinders were stored in a 100% RH fog room at 73°F for the period between casting and initial exposure to elevated temperatures. Prior to heating, specimens were removed from the moist room and cylinder ends leveled. This was done to assure uniform distribution of load when cylinders were tested in compression.

2.4.1.2 Thermal Cycling Strength Test Temperatures. Two temperature cycling regimes were studied. Maximum test temperature and rates of heating and cooling were the same for both test series. The major difference was the duration of the heating cycle. In the earlier program, each thermal cycle had a period of 14 days; in the later program,

28 days. This was done to determine if lengthening elevated temperature exposure during each thermal cycle would cause deterioration of the concrete above the changes caused by the number of thermal cycles applied.

In each thermal cycling program, 24 cylinders were removed from the moist room, weighed, and measured. Weights and measurements are given in Table G-1 of Appendix G. Series 3K14 and 4.5K12 cylinders were used in the 14 day cycle program, while specimens from Series 3K10 and 4.5K10 were used in the 28 day cycle program. Cylinders were then placed in an oven, initially at room temperature. Oven temperature was then increased at a rate of 140°F/day until 350°F was reached. In the earlier program, this temperature was maintained for 10 days; in the later program, for 24 days. At that time, oven temperature was reduced at a rate of 140oF/day until room temperature was reached. The oven was maintained at ambient conditions for 24 hours prior to the initiation of the next temperature cycle. This procedure was repeated until a maximum of 17 or 18 cycles had been applied. The temperature cycles for each program are shown schematically in Figure 2-9.

2.4.1.3 Thermal Cycling Strength Test Apparatus and Procedures. At the end of selected thermal cycles, two cylinders from Series 3K10, 3K14, 4.5K10, and 4.5K12 were removed from the oven, weighed, and tested to determine strength and elastic properties. Tests were conducted after 1, 3, 5, 8, 12 or 13, and 17 or 18 thermal cycles. Tests were conducted at ambient conditions within 24 hours after the oven had reached room temperature.

In addition, two unheated cylinders from each batch used in heat cycling programs were tested at ambient conditions. Test results from these cylinders were used to evaluate the effects of thermal cycling.

Moduli of elasticity and Poisson's ratios were measured using equipment and test procedures similar to those described in ASTM Designation C469.[27] After elastic properties tests had been conducted, the same cylinders were used for determining concrete compressive strength, using procedures described in ASTM Designation C39.[25]
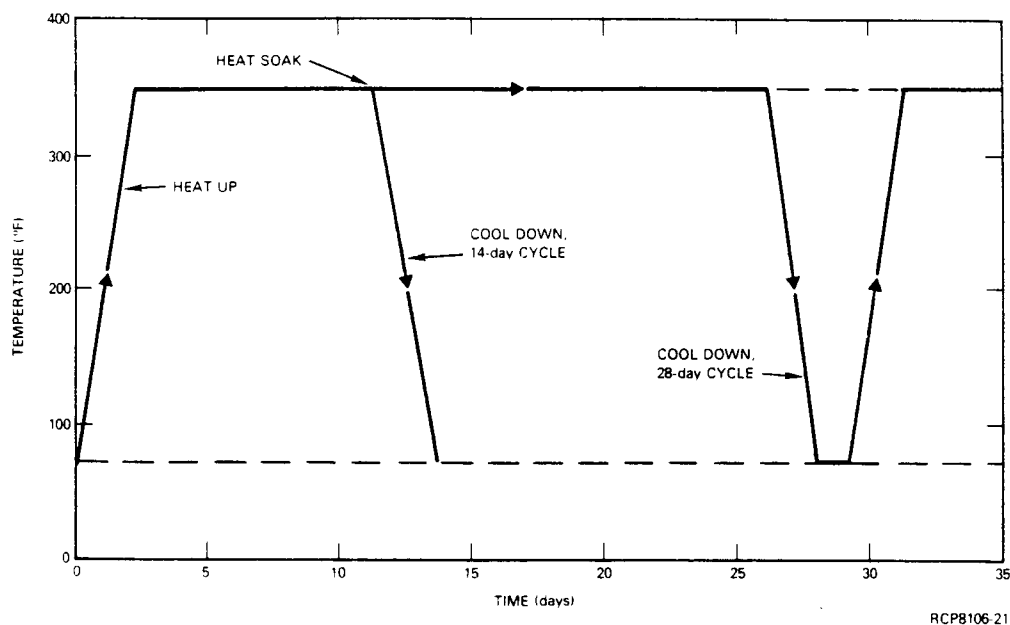
FIGURE 2-9. Temperature Cycles for 14- and
28- Day Temperature Cycle Programs.

2.4.2 Cyclic Thermal Expansion Tests

Changes in the thermal expansion characteristics of Hanford con-
cretes caused by repeated exposure to elevated temperatures were also
studied in this test program.

Specimens used in this study were fabricated from 6- by 12-in.
concrete cylinders 3K8-7, 3K9-18, 4.5K8-9, and 4.5K9-10, cast at CTL/PCA
in May 1975, and 3K14-22 and 4.5K12-12, cast in September 1977. Methods
of specimen preparation and curing were identical to those used for
dilatometer specimens previously described (see Section 2.3.1). Concrete
cast in 1975 was tested at an age of approximately 50 months. Specimens
made from concrete cast in 1977 were tested at an age of about
22 months. The test equipment used in the cyclic thermal expansion
program was the same as that described earlier (see Section 2.3.2.1).

A total of 8 dilatometer specimens were tested in this program at temperatures ranging from ambient to 450°F. Procedures used in cyclic thermal expansion tests were as follows:

A test specimen was positioned in the fused silica tube of the dilatometer (see Figures 2-6 and 2-8). The fused silica rod was seated against the end of the specimen. Temperature then was increased with the electric furnace at a rate of 10°F/min. from room temperature to approximately 450°F. Temperature and thermal expansion were recorded continuously on the X-Y plotter.

When 450°F was reached, the specimen was cooled to ambient temperature, again at a rate of 10°F/min. The time/temperature curve is shown in Figure 2-10. The heating-cooling cycle then was repeated 3 or 4 times, and thermal strain behavior of the specimen was recorded during the heating portion of each cycle. Thus, the maximum number of cycles was 5. This was the largest number of temperature cycles that could be completed during one working day.
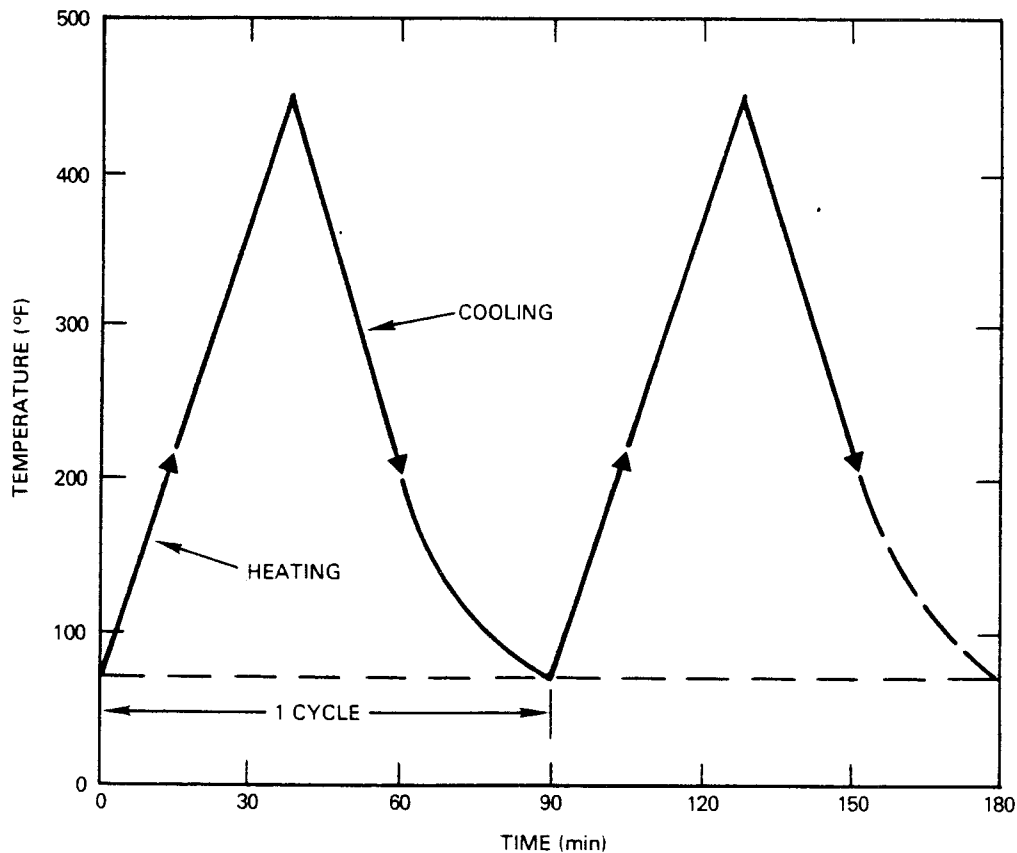
RCP8106-22

FIGURE 2-10. Cyclic Time/Temperature Curve.

2.5 STEAM CURING TESTS

Due to the relatively long time required to produce mature test specimens for strength and elastic properties tests, the possibility of accelerating strength development by steam curing was investigated. Specimens and test procedures used in this study are described below.

One group of 24 cylinders was selected to determine the affect of steam curing on the acceleration of strength development of Hanford concrete. These cylinders were cast at CTL/PCA on October 17, 1977, from a single batch of concrete using the mix design for 3,000 psi Hanford concrete. This batch was identified as 3K16. Mix proportions for this batch may be found in Table A-16 in Appendix A.

Eighteen cylinders were steam cured for varying times, following the American Concrete Institute's (ACI) proposed guidelines for atmospheric pressure steam curing of concrete.[29] The remaining 6 cylinders were conditioned in the 100% RH fog room at 73°F to provide comparison specimens.

According to ACI, steam curing procedures may vary, depending on the time allotted for each of the following operations:

- Presteaming period
- Temperature rise period
- Maximum temperature period.

Presteaming period is the time between casting the concrete and the beginning of heating to desired curing temperature. The ACI recommends that heating of concrete should not begin sooner than 1 to 7 hr after casting. Other investigators[30] suggest that longer presteaming times may increase long-term strength.

The temperature rise period is the time required to reach the maximum cure temperature from ambient conditions. The ACI recommendation is that the rate of heating should not exceed 20°F/hr.

Maximum temperature period is the time concrete is exposed to the highest curing temperature. Generally, this time is 24 hr or less, but is increased to as much as 3 days for some applications. Curing beyond three days is not recommended for economic reasons. Maximum temperature is usually in the range of 130° to 180°F. Higher temperatures are not recommended. Maximum temperatures should not exceed 150°F if steam curing exceeds 24 hr. For longer curing times, a maximum temperature of 130°F may yield higher strengths at later ages than curing at 160°F for the same length of time.

Based on these recommendations, the curing and testing program outlined below was selected.

- Twenty-four 6- by 12-in. cylinders were cast into metal molds and covered with close-fitting lids.

- Five hr after casting, 18 cylinders (still inside molds) were placed in a steam box and heated to 137°F at a rate of 20°F/hr. The remaining 6 cylinders were stripped from molds after one day and placed in a fog room maintained at 100% RH and 73°F.

- After 24, 48, and 72 hr of steam curing, 6 cylinders were removed from the steam box. Three cylinders were tested in compression after cooling, and three were placed in the fog room to cure normally for testing at 28 days.

- Cylinders that had not been steam cured were tested in compression at 1, 3, and 28 days. Two specimens were tested on each date.

All specimens were tested in compression at room temperature, using equipment and procedures described in ASTM Designation C39.[25]

2.6 THERMAL PROPERTIES TESTS

The influence of elevated temperatures on the thermal properties of Hanford concrete was studied in tests on two specimens of concrete cast at CTL/PCA. In these tests, specific heat, thermal conductivity, and

thermal diffusivity were measured from 79° to 1,175°F. Testing was conducted by personnel of the Research Section, Division of Building Research of the National Research Council in Ottawa, Canada.

2.6.1 Thermal Properties Test Specimen

Two specimens were obtained from 6- by 12-in. cylinders cast at CTL/PCA in September 1977. Specimens obtained from these cylinders were identified as 3K14-20 and 4.5K12-4. Mix designs for these specimens may be found in Tables A-14 and A-28 in Appendix A.

All test specimens were dried at 105°C (221°F) to constant weight prior to testing.

2.6.2 Thermal Properties Test Apparatus and Procedures

Test methods used permitted the determination of specific heat, thermal conductivity, and thermal diffusivity by using pulsed or rapid application of heat to the specimen. By monitoring temperature response at various specimen locations and by assuming linear heat flow in a localized area, thermal properties were determined, using curve fitting techniques.

These methods are suited for measurement of thermal properties of materials such as concrete, that undergo rapid physico-chemical changes on heating. These variable state methods were developed at the Fire Section, Division of Building Research of the National Research Council in Ottawa, Canada.

A detailed description of the test methods may be found in a paper by Harmathy.[31] A copy of this paper has been included in Appendix I.

2.7 PETROGRAPHIC ANALYSIS

Test cylinders representing specified time and temperature combinations were removed from the ovens. After a few hours of cooling at room temperature, a 1-in. thick slice was cut transversely, using a water-cooled saw. A small block, cut from the interior of the slice with an

air-cooled saw, was planed, dried at 122°F, and mounted on a standard petrographic slide with epoxy adhesive. The section was ground to 10 to 20 microns thickness and protected with cover glass, loose mounted in epoxy. The thin sections were labeled and were numerically coded so that they could be described without prior bias as to duration of storage and temperature.

Birefringence is the numerical difference between the maximum and minimum indices of refraction of an anistropic crystalline solid and is related to the crystal thickness (thin section thickness) by the following equation:

$$t = \frac{\lambda\theta}{180}/B$$

where λ is the wavelength of transmitted light, in millimicrons (540)

   θ is the analyzer rotation on the microscope, in degrees

   B is the birefringence of the crystal solid

   t is the thickness, in microns.

Assuming a quartz birefringence of 0.009, thickness of the concrete thin section was determined by averaging several measurements of on 6 to 8 grains of quartz. Using this calculated value of thickness, the average birefringence of calcuim hydroxide in the same thin section was determined by examination of 8 to 10 crystals in the portland cement paste of the concrete. More information on the petrographic and fractographic analyses is given in Appendix J.

3.0 SUMMARIZED RESULTS

In the following sections, data from physical and mechanical properties tests on Hanford concrete mixes at room and elevated temperatures are presented. Each section covers one aspect of properties testing. Normally, data are shown in graphical form, accompanied by a brief description of material behavior as a function of significant test variables.

For convenience, data are also given in tabular form in Appendices A through J. Where more detailed descriptions of test methods and results were required, such as for thermal properties tests or petrographic analyses, they have been included in the relevant appendices.

3.1 STRENGTH AND ELASTIC PROPERTIES

The strength and elastic properties test program consisted of several consecutive test series that measured the effects of elevated temperatures on concrete mechanical properties for varying periods of time. The first phase of this work, begun in 1975, studied, in detail, the mechanical behavior of concrete mixes heated for up to 35 days. Later phases examined the behavior of concrete heated for up to 2 3/4 years.

The test program included measurement of compressive strengths, splitting tensile strengths, moduli of elasticity, and Poisson's ratios of Hanford concrete mixes. Determination of concrete strengths was made using static methods. Concrete elastic properties were determined using static and dynamic (sonic) methods. Tests were conducted on unheated concrete and on specimens heated for varying periods of time at 250°, 350°, and 450°F.

3.1.1 Modulus of Elasticity

Results of tests to determine the influence of age, mix design, and elevated temperatures on the elastic moduli of Hanford concrete mixes are described in the following two sections.

3.1.1.1 <u>Elastic Modulus - Static Method</u>. Modulus of elasticity data at room temperature, determined by the static method for 3K and 4.5K mixes, are given in Table B-2 in Appendix B and plotted as a function of age in Figure 3-1.
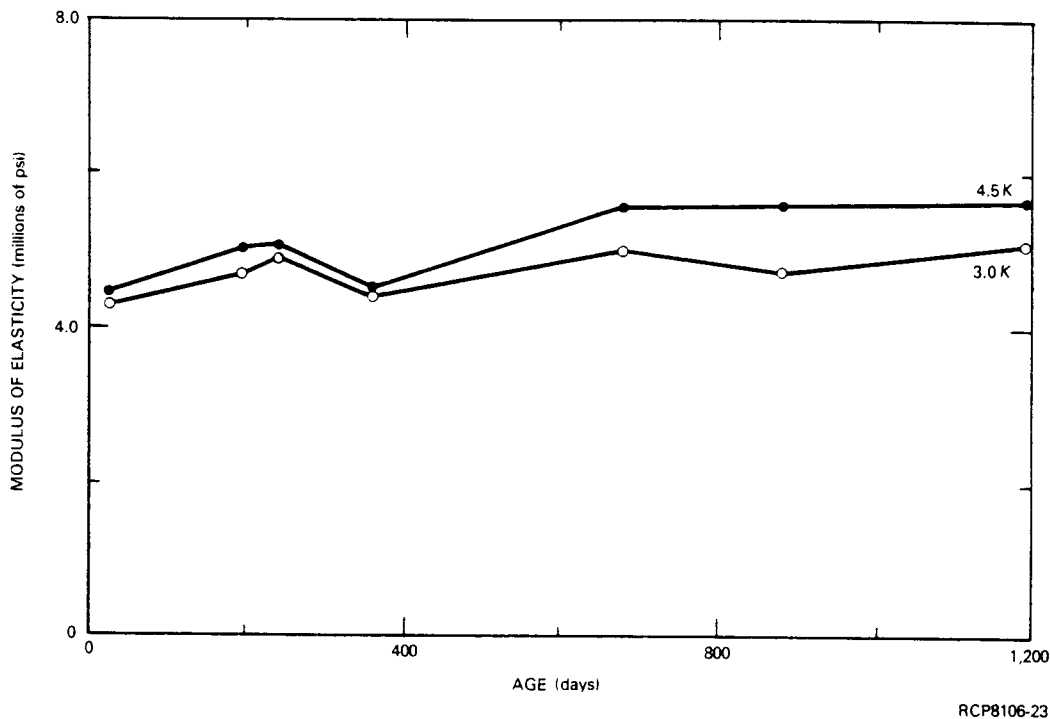
FIGURE 3-1. Modulus of Elasticity for Moist Cured Cylinders Using the Static Method.

The static moduli of elasticity of the moist-cured concretes generally increased with age. Higher values of static modulis were obtained for the 4.5K mix at room temperature. The increase in modulus of elasticity did not differ appreciably for either mix.

Modulus of elasticity values, obtained from tests of cylinders heated at 250°, 350°, and $450^\circ F$ for periods ranging from 3 to 926 days, are given in Table B-2 in Appendix B and are shown in Figures 3-2, 3-3, and 3-4. Generally, the modulus of elasticity for both concrete mixes decreased as the heating time increased. At all temperatures, the rate of decrease in modulus was greatest between 3 and about 150 days. Lower values of the modulus of elasticity were generally obtained for the 3K mix rather than for the 4.5K mix at all three temperatures. However, the data are not as clearly defined at $450^\circ F$.
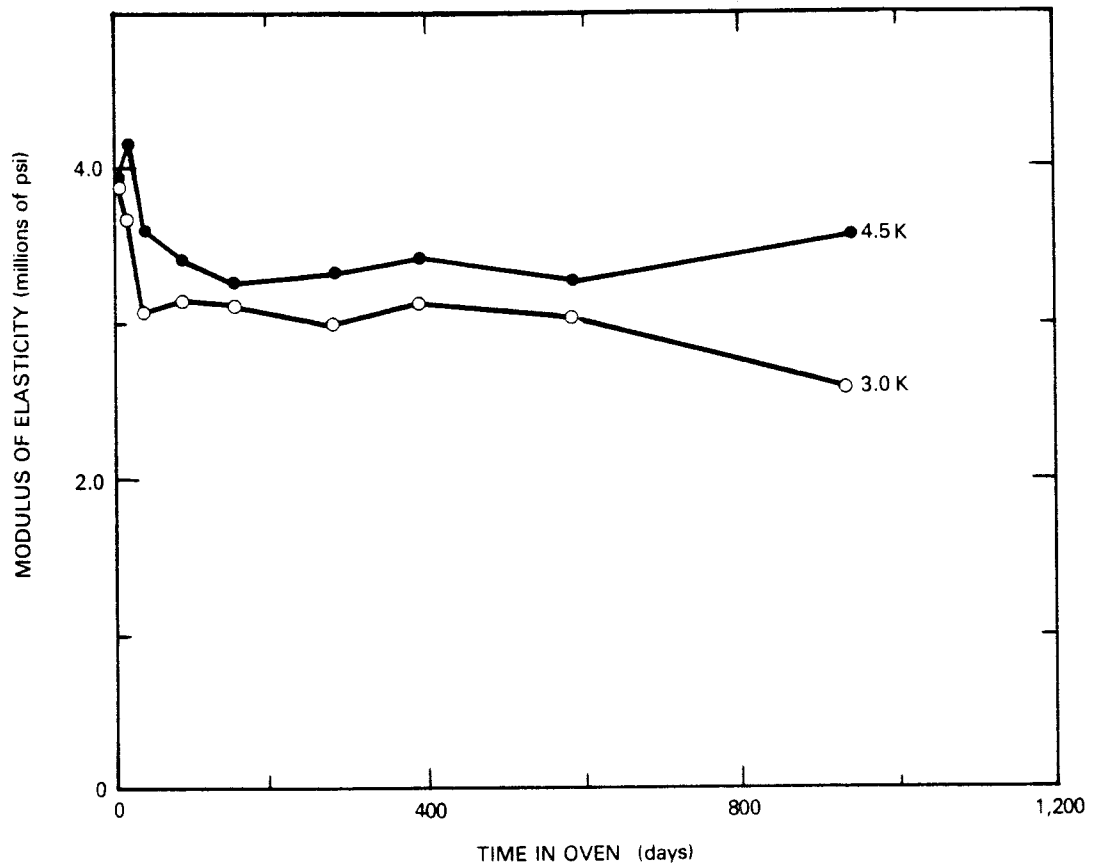
RCP8106-24

FIGURE 3-2. Modulus of Elasticity for Cylinders at 250°F,
Using the Static Method.
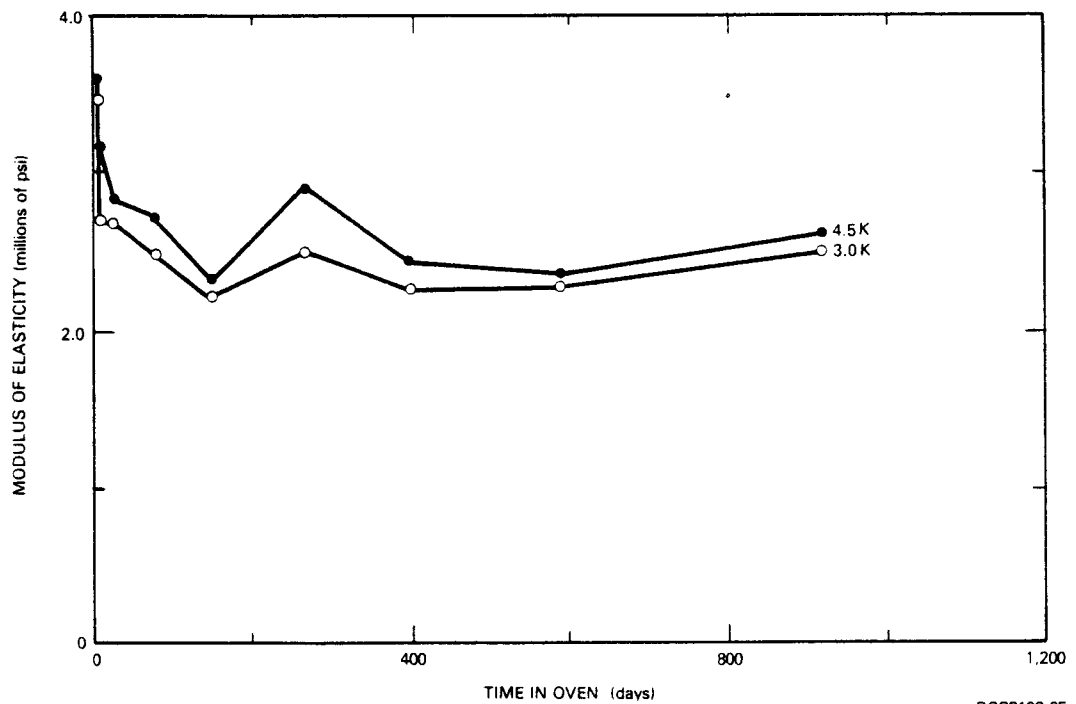
RCP8106-25

FIGURE 3-3. Modulus of Elasticity for Cylinders at 350°F,
Using the Static Method.
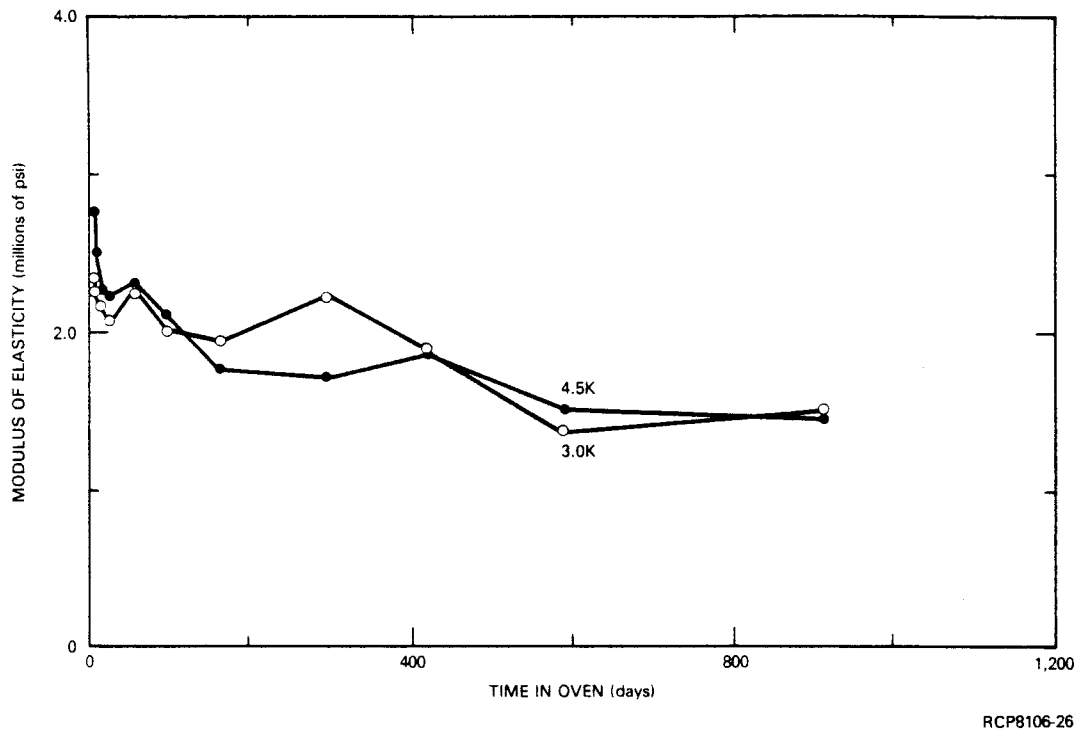
FIGURE 3-4. Modulus of Elasticity for Cylinders At 450°F, Using the Static Method.

Temperature has a very significant effect on the elastic moduli of the concretes. At 250°F, values of the elastic modulus dropped from an average initial value of 4.3 million psi for unheated concrete to about 3.8 million psi. After 926 days, the average modulus for both mixes was about 3 million psi. After three days of heating at 350°F, the initial modulus value of 4.3 million psi was reduced to 3.5 million psi. After 926 days of heating, the modulus values were about 2.5 million psi. The moduli of concrete mixes, after only three days of heating at 450°F, were significantly lower than unheated concrete, decreasing from 4.3 to 2.5 million psi. At the end of about 922 days of heating at 450°F, modulus values for both concrete mixes were about 1.5 million psi.

3.1.1.2 Elastic Modulus - Sonic Method. Values of modulus of elasticity of Hanford mixes, determined by the sonic method at room temperature, are given in Table C-1 in Appendix C, and shown as a function of age in Figure 3-5. For both mix designs, sonic moduli increase with length of moist cure period. The largest increases occurred between 30 and
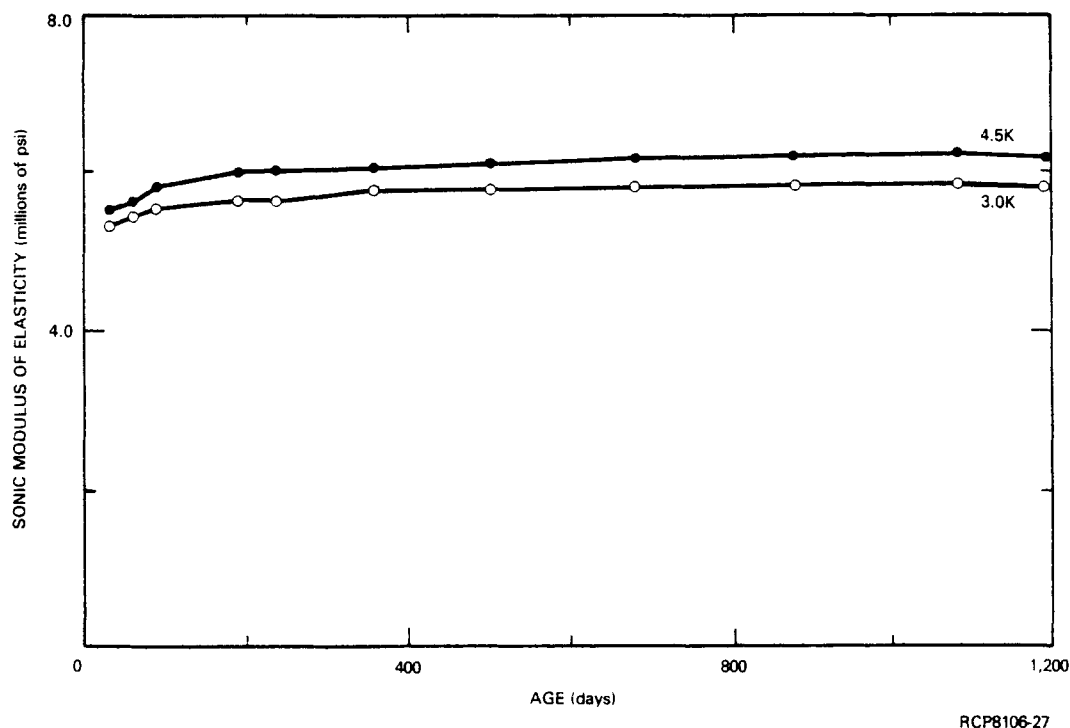
FIGURE 3-5. Modulus of Elasticity for Moist Cured
Cylinders, Using the Sonic Method.

200 days. Over the next 1,000 days, however, the increases in moduli were quite small. Higher values of the sonic modulus were obtained for the 4.5K mix at room temperature. The increases in moduli did not differ appreciably for either mix.

All of the sonic modulus values were determined from tests of the same cylinders for each mix. Consequently, in-batch and batch-to-batch variations of the test specimens did not affect the sonic modulus age relationships of the two concrete mixes. Comparison of these data with those obtained from static test methods shows that sonic modulus values were larger than their statically determined counterparts at all ages.

In addition to room temperature tests, moduli of elasticity were determined sonically on concrete cylinders heated from ambient to 450°F. Values for sonically determined elastic constants are given in Table C-2 in Appendix C. These data are compared to sonic room temperature and statically determined ambient and elevated temperature moduli in Figures 3-6 and 3-7. The magnitude of modulus of elasticity of concrete decreases very rapidly on initial heating, as shown in the
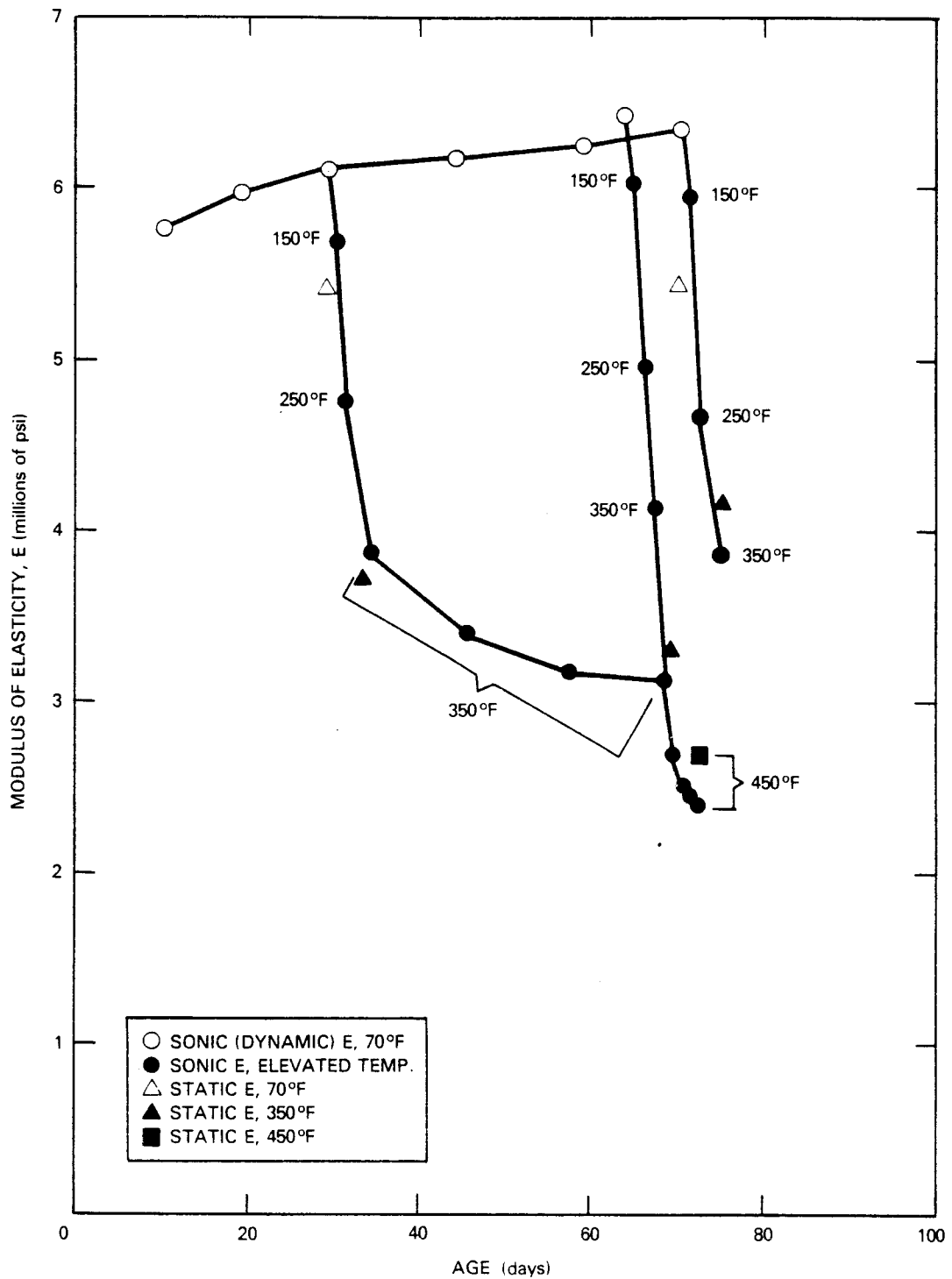
FIGURE 3-6. Modulus of Elasticity for the
3K Mix at Elevated Temperatures.

RCP8106-28
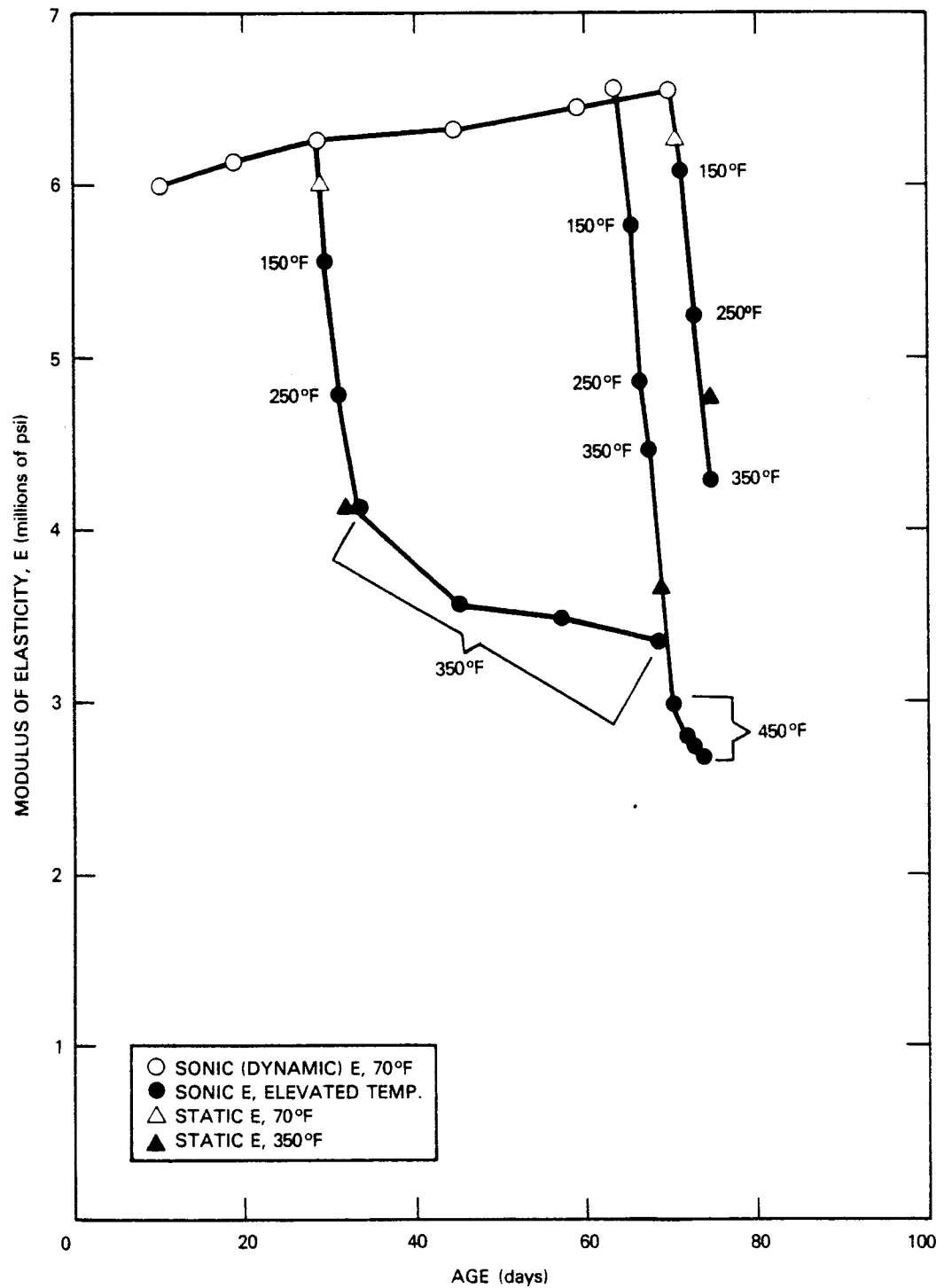
FIGURE 3-7. Modulus of Elasticity for the
4.5K Mix at Elevated Temperatures.

RCP8106-29

figures. This loss is equally severe for concrete of different ages, as shown in Figures 3-6 and 3-7. Higher temperatures produced larger reductions in modulus values. Comparison of static and sonic modulus values in Figures 3-6 and 3-7 shows good agreement at both ambient and elevated temperatures.

3.1.2 Poisson's Ratio

Poisson's ratio data on Hanford concrete mixes determined from static and sonic tests are described in the following two sections.

3.1.2.1 Poisson's Ratio - Static Method. Information on Poisson's ratio, obtained by the static test method at 73°F for both mixes over a period of 1,204 days, is shown in Figure 3-8 and in Table B-2 in Appendix B. Poisson's ratio values appear to increase somewhat with age. Generally, higher values were obtained for the 4.5K mix than for the 3K mix. For the 3K mix, static values ranged from 0.15 to 0.17. The range of values for the 4.5K mix was from 0.16 to 0.19.

RCP8106-30
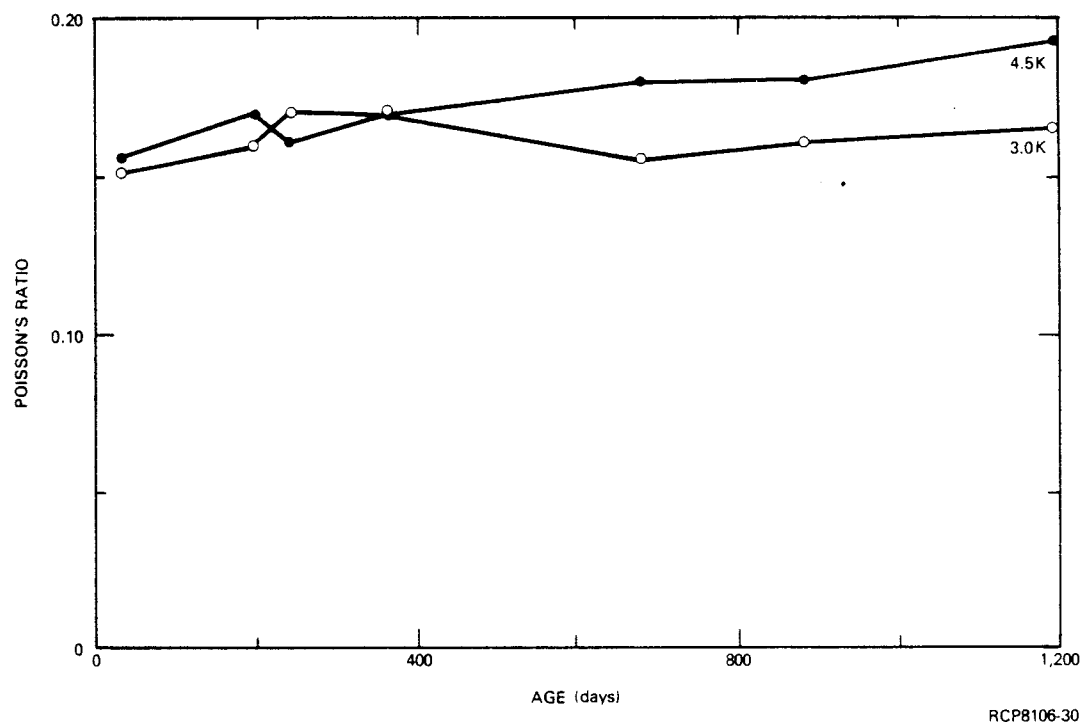
FIGURE 3-8. Poisson's Ratio for Moist Cured
Cylinders, Using the Static Method.

Data for Poisson's ratio determined by the static method at temperatures of 250°, 350°, and 450°F, respectively, are shown in Figures 3-9, 3-10, and 3-11 and Table B-2 in Appendix B. Poisson's ratio data were very erratic. The largest fluctuation in the data occurred at 450°F. There are numerous crossovers in the Poisson's ratio curves for the 3K and 4.5K mixes at all three temperatures. However, notwithstanding these variations, the high temperature values for Poisson's ratio varied between 0.10 and 0.14. In general, age and temperature did not have a large effect on the values of Poisson's ratio obtained at the various test dates.

3.1.2.2 Poisson's Ratio - Sonic Method. Poisson's ratios of Hanford concrete mixes, determined by the sonic method at 73°F, are shown in Table C-1 of Appendix C, and plotted as a function of age in Figure 3-12. Poisson's ratio determined by the sonic method remained relatively constant for both mixes. With the exception of the data obtained at 240 days, Poisson's ratios for the 3K mix varied from 0.21 to 0.25. For the 4.5K mix, values of Poisson's ratio determined sonically ranged from 0.20 to 0.27. Generally, higher values were obtained for the 4.5K mix. Comparison with static Poisson's ratio data shows that the sonically determined values were larger at all ages.

Poisson's ratios, sonically determined from concrete mixes heated to 350° and 450°F, are shown in Figures 3-13 and 3-14 and tabulated in Table C-2 of Appendix C. As with elastic modulus, Poisson's ratio values decreased rapidly with increasing temperature. Also, length of moist curing prior to heating did not appear to significantly affect the amount of loss in Poisson's ratio values.

Comparison with static values, also plotted in Figures 3-13 and 3-14, showed fairly good correlation between Poisson's ratios determined from both test methods.

3.1.3 Compressive Strength

Compressive strengths of the two concrete mixes determined at 73°F on moist cured cylinders are shown in Figure 3-15 and given in Table B-2 in Appendix B. Generally, compressive strength increased with age. The greatest increase was between 30 and 200 days. Beyond this point, the increase was much smaller.
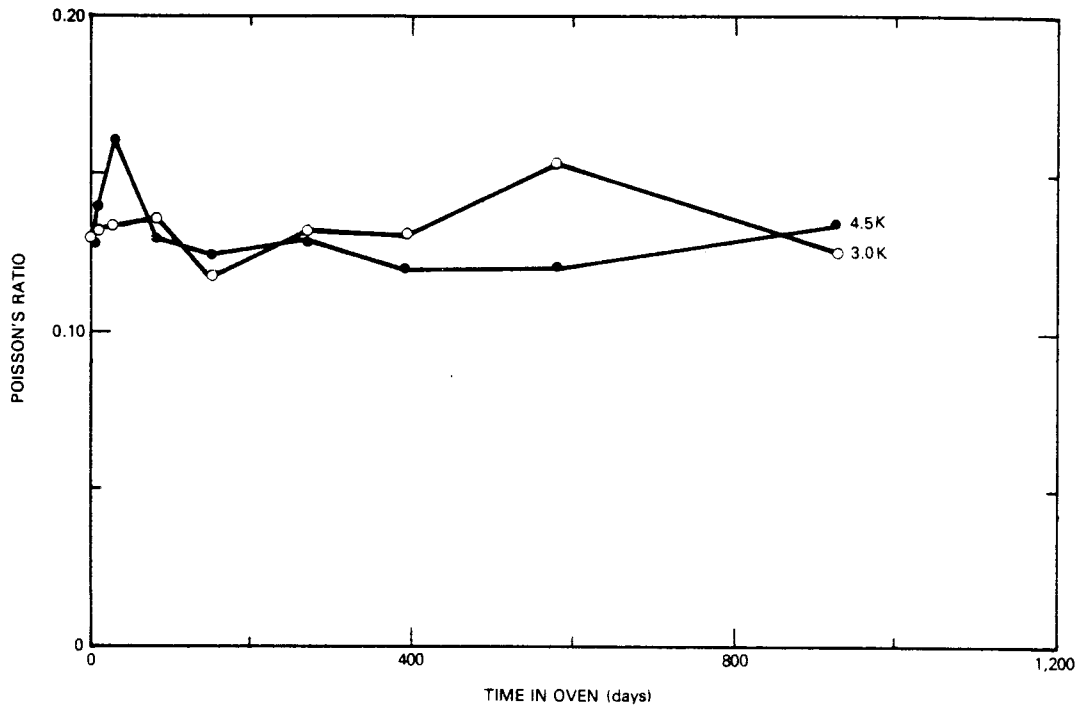
FIGURE 3-9. Poisson's Ratio for Cylinders at 250°F, Using the Static Method.
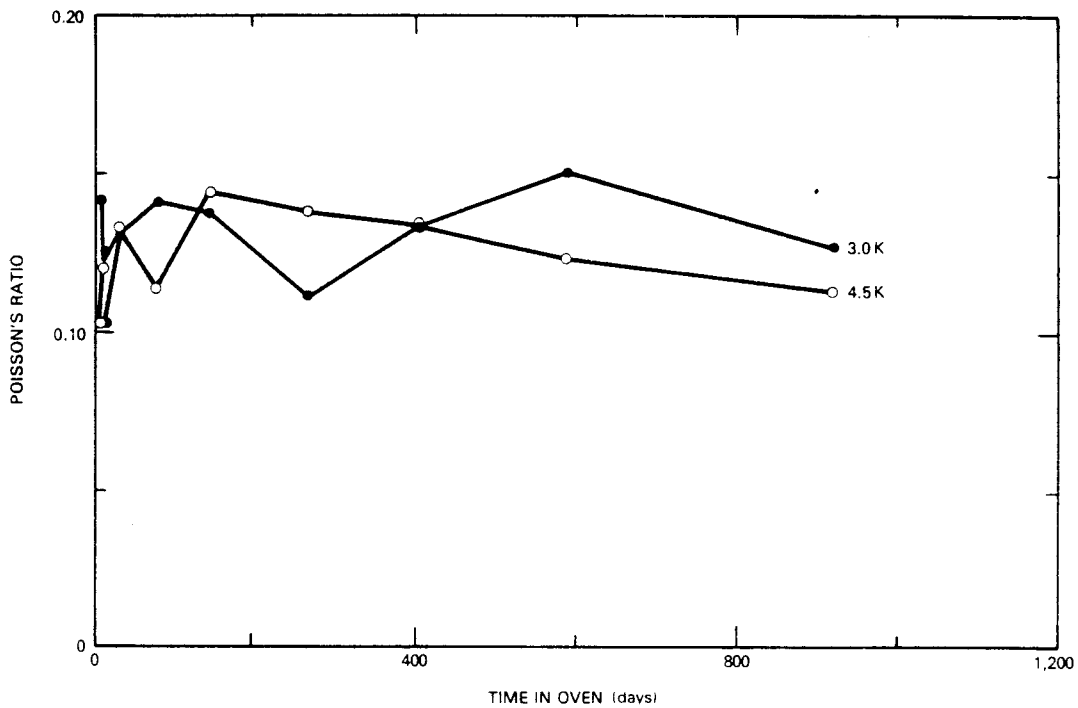
FIGURE 3-10. Poisson's Ratio for Cylinders at 350°F, Using the Static Method.
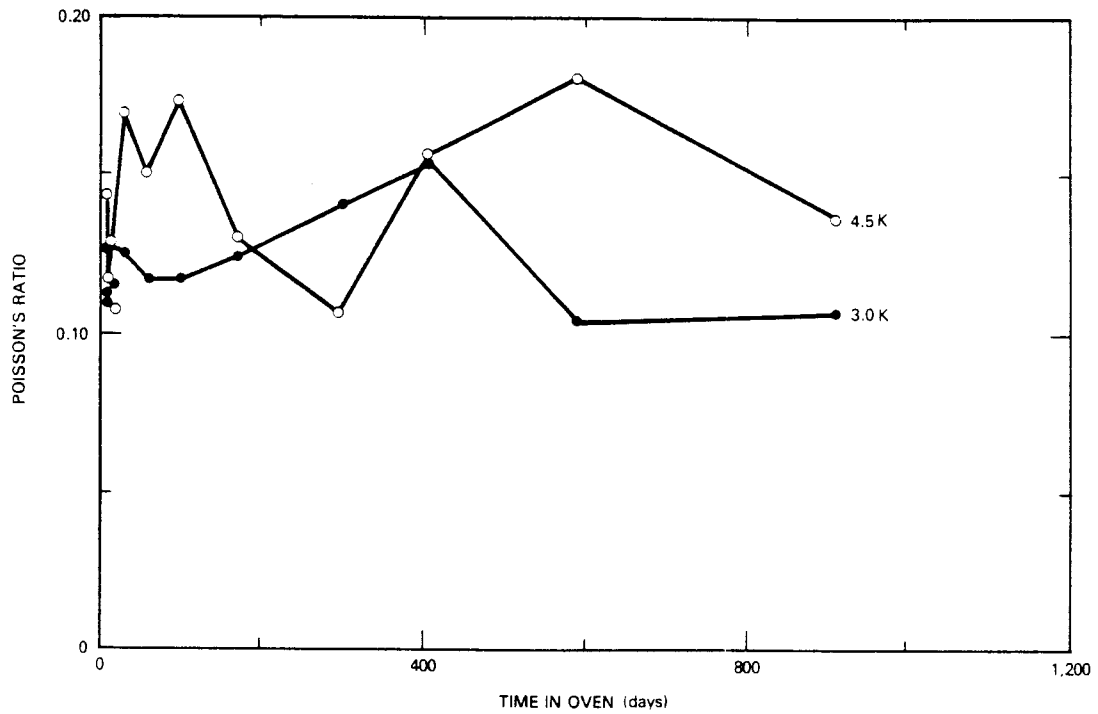
FIGURE 3-11. Poisson's Ratio for Cylinders at 450°F, Using the Static Method.
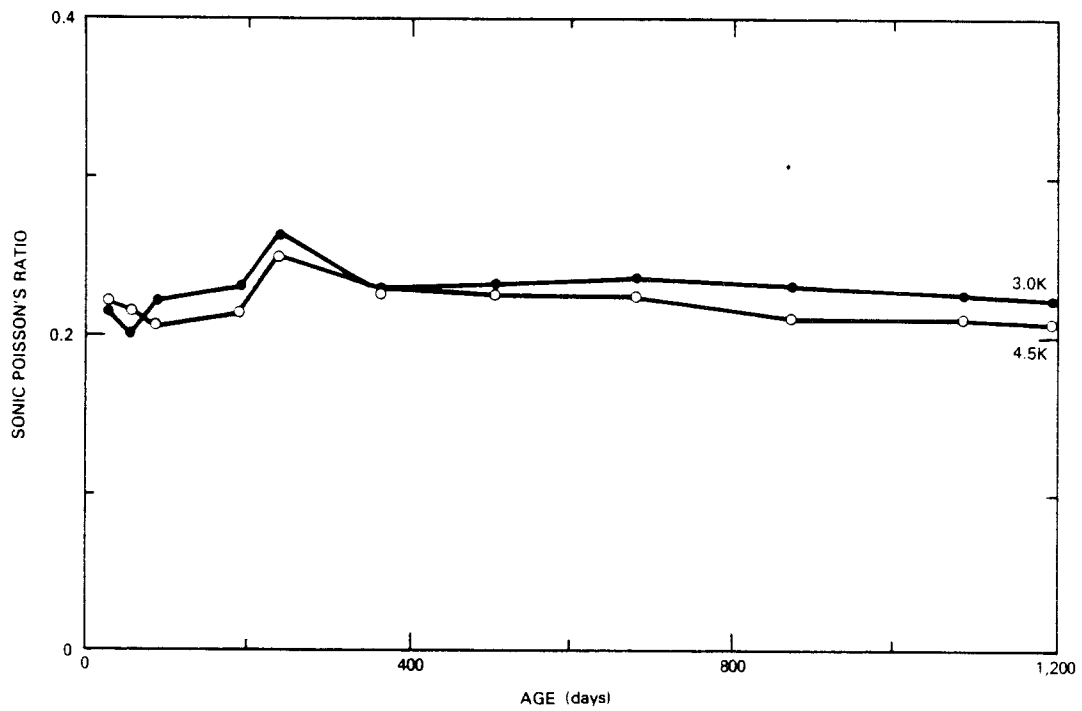
FIGURE 3-12. Poisson's Ratio for Moist Cured Cylinders, Using the Sonic Method.
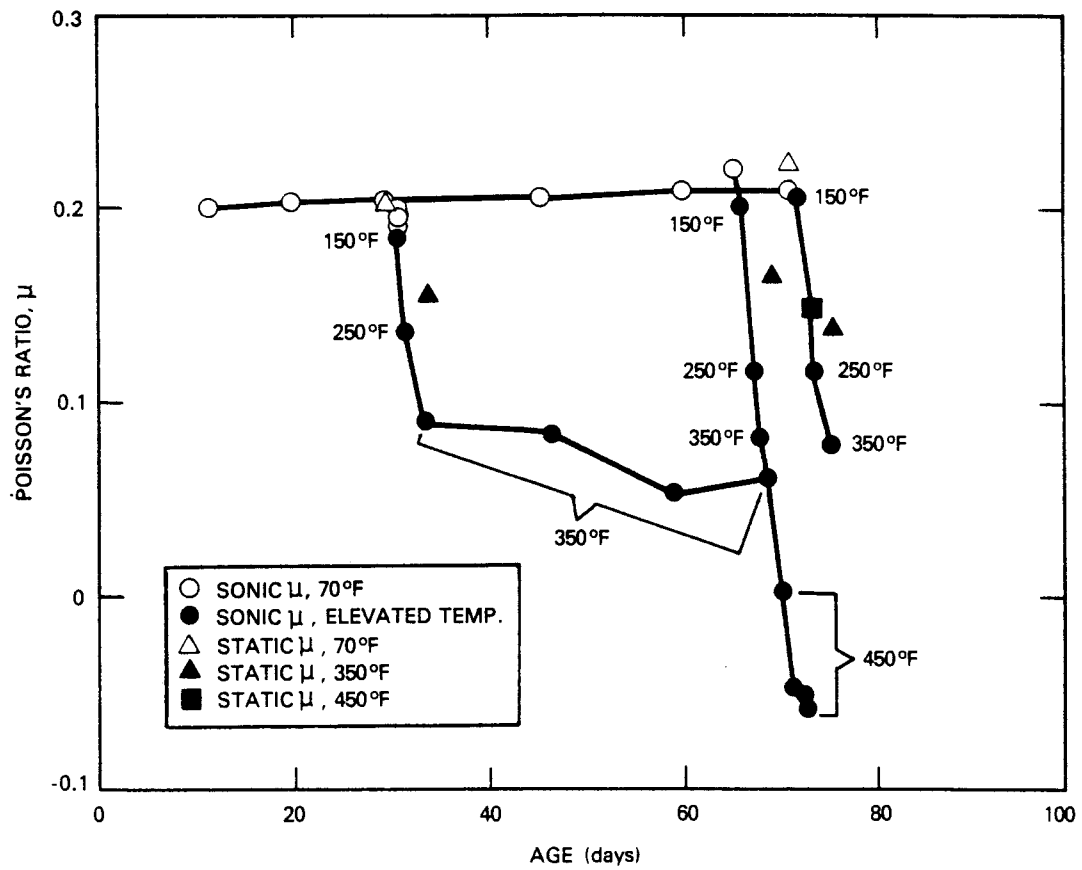
FIGURE 3-13.   Poisson's Ratio for 3K Mix at
Room and Elevated Temperatures.
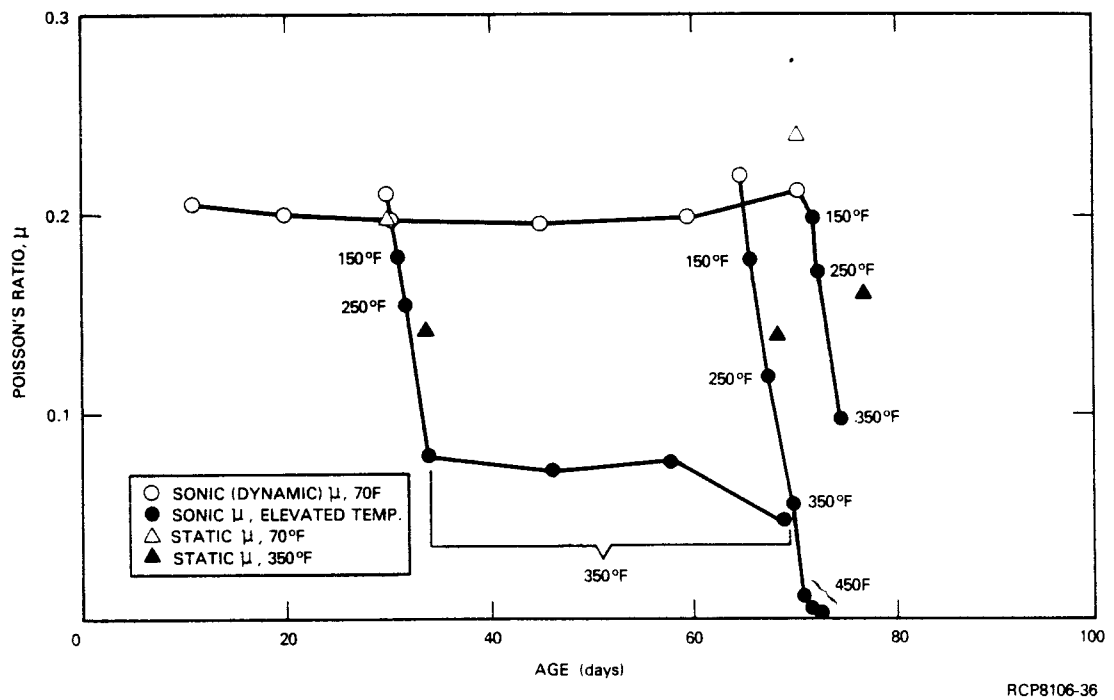
FIGURE 3-14.   Poisson's Ratio for 4.5K Mix at
Room and Elevated Temperatures.
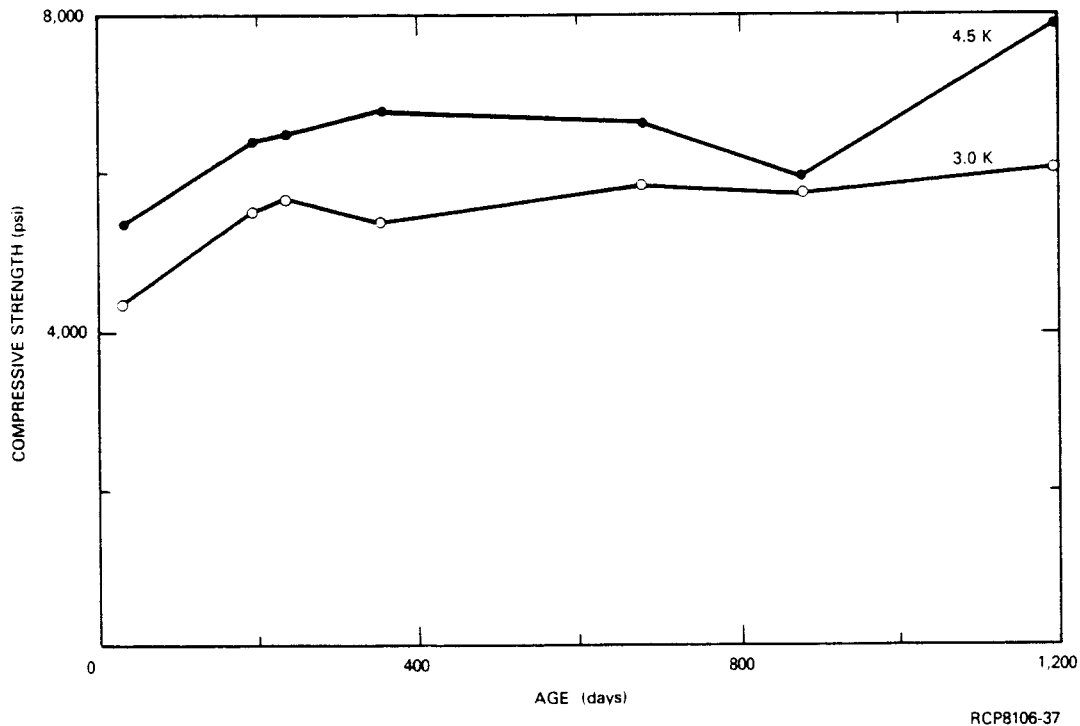
FIGURE 3-15. Compressive Strength of Moist Cured Cylinders.

This type of strength increase is normal for these concrete mixes. A representative age/strength relationship for moist cured concrete, expressed as a percentage of that obtained at 28 days, is shown in Figure 3-16. This curve represents results of many tests obtained over a period of years at the PCA. It can be seen that the most rapid increase in strength occurs during the first 180 days of the period. Beyond that point, strength increases at a much slower rate.

Compressive strength test data for the 3K and 4.5K mixes, heated at 250^0, 350^0, and 450^0F for about 920 days, are shown in Figures 3-17, 3-18, and 3-19. These data are also given in Table B-2 in Appendix B. For the most part, the compressive strength data are very erratic. For the 3K mix, strength decreased with increasing age at all three temperatures, with the exception of the data at 450^0F between 100 and 400 days of exposure to heat. Generally, the compressive strength of the 4.5K concrete decreased with increasing time at elevated temperatures. This trend is most pronounced at 450^0F.
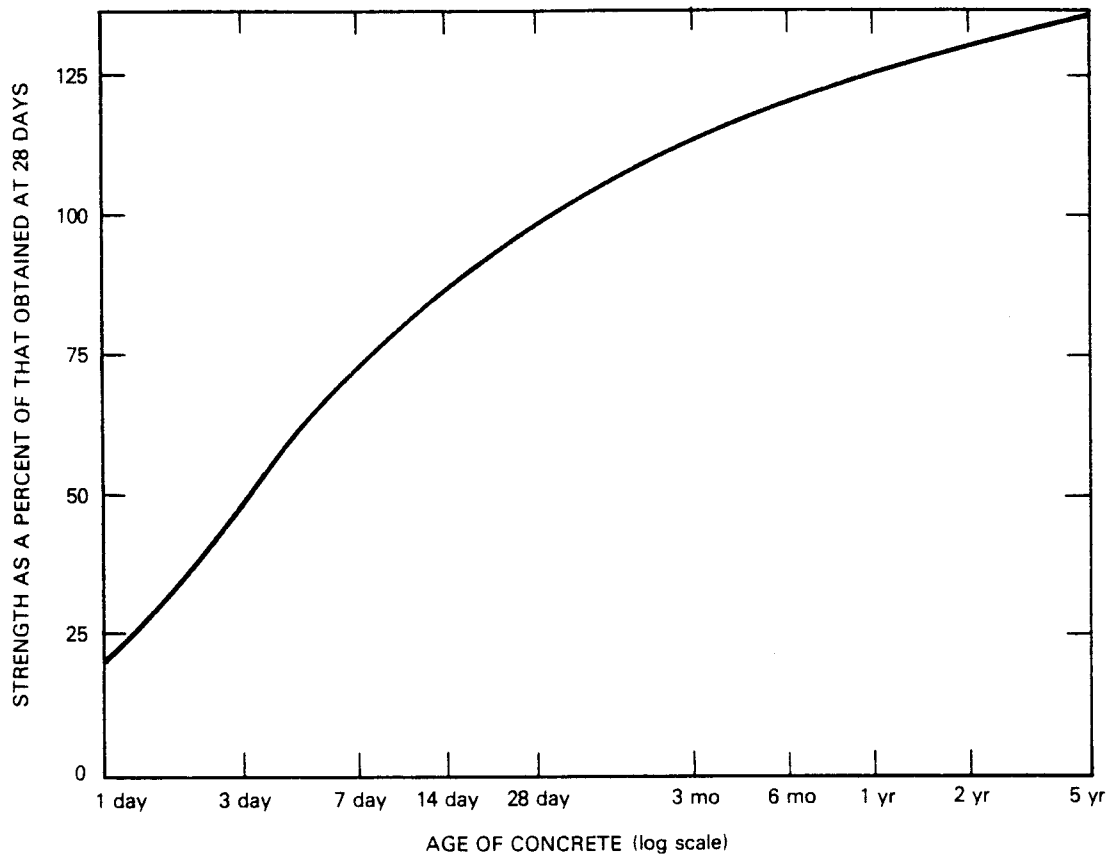
FIGURE 3-16. Age Strength Relationships for Moist Cured Concrete.
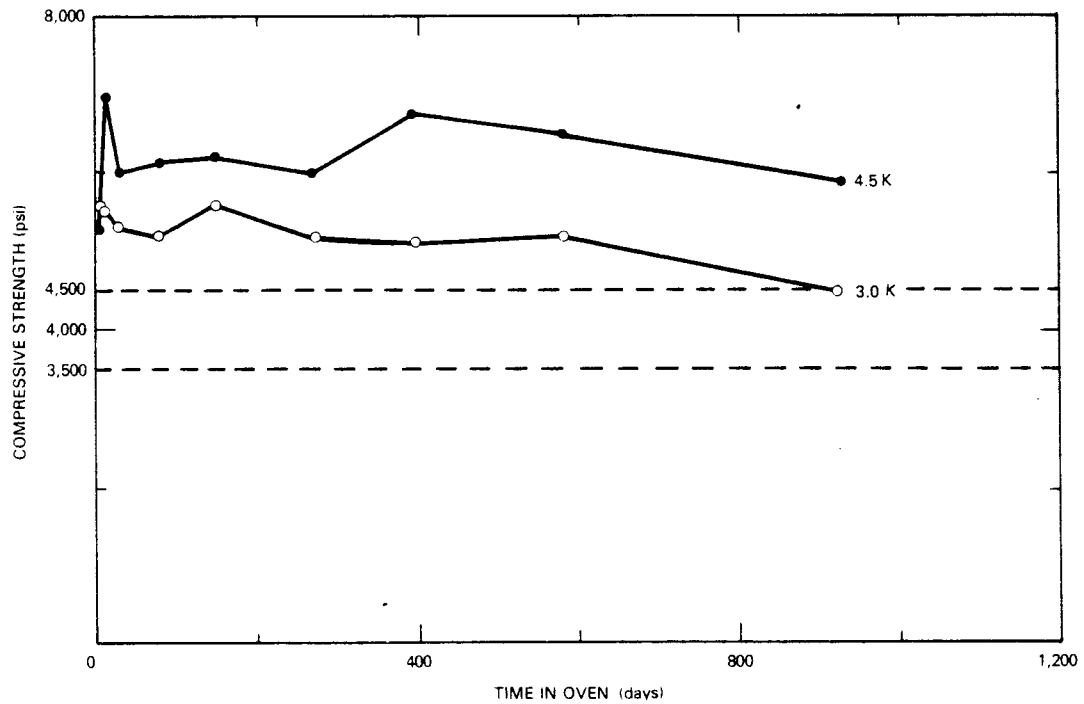
FIGURE 3-17. Compressive Strength of Cylinders at 250°F.
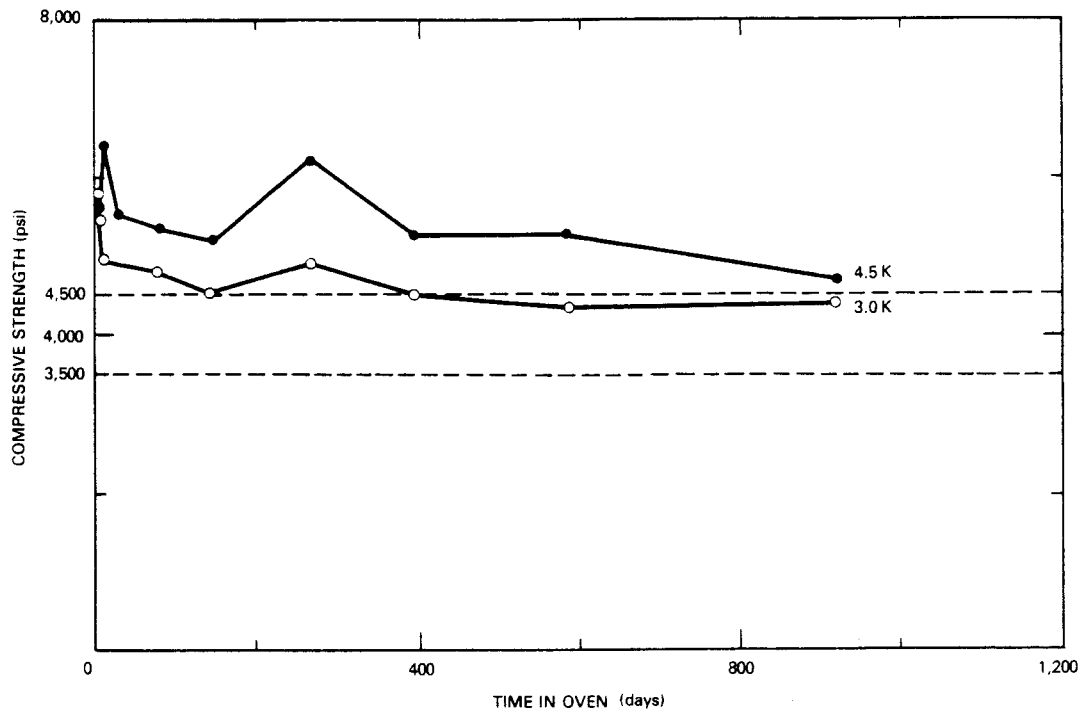
FIGURE 3-18. Compressive Strength of Cylinders at 350°F.
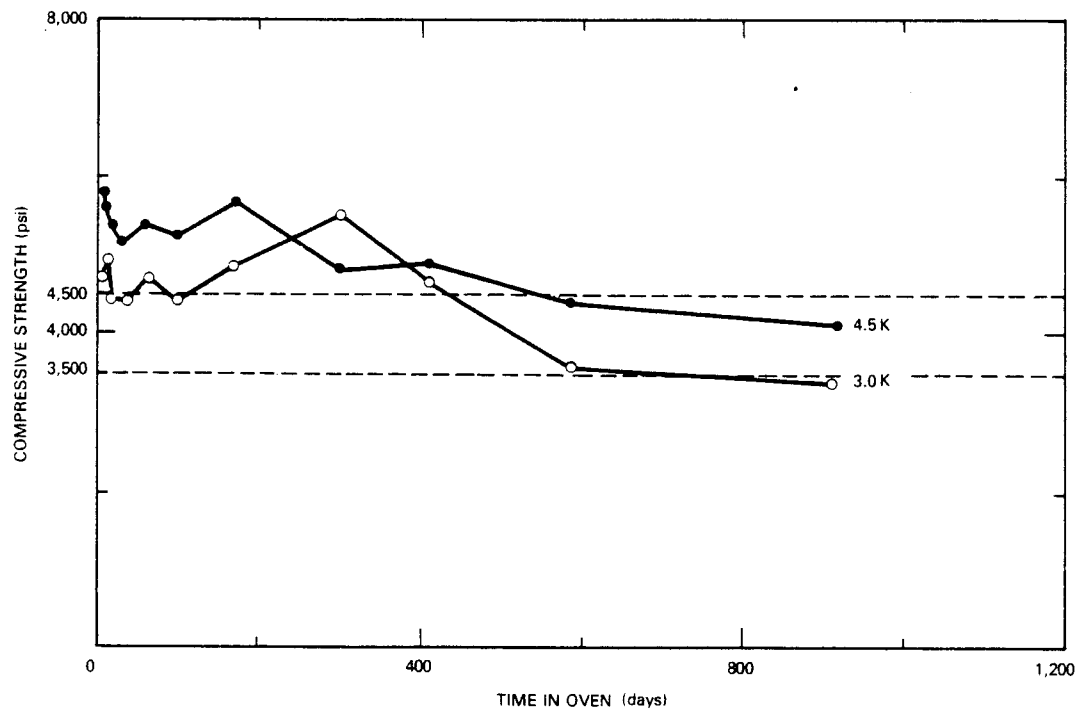
FIGURE 3-19. Compressive Strength of Cylinders at 450°F.

Strength decreased also with increasing temperature. The decrease was most pronounced at 450°F. The lowest strength values obtained were those after about 920 days at 450°F. It is interesting to note that even after over 900 days exposure at 450°F, the compressive strengths of both mixes barely decreased below the specification levels of 3,000 and 4,500 psi.

Reasons for the fluctuations in some of the test data, particularly the compressive strength data, are not clearly defined. Some variations in test results are probably due to testing at elevated temperatures. Usually, test results obtained at elevated temperatures show more scatter than those obtained at room temperature.

The greatest difficulty in analyzing the data probably results from batch-to-batch and in-batch variations in the original strength of the specimens. Tests were made on two cylinders from each batch of the 3K and 4.5K mixes after 879 days of moist curing to determine the room temperature strengths.

For the 3K mix, strengths varied from about 4,200 to 6,200 psi; for the 4.K mix, variations in strength were from about 5,100 psi to around 7,200 psi. In-batch variations ranged from about 200 psi to 1,300 psi. Undoubtedly, these variations in strength affected the test results. It is possible that these variations in strength are masking the indicated downward trend of compressive strength with increasing time of exposure to elevated temperatures. For example, if the 3-day strengths were determined on cylinders having compressive strength at the lower range of initial strengths, and the 900-day strengths were determined on cylinders having initially high compressive strengths, the effect of exposure time and temperature on the compressive strengths would be difficult to evaluate.

3.1.4 Splitting Tensile Strength

Splitting tensile strength information on moist cured cylinders of both mixes, over a period of 1,204 days, is shown in Figure 3-20 and Table B-3 in Appendix B. For both mixes, the splitting tensile strength increased rapidly up to about 190 days of age. Beyond that point,
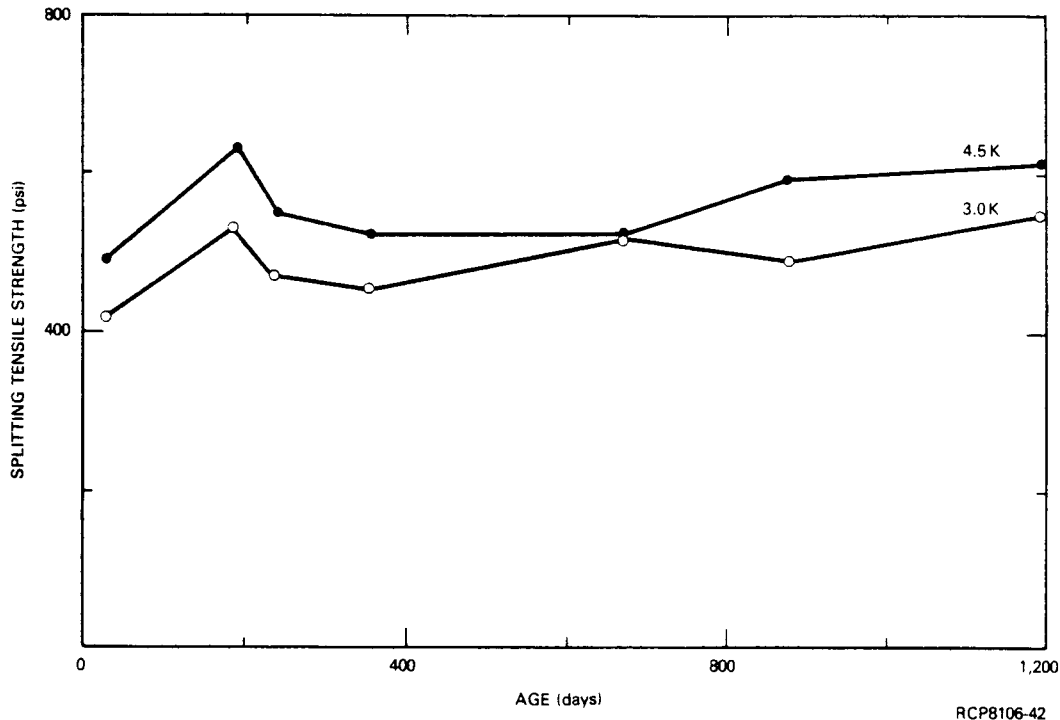
FIGURE 3-20. Splitting Tensile Strength
of Moist Cured Cylinders.

strength decreased to about 350 days, and either leveled off or increased
from that point on. The rapid increase followed by a decrease during the
first 400 days of moisture cure at room temperature is not easily
explained. Generally, it would be expected that the splitting tensile
strength would increase with age during the moist curing period. It is
possible that the in-batch and batch-to-batch variations of the test
cylinders affected the test results. Notwithstanding the irregularities
in the data, the 1,204 day strength values are higher by over 100 psi
than the values obtained at 30 days.

The effect of heat soaking the specimens at temperatures of 250°F,
350°F, and 450°F for over 900 days is shown in Figures 3-21, 3-22,
and 3-23. Although there were some crossovers in the data, generally the
tensile splitting strengths of the mixes decreased with increased time at
elevated temperatures. Generally, the splitting tensile strengths
decreased with temperature. The greatest decrease was obtained at the
450°F level. For the 3K mix, the splitting tensile strength was
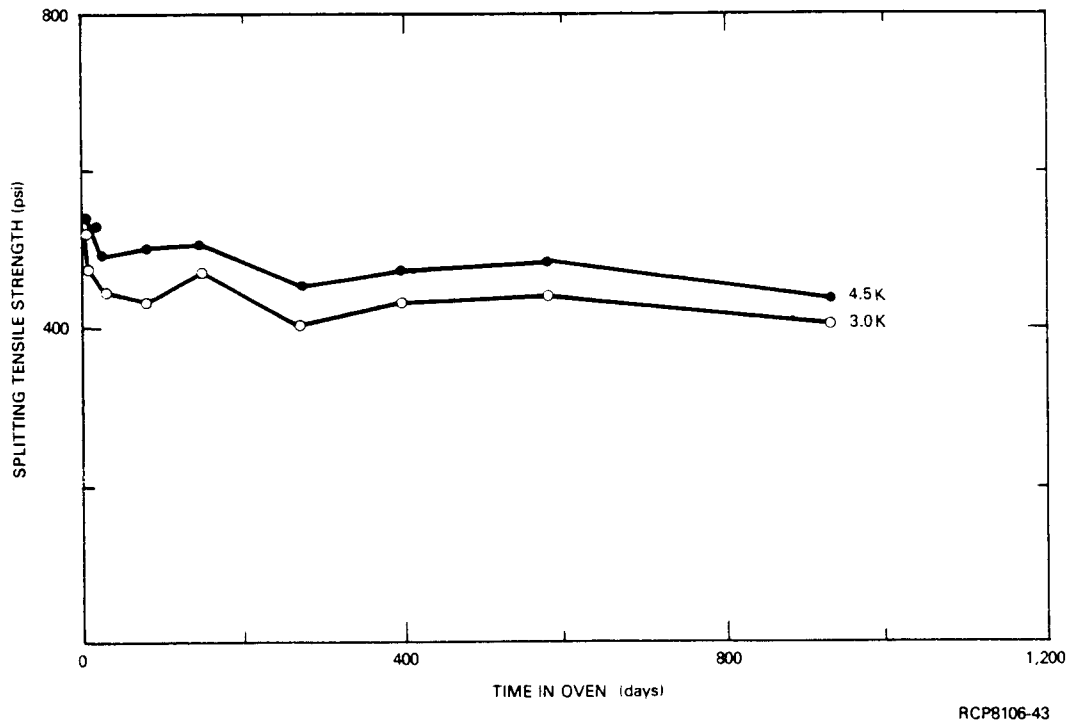
FIGURE 3-21. Splitting Tensile Strength of Cylinders at 250°F.
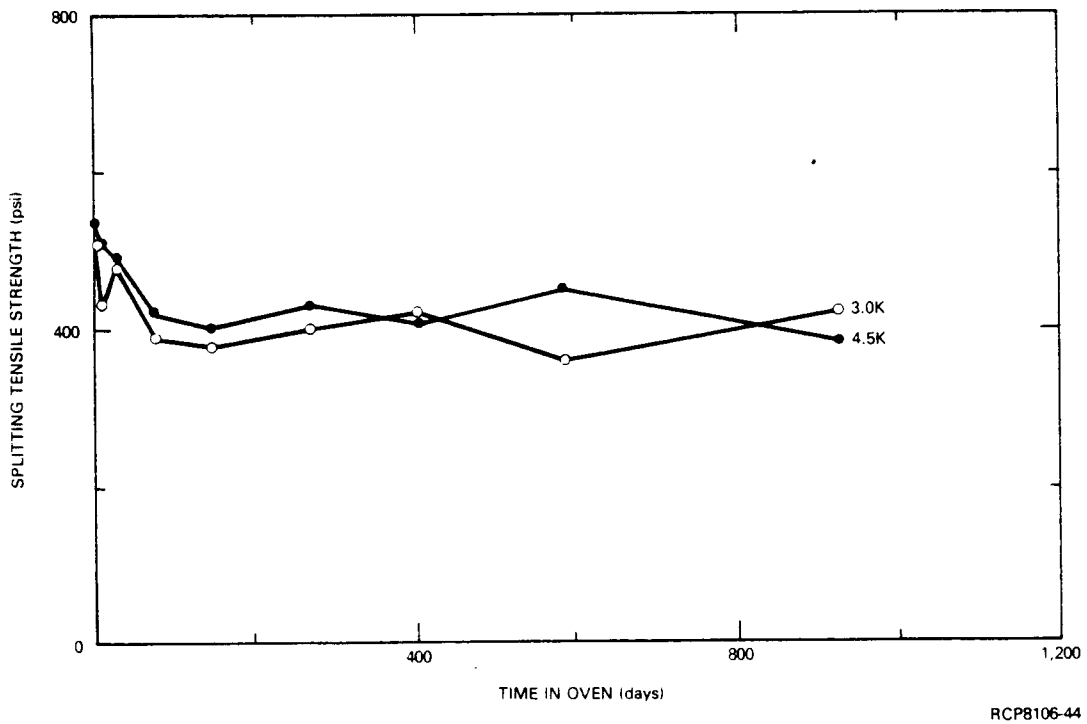
FIGURE 3-22. Splitting Tensile Strength of Cylinders at 350°F.
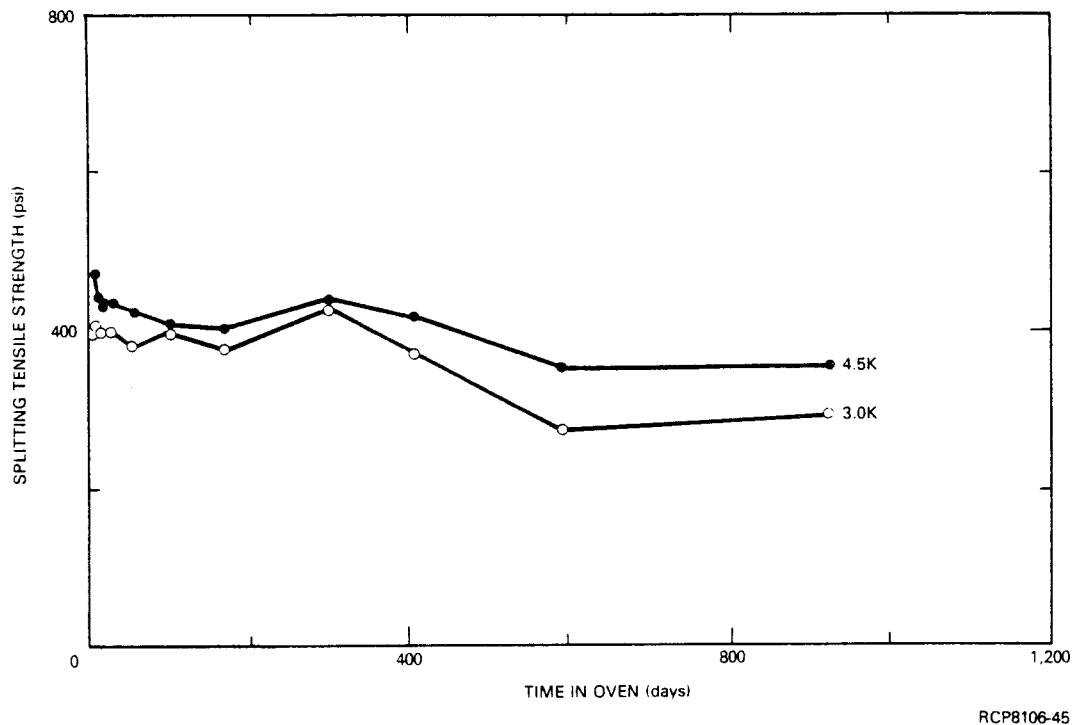
FIGURE 3-23. Splitting Tensile Strength of Cylinders at 450°F.

295 psi after 920 days in the oven. This compared with an initial value prior to heating of about 460 psi. Splitting tensile strength of the 4.5K mix dropped from an initial value of 540 psi 'to a final value of 352 psi.

3.1.5 Size Effects

In order to determine influence of specimen size effects on elevated temperature properties tests of Hanford concrete mixes, a test program was conducted to determine mechanical properties of 3- by 6-in. and 6- by 12-in. concrete cylinders and 3-in. cubes. Test specimens were 6- by 12-in. concrete cylinders cast at CTL/PCA in May 1975, and 3- by 6-in. cylinders and 3-in. cubes cored or cut from 6- by 12-in. cylinders.

After cutting, 3- by 6-in. cylinders and 3 in. cubes were cured at 50% RH until heated or tested. A list of weights and dimensions of test specimens is given in Tables D-1, D-2, and D-3 in Appendix D.

Moduli of elasticity, Poisson's ratios, and compressive strengths or splitting tensile strengths were determined from 6- by 12-in. or 3- by 6-in. cylinders. Elastic properties and compressive strengths only were determined from 3-in. concrete cubes. Tests were conducted at room temperature and on specimens heated at 250°F for 30 days. Test apparatus and procedures used for 3- by 6-in. cylinders and 3-in. cubes were similar to those used in testing 6- by 12-in. concrete cylinder properties. Results of properties tests are listed in Tables D-4 through D-8 and Appendix D.

A comparison of strengths and elastic properties determined that using different specimen geometries shows varying degrees of agreement. The room temperature moduli of elasticity was about 4.0 million psi for the 3- by 6-in. cylinders and 3-in. cubes. After 30 days of heating at 250°F, modulus of elasticity values for the 3- by 6-in. cylinders dropped to under 2.8 million psi, while the 3-in. cubes values increased to over 4.2 million psi. A similar trend was observed for Poisson's ratios for these same specimens.

The effect of specimen geometry on measurement of compressive strength is illustrated in Figure 3-24. Specimens strengths of three different geometries are compared at room temperature and after 30 days at 250°F.

Neville has shown that, for cast specimens at room temperature, smaller specimen geometries yield higher measured strengths.[32] This was only partially true for cored specimens at 70° and 250°F in this study.

Strengths of 3-in. cube specimens were larger than those of 6- by 12-in. cylinders at room and elevated temperatures. However, 3- by 6-in. cylinders had strengths lower than cubes and larger cylinders at both test temperatures. Cylindrical specimens suffered a loss in strength on heating. However, cube specimens showed an increase in strength on heating from 70° to 250°F.
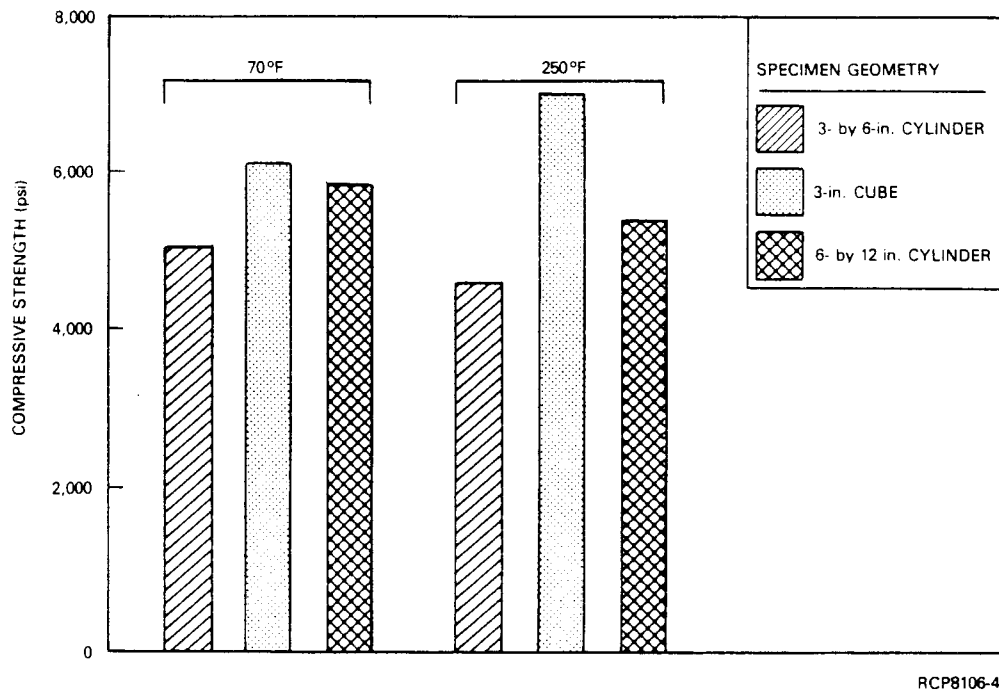
FIGURE 3-24. Comparison of Compressive Strength Versus Specimen Geometry for Concrete at Room Temperature and After 30 Days at 250°F.

Overall, the cube specimens indicated trends in strength and elastic properties contrary to both sets of cylindrical specimens. Also, within a given series, there appeared to be larger property variations measured between cube specimens than between cylinders. No simple explanation for these differing results is apparent.

3.2 CREEP BEHAVIOR

The six 6- by 12-in. cylinders used in elevated temperature creep tests were initially heated during November 1978. Measurements of length changes were taken at different times during the following 21 months. On September 11, 1980, furnaces on all three creep frames were turned off. On the following day, after specimens had cooled to room temperature, loads were removed and final length readings taken.

Strain readings are given in tabular form in Table E-1 in Appendix E, and plotted graphically in Figures 3-25, 3-26, and 3-27. Individual strain measurements are shown as discrete points in the graphs. Average strains of cylinders, subjected to the same tests conditions, have been plotted as a solid line.

Influence of test temperature on creep of concrete cylinders can be seen in Figures 3-25 and 3-27. Comparison of results of specimens loaded to 1,500 psi shows that creep of concrete at 350°F was approximately twice as great as concrete heated to only 250°F over equivalent intervals of time.

Influence of static test load on creep can be seen by comparing results shown in Figures 3-26 and 3-27. Test temperature for both sets of cylinders was 350°F. However, specimens in Frame No. 2 were loaded to 500 psi, while in Frame No. 3, the test load was 1,500 psi. Creep of specimens at 1,500 psi was approximately a factor of 2 greater than that of specimens loaded to only 500 psi.
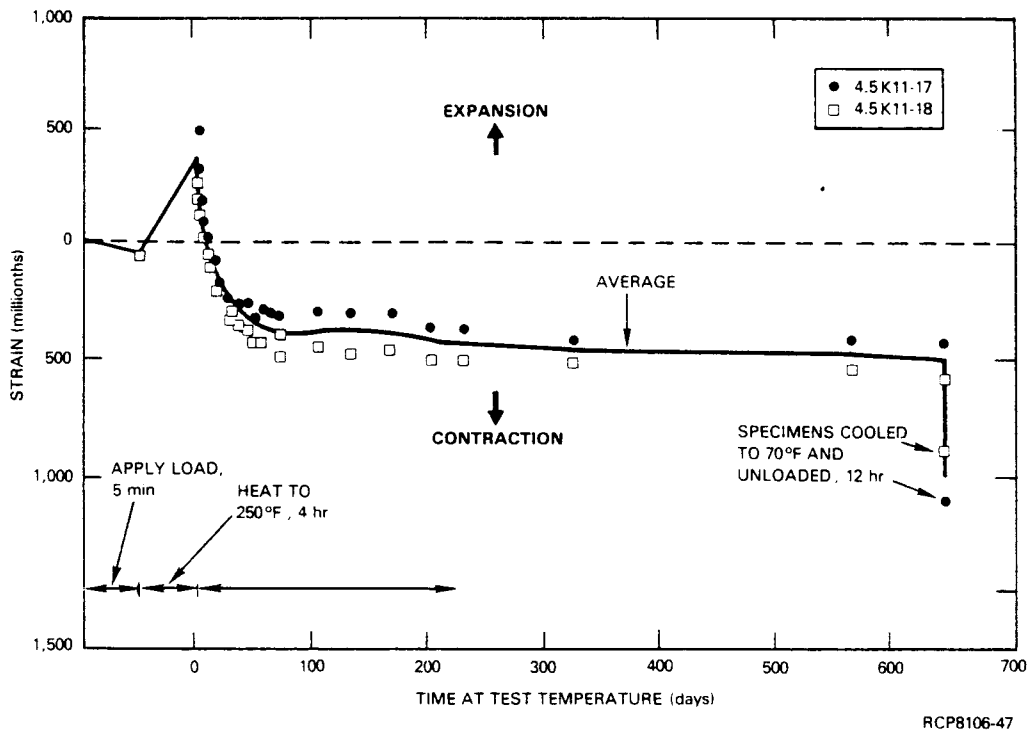
FIGURE 3-25. Deformation of Specimens on Frame No. 1 at 1,500 psi and 250°F.
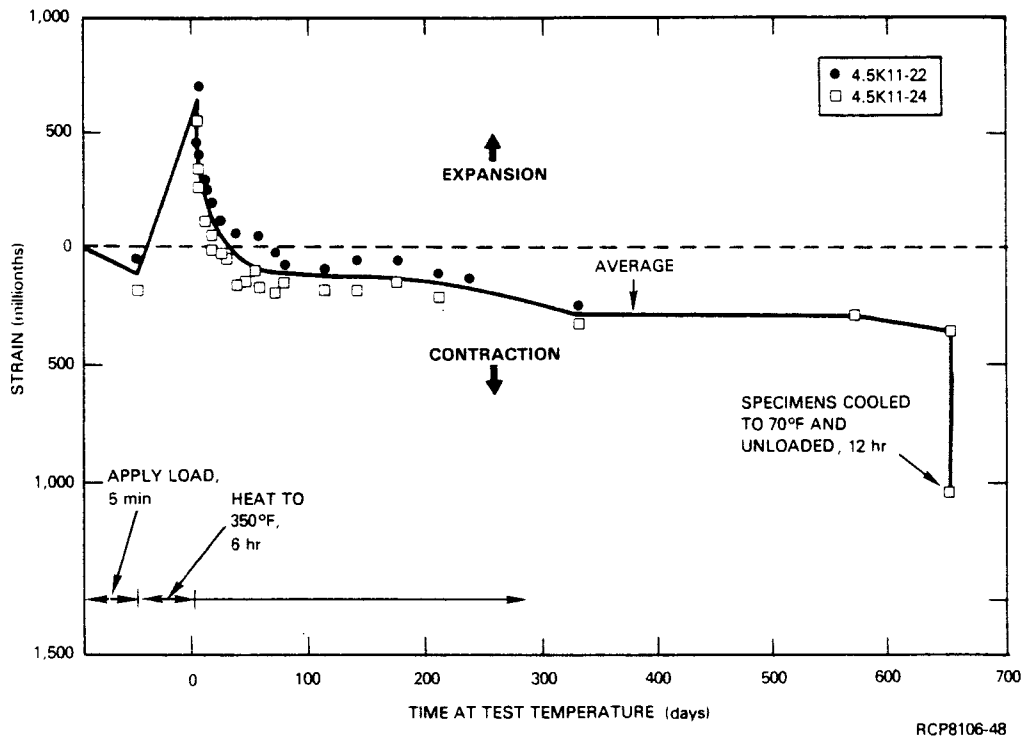
FIGURE 3-26. Deformation of Specimens on Frame No. 2 at 500 psi and 350°F.
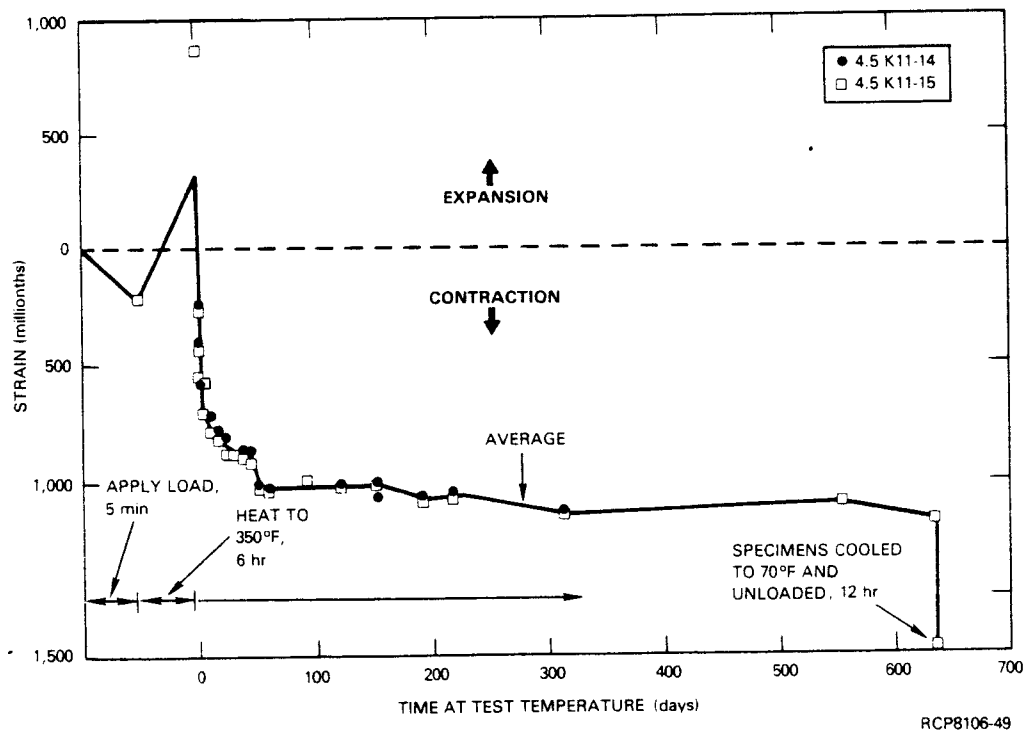
FIGURE 3-27. Deformation of Specimens on Frame No. 3 at 1,500 psi and 350°F.

Restraining effect of static load on thermal expansion of concrete can also be seen in Figures 3-25, 3-26 and 3-27. Since specimens in Frame Nos. 2 and 3 were heated to the same test temperature, free thermal expansion of both sets of cylinders should have been similar. Using an average value of coefficient of thermal expansion determined for Hanford concretes subject to only a single heating (see Table F-2 in Appendix F), free expansion of cylinders heated to 250° and 350°F should have been of the order of 550 and 850 millionths, respectively. Under a load of 1,500 psi, specimens heated to 250°F expanded an average of 415 millionths. At 500 psi, specimens heated to 350°F expanded 740 millionths. For specimens at 1,500 psi, heating at 350°F resulted in an average expension of only 530 millionths.

The development of creep strains in specimens at each test condition are compared in Figures 3-28. Here the effects of elastic strain and thermal expansion have been removed, and only strains measured after one day of heating are plotted versus $\log_{10}$ (time).
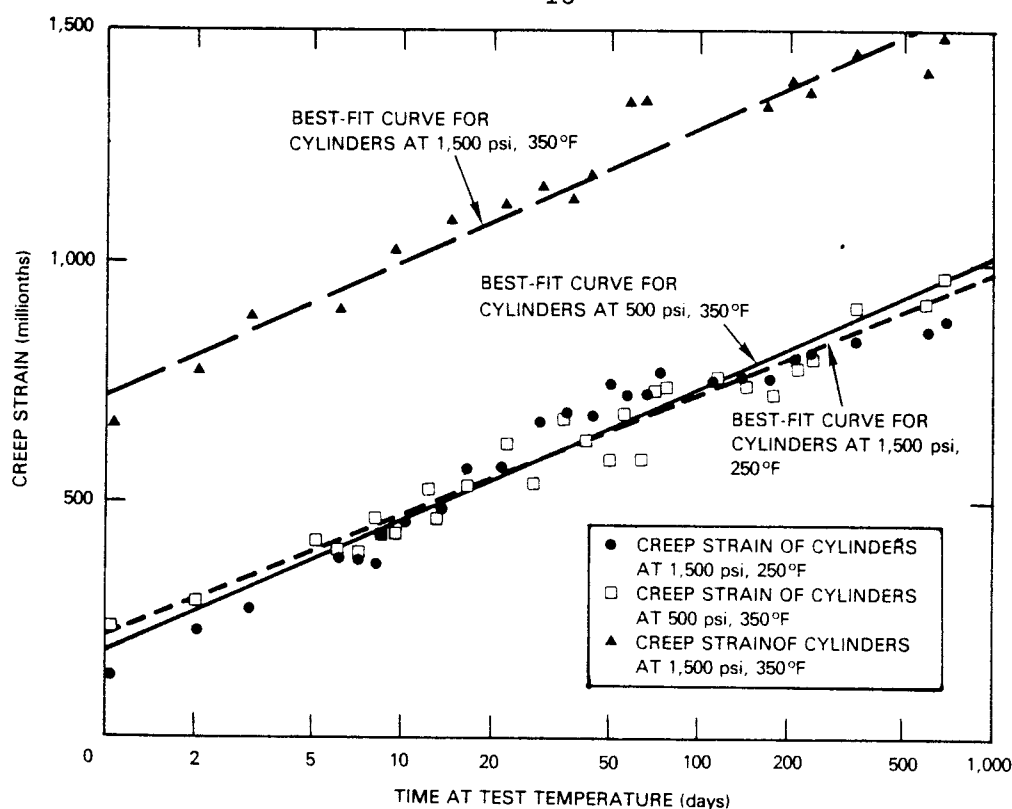
FIGURE 3-28. Best-Fit Curve of Creep Strain Data to Logarithmic Equation, $\varepsilon_{CR} = K \log_{10} (t) + \varepsilon_0$.

A linear regression analysis showed that creep data were adequately modeled by an expression of the form:

$$\varepsilon_{CR} = K \log_{10}(t) + \varepsilon_0$$

where

ε_{CR} is creep strain, in millionths,
t is time at test temperature, in days.

Calculated values for K and ε_0 are given in Table 3-1. Magnitude of the constant, ε_0, varied with load and temperature. However, values for the coefficient K did not appear to be strongly dependent on test conditions.

These trends are in general agreement with creep behavior reported in the literature.[32,33]

TABLE 3-1. Calculated Values of K, ε_0, and R.

Test Conditions	K^{*}	ε_0^{*}	R^{**}
1,500 psi/250°F	276.1	182.1	0.967
500 psi/350°F	255.6	214.5	0.979
1,500 psi/350°F	286.9	718.6	0.976

*Calculated from best-fit of Equation:

$\varepsilon_{CR} = K \log_{10}(t) + \varepsilon_0$ to creep data.

**R, correlation coefficient, a measure of the closeness of model expression fit to data. R may vary from ±1. If R = 0, there is no correlation; if R = ±1, there is a perfect fit.

3.3 THERMAL EXPANSION

Concrete cylinders were cast at CTL/PCA in 1975 and 1977 using materials and mix designs simialar to those used in construction of Hanford factilties. Thermal expansion of specimens fabricated from these cylinders are described below.

Thermal expansion of specimens fabricated from concrete cast at CTL/PCA in May 1975 is shown as a function of temperature in Figure 3-29. Thermal expansion for each of the four specimens increased approximately linearly with temperature from 73° to $1,000^\circ F$.

At about $1,000^\circ F$, slopes of the expansion versus temperature curves increased rapidly for all specimens. The most probable explanation for this change is volumetric expansion of aggregate resulting from the inversion of quartz from the alpha to beta form.[1,9] Temperature for this transition is usually reported as $1,063^\circ F$. The relatively large increases in expansion near this temperature indicate the presence of quartz in significant quantities in the aggregate.

No increase in thermal strain was observed for three of the four specimens from $1,250^\circ F$ to maximum test temperature. This plateau in the expansion versus temperature curve has been reported by other investigators for siliceous aggregates.[2,9]

Thermal strain at maximum temperature ranged from a low of about 4,000 millionths to a high of approximately 6,700 millionths for these specimens. Expansion of concrete from specimens 3K8-7 and 3K9-18, was larger on average than that of specimens 4.5K8-19 and 4.5K9-10. Average thermal strain for 4.5K-specimens was approximately 840 millionths at $400^\circ F$, and 5,180 millionths at $1,400^\circ F$.

Thermal expansion of specimens, fabricated from concrete and cast at CTL/PCA in September 1977, is plotted against temperature in Figure 3-30. Concrete thermal expansion curves followed trends observed in expansion of concrete cast in 1975. Thermal expansion of concrete cast in 1977 was, on average, slightly greater than concrete cast in 1975 in the temperature range from 73° to $400^\circ F$. Average thermal strain at $400^\circ F$ was approximately 1,040 millionths. Between 400° and $1,000^\circ F$, thermal strains for concrete of both ages were approximately equal.
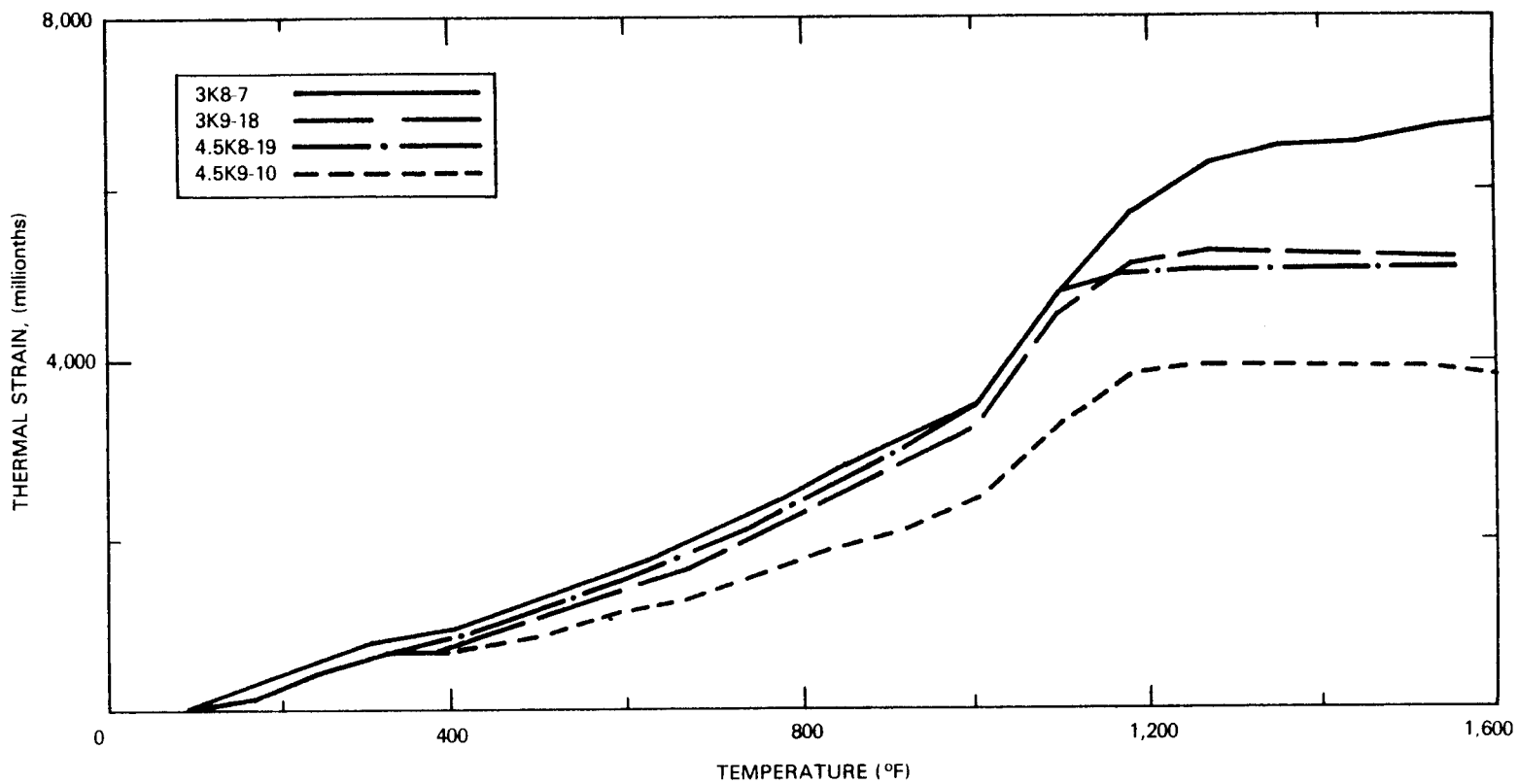
FIGURE 3-29. Thermal Expansion of Concrete Cast in 1975 as a Function
of Temperature.
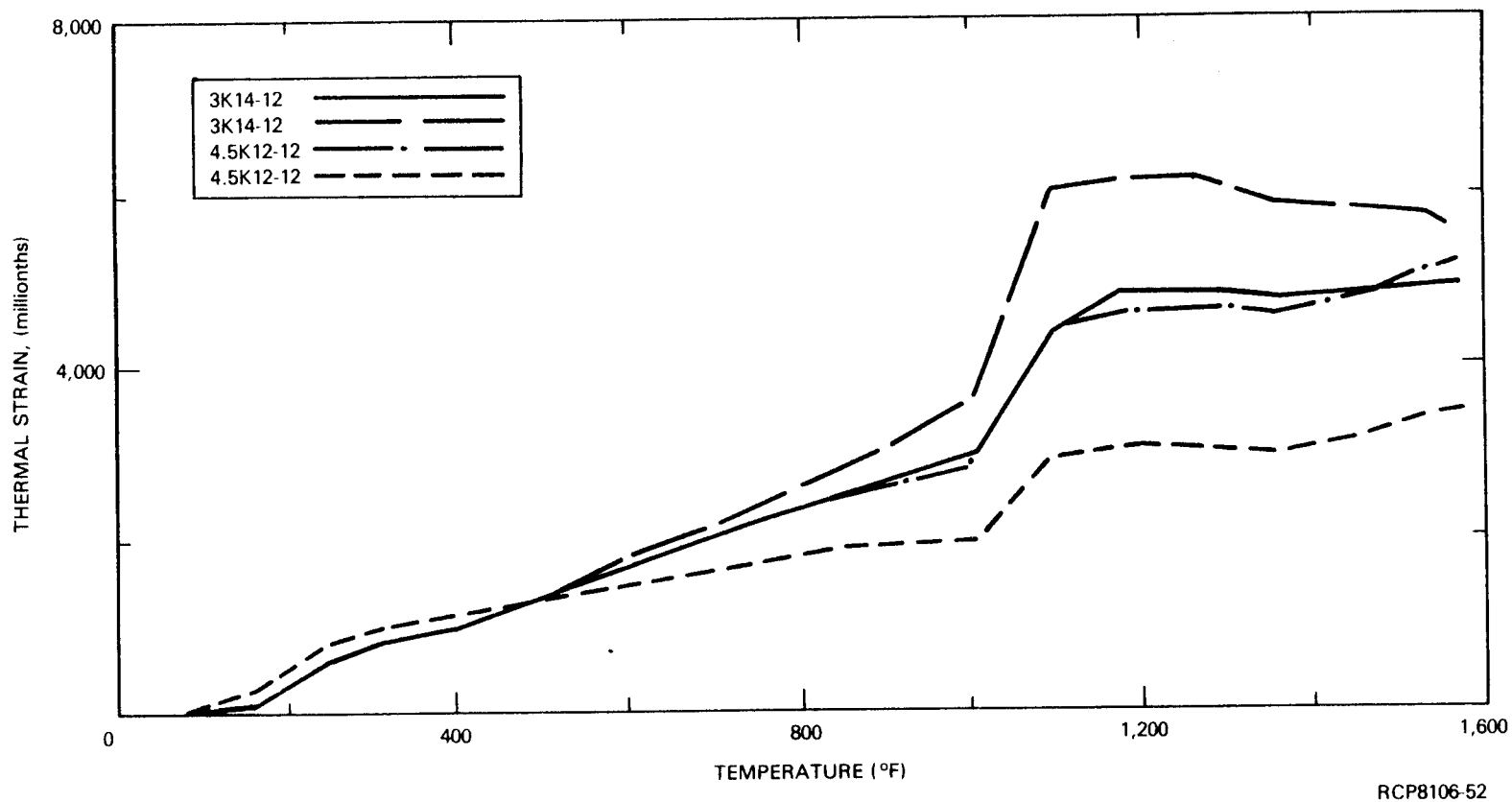
RCP8106-51

FIGURE 3-30. Thermal Expansion of Concrete Cast in 1977 as a Function of Temperature.

RCP8106-52

At 1,000°F, the slope of expansion curves of concrete specimens cast in 1977 increased more rapidly than was observed with older specimens. The flattened portion of the expansion curve seen with older specimens above 1,170°F is also present in plots of test results of the younger concrete. However, for younger specimens this post-quartz inversion plateau appears to begin at a temperature of approximately 1,080°F. This is lower than observed for older specimens. In Test No. 6, the specimen contracted at temperatures above 1,260°F.

Average thermal strain of younger specimens at 1,400°F was approximately 4,600 millionths. As with older concrete, average strains of 3K concrete cast in 1977 were greater than 4.5K concrete over most of the test temperature range.

Thermal strain behavior is described completely only by curves such as those in Figures 3-29 and 3-30. However, average coefficients of expansion are useful for calculations and comparison purposes. Average coefficients, $\bar{\alpha}$, of test specimens calculated from a linear regression analysis of thermal strains in the range from 73° to 1,000°F are listed in Table F-2 in Appendix F.

The mean value of $\bar{\alpha}$ for the eight test specimens was 3.29 X 10^{-6}/°F. This value is somewhat lower than that found in normal structural concretes, which are usually in the range from 5 to 10 X 10^{-6}/°F.

3.4 THERMAL CYCLING RESPONSE

Results of tests to determine the influence of cyclically varying elevated temperatures on Hanford concrete mechanical properties and thermal expansion behavior are described below.

3.4.1 Thermal Cycling Effects on Mechanical Properties

Tests were conducted to determine the compressive strengths, moduli of elasticity, and Poisson's ratios of unheated Hanford concrete cylinders and specimens subjected to 1, 3, 5, 8, 12 or 13, and 17 or 18 thermal cycles. Temperatures varied from ambient to 350°F during cycling. The length of each thermal cycle was 14 days for one test

series and 28 days for the second test program. All tests were conducted at ambient temperature. Results from strength and elastic properties tests are given in tabular form in Tables G-1 and G-2 in Appendix G.

3.4.1.1 Compressive Strength. The affect of heat cycling on compressive strength of concrete, subjected to 28 day thermal cycles, is shown in Figure 3-31. Strengths decreased linearly with number of exposures for the first 5 thermal cycles. Compressive strengths of both Series 3K10 and 4.5K10 specimens subjected to 5 heat cycles were about 15% lower than for unheated concrete. Additional thermal cycling produced relatively smaller decreases in strength. The largest strength loss measured was 20% for Series 3K10 specimens subjected to 18 temperature cycles.

Also plotted in Figure 3-31 are test results from the 14-day cycle test program. Comparison of data from both heat cycle programs shows that strength losses were more immediate for specimens subjected to the longer thermal cycles. However, it should be noted that total time of exposure to maximum elevated temperatures per cycle is more than twice as long (24 versus 10 days) for the 28-day temperature cycle regime as for the 14-day cycle program. When data from both test series are compared on the basis of time of exposure to 350°F, as in Figure 3-32, differences in strength-loss trends are reduced.

3.4.1.2 Modulus of Elasticity. Influence of thermal cycling on the modulus of elasticity of Hanford concrete cylinders is shown in Figure 3-33. The decrease in magnitude of elastic moduli of cylinders subjected to only one 28-day temperature cycle amounted to over 40% of the value of unheated specimens. Additional thermal cycles produced a gradual additional loss in stiffness of both Series 3K10 and 4.5K10 specimens. The greatest loss, 50% in moduli values, was measured with specimens from Series 3K10 subjected to 18 twenty-eight day thermal cycles.

Comparison of these data with results of moduli tests on 14-day cycled cylinders, also plotted in Figure 3-34, shows more severe losses for the longer cycle tests. Moreover, these differences remain large
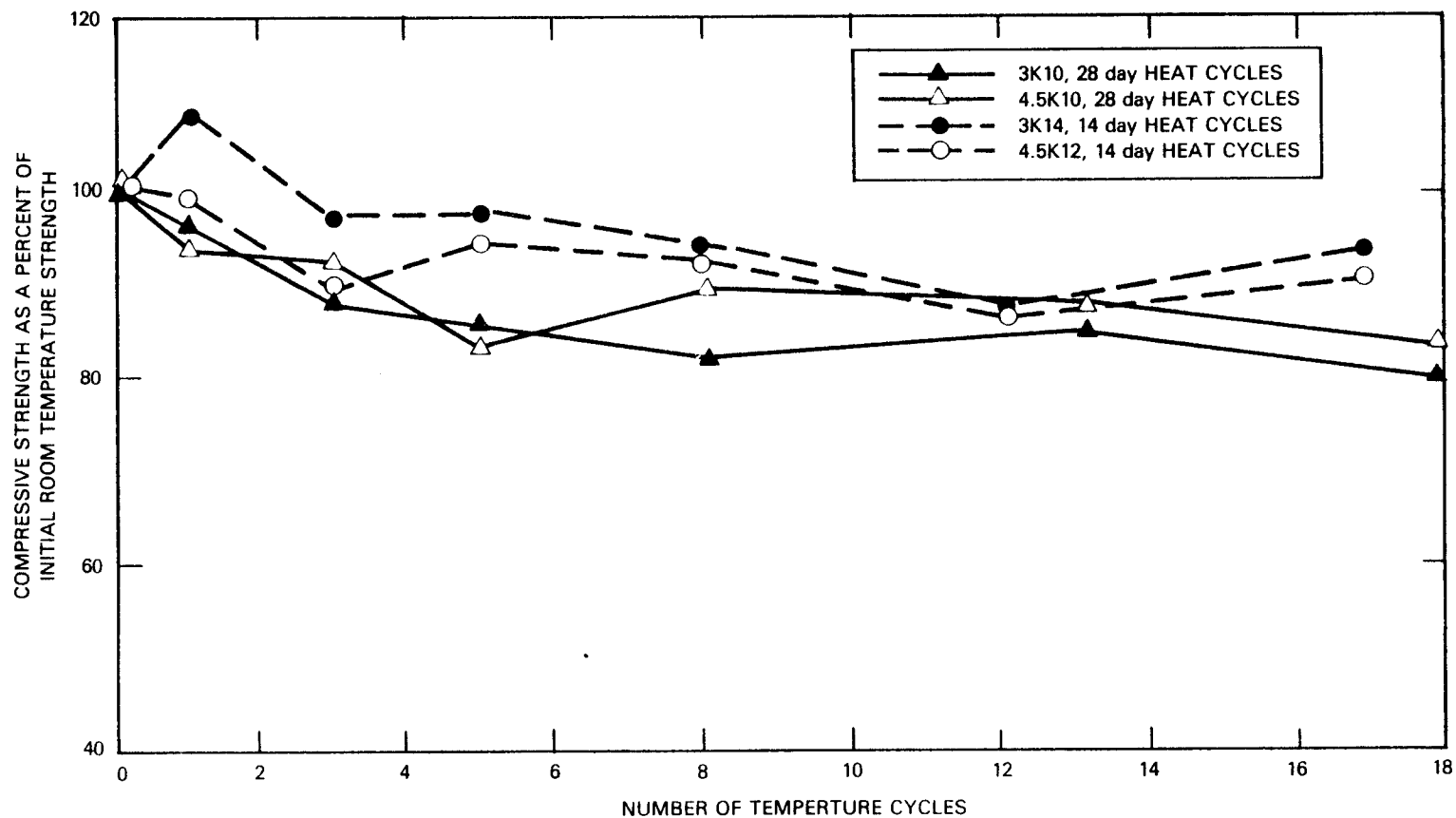
FIGURE 3-31. Variation of the Concrete's Compressive Strength
With the Number of Thermal Cycles.
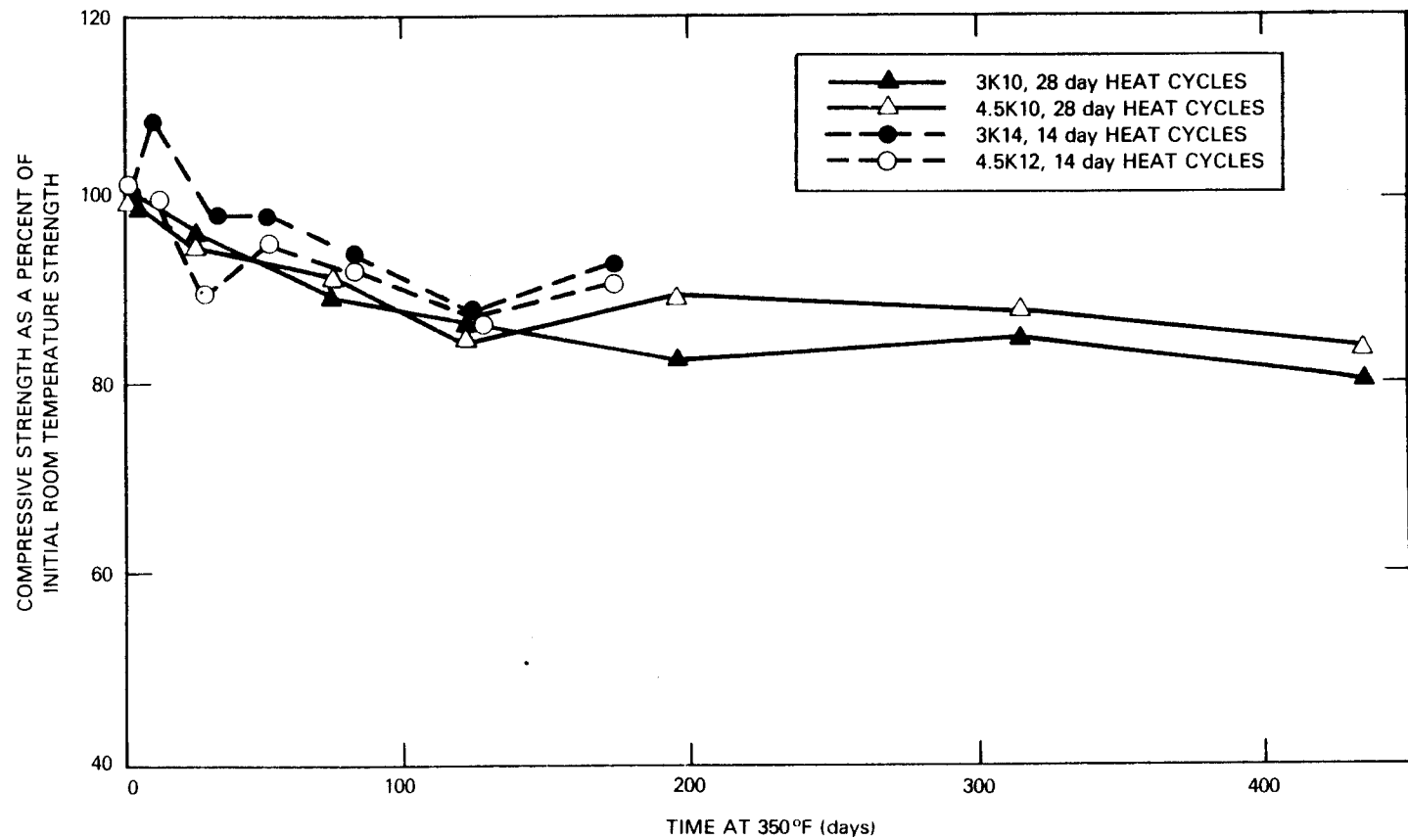
FIGURE 3-32. Variation of the Concrete's Compressive Strength With Length of Exposure to the Maximum Test Temperature.
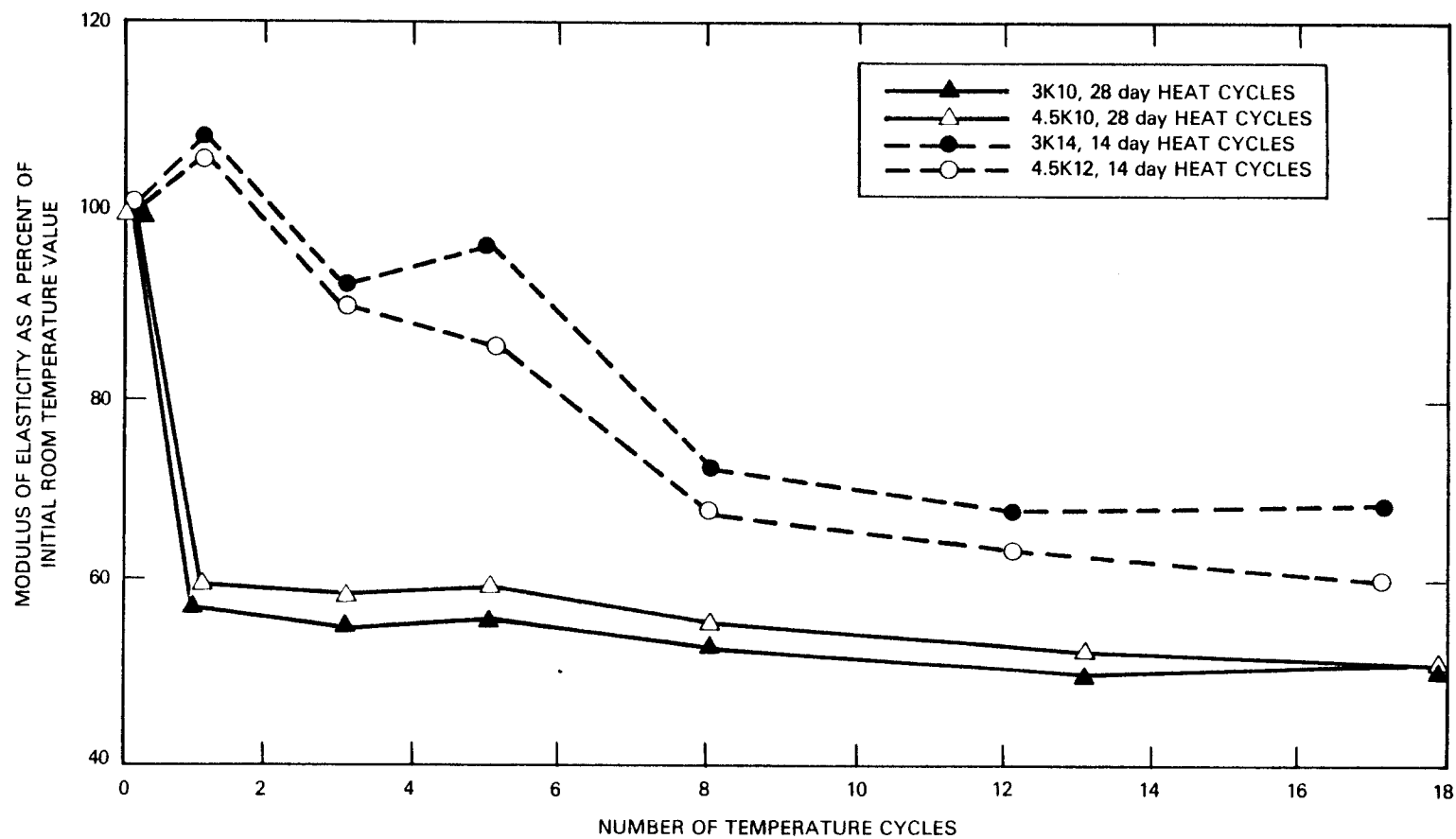
RCP8106-55

FIGURE 3-33. Variation of the Concrete's Modulus of Elasticity
With the Number of Thermal Cycles.

when results from both testing programs are plotted versus time of exposure to the 350°F maximum test temperature. This trend, shown in Figure 3-34, is contrary to that observed for compressive strength data.

Due to equipment malfunction at time of test, data for calculating modulus of elasticity and Poisson's ratio were not obtained for 3 cylinders subjected to 18 twenty-eight day thermal cycles.

3.4.1.3 Poisson's Ratio. The effect of temperature cycling on Poisson's ratio is shown in Figure 3-35. Measured values after one 28-day thermal cycle were approximately 35% lower than for unheated cylinders. Continued thermal cycling produced some increase from this minumum. For example, after 5 thermal cycles, Poisson's ratio of specimens averaged 83% of initial ambient temperature values.

Also shown in Figure 3-35 are values of Poisson's ratio obtained from the 14-day temperature cycle program. Data from this test series follow trends similar to those of the 28-day cycle tests. However, the minimum occurs later, after 3 cycles, and overall reductions are not as great as those observed in the current program.

In Figure 3-36, data from both test programs are plotted as a function of length of exposure to the maximum test temperature. Data from both cycle tests correlate fairly well. However, loss trends are still less severe for the shorter heat cycle program.

3.4.2 Thermal Cycling Effects on Thermal Expansion

Eight dilatometer specimens, fabricated from concrete cast at CTL/PCA in 1975 and 1977, were used to study the influence of cyclically varying temperatures on concrete thermal expansion behavior. Specimens were repeatedly heated and cooled between room temperature and 450°F at a rate of about 10°F/min. Specimen temperatures and thermally induced strains were continuously measured for a maximum of 5 thermal cycles.

Thermal expansions of specimens, made from concrete cylinders cast in May 1975, are shown as a function of temperature in Figures 3-37 through 3-40. In each case, the thermal strain/temperature relationship
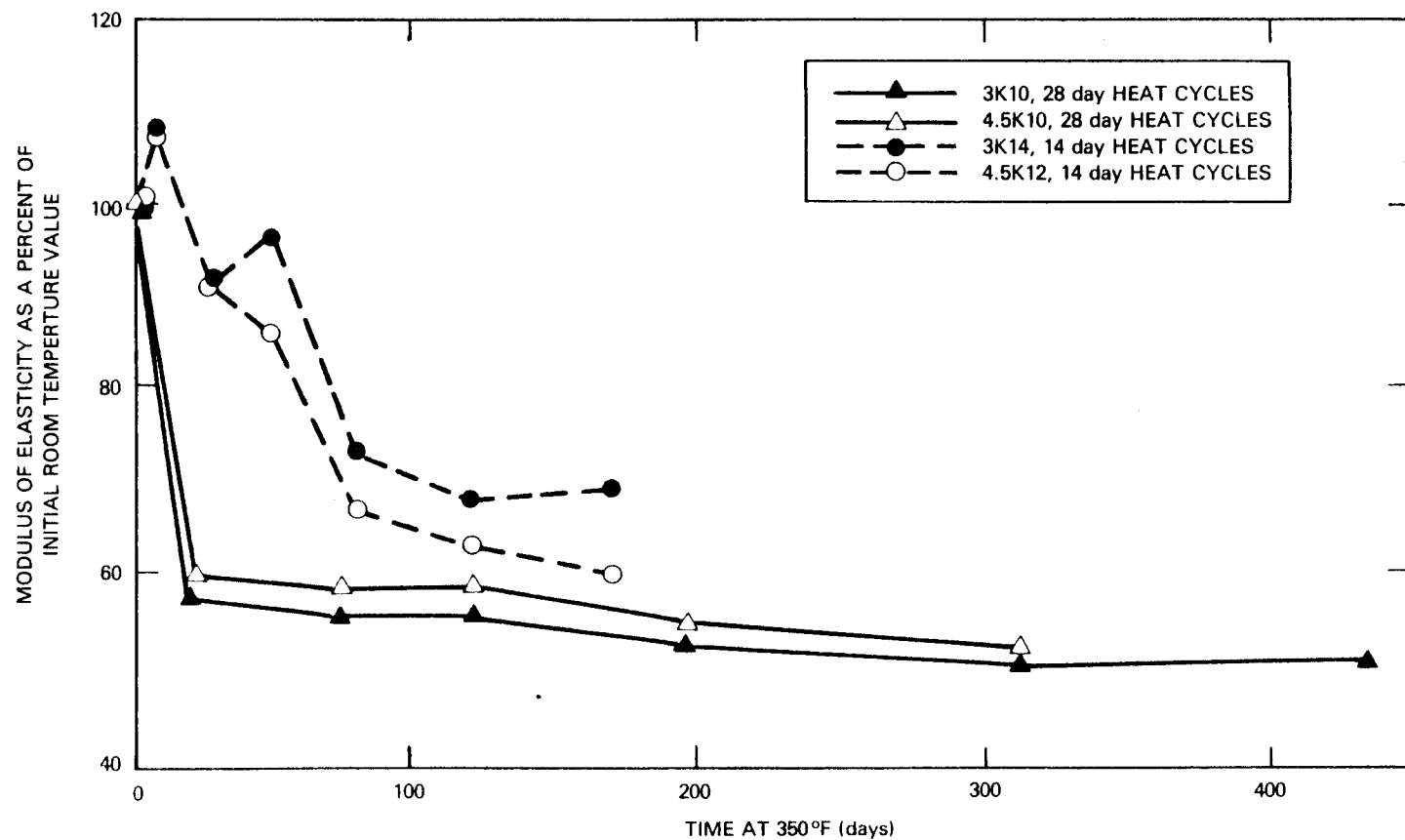
FIGURE 3-34. Variation of the Concrete's Modulus of Elasticity
With the Length of Exposure to the Maximum Test Temperature.
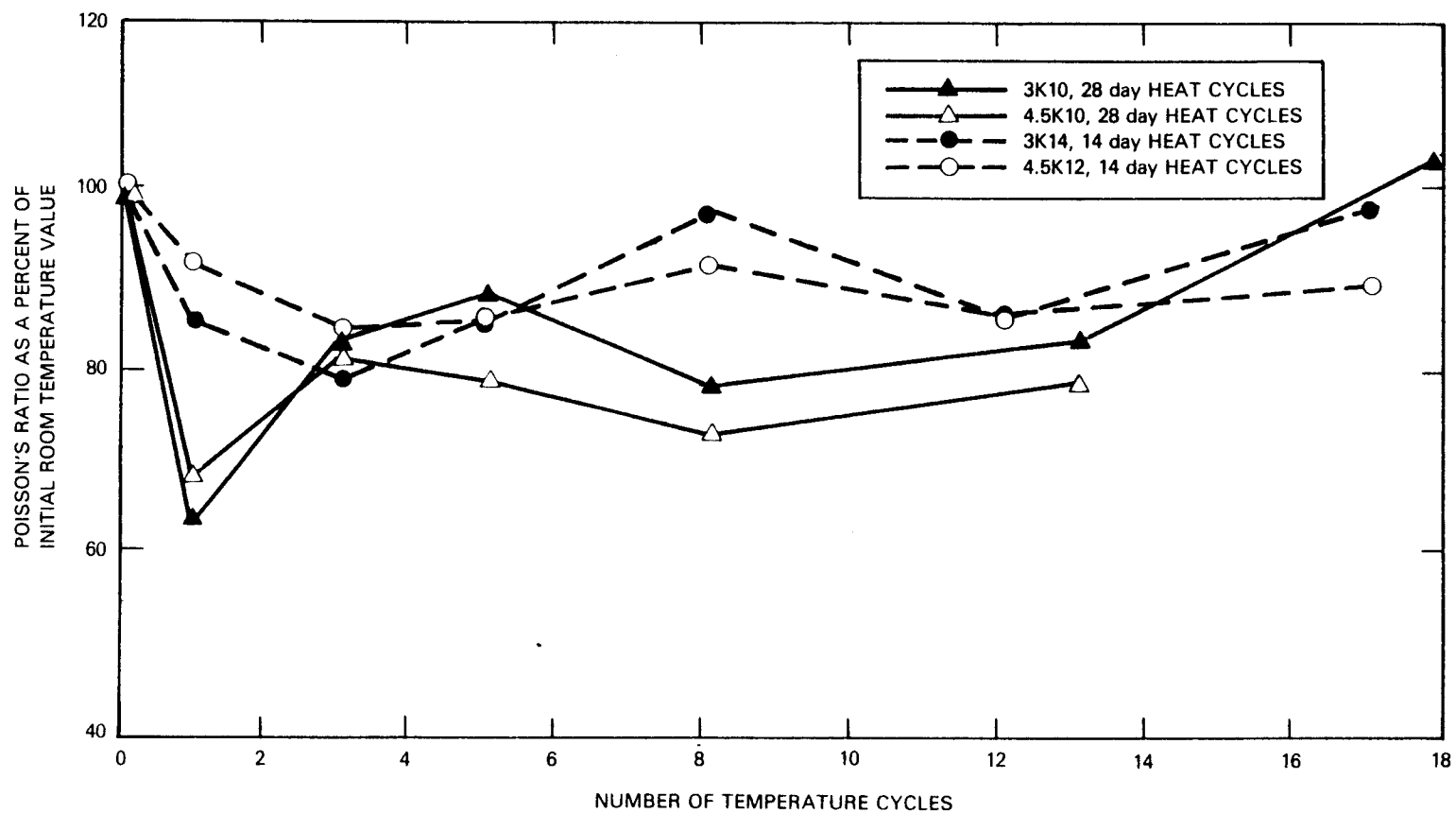
FIGURE 3-35. Variation of Poisson's Ratio With the Number of Thermal Cycles.
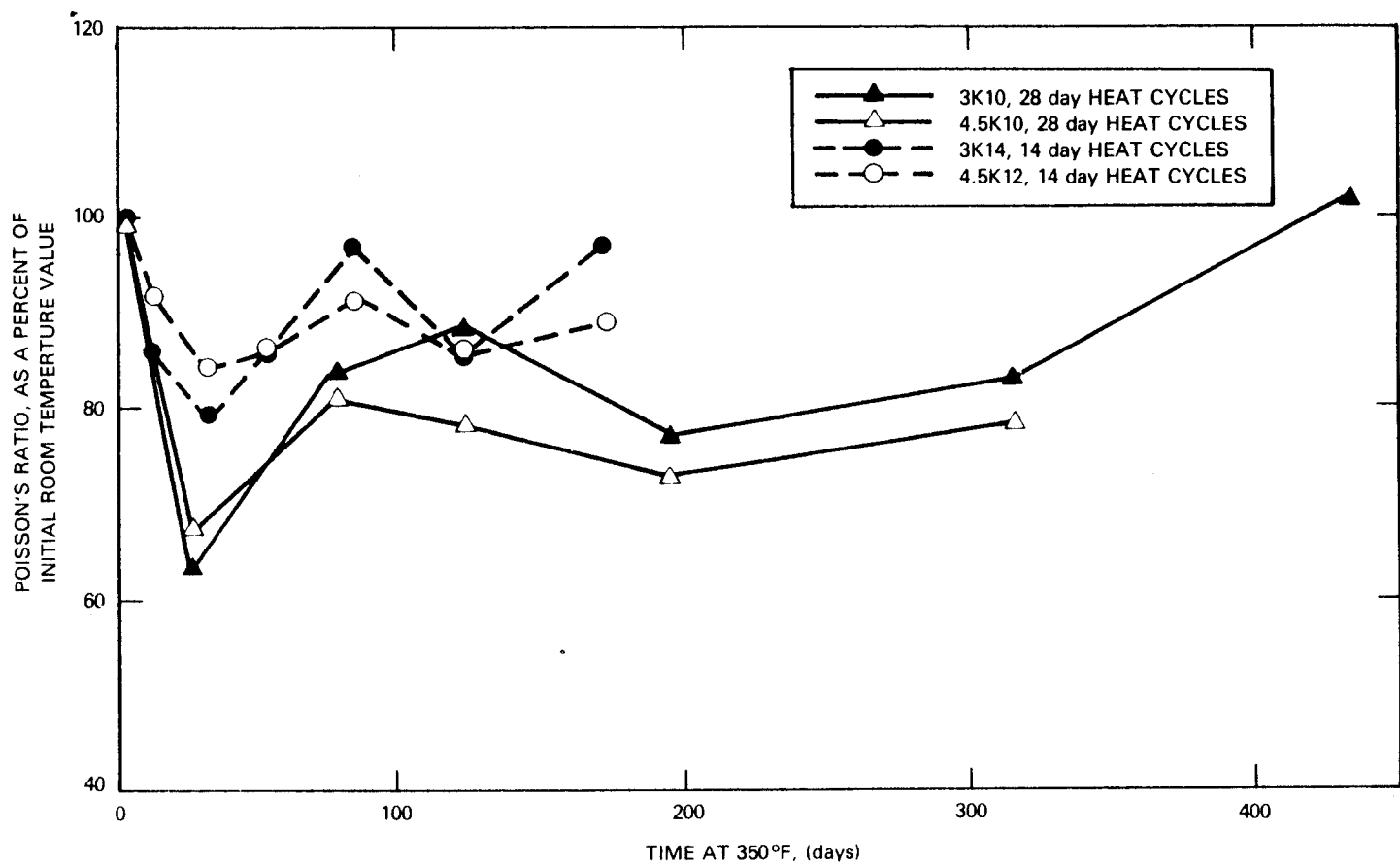
FIGURE 3-36. Variation of Poisson's Ratio With the Length of
Exposure to the Maximum Test Temperature.
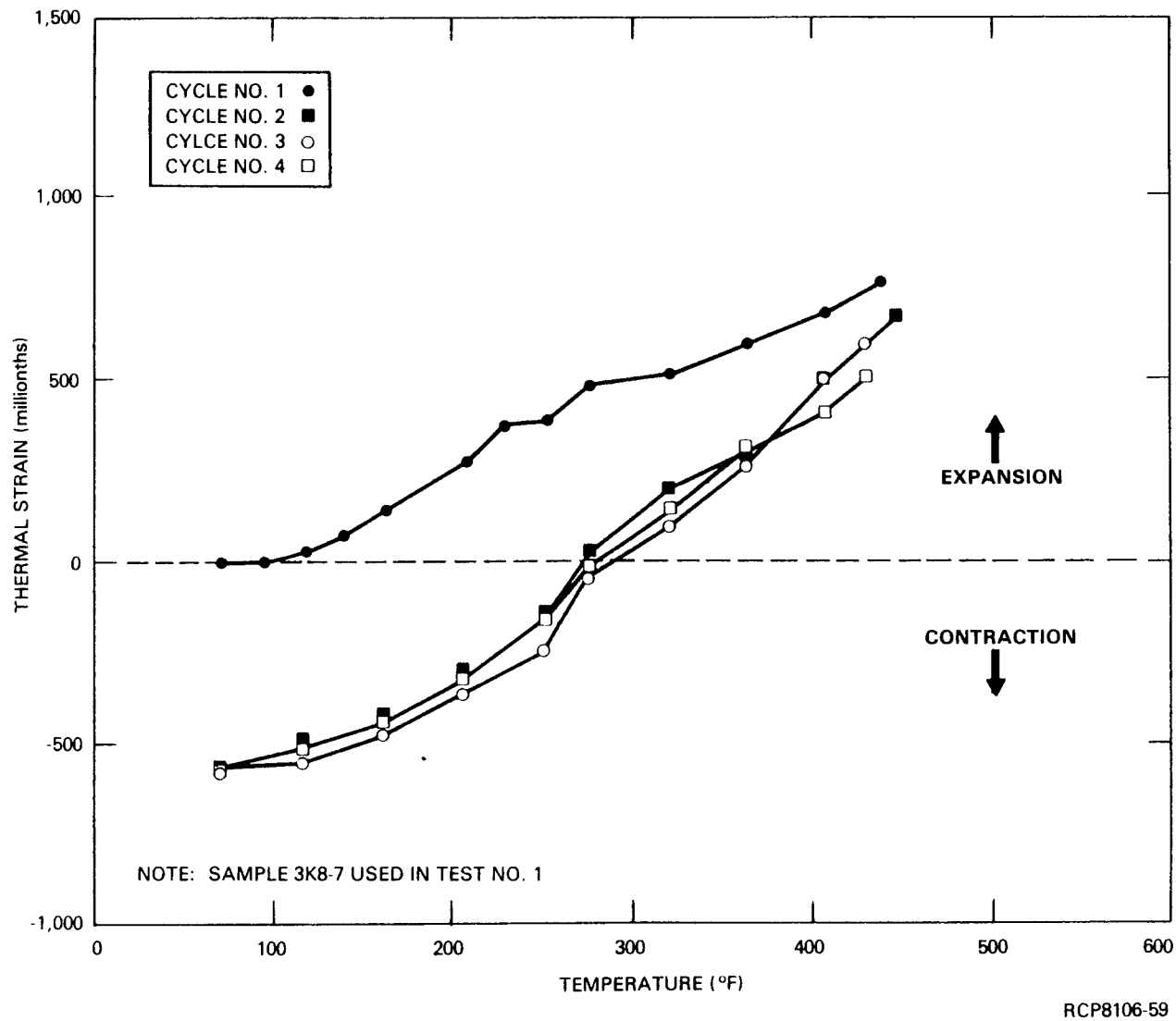
FIGURE 3-37. Cyclic Thermal Strain Versus Temperature Curves for Test No. 1.
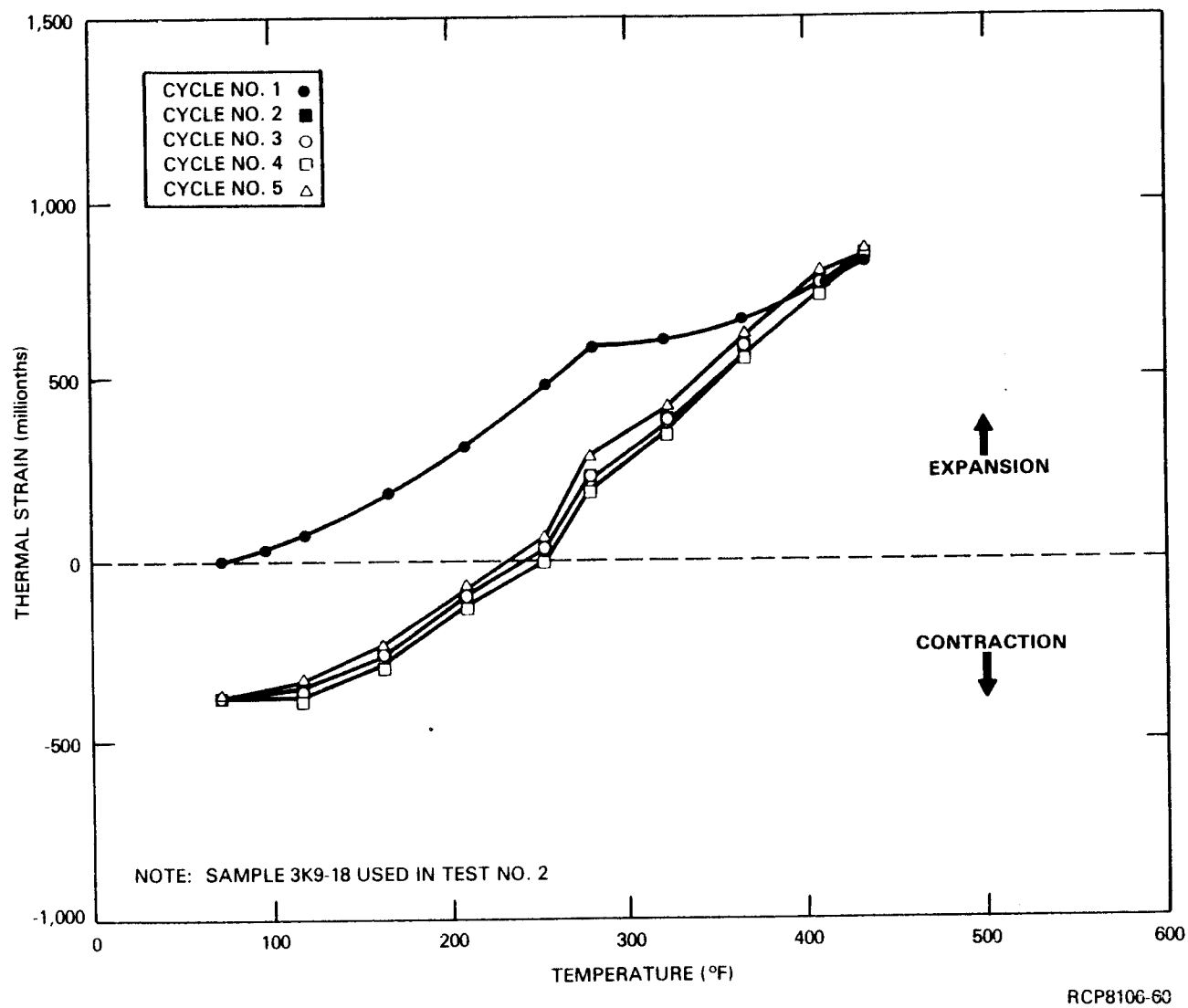
FIGURE 3-38. Cyclic Thermal Strain Versus Temperature Curves
for Test No. 2.
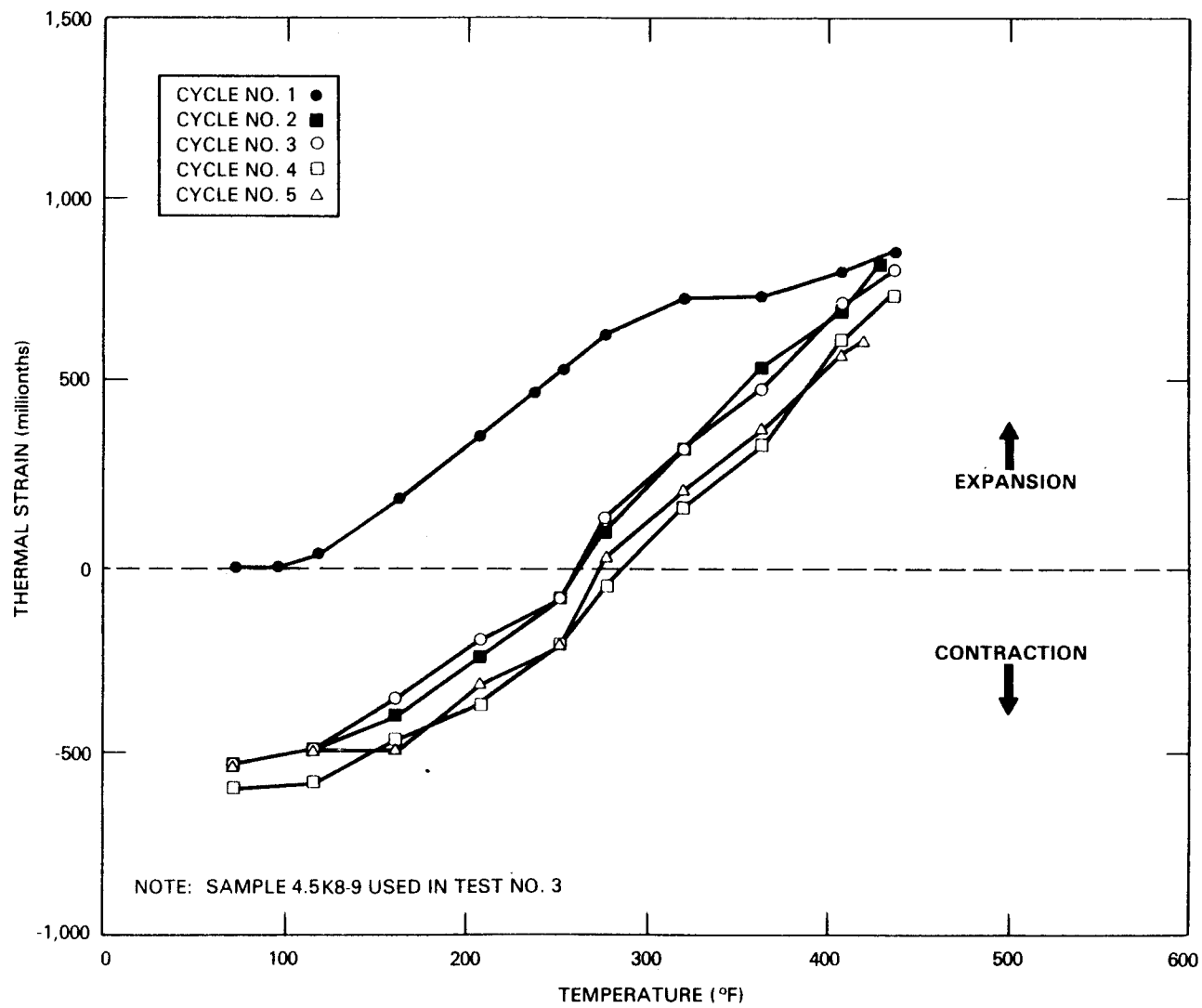
FIGURE 3-39. Cyclic Thermal Strain Versus Temperature Curves for Test No. 3.
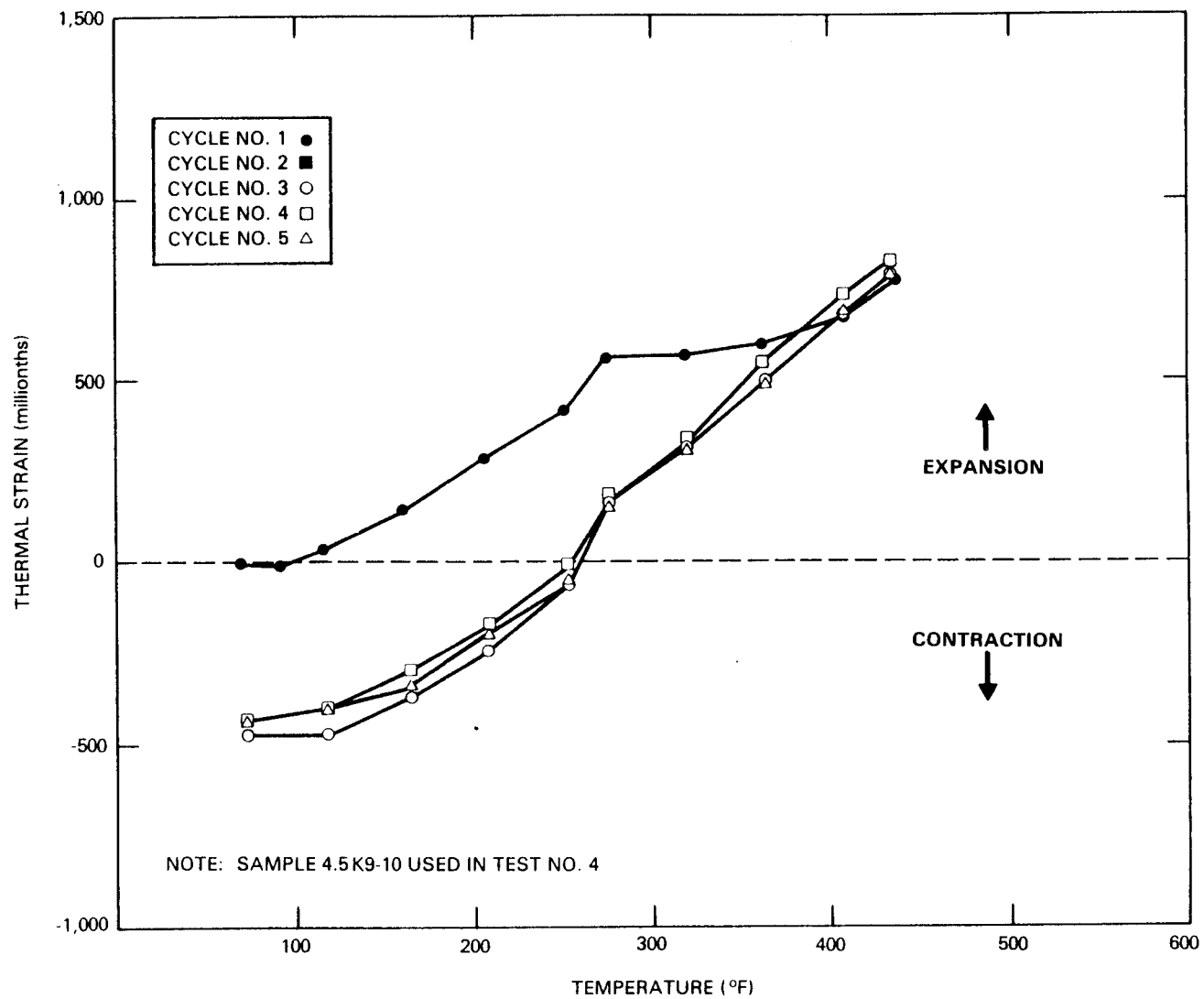
RCP8106-61

FIGURE 3-40. Cyclic Thermal Strain Versus Temperature Curves for Test No. 4.

was approximately linear during the first temperature cycle. Thermal strain of these specimens averaged 800 millionths at maximum test temperature.

After cooling to room temperature, all specimens exhibited a net length loss of approximately 1,500 millionths of an inch. Repeated heating did not produce any additional contraction. The shortening of the test specimen after the first temperature cycle is attributed to permanent shrinkage caused by loss of free water, and possibly some chemically combined water, from the cement paste matrix.[3,9]

On the second heat cycle, thermal expansion again was approximately a linear function of temperature. However, the slope of the strain/ temperature curve was steeper in all cases than that produced by the initial heating cycle. Thermal strains of specimens at maximum temperature on the second heat cycle were similar to that observed during the initial heat cycle. No additional changes in strain behavior were noted when specimens were heated beyond two thermal cycles. Strain/temperature curves were very similar to those produced during the second heat cycle.

Thermal strain versus temperature curves of specimens cored from concrete cylinders cast at CTL/PCA in September 1977 are shown in Figures 3-41 through 3-44. As with older specimens, there was an approximately linear relationship between strain and .temperature during the initial heating for the younger concrete. However, slopes of the strain temperature curves were somewhat steeper than those observed with older concrete. Average strain values of 1,050 millionths were measured at maximum test temperature for the concrete cast in 1977.

A net length loss on cooling of about 300 millionths was measured on the younger specimens. Reheating produced steeper sloped strain versus temperature curves than observed with the initial heat cycle. However, thermal strains at maximum test temperature were essentially the same as those observed during the initial heat cycle.
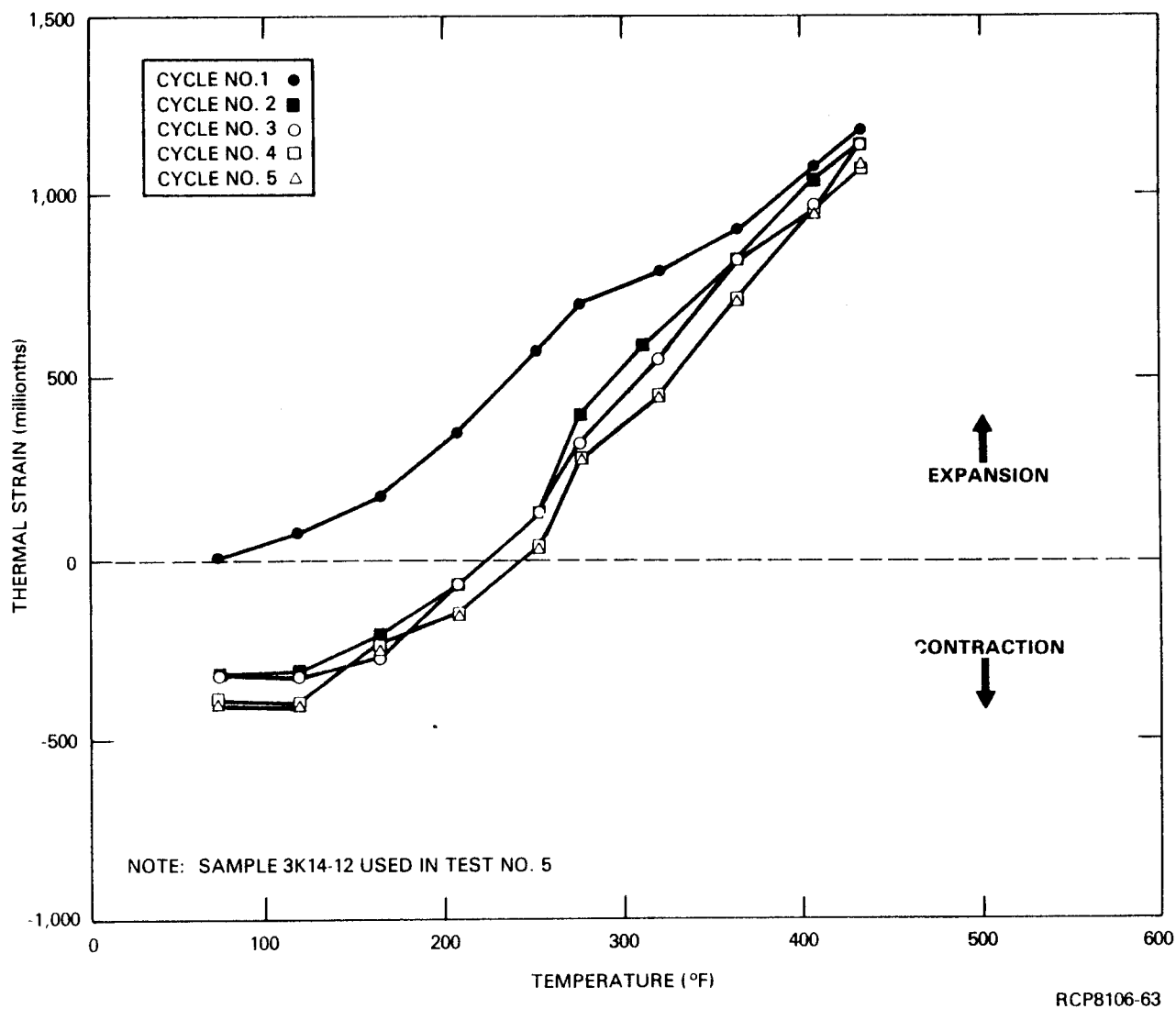
FIGURE 3-41. Cyclic Thermal Strain Versus Temperature Curves
for Test No. 5.

RCP8106-66
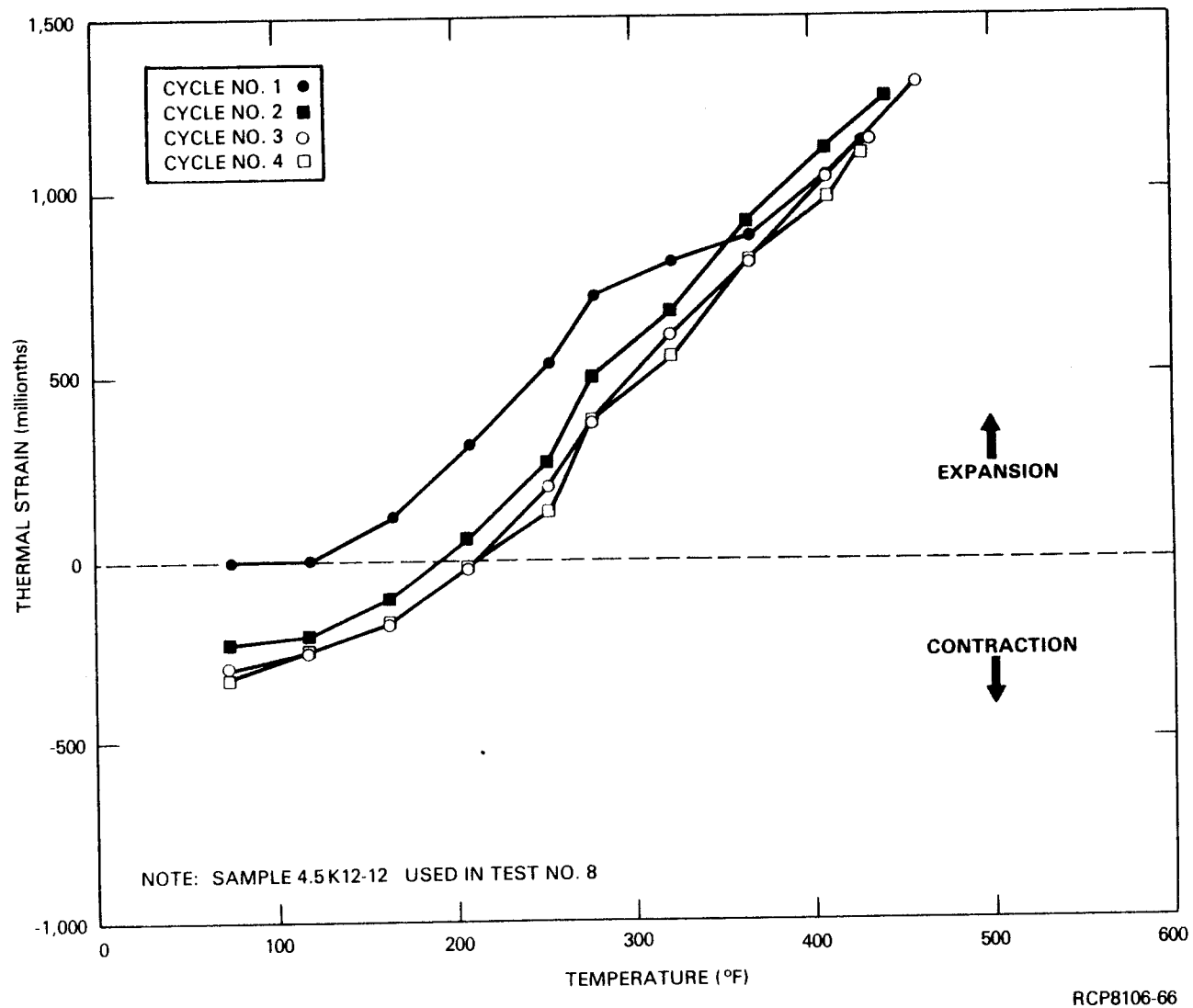
FIGURE 3-42. Cyclic Thermal Strain Versus Temperature Curves
for Test No. 6.
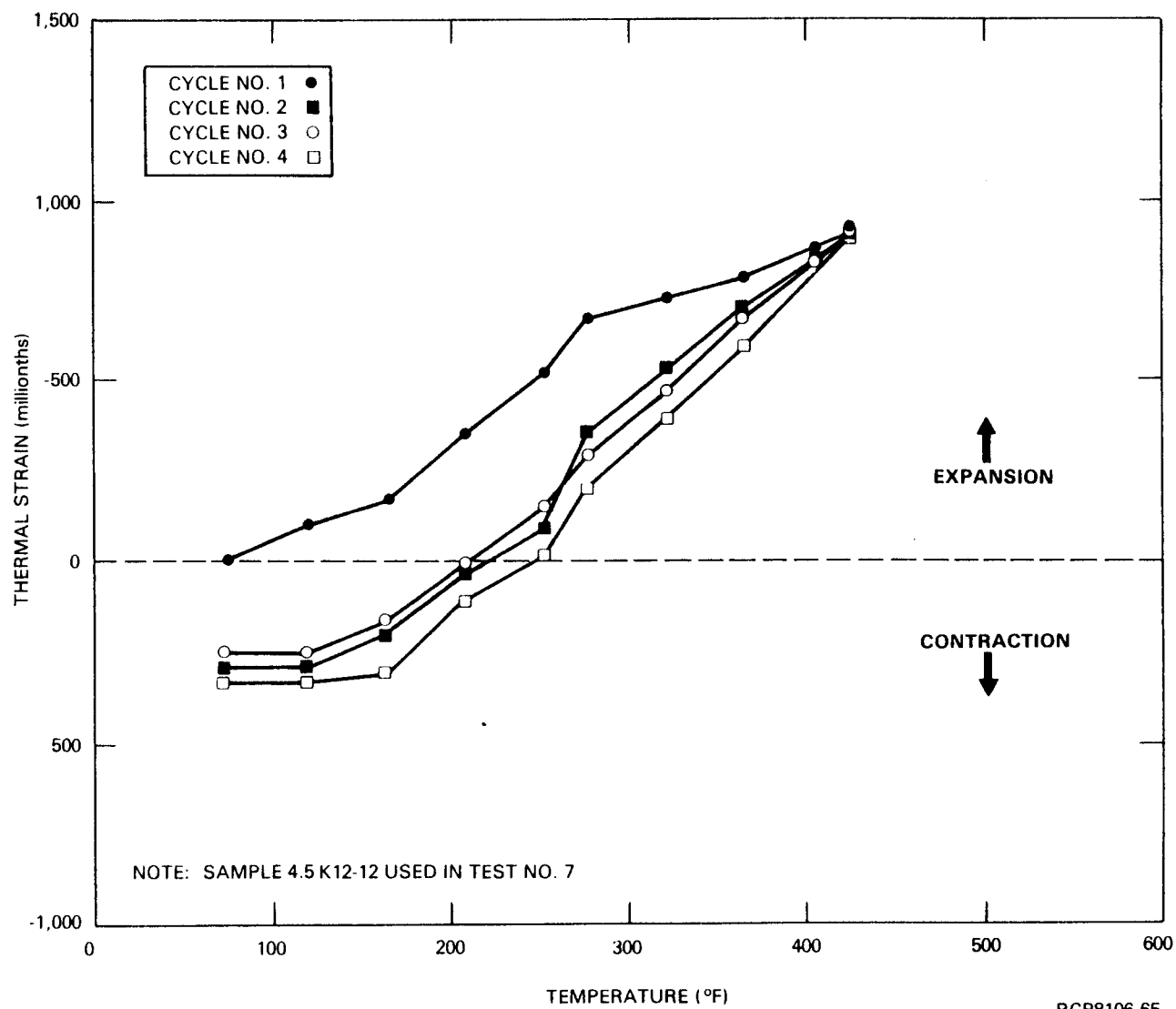
FIGURE 3-43. Cyclic Thermal Strain Versus Temperature Curves for Test No. 7.
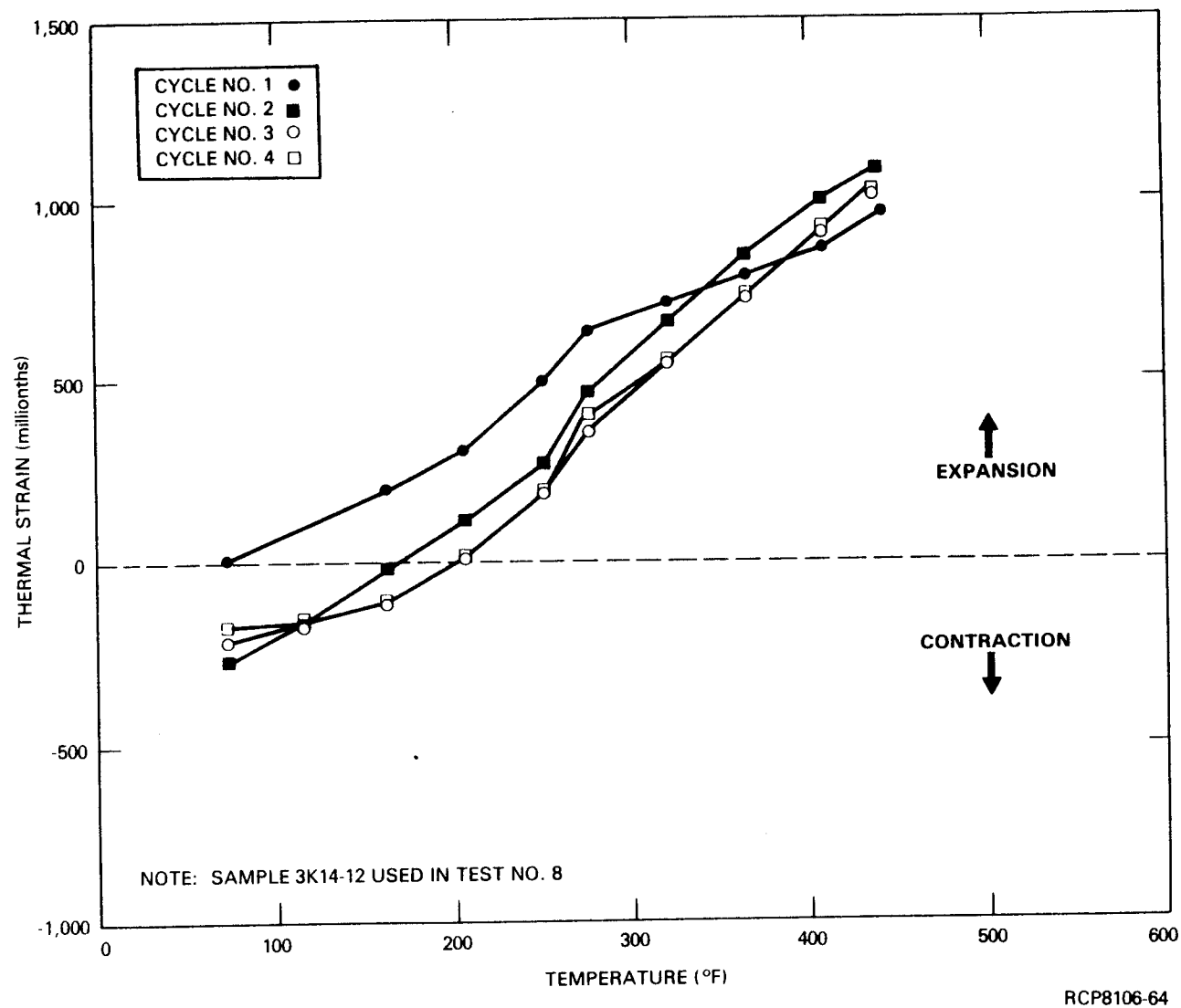
FIGURE 3-44. Cyclic Thermal Strain Versus Temperature Curves
for Test No. 8.

RCP8106-64

The strain versus temperature curves of specimens heated from the third to fifth cycle had characteristics similar those produced during the second thermal cycle. Heating beyond two thermal cycles produced some additional permanent shrinkage when 3 of the 4 specimens cast in 1977 were cooled to room temperature. The effect was rather small, however, amounting only to about 30 millionths in the worst case.

The curves in Figures 3-37 through 3-44 show the thermal strain behavior of test specimens in detail. However, average values for the coefficient of thermal expansion, α, are useful for calculations and comparison purposes. Therefore, test data from each of the 8 tests shown in these figures were used to calculate values for the coefficient of thermal expansion of the concrete, based on the formula:

$$\varepsilon_{TH} = \alpha T$$

where

ε_{TH} is the thermal strain, millionths

α is the coefficient of thermal expansion, in millionths/^{O}F

T is the temperature, in ^{O}F.

Coefficients were determined from best fit of a straight line to the thermal strain versus temperature curves.

Two values for α were determined for each test. The first, α_0, is the value of the coefficient of thermal expansion calculated from results of the initial heating of the specimen. The second, $\bar{\alpha}$, is the average coefficient of thermal expansion determined from thermal strain versus temperature curves produced during heat cycles 2 through 4 or 5. Thus, α_0 is a measure of the thermal expansion of the concrete in the as-cured condition, while $\bar{\alpha}$ represents the response of concrete previously subjected to one or more thermal cycles. Both values are reported in Table G-3 in Appendix G for each test.

In most cases, values obtained for the coefficient $\bar{\alpha}$ for different specimens were in reasonable agreement. Variations that do occur are believed to be attributable to differing volumes of aggregate from specimen to specimen. Also, it should be noted that free moisture would not be present within concrete previously heated above 212°F. The coefficient, $\bar{\alpha}$, was determined from tests on concrete that previously had been heated once or more to 450°F, and thus had free pore water removed. Therefore, $\bar{\alpha}$ essentially was a measure of the thermal expansion of dried concrete.

3.5 STEAM CURING

Results of compressive strength tests on steam cured and companion moist cured concrete cylinders are given in Table H-1 in Appendix H, and plotted as a function of time in Figure 3-45.
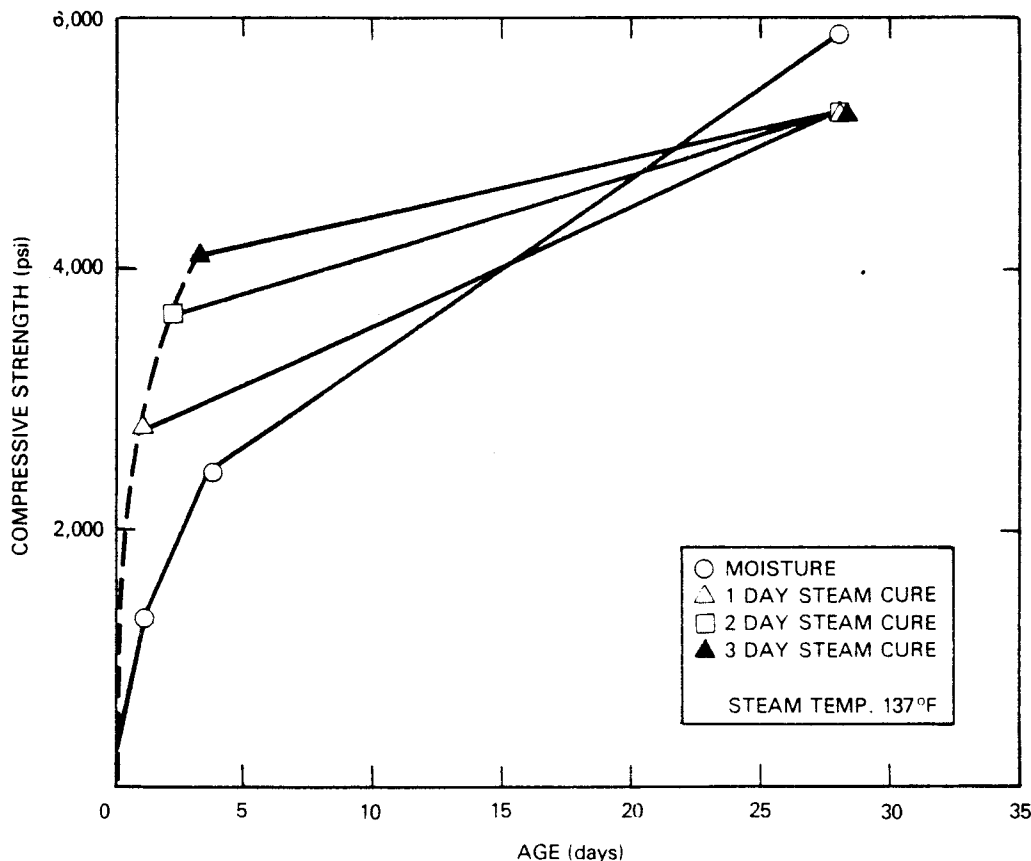
RCP8106-67

FIGURE 3-45. Steam Curing of Hanford Cylinders.

Early strength of steam cured cylinders increased with length of steam curing time. However, strength development after steam curing was slower than that of moist cured concrete. Cylinders with the longest steam exposure had the lowest strength development after steam curing.

The 28-day compressive strength of steam cured cylinders averaged about 5,200 psi, regardless of length of curing. For comparison, strengths of moist cured cylinders averaged 5,860 psi at 28 days.

3.6 THERMAL PROPERTIES

Results of tests to determine the influence of elevated temperatures on thermal properties of Hanford concrete mixes are given in the following sections. Tests were conducted to measure thermal diffusivity, thermal conductivity, and specific heat of concrete from 79° to $1,175^oF$. Test specimens were fabricated from two 6- by 12-in. concrete cylinders cast at CTL/PCA in September 1977. Results of each test are given in tabular form in Table I-1 of Appendix I.

3.6.1 Thermal Diffusivity

Thermal diffusivity, κ, measures the rate at which temperature changes may take place within a material. Diffusivity is related to specific heat, c, and thermal conductivity, k, by the following equation:

$$\kappa = \frac{k}{c\rho}$$

where

ρ is the material density.

Neville states that typical values for diffusivity of normal weight concrete ranges from 0.02 to 0.06 ft^2/hr, depending upon the type of aggregate incorporated into the concrete.[32] He further states that basalt rock aggregates, of the type used in Hanford concretes, produce lower than average values for concrete diffusivity than concrete incorporating other normal weight mineral aggregates.

Examination of Figures 3-46 and 3-47 shows this to be true. Diffusivity of Hanford concrete cast at CTL/PCA varied from a maximum of 0.0322 ft^2/hr at room temperature to a minimum of about 0.015 ft^2/hr at 1,175°F.

3.6.2 Thermal Conductivity

Thermal conductivity, k, is a measure of the rate at which heat will flow down temperature gradient in a material. For concrete, thermal conductivity is strongly dependent on aggregate mineral composition. As with diffusivity, thermal conductivity of concrete made with basalt aggregate tends to have lower values than concrete fabricated from most other natural mineral aggregates.[32]

The presence of moisture inside concrete also has a major influence on measured values of thermal conductivity. Lower moisture content reduces conductivity in concrete because air has a lower thermal conductivity than water. However, moisture content of concrete can vary greatly, making it difficult to state a "typical" value for concrete thermal conductivity. Neville quotes a representative value for concrete with a density of 140 lb/ft^3 to be about 1.1 Btu/ft·hr·°F.[32]

Examination of Figures 3-48 and 3-49 shows that Hanford concretes do exhibit smaller values for thermal conductivity than the stated typical value. Samples from concrete cast at CTL/PCA had room temperature values of approximately 0.81 and 0.95 Btu/ft·hr·°F. Heating specimens of concrete cast at CTL/PCA tended to reduce thermal conductivity below ambient temperature values.

3.6.3 Specific Heat

Specific heat, c, is a measure of the heat capacity of a material. For concrete, c is reported to be little influenced by the minerology of the aggregates, but does increase with increased free moisture within the concrete mass. Typical values for concrete made with normal weight aggregates range from 0.2 to 0.28 Btu/lb·°F.[32]
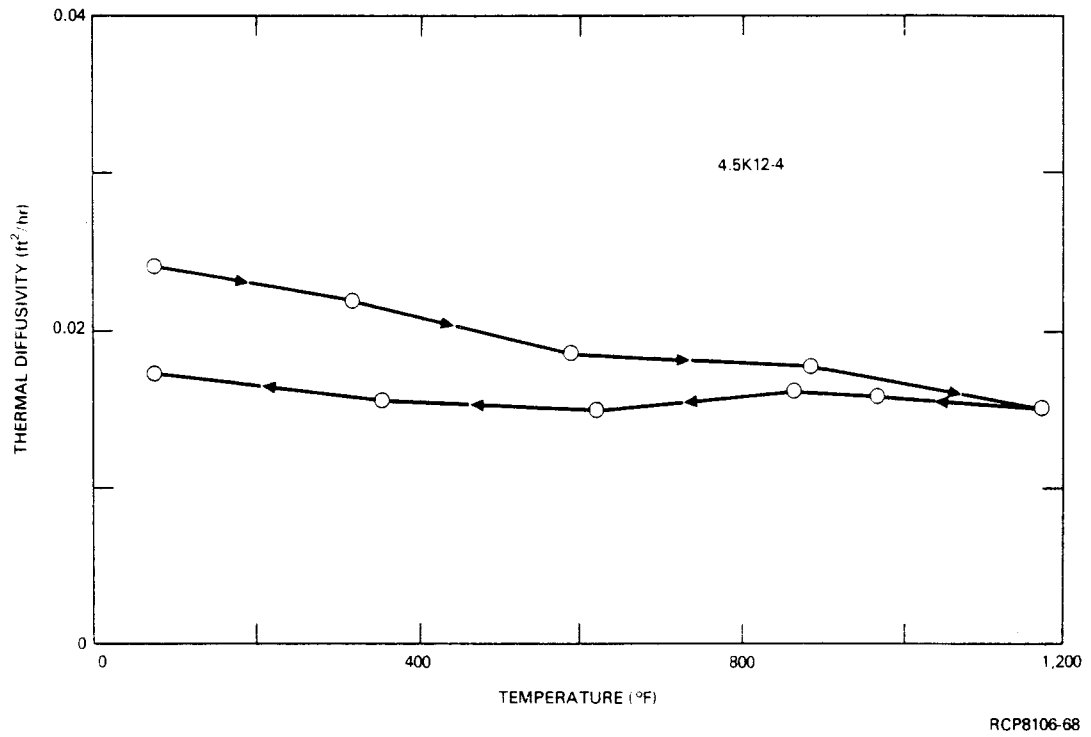
FIGURE 3-46. Thermal Diffusivity of 4.5K Hanford Concrete.
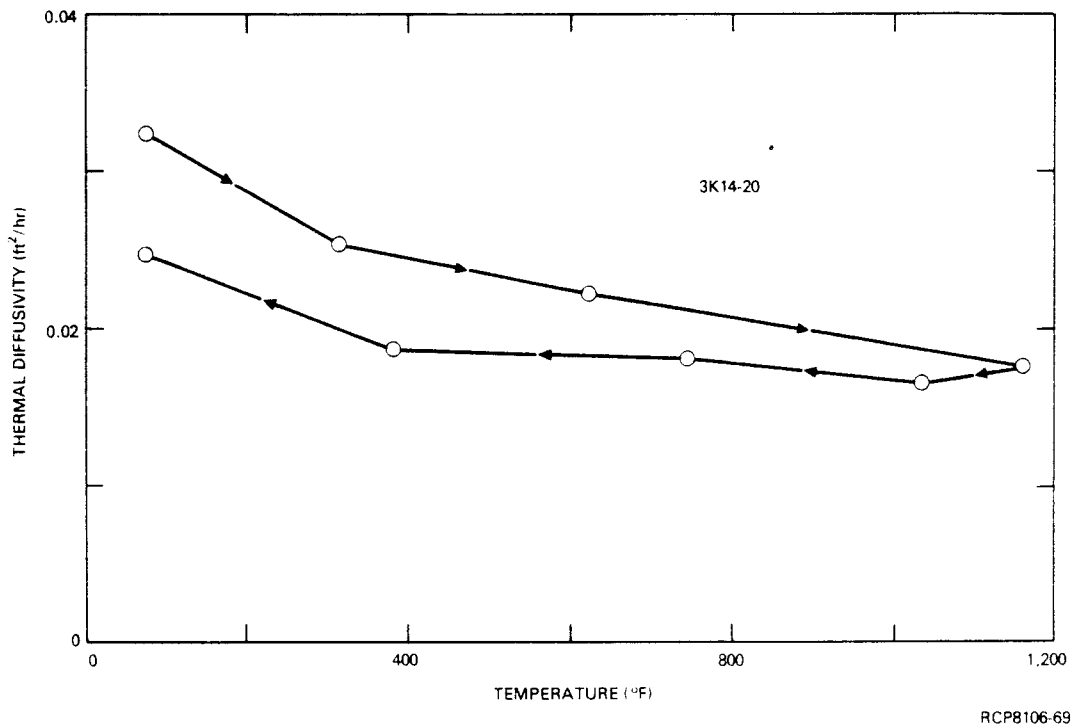
FIGURE 3-47. Thermal Diffusivity of 3K Hanford Concrete.
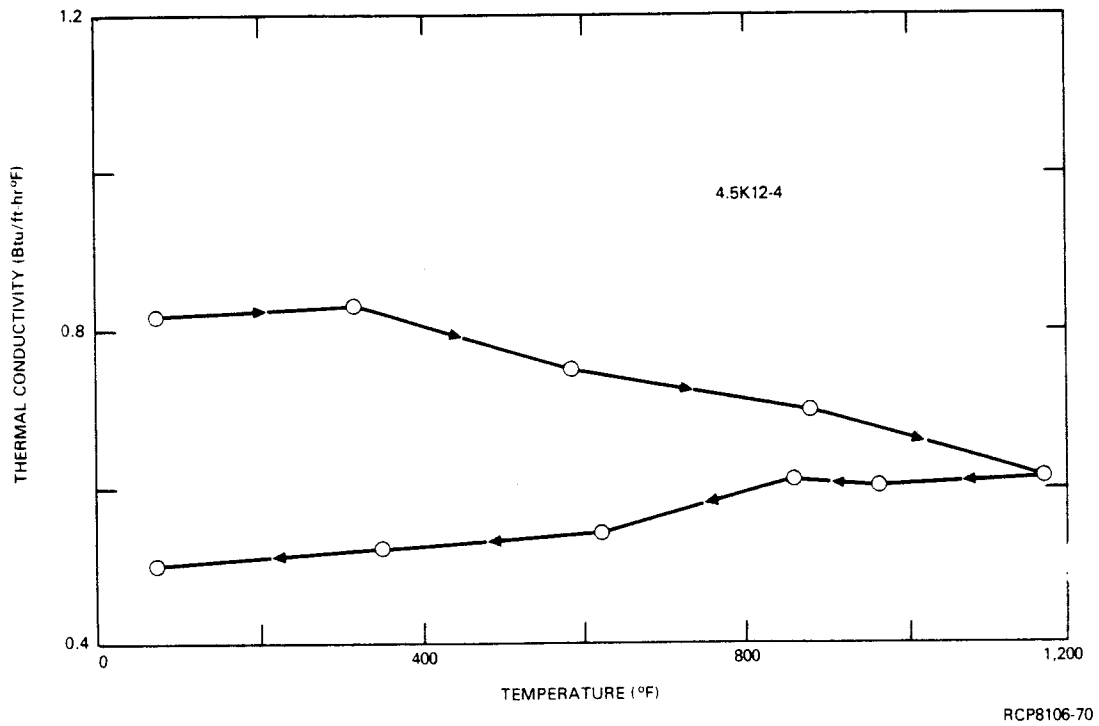
FIGURE 3-48.   Thermal Conductivity of 4.5K Hanford Concrete.
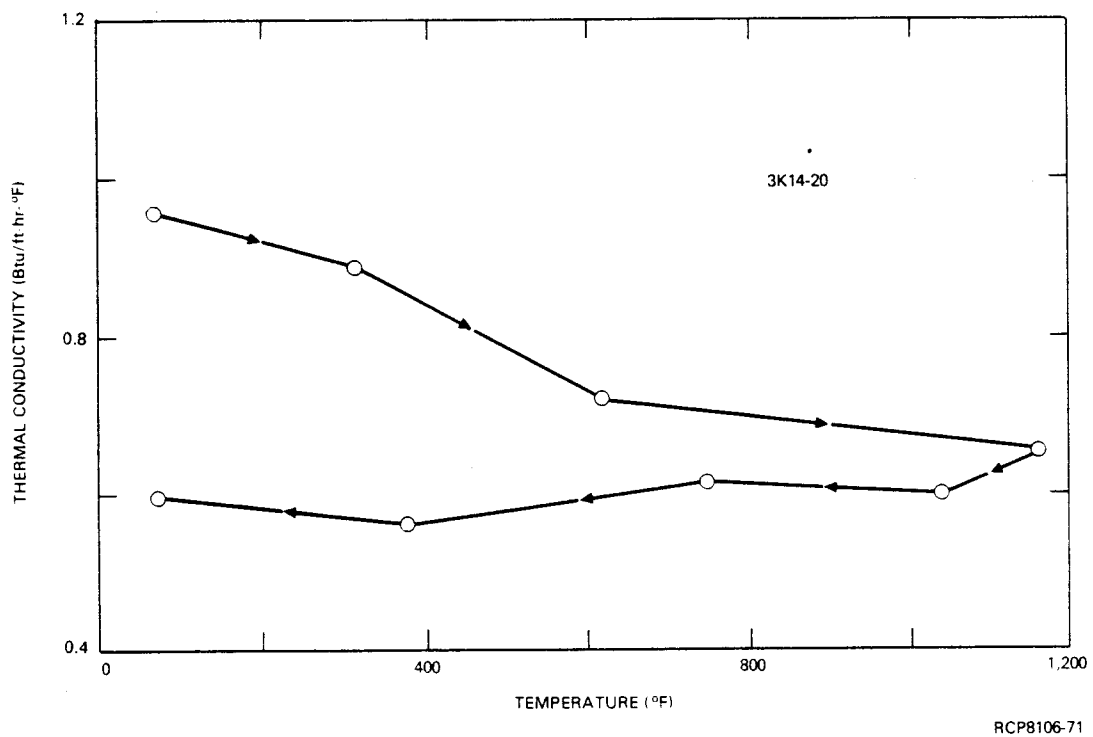
FIGURE 3-49.   Thermal Conductivity of 3K Hanford Concrete.

In Figures 3-50 and 3-51, it can be seen that specific heat of Hanford concretes had room temperature values near the lower limit of the stated range. Heating specimens produced an increase in values of specific heat. Near the maximum test temperature, both specimens had values of c approximately 0.30 Btu/lb °F.

3.7 PETROGRAPHIC AND FRACTOGRAPHIC ANALYSES

Detailed information concerning the petrographic and fractographic work is given in Appendix J. A summary of the major findings of these analyses follows.

3.7.1 Petrographic Analysis

Samples of 28 cylinders of laboratory prepared concrete, stored at various temperatures for different lengths of time, were examined with a polarized light microscope and stereomicroscope to determine the microstructural effects on the paste and the paste-aggregate bond. An attempt was made to discern the progressive changes in microcrystalline texture of the paste as functions of duration and temperature of storage. The duration of storage ranged from 3 to 270 days. Temperatures were 250°, 350°, and 450°F.

From the test, it was concluded that calcium hydroxide birefringencies showed no clearly defined correlation with temperature of storage. A Students t-Distribution Test (a statistical method) for comparing significant differences between the 250° and 350°F data when compared with the 450°F data gives a value of 1.28. This suggests the possibility that a real difference exists, but implies the necessity for additional data. In terms of storage time, samples stored at 270 days revealed relatively high birefringencies. A Students t-Distribution Test for significant differences in the birefringencies of the 1- to 100-day samples as compared with 150- to 270-day samples results in a value of 1.37. This again suggests a defined relationship and need for additional data.
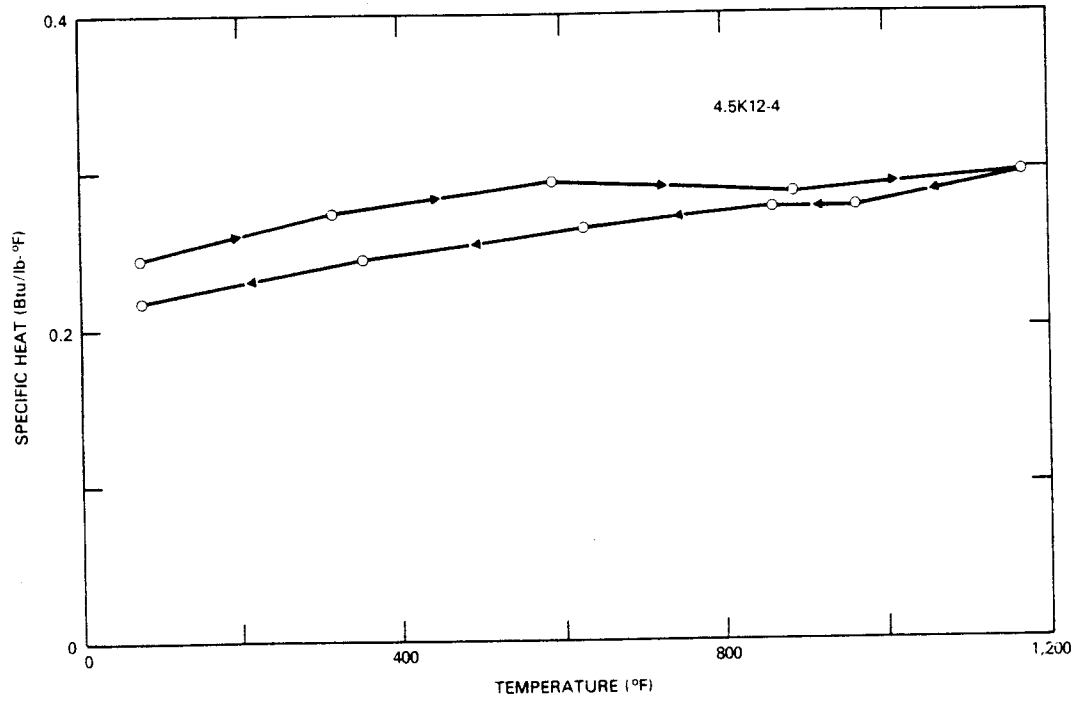
FIGURE 3-50. Specific Heat of 4.5K Hanford Concrete.
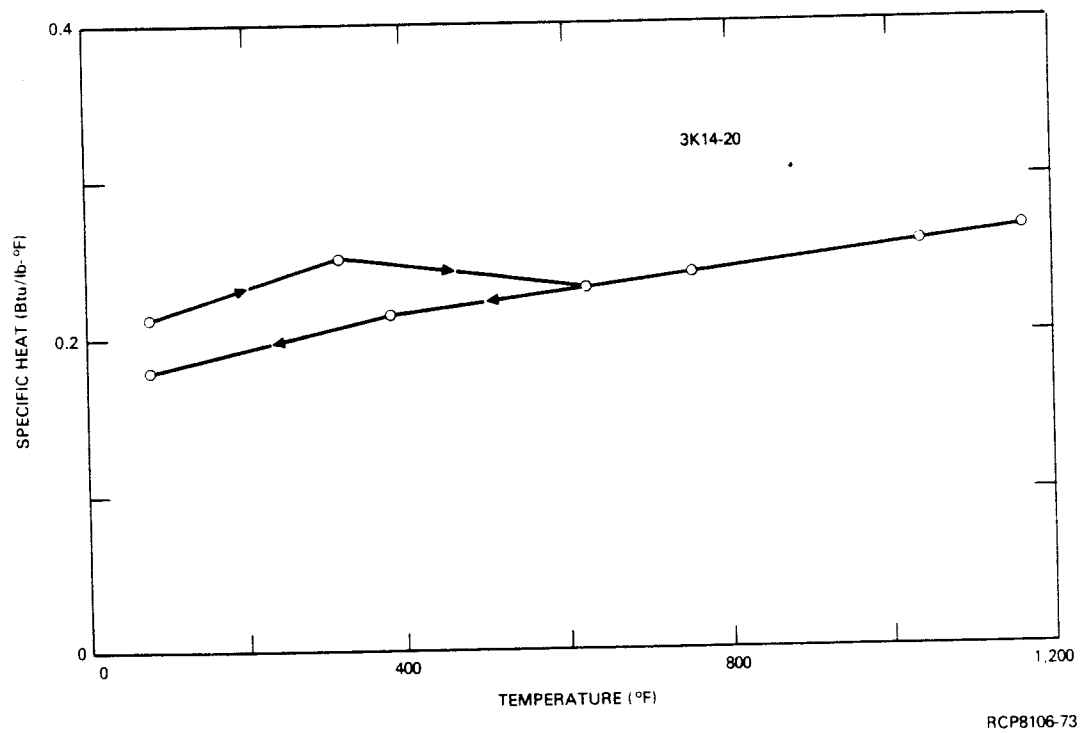
FIGURE 3-51. Specific Heat of 3K Hanford Concrete.

4.0 EVALUATION OF THE TEST PROGRAM

The purpose of this test program was to obtain sufficient data to permit evaluation of Hanford concrete waste tanks exposed to elevated temperatures for prolonged periods. To provide this information, strength and elastic properties tests were conducted on concrete cylinders heated at 250°, 350°, and 450°F for periods of up to 2 3/4 years. Tests were also conducted to determine the influences of elevated temperatures on concrete creep, thermal expansion, thermal conductivity, and other physical properties. In addition, petrographic and fractographic analyses were conducted to determine if degradation in mechanical properties caused by heat exposure could be related to specific changes in concrete microstructure.

Influences of elevated temperatures on concrete physical/mechanical properties are summarized and their relations to concrete integrity are described in the following sections.

4.1 ELASTIC PROPERTIES

Of all concrete properties examined in this study, modulus of elasticity was the most sensitive to elevated temperature exposure. Elastic modulus of Hanford concrete was affected by both the magnitude and length of exposure to elevated temperatures.

For example, the average modulus of concrete heated to 250°F for only 3 days dropped about 20% from values for unheated concrete. By comparison test cylinders heated at 350°F for 4 days or 450°F for 6 days lost approximately 27 and 38%, respectively. After about 900 days heating, concrete at 250°, 350°, and 450°F had modulus values that were approximately 37, 48, and 70% below that measured for unheated concrete.

Lankard, et al, have compared results of a number of investigators studying effects of elevated temperatures on the modulus of elasticity of various concretes.[3] In Figure 4-1, the range of values reported by Lankard has been plotted with those obtained from the present study.
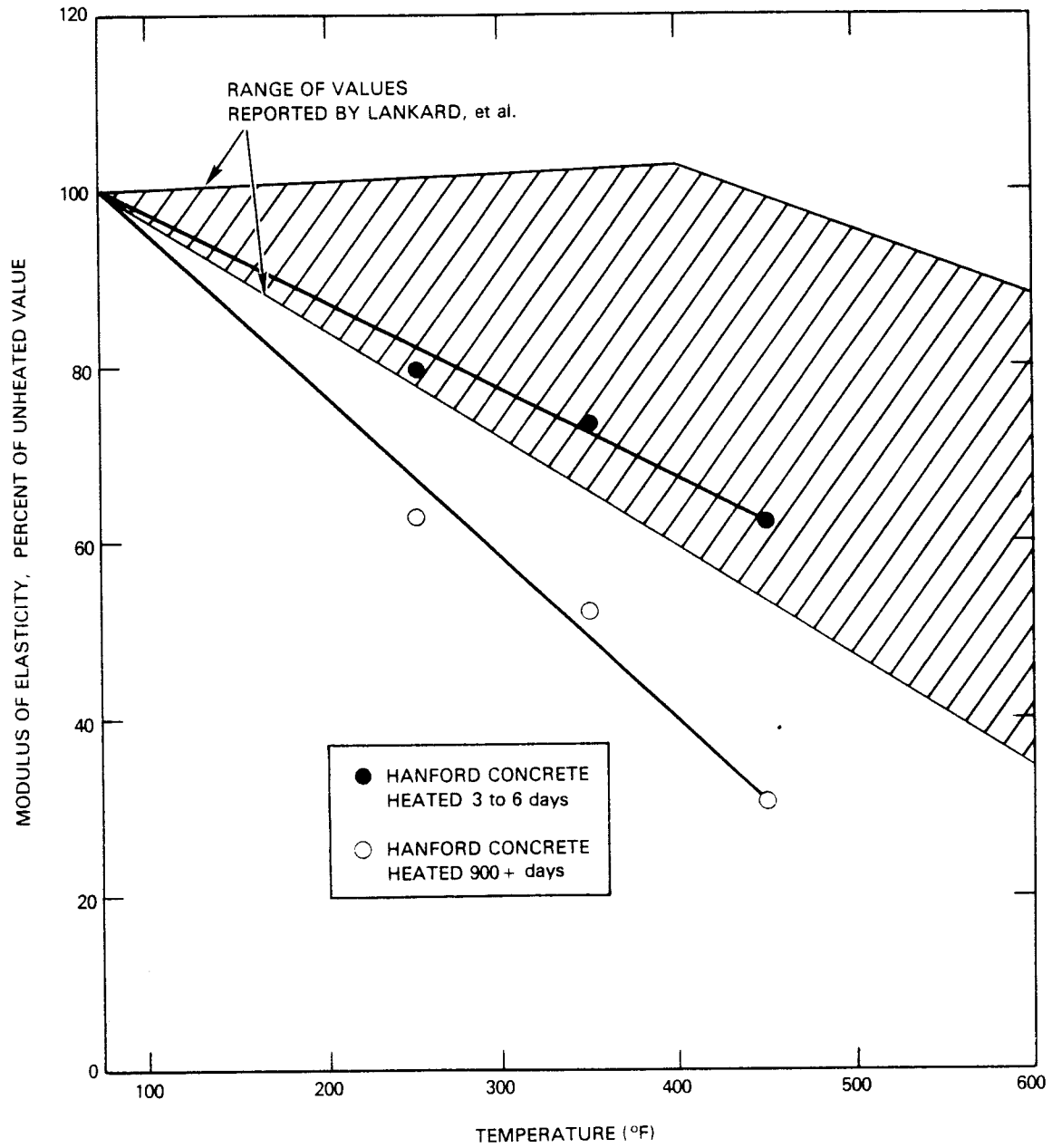
FIGURE 4-1. Modulus of Elasticity of Hanford Concrete
Compared to Other Elevated Temperature Test Data.

Results of studies on concrete high temperature elastic behavior more recent than those examined by Lankard also fall within those limits. Modulus values obtained from Hanford concrete subjected to less than 7 days heating are near the lower bound of the range reported by Lankard. Elastic moduli of Hanford concrete heated at 250°, 350°, and $450^\circ F$ for more than 900 days, however, falls wholely outside this range.

This result would seem to confirm that long-term exposure to elevated temperatures does produce losses in concrete stiffness larger than those determined from relatively short-term tests. This difference is most noticeable at $450^\circ F$, where short-term test results indicated moduli losses on the order of 35%. Long-term tests, however, show cumulative losses almost twice as large as this.

When modulus of elasticity is considered as a function of heating time (see Figures 3-2, 3-3, and 3-4), three types of behavior can be seen. During early heating, from about 3 to 30 days, modulus values decreased rapidly. The rate and magnitude of loss depended on heating temperature; higher temperatures produced steeper loss rates.

For heating times beyond 200 days, modulus losses were smaller and fairly linear with respect to time. Again, largest loss rates occurred for concrete at $450^\circ F$. At intermediate times, ·approximately 30 to 200 days, modulus loss rates decreased smoothly from the steep losses of the earlier heating period to the roughly linear loss behavior beyond 200 days heating.

Poisson's ratio of heated concrete exhibited no well defined relationships with respect to time or temperature. Poisson's ratio data were very erratic (see Figures 3-9, 3-10, and 3-11). For heated concrete, Poisson's ratios varied from 0.10 to 0.14, compared to values of 0.15 to 0.20 for mature, unheated concrete. Most of this reduction occurred during initial heating. No systematic changes were observed in the data with additional exposure to elevated temperatures.

4.2 COMPRESSIVE STRENGTH

Compressive strength data for heated concrete, (see Figures 3-17, 3-18, and 3-19), exhibit noticeable scatter that make accurate assessment of temperature effects difficult. However, for most cases, strength decreased with increasing length of exposure to elevated temperatures, and also decreased with increasing temperatures.

For example, just prior to heating, the average compressive strength of 6- by 12-in. test cylinders was 5,955 psi, well above the minimum design strengths of 4,500 and 3,000 psi. After 3 days heating, specimens at 250°F had strengths averaging 5,435 psi, a 9% decrease from values of unheated concrete. For concrete heated 4 days to 350°F or 6 days to 450°F, strengths averaged 5,730 and 5,260, respectively, representing losses of 4 and 12 1/2% from the unheated control concrete. Note that these modest reductions are in sharp contrast to the large early losses observed in concrete elastic moduli.

Concrete heated for extended times showed greater strength reductions. The magnitude of the additional losses depended upon the test temperature. This can be seen from the results of tests conducted on specimens heated for approximately 900 days. Average compressive strengths of cylinders heated at 250°, 350°, and 450°F were 5,225 psi (-12%), 4,580 psi (-23%), and 3,930 psi (-34%), respectively, where the percentages in parentheses are the changes from values measured for unheated concrete.

It should be noted that concrete strengths remained above specification levels for the 3K mix design at all three test temperatures throughout the study period. Concrete made from the 4.5K mix design also remained above the specified strength level at 250° and 350°F, and fell only slightly below requirements after 590 days at 450°F. After 915 days of heating, compressive strengths of 4.5K concrete averaged less than 10% below the minimum design strength.

A comparison of these test data to those reported in Lankard's survey for unsealed concrete[3] is shown in Figure 4-2. Unlike moduli of elasticity, compressive strength values for Hanford concrete heated for extended times remained within the Lankard survey range.
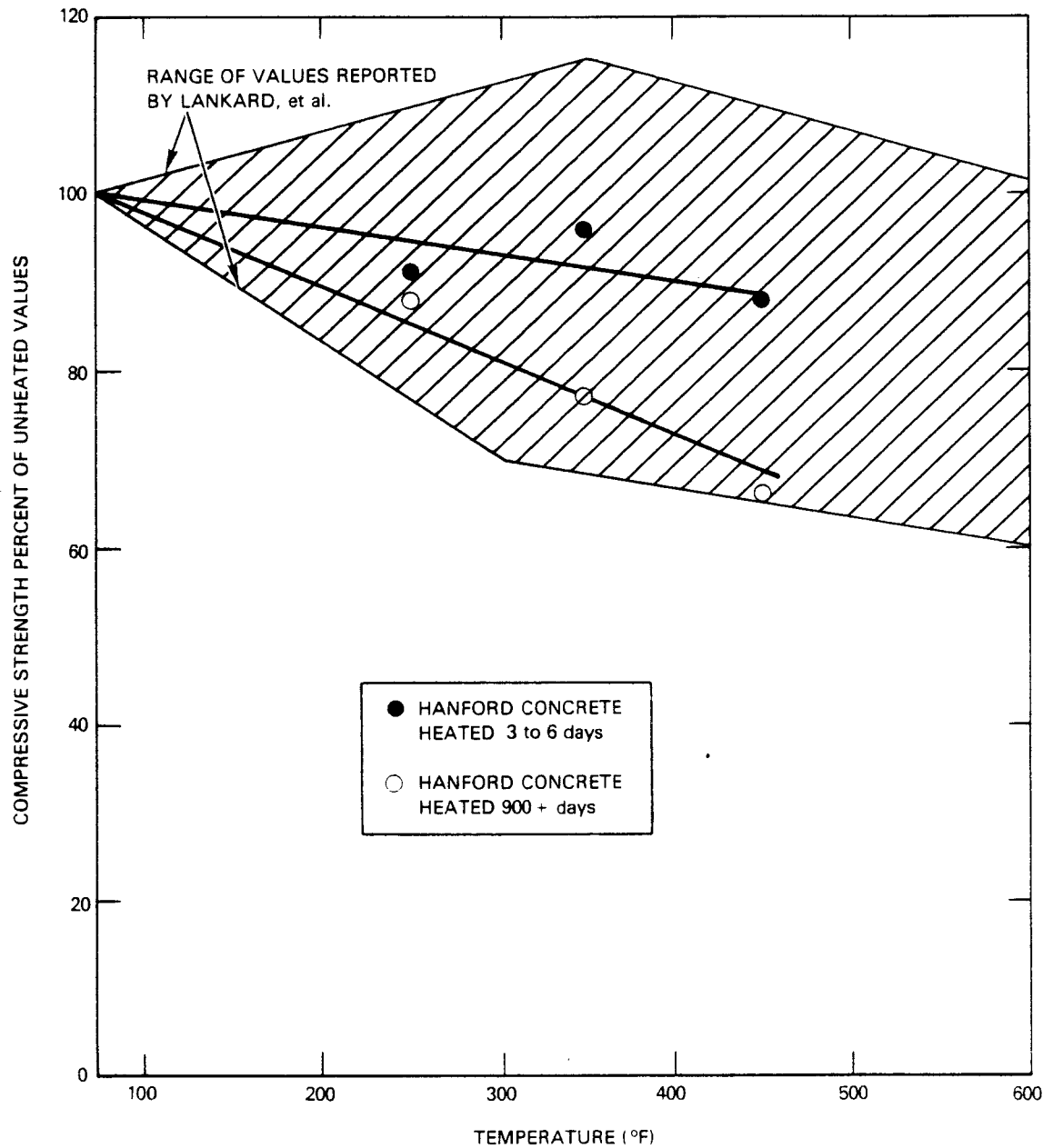
FIGURE 4-2. Compressive Strength of Hanford Concrete Compared to Other Elevated Temperature Test Data.

However, average strength loss percentage of Hanford concrete heated at 450°F was at the lower limit of this range. The strength loss/temperature trend for Hanford concrete heated for extended times would seem to indicate that at temperatures above 450°F, strength losses would exceed those reported by Lankard.

4.3 SPLITTING TENSILE STRENGTH

From the curves in Figures 3-21, 3-22, and 3-23, it can be seen that splitting tensile strength of Hanford concrete decreased with length and degree of exposure to elevated temperatures in a manner similar to that observed in compressive strength data. The combined average strength of unheated concrete cylinders was 582 psi. Three days of heating to 250°F reduced strengths to an average of about 530 psi. Four days of heating to 350°F reduced strengths by a similar amount, approximately a 9% reduction from unheated values. Heating 6- by 12-in. cylinders for 6 days to 450°F reduced strengths to an average of only 433 psi, a 26% reduction.

Concrete specimens heated for extended periods had losses from two to three times greater than the values quoted above. Cylinders heated for approximately 900 days at 250°, 350°, and 450°F had strengths reduced by an average of 28, 30, and 44% respectively. .

Relatively few studies have been made of the effects of temperature on concrete tensile strength using either the flexural or split cylinder method. In Figure 4-3 the range of strength values determined by both methods reported in Lankard's survey[3] is shown as a function of temperature. Several more recent studies, most notably by Thelandersson,[16] have also produced data that fall within those limits.

Splitting tensile strength data from Hanford concrete, subjected to short and extended periods of heating, are also plotted in Figure 4-3. Data from concrete subjected to short-term heating fall near the middle of Lankard's range of strengths. However, concrete exposed to extended periods of heating had strengths somewhat below the lower limit of this range.
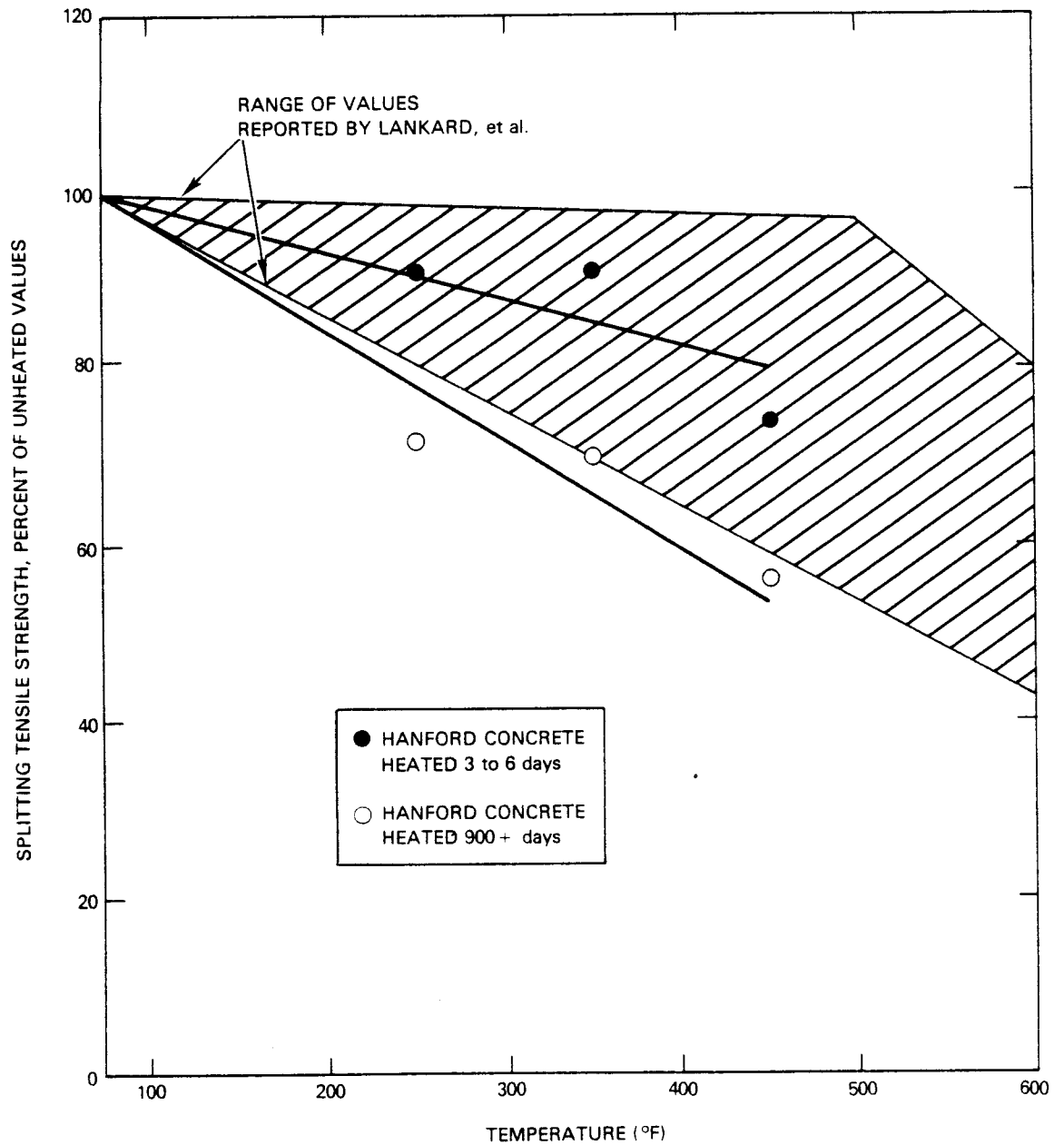
FIGURE 4-3. Splitting Tensile Strength of Hanford Concrete
Compared to Other Elevated Temperature Data.

RCP8106-76

A comparison of Figures 4-2 and 4-3 shows that the tensile strength of Hanford concrete was somewhat more susceptible to degradation due to heat exposure than was compressive strength. As explained earlier, the ratio of splitting tensile strength f_{st}, to compressive strength, f_c is about 0.1 for normal concrete. For Hanford concrete, the ratio was f_{st}/f_c = 582 psi/5,955 psi = 0.098, very close to the accepted normal value. Comparing tensile to compressive strengths of Hanford concrete heated for equivalent times and temperatures, the greater relative reduction in tensile strength on heating is shown quantitatively in Table 4-1. Strength ratios of concrete heated for extended times were lower than those for short-term heating of 250° and $350^\circ F$, and were equal at $450^\circ F$.

TABLE 4-1 - Ratio of Splitting Tensile Strength
and Compressive Strength of Hanford Concrete.

Temperature, $^\circ F$	Splitting Tensile Strength/ Compressive Strength (f_{st}/f_c)		
	Unheated	Heated for 3 to 6 days	Heated for 900 days
73	0.098	-	-
250	-	0.098	0.080
350	-	0.092	0.088
450	-	0.082	0.082

4.4 CREEP

In Section 3.2, it was shown that creep strain data from tests on Hanford concrete at 250° and $350^\circ F$ could be accurately modeled by a relatively simple logarithmic expression, $\varepsilon_{cr} = K \log_{10} (t) + \varepsilon_0$ where K and ε_0 are constants dependent on load, temperature, and material variables. This equation has been found to satisfactorily model concrete creep behavior at elevated temperatures by a number of investigators.[19,33]

For example, Marechal measured creep strains of a quartzite aggregate concrete at temperatures from 20° to $400^\circ C$ (68° to $752^\circ F$) and found that his data fit the logarithmic model over the whole temperature range. Marechal's data for concrete loaded to about 1,450 psi are shown in Figure 4-4. Unfortunately, the compressive strength of the concrete was not given. Therefore, it is not possible to determine the magnitude of the applied load relative to the material strength and make a direct comparison to creep data in the current study.

More important, however, is the creep behavior of concrete at temperatures below $105^\circ C$ ($221^\circ F$), shown in Figure 4-4. Instead of looking at creep strain, examine the rate of creep strain by differentiating the equation $\varepsilon_{cr} = K \log_{10}(t) + \varepsilon_0$ with respect to time:

$$\text{rate of creep} = \frac{d\,\varepsilon_{cr}}{dt} = K/t.$$

By plotting K/t versus temperature for some arbitrary fixed time t, the creep rate is shown to have a strong local maximum in the neighborhood of $50^\circ C$ ($\sim 120^\circ F$) (see Figure 4-5). This maximum produces larger strains than found at temperatures comparable to those used in the current study of Hanford concrete.

The migration of moisture within the hardened concrete is the suspected cause of the large creep strains in this temperature region. Many mechanisms have been proposed to explain this phenomenon.[3] However, there is no general agreement on the exact nature of the processes involved.

This behavior suggests that creep strain of Hanford concrete may be greater at temperatures in the range from ambient to $150^\circ F$ than at temperatures examined in the present program. Further study is needed to determine the significance of creep behavior of Hanford concrete at these lower temperatures.

4.5 THERMAL EXPANSION

Typical quoted values for coefficient of thermal expansion, α, of normal weight concrete are on the order of 5×10^{-6} to $1.0 \times 10^{-5}/^\circ F$. The mean value of α for Hanford concrete measured in this study was
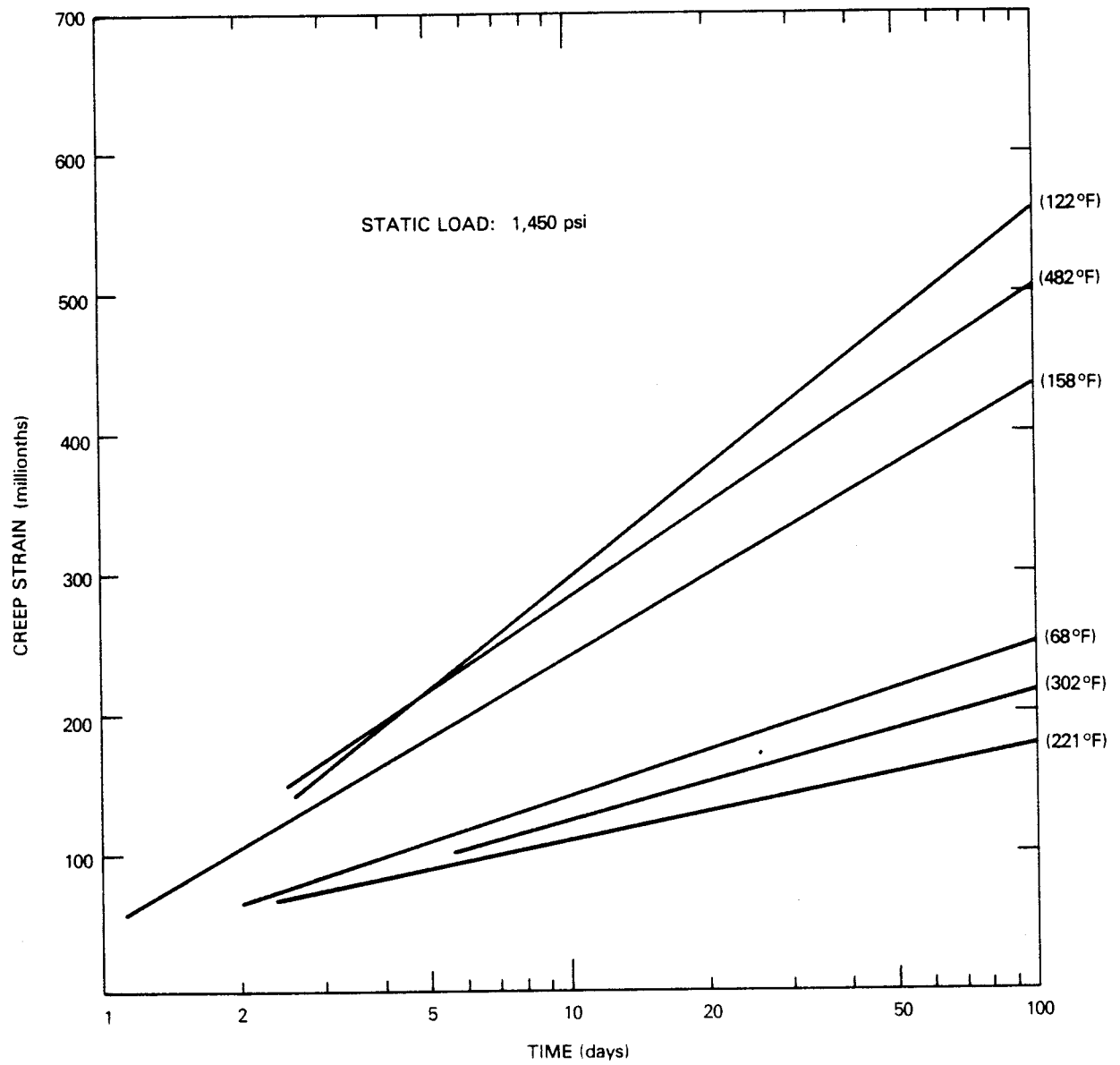
FIGURE 4-4. Creep Data of Marechal. (33)
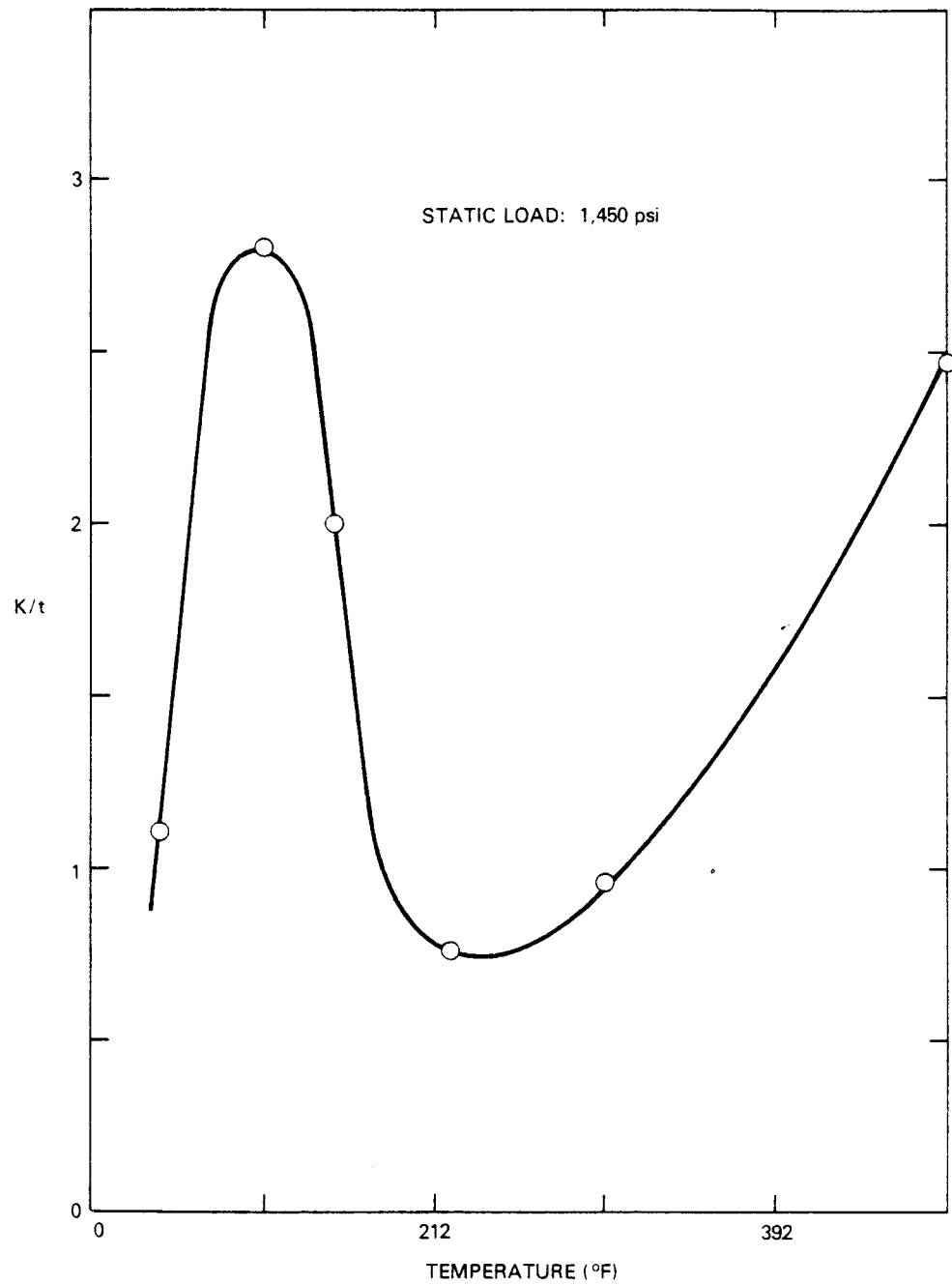
RCP8106-77

FIGURE 4-5. Strain Rate as a Function of Temperature, Derived from Creep Data of Marechal. [33]

about 3.3 x 10^{-6}/°F. By itself, a lower α value means that, at a given temperature, thermally induced stresses and strains should be smaller than that of a concrete with a more typical value of α, and for that reason is a desirable property for high temperature applications.

However, if steel reinforcement is present within the concrete, it is necessary to have a good match in thermal expansion behavior between concrete and steel. Poor matching will produce different rates of expansion on heating that may result in bond breaking at the concrete/steel interface and may even cause rupture of the concrete.

Normally, this is not a serious problem in reinforced concrete structures because the expansion behavior of most concrete mixes is similar to that of structural steel at moderate temperature levels, as shown in Figure 4-6. By comparison, expansion of Hanford concrete, also shown in Figure 4-6, is about half that of steel. This difference may indicate a potential for disruption of the concrete/steel bond at elevated temperatures. Further study of the bonding characteristics of Hanford concrete to steel is needed to determine if this is, in fact, a serious problem.

4.6 THERMAL CYCLING

The purpose of the thermal cycling program was to determine if cyclically varying temperatures had additional deleterious effects on mechanical properties of Hanford concrete above that observed with sustained exposure to constant elevated temperatures. Hanford concrete mechanical properties, particularly modulus of elasticity, were susceptible to degradation, proportional to increasing period and number of thermal cycles from ambient to 350°F (see Figures 3-33 and 3-38).

When compared to data in Figures 3-1 through 3-19, however, it can be seen that thermally cycled concrete suffered relatively less material properties degradation, than did concrete held at constant temperature for an equivalent length of time. Reductions in concrete strength and
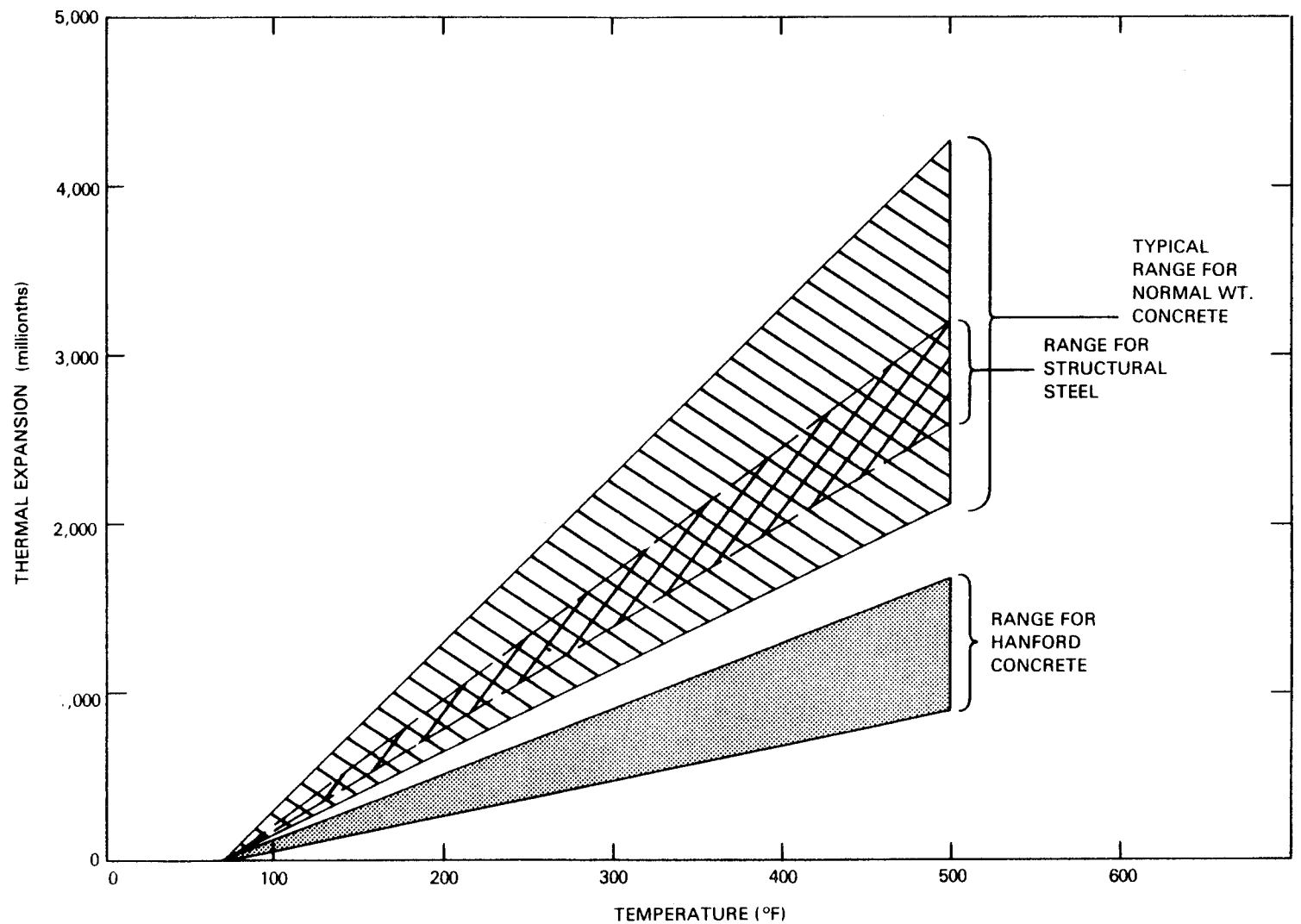
FIGURE 4-6. Thermal Expansion Behavior of Typical Concrete Mixes, Structural Steel, and Hanford Concrete.

elastic properties for the heat cycled condition approached, but never exceeded losses observed at constant temperature. Therefore, in the case of unsealed concrete heated with no external load applied, constant exposure to 350°F was a more severe environment than was cyclically varying temperatures between ambient and 350°F.

Thermal cycling also produced changes in the thermal expansion behavior of Hanford concrete. When concrete specimens were repeatedly heated from ambient to about 450°F, two distinct types of expansion behavior were observed. The initial heat cycle produced thermal strains with a linear coefficient of thermal expansion, α_0 that averaged 2.74 x 10^{-6}/°F. On cooling, all specimens exhibited a net length loss. This permanent length change is caused by the loss of internal moisture on heating and resultant volumetric shrinkage.

The second heat cycle produced thermal strains with a coefficient of expansion that averaged about 3.9 x 10^{-6}/°F, an increase of approximately 40% from that measured with the first cycle. Additional cycling resulted in thermal strain behavior that was essentially identical to that observed during the second thermal cycle.

Two major results obtained from these data, that are important from a structural analysis standpoint, are the permanent shrinkage and the change in α values caused by initial heating. Shrinkage is important because it produces internal tensile stresses within the concrete. These internal stresses can cause cracking, even in the absence of an externally applied load.

Changes in the linear coefficient of thermal expansion must be considered if thermal stresses and strains within a structure in service are to be accurately determined. Any stress analysis of structures in operation should use the $\bar{\alpha}$ value, given in Table G-3, Appendix G, for concrete subjected to prior heating rather than the value determined from concrete with no previous heating. Since α_0 is greater than $\bar{\alpha}$, the use of α_0 in thermal stress analysis would yield calculated strain and stress values much smaller than may actually occur in a heated structure.

4.7 STEAM CURING

The use of low pressure steam curing was found to produce higher early strengths than conventional moist curing for Hanford concrete. However, these increases were not maintained with post-steam curing. After 28 days, compressive strengths of concrete specimens subjected to various periods of steam curing were, in all cases, lower than that of moist cured specimens.

Furthermore, rate of strength increase with time for steam cured cylinders during the post-steam cure was much below that of moist cured concrete. This indicates that long-term strength of steam cured concrete would be measurably lower than that derived with moist curing. For these reasons, steam curing does not appear to be a useful tool for producing test specimens representative of Hanford concrete cured in situ.

4.8 THERMAL PROPERTIES

Tests to determine thermal diffusivity, thermal conductivity, and specific heat confirmed that values for Hanford concrete were near the lower limit of the range of typical concrete values published by other investigators. Moreover, thermal properties of Hanford specimens, on heating, were different from those measured on subsequent cooling.

As in the case of thermal expansion tests, heating appeared to cause a reduction in the magnitude of thermal properties from their initial values. Unfortunately, no tests were conducted to determine if these reductions were permanent by measuring properties of concrete subjected to more than one thermal cycle. Further study of thermal properties behavior of concrete exposed to repeated heating will be necessary in order to provide data for any analysis of in service structural performance of Hanford concrete at elevated temperatures.

5.0 CONCLUSIONS

Based on data from the various types of tests conducted in this program, a number of conclusions can be made about the long-term effects of elevated temperatures on the thermal and mechanical properties of Hanford concrete mixes. These are outlined below.

- The mechanical properties of Hanford concrete were susceptible to degradation when concrete was exposed to elevated temperatures in the range from 250° to 450^OF. The amount of degradation was dependent on both the length and degree of elevated temperature exposure.

- Heat induced strength losses did not reduce Hanford concrete mixes' compressive strengths below minimum design levels, except for the 4.5K mix heated at 450^OF for time spans greater than or equal to 590 days. Maximum strength loss for the 4.5K mix occurred when concrete was heated for approximately 920 days at 450^OF, reducing concrete strength less than 10% below minimum design level.

- Relative sensitivity of mechanical properties to degradation by concrete heat exposure was as follows:

modulus of elasticity	(most sensitive)
splitting tensile strength	
compressive strength	
Poisson's ratio	(least sensitive).

  Most severe properties losses were measured with concrete subjected to 920 days heating at 450^OF. The modulus of elasticity of heated concrete was only about 30% of that measured with unheated concrete.

- Long-term tests at elevated temperatures produced properties losses that were more severe than those measured with short term tests of heated concrete. Moreover, at maximum test temperature, 450^OF, losses did not appear to approach limiting values even after more than 2 1/2 years heating.

- Creep behavior of Hanford concrete mixes at elevated temperatures was found to be adequately modeled by a logarithmic expression of the form:

$$\varepsilon_{CR} = K \log_{10} (time) + \varepsilon_0.$$

Where K and ε_0 are constants that varied with temperature and load.

- Thermal expansion of Hanford concrete mixes was only about one half that generally reported for normal weight structural concrete. The difference in α values between Hanford concrete and steel may cause large internal stresses in concrete near steel reinforcement in a heated structure.

- Cyclically varying temperatures produced smaller changes in concrete mechanical properties than equivalent exposure to fixed maximum temperature. In general, magnitude of properties losses increased with increasing number and length of temperature cycles.

- Effects of temperature cycling on Hanford concrete thermal expansion behavior were mixed. Application of one thermal cycle produced a permanent increase in concrete coefficient of thermal expansion, α. Further cycling, however, produced no additional changes in concrete thermal strain behavior.

- Measured values of the thermal properties of Hanford concrete mixes; diffusivity, conductivity, and specific heat were lower than those typically quoted for normal structural concrete. This is thought to be due to the thermal properties of the aggregates used in Hanford concrete mixes. Application of heat appears to further reduce these values.

6.0 RECOMMENDATIONS

In Section 4 of this report, it was indicated that analysis of some aspects of the test data raised questions about the high temperature performance of Hanford concrete mixes. To determine if these potential problems areas actually have adverse effects on concrete performance in service, it is recommended that the additional investigations outlined below be conducted.

6.1 STRENGTH BEHAVIOR BEYOND 2 1/2 YEARS HEATING

Concrete mixes at 450°F continued losing strength at an appreciable rate after more than 2 1/2 years of heating. There was no "limit strength" apparent from analysis of the trends of this data. Considering that the service life of a structure may be more than 25 years, detailed knowledge of anticipated strength losses is essential for adequate design. Additional elevated temperature testing over a period of 5 to 10 years would be needed to provide this information.

6.2 CONCRETE/STEEL BOND STRENGTH

The large difference in α values between Hanford concrete mixes and steel could conceivably produce disruption of the concrete/steel bond in a reinforced structure, subjected to heating. The extent to which this is a problem could be determined by bond strength tests described in ASTM Designation C234.

Tests should be conducted on steel reinforced specimens while at elevated temperatures and also at ambient conditions on specimens subjected to prior heating. Companion tests on unheated specimens would give baseline data for evaluation of the degree of bond disruption, if it occurs.

6.3 HEAT INDUCED CHANGES IN CONCRETE THERMAL PROPERTIES

The thermal properties of Hanford concrete mixes (k, κ, c) were found to be smaller in magnitude than those normally attributed to concrete. Heating the concrete appeared to reduce properties values

still further. Given their importance for analytical purposes, the influence of heat on Hanford concrete thermal properties should be studied more closely. In particular, changes brought about by repeated heating in the range from ambient to 450°F should be studied thoroughly. Tests should include determination of thermal properties values of concrete subjected to at least 2 temperature cycles in this temperature range, and preferably more.

Also, thermal properties tests should be conducted on Hanford concrete mixes subjected to prior heating at 350° to 450°F for a prolonged period to determine if long-term heating produces any additional changes in these properties.

6.4 CREEP BEHAVIOR AT ELEVATED TEMPERATURES

Creep tests were conducted on Hanford concrete mixes at 250° and 350°F in the current study. However, studies by other investigators have indicated that creep strains of normal weight concrete may have a local maximum in the region 120° to 150°F. Creep of Hanford concrete should be investigated in this temperature region to determine if large strains do, in fact, occur. In addition, creep tests should also be conducted at ambient temperature to provide control data against which effects of elevated temperature on creep behavior can be evaluated.

7.0 REFERENCES

1. S. P. Clark, ed., Handbook of Physical Constants, Memoir 97, p. 91, Geological Society of America (1966).

2. L. J. Mitchell, "Thermal Expansion Tests on Aggregates, Neat Cements, and Concretes," Proceedings, ASTM, Vol. 53, pp. 963-977 (1953).

3. D. R. Lankard, D. L. Birkimer, and et al, "Effects of Moisture Content on the Structural Properties of Portland Cement Concrete Exposed to Temperatures up to 500°F," Temperature and Concrete, ACI SP-25, American Concrete Institute, pp. 59-102 (1971).

4. N. G. Zoldners, and H. S. Wilson, "Effect of Sustained and Cyclic Temperatures on LIghtweight Concrete," Temperature Extremes, ACI SP-39, American Concrete Institute, pp. 149-178 (1973).

5. K. W. Nasser, and R. P. Lahtia, "Mass Concrete Properties at High Temperatures," ACI Journal, pp. 180-186 (March, 1971).

6. M. S. Abrams, "Compressive Strength of Concrete at Temperatures to 1600°F," Temperature and Concrete, ACI SP-25, American Concrete Institute, pp. 33-58 (1971).

7. R. Philleo, "Some Physical Properties of Concrete at High Temperature," Portland Cement Association Research Bulletin 97 (1958).

8. C. R. Cruz, "Elastic Properties of Concrete at High Temperatures," Portland Cement Association Research Bulletin 191 (1966).

9. N. G. Zoldners, "Thermal Properties of Concrete Under Sustain Elevated Temperatures,: ACI SP-25, American Concrete Institute, pp. 1-32 (1971).

10. H. L. Malhotra, "The Effect of Temperature on the Compressive Strength of Concrete," Magazine of Concrete Research, Vol. 8, No. 22, pp. 85-94 (1956).

11. Y. Anderberg, "Mechanical Behavior at Fire of Concrete and Hyperstatio Structures," Division of Structural Mechanics and Concrete Construction Bulletin 56, Lund Institute of Technology, Lund, Sweden (1976).

12. U. Schneider, "Behavior of Concrete Under Thermal Steady State and Non-Steady State Conditions," Fire and Materials, Vol. 1, No. 3, pp. 103-115 (1976).

13. ASTM Designation C293, "Standard Method of Test for Flexural Strength of Concrete (Using a Simple Beam with Center-Point Loading)," American Society for Testing and Materials, Philadelphia, Pennsylvania (1967).

14. ASTM Designation C496, "Standard Method of Test for Splitting Tensile Strength of Molded Concrete Cylinders," American Society for Testing and Materials, Philadelphia, Pennsylvania (1967).

15. P. J. Sullivan, and M. P. Pocher, "The Influence of Temperature on the Physical Properties of Concrete and Mortar in the Range 20°C to 400°C," Temperature and Concrete, ACI SP-25, American Concrete Institute, pp. 103-135 (1971).

16. S. Thelandersson, "Effect of High Temperatures on Tensile Strength of Concrete," Division of Structural Machanics and Concrete Construction Bulletin 26, Lund Institute of Technology, Lund, Sweden (1972).

17. K. W. Nasser, "Creep of Concrete at Low Stress-Strength Ratios and Elevated Temperatures," Temperature and Concrete, ACI SP-25, American Concrete Institute, pp. 137-147, (1971).

18. T. E. Northrup, and F. S. Ople, "Effects of Temperature on a Prestressed Concrete Reactor Vessel Model," Temperature and Concrete, ACI SP-25, American Concrete Institute, pp. 149-171. (1971).

19. R. D. Browne, and R. Blundell, "The Influence of Loading Age and Temperature on the Long-Term Creep Behavior of Concrete in a Sealed, Moisture Stable State," Materials & Structures (RILEM), Vol. 2, No. 8, pp. 133-144 (1969).

20. C. R. Cruz, "Apparatus for Measuring Creep of Concrete at High Temperatures," Portland Cement Association Research Department Bulletin 225, Skokie, Illinois (1968).

21 M. P. Gillen, "Short Term Creep of Concrete at Elevated Temperatures," Fire and Materials Journal (1981).

22. Y. Anderberg, and S. Thelandersson, "Stress and Deformation Charactertistics of Concrete at High Temperatures," Division of Structural Mechanics and Concrete Construction Bulletin 54, Lund Institute of Technology, Lund, Sweden (1976).

23. D. Campbell-Allen, E. W. E. Low, and H. Roper, "An Investigation of the Effect of Elevated Temperatures on Concrete for Reactor Vessels," Nuclear Structural Engineering (Amsterdam), Vol. 2, pp. 382-388 (1965).

24. ASTM Designation C42, "Standard Method of Obtaining and Testing Drilled Cores and Sawed Beams of Concrete," American Society of Testing and Materials, Philadelphia, Pennsylvania (1967).

25. ASTM Designation C39, "Standard Method of Test for Compressive Strength of Molded Concrete Cylinders," American Society for Testing and Materials, Philadelphia, Pennsylvania (1967).

26. ASTM Designation C215, "Standard Method of Test for Fundamental Transverse, Longitudinal and Torsional Frequencies of Concrete Specimens," American Society for Testing and Materials, Philadelphia, Pennsylvania (1967).

27. ASTM Designation C469, "Standard Method of Test for Static Young's Modulus of Elasticity and Poisson's Ratio in Compression of Cylindrical Concrete Specimens," American Society for Testing and Materials, Philadelphia, Pennsylvania (1967).

28. ASTM Designation C512, "Tentative Method of Test for Creep of Concrete in Compression," American Society for Testing and Materials, Philadelphia, Pennsylvania (1967).

29. ACI Committee 517, "Proposed ACI Standard: Recommended Practice for Atmospheric Pressure Steam Curing of Concrete," ACI Journal, Vol. 66, No. 8, pp. 629-646 (1969).

30. R. Farsky, and B. S. Basavarajaiah, "Some Studies on (Atmospheric Pressure) Steam Curing of Cement Mortars, "Indian Concrete Journal, Vol. 45, No. 1, pp. 35-41 (1971).

31. T. Z. Harmathy, "Variable State Methods of Measuring the Thermal Properties of Solids," Division of Building Research Paper No. 221, National Research Council, Ottawa, Canada (1964).

32. A. M. Neville, Properties of Concrete, John Wiley & Sons (1973).

33. J. E. Marechal, "Le Fluage du Beton en Fonction de La Temperature, "Materials & Structures (RILEM), Vol. 2, No. 8, pp. 111-115 (1969).

APPENDIX A

MIX DESIGN INFORMATION

TABLE A-1. Batch Ingredients and Physical Properties
for Mix No. 3K1 (Date: April 5, 1975).

Materials
  Cement   Portland Cement Type II
  Fine Aggregate   1-S
                    2-None
  Coarse Aggregate 1-R
                    2-None
  Admixture   1-Darex Air Entrained Additive (AEA)
                    2-None

Batch Ingredients

Cement		505.0 lb/yd^3	5.38 bags
Fine Aggregate	1	1,262.0 lb/yd^3	
	2	0.0 lb/yd^3	
Coarse Aggregate	1	2,131.0 lb/yd^3	
	2	0.00 lb/yd^3	
Admixture	1	0.36 lb/yd^3	
	2	0.00 lb/yd^3	
Water		244.0 lb/yd^3	29.32 gal/yd^3
Total Weight		4,144.34 lb/yd^3	

Physical Properties
of Plastic Concrete
  Slump in inches   2.5
  Air Content, %   1.5
  Unit wt, lb/ft^3 153.4

Batch Analysis

Water cement ratio	0.48 by wt	5.44 gal/bag
% of fine to total aggregate	37.1 by wt	37.5 abs vol
Voids/cement ratio, by absolute vol	1.67 press	1.81 unit wt

Additional Data
  Specimen size: 6- by 12-in. cylinders,
                   cast 15 per batch
  Cure: continuous moist
  Mixer: 6.0 ft^3 tilting drum
  Mix cycle: 5 min all in

TABLE A-2. Batch Ingredients and Physical Properties
for Mix No. 3K2 (Date: April 5, 1975).

Materials

Cement	Portland Cement Type II
Fine Aggregate	1-S
	2-None
Coarse Aggregate	1-R
	2-None
Admixture	1-Darex AEA
	2-None

Batch Ingredients

Cement		507.0	lb/yd^3	5.39 bags/yd^3
Fine Aggregate	1	1,266.0	lb/yd^3	
	2	0.0	lb/yd^3	
Coarse Aggregate	1	2,139.0	lb/yd^3	
	2	0.00	lb/yd^3	
Admixture	1	0.36	lb/yd^3	
	2	0.00	lb/yd^3	
Water		245.0	lb/yd^3	29.42 gal/yd^3
Total Weight		4,158.09	lb/yd^3	

Physical Properties of Plastic Concrete

Slump in inches	1.0
Air Content, %	1.9
Unit wt, lb/ft^3	154.0

Batch Analysis

Water cement ratio	0.48	by wt	5.44 gal/bag
% of fine to total aggregate	37.1	by wt	37.5 abs vol
Voids/cement ratio, by absolute vol	1.71	press	1.78 unit wt

Additional Data

Specimen size:	6- by 12-in. cylinders, cast 17 per batch
Cure:	continuous moist
Mixer:	6.0 ft^3 tilting drum
Mix cycle:	5 min all in

TABLE A-3. Batch Ingredients and Physical Properties
for Mix No. 3K3 (Date: May 22, 1975).

Materials			
Cement	Lone Star Portland Cement Co Type II		
Fine Aggregate	1-S		
	2-None		
Coarse Aggregate	1-R		
	2-None		
Admixture	1-Darex AEA		
	2-None		

Batch Ingredients			
Cement		498.0 lb/yd^3	5.30 bags
Fine Aggregate	1	1,217.0 lb/yd^3	
	2	0.0 lb/yd^3	
Coarse Aggregate	1	2,102.0 lb/yd^3	
	2	0.00 lb/yd^3	
Admixture	1	0.20 lb/yd^3	
	2	0.00 lb/yd^3	
Water		277.00 lb/yd^3	33.28 gal/yd^3
Total Weight		4,096.21 lb/yd^3	

Physical Properties
of Plastic Concrete

Slump in inches	3.0
Air Content, %	3.8
Unit wt, lb/ft^3	151.7

Batch Analysis		
Water cement ratio	0.55 by wt	6.27 gal/yd^3
% of fine to total aggregate	36.6 by wt	37.0 abs vol
Voids/cement ratio, by absolute vol	2.14 press	2.02 unit wt

Additional Data	
Specimen size:	6- by 12-in. cylinders, cast 27 in summ.
Cure:	moist cure 70°F 100% RH 90 days
Mixer:	6.0 ft^3 tilting drum
Mix cycle:	5 min all in

TABLE A-4. Batch Ingredients and Physical Properties
for Mix No. 3K4 (Date: May 22, 1975).

Materials
Cement	Lone Star Portland Cement Co Type II
Fine Aggregate	1-S
	2-None
Coarse Aggregate	1-R
	2-None
Admixture	1-Darex AEA
	2-None

Batch Ingredients
Cement		490.0	lb/yd^3	5.22 bags/yd^3
Fine Aggregate	1	1,198.0	lb/yd^3	
	2	0.0	lb/yd^3	
Coarse Aggregate	1	2,068.0	lb/yd^3	
	2	0.00	lb/yd^3	
Admixture	1	0.29	lb/yd^3	
	2	0.00	lb/yd^3	
Water		247.0	lb/yd^3	29.73 gal/yd^3
Total Weight		4,005.46	lb/yd^3	

Physical Properties of Plastic Concrete
Slump in inches	3.25
Air Content, %	4.9
Unit wt, lb/ft^3	148.3

Batch Analysis
Water cement ratio	0.50 by wt	5.69 gal/yd^3
% of fine to total aggregate	36.6 by wt	37.0 abs vol
Voids/cement ratio, by absolute vol	2.08 press	2.19 unit wt

Additional Data
Specimen size:	6- by 12-in. cylinders, cast 30 in summ.
Cure:	moist cure 70°F 100% RH 90 days
Mixer:	6.0 ft^3 tilting drum
Mix cycle:	5 min all in

TABLE A-5. Batch Ingredients and Physical Properties
for Mix No. 3K5 (Date: May 22, 1975).

Materials
  Cement   Lone Star Portland Cement Co Type II
  Fine Aggregate   1-S
                    2-None
  Coarse Aggregate 1-R
                    2-None
  Admixture   1-Darex AEA
                    2-None

Batch Ingredients
  Cement   494.0   lb/yd^3 5.26 bags/yd^3
  Fine Aggregate   1   1,202.0   lb/yd^3
                      2   0.0   lb/yd^3
  Coarse Aggregate   1   2,083.0   lb/yd^3
                      2   0.00 lb/yd^3
  Admixture   1   0.34 lb/yd^3
                      2   0.00 lb/yd^3
  Water   255.0   lb/yd^3 30.72 gal/yd^3

  Total Weight   4,037.08 lb/yd^3

Physical Properties
of Plastic Concrete
  Slump in inches   3.0
  Air Content, %   4.5
  Unit wt, lb/ft^3 149.5

Batch Analysis
  Water cement ratio   0.51 by wt   5.84 gal/yd^3
  % of fine to total
    aggregate   36.5 by wt   36.9 abs vol
  Voids/cement ratio,
    by absolute vol   2.09 press   2.12 unit wt

Additional Data
  Specimen size: 6- by 12-in. cylinders,
                    cast 30 in summ.
  Cure: moist cure 70°F
                    100% RH 90 days
  Mixer: 6.0 ft^3 tilting drum
  Mix cycle: 5 min all in

TABLE A-6. Batch Ingredients and Physical Properties
for Mix No. 3K6 (Date: May 22, 1975).

Materials
Cement   Lone Star Portland Cement Co Type II
Fine Aggregate   1-S
                  2-None
Coarse Aggregate 1-R
                  2-None
Admixture   1-Darex AEA
                  2-None

Batch Ingredients

Cement		489.0	lb/yd^3	5.21 bags/yd^3
Fine Aggregate	1	1,179.0	lb/yd^3	
	2	0.0	lb/yd^3	
Coarse Aggregate	1	2,071.0	lb/yd^3	
	2	0.00	lb/yd^3	
Admixture	1	0.39	lb/yd^3	
	2	0.00	lb/yd^3	
Water		260.0	lb/yd^3	31.24 gal/yd^3
Total Weight		4,001.33	lb/yd^3	

Physical Properties
of Plastic Concrete
 Slump in inches   3.50
 Air Content, %   5.0
 Unit wt, lb/ft^3 148.1

Batch Analysis

Water cement ratio	0.53 by wt	5.99 gal/yd^3
% of fine to total aggregate	36.2 by wt	36.6 abs vol
Voids/cement ratio, by absolute vol	2.18 press	2.24 unit wt

Additional Data
 Specimen size: 6- by 12-in. cylinders,
                  cast 30 in summ.
 Cure: moist cure 70°F
                  100% RH 90 days
 Mixer: 6.0 ft^3 tilting drum
 Mix cycle: 5 min all in

TABLE A-7. Batch Ingredients and Physical Properties
for Mix No. 3K7 (Date: May 23, 1975).

Materials

Cement	Lone Star Portland Cement Co Type II
Fine Aggregate	1-S
	2-None
Coarse Aggregate	1-R
	2-None
Admixture	1-Darex AEA
	2-None

Batch Ingredients

Cement		484.0 lb/yd^3	5.15 bags/yd^3
Fine Aggregate	1	1,169.0 lb/yd^3	
	2	0.0 lb/yd^3	
Coarse Aggregate	1	2,047.0 lb/yd^3	
	2	0.00 lb/yd^3	
Admixture	1	0.38 lb/yd^3	
	2	0.00 lb/yd^3	
Water		261.0 lb/yd^3	31.42 gal/yd^3
Total Weight		3,962.83 lb/yd^3	

**Physical Properties
of Plastic Concrete**

Slump in inches	3.0
Air Content, %	6.3
Unit wt, lb/ft^3	146.7

Batch Analysis

Water cement ratio	0.53 by wt	6.09 gal/yd^3
% of fine to total aggregate	36.3 by wt	36.6 abs vol
Voids/cement ratio, by absolute vol	2.34 press	2.35 unit wt

Additional Data

Specimen size:	6- by 12-in. cylinders, cast 29 in summ.
Cure:	moist cure 70°F 100% RH 90 days
Mixer:	6.0 ft^3 tilting drum
Mix cycle:	5 min all in

TABLE A-8. Batch Ingredients and Physical Properties
for Mix No. 3K8 (Date: May 23, 1975).

Materials

Cement	Lone Star Portland Cement Co Type II
Fine Aggregate	1-S
	2-None
Coarse Aggregate	1-R
	2-None
Admixture	1-Darex AEA
	2-None

Batch Ingredients

Cement		491.0	lb/yd^3	5.22 bags/yd^3
Fine Aggregate	1	1,183.0	lb/yd^3	
	2	0.0	lb/yd^3	
Coarse Aggregate	1	2,072.0	lb/yd^3	
	2	0.00	lb/yd^3	
Admixture	1	0.34	lb/yd^3	
	2	0.00	lb/yd^3	
Water		267.0	lb/yd^3	32.13 gal/yd^3
Total Weight		4,015.08	lb/yd^3	

Physical Properties
of Plastic Concrete

Slump in inches	3.25
Air Content, %	4.9
Unit wt, lb/ft^3	148.7

Batch Analysis

Water cement ratio	0.54	by wt	6.14	gal/yd^3
% of fine to total aggregate	36.3	by wt	36.6	abs vol
Voids/cement ratio, by absolute vol	2.21	press	2.22	unit wt

Additional Data

Specimen size:	6- by 12-in. cylinders, cast 30 in summ.
Cure:	moist cure 70°F 100% RH 90 days
Mixer:	6.0 ft^3 tilting drum
Mix cycle:	5 min all in

TABLE A-9. Batch Ingredients and Physical Properties
for Mix No. 3K9 (Date: May 23, 1975).

Materials
  Cement   Lone Star Portland Cement Co Type II
  Fine Aggregate   1-S
                      2-None
  Coarse Aggregate   1-R
                      2-None
  Admixture   1-Darex AEA
                      2-None

Batch Ingredients
  Cement   489.0   lb/yd^3 5.21 bags/yd^3
  Fine Aggregate   1   1,179.0   lb/yd^3
                       2   0.0   lb/yd^3
  Coarse Aggregate   1   2,068.0   lb/yd^3
                       2   0.00   lb/yd^3
  Admixture   1   0.36   lb/yd^3
                       2   0.00   lb/yd^3
  Water   263.0   lb/yd^3 31.65 gal/yd^3

  Total Weight   4,001.33   lb/yd^3

Physical Properties
of Plastic Concrete
  Slump in inches   3.00
  Air Content, %   5.0
  Unit wt, lb/ft^3 148.1

Batch Analysis
  Water cement ratio   0.53 by wt   6.07 gal/yd^3
  % of fine to total
    aggregate   36.3 by wt   36.6 abs vol
  Voids/cement ratio,
    by absolute vol   2.20 press   2.24 unit wt

Additional Data
  Specimen size: 6- by 12-in. cylinders,
                     cast 29 in summ.
  Cure: moist cure 70°F
                     100% RH 90 days
  Mixer: 6.0 ft^3 tilting drum
  Mix cycle: 5 min all in

TABLE A-10. Batch Ingredients and Physical Properties
for Mix No. 3K10 (Date: Sept. 21, 1977).

Materials

Cement	Type II
Fine Aggregate	1-S
	2-None
Coarse Aggregate	1-R
	2-None
Admixture	1-Darex, 1/3 Normal Strength)
	2-None
	3-None

Batch Ingredients

Cement		513.0	lb/yd^3	5.46 bags/yd^3
Fine Aggregate	1	1,274.0	lb/yd^3	
	2	0.0	lb/yd^3	
Coarse Aggregate	1	2,191.0	lb/yd^3	
	2	0.00	lb/yd^3	
Admixture	1	0.37	lb/yd^3	
	2	0.00	lb/yd^3	
	3	0.00	lb/yd^3	
Water		222.0	lb/yd^3	26.68 gal/yd^3
Total Weight		4,200.0	lb/yd^3	

Physical Properties of Plastic Concrete

Slump in inches	1.1
Air Content, %	2.5
Unit wt, lb/ft^3	155.6

Batch Analysis

Water cement ratio	0.43	by wt	4.89 gal/yd^3
% of fine to total aggregate	36.8	by wt	37.1 abs vol
Voids/cement ratio, by absolute vol	1.62	press	0.00 unit wt
Paste/aggregate ratio	0.21	by wt	0.31 abs vol
Mix ratio, by wt	1:2.48:4.27		

Additional Data

Specimen size:	6- by 12-in. cylinders,
Cure:	100% RH
Mixer:	6.0 ft^3 tilting drum
Mix cycle:	5 min all in

TABLE A-11. Batch Ingredients and Physical Properties
for Mix No. 3K11 (Date: Sept. 21, 1977).

<u>Materials</u>

Cement	Type II
Fine Aggregate	1-S
	2-None
Coarse Aggregate	1-R
	2-None
Admixture	1-Darex, 1/3 Normal Strength
	2-None
	3-None

<u>Batch Ingredients</u>

Cement		517.0	lb/yd^3	5.50 bags/yd^3
Fine Aggregate	1	1,283.0	lb/yd^3	
	2	0.0	lb/yd^3	
Coarse Aggregate	1	2,206.0	lb/yd^3	
	2	0.00	lb/yd^3	
Admixture	1	0.37	lb/yd^3	
	2	0.00	lb/yd^3	
	3	0.00	lb/yd^3	
Water		224.0	lb/yd^3	26.87 gal/yd^3
Total Weight		4,230.0	lb/yd^3	

<u>Physical Properties</u>
<u>of Plastic Concrete</u>

Slump in inches	2.1
Air Content, %	1.8
Unit wt, lb/ft^3	156.7

<u>Batch Analysis</u>

Water cement ratio	0.43	by wt	4.89 gal/yd^3
% of fine to total aggregate	36.8	by wt	37.1 abs vol
Voids/cement ratio, by absolute vol	1.55	press	0.00 unit wt
Paste/aggregate ratio	0.21	by wt	0.31 abs vol
Mix ratio, by wt	1:2.48:4.27		

<u>Additional Data</u>

Specimen size:	6- by 12-in. cylinders,
Cure:	70°F, 100% RH
Mixer:	6.0 ft^3 tilting drum
Mix cycle:	5 min all in

TABLE A-12. Batch Ingredients and Physical Properties
for Mix No. 3K12 (Date: Sept. 21, 1977).

Materials
 Cement   Type II
 Fine Aggregate   1-S
                   2-None
 Coarse Aggregate 1-R
                   2-None
 Admixture   1-Darex, 1/3 Nor-
                   mal Strength
                   2-None
                   3-None

Batch Ingredients

Cement		516.0	lb/yd^3	5.49 bags/yd^3
Fine Aggregate	1	1,281.0	lb/yd^3	
	2	0.0	lb/yd^3	
Coarse Aggregate	1	2,202.0	lb/yd^3	
	2	0.00	lb/yd^3	
Admixture	1	0.37	lb/yd^3	
	2	0.00	lb/yd^3	
	3	0.00	lb/yd^3	
Water		223.0	lb/yd^3	26.82 gal/yd^3
Total Weight		4,222.0	lb/yd^3	

Physical Properties
of Plastic Concrete
 Slump in inches   3.0
 Air Content, %   2.0
 Unit wt, lb/ft^3 156.4

Batch Analysis

Water cement ratio	0.43	by wt	4.89 gal/yd^3
% of fine to total aggregate	36.8	by wt	37.1 abs vol
Voids/cement ratio, by absolute vol	1.57	press	0.00 unit wt
Paste/aggregate ratio	0.21	by wt	0.31 abs vol
Mix ratio, by wt	1:2.48:4.27		

Additional Data
 Specimen size: 6- by 12-in. cylinders,
 Cure: 70°F, 100% RH
 Mixer: 6.0 ft^3 tilting drum
 Mix cycle: 5 min all in

TABLE A-13. Batch Ingredients and Physical Properties
for Mix No. 3K13 (Date: Sept. 21, 1977).

Materials

Cement	Type II
Fine Aggregate	1-S
	2-None
Coarse Aggregate	1-R
	2-None
Admixture	1-Darex, 1/3 Normal Strength
	2-None
	3-None

Batch Ingredients

Cement		516.0	lb/yd^3	5.49 bags/yd^3
Fine Aggregate	1	1,281.0	lb/yd^3	
	2	0.0	lb/yd^3	
Coarse Aggregate	1	2,202.0	lb/yd^3	
	2	0.00	lb/yd^3	
Admixture	1	0.37	lb/yd^3	
	2	0.00	lb/yd^3	
	3	0.00	lb/yd^3	
Water		223.0	lb/yd^3	26.82 gal/yd^3
Total Weight		4,222.0	lb/yd^3	

Physical Properties of Plastic Concrete

Slump in inches	4.0
Air Content, %	2.0
Unit wt, lb/ft^3	156.4

Batch Analysis

Water cement ratio	0.43	by wt	4.89 gal/yd^3
% of fine to total aggregate	36.8	by wt	37.1 abs vol
Voids/cement ratio, by absolute vol	1.57	press	0.00 unit wt
Paste/aggregate ratio	0.21	by wt	0.31 abs vol
Mix ratio, by wt	1:2.48:4.27		

Additional Data

Specimen size:	6- by 12-in. cylinders,
Cure:	70°F, 100% RH
Mixer:	6.0 ft^3 tilting drum
Mix cycle:	5 min all in

TABLE A-14. Batch Ingredients and Physical Properties
for Mix No. 3K14 (Date: Sept. 23, 1977).

Materials

Cement	Type II
Fine Aggregate	1-S
	2-None
Coarse Aggregate	1-R
	2-None
Admixture	1-Darex, 1/3 nor- mal strength
	2-None
	3-None

Batch Ingredients

Cement		513.0	lb/yd^3	5.45 bags/yd^3
Fine Aggregate	1	1,269.0	lb/yd^3	
	2	0.0	lb/yd^3	
Coarse Aggregate	1	2,193.0	lb/yd^3	
	2	0.00	lb/yd^3	
Admixture	1	0.41	lb/yd^3	
	2	0.00	lb/yd^3	
	3	0.00	lb/yd^3	
Water		228.0	lb/yd^3	27.42 gal/yd^3
Total Weight		4,203.0	lb/yd^3	

Physical Properties of Plastic Concrete

Slump in inches	3.00
Air Content, %	2.2
Unit wt, lb/ft^3	155.7

Batch Analysis

Water cement ratio	0.45	by wt	5.03 gal/yd^3
% of fine to total aggregate	36.7	by wt	37.0 abs vol
Voids/cement ratio, by absolute vol	1.63	press	0.00 unit wt
Paste/aggregate ratio	0.21	by wt	0.31 abs vol
Mix ratio, by wt	1:2.48:4.28		

Additional Data

Specimen size:	6- by 12-in. cylinders,
Cure:	70°F, 100% RH
Mixer:	6.0 ft^3 tilting drum
Mix cycle:	5 min all in

TABLE A-15. Batch Ingredients and Physical Properties
for Mix No. 3K15 (Date: Sept. 23, 1977).

Materials
 Cement   Type II
 Fine Aggregate   1-S
                         2-None
 Coarse Aggregate   1-R
                         2-None
 Admixture   1-Darex, 1/3 nor-
                         mal strength
                         2-None
                         3-None

Batch Ingredients

Cement		509.0	lb/yd^3	5.41 bags/yd^3
Fine Aggregate	1	1,259.0	lb/yd^3	
	2	0.0	lb/yd^3	
Coarse Aggregate	1	2,175.0	lb/yd^3	
	2	0.0	lb/yd^3	
Admixture	1	0.41	lb/yd^3	
	2	0.00	lb/yd^3	
	3	0.00	lb/yd^3	
Water		227.0	lb/yd^3	27.20 gal/yd^3
Total Weight		4,169.0	lb/yd^3	

Physical Properties
of Plastic Concrete
 Slump in inches   4.00
 Air Content, %   3.0
 Unit wt, lb/ft^3 154.4

Batch Analysis
 Water cement ratio   0.45 by wt   5.03 gal/yd^3
 % of fine to total
   aggregate   36.7 by wt   37.0 abs vol
 Voids/cement ratio,
   by absolute vol   1.72 press   0.00 unit wt
 Paste/aggregate
   ratio   0.21 by wt   0.31 abs vol
 Mix ratio, by wt   1:2.48:4.28

Additional Data
 Specimen size: 6- by 12-in. cylinders,
 Cure: 70°F, 100% RH
 Mixer: 6.0 ft^3 tilting drum
 Mix cycle: 5 min all in

TABLE A-16. Mix Design for Steam-cured Cylinders.

Batch number	-	3K16
Date cast	-	October 17, 1977
Type II cement	-	119.3 lb
Sand	-	290.3 lb
Larger aggregates	-	501.6 lb
Water	-	64.9 lb
Darex AEA*	-	39 mL
Slump	-	3.5 in.
Unit weight	-	154.4 lb/ft^3
Number of cylinders cast	-	24

*AEA at 1/3 normal strength

TABLE A-17. Batch Ingredients and Physical Properties
for Mix No. 4.5K1 (Date: April 15, 1975).

Materials

Cement	Portland Cement Type II
Fine Aggregate	1-S
	2-None
Coarse Aggregate	1-R
	2-None
Admixture	1-Darex, 1/3 normal strength
	2-None

Batch Ingredients

Cement		671.0	lb/yd^3	7.14 bags/yd^3
Fine Aggregate	1	1,296.0	lb/yd^3	
	2	0.0	lb/yd^3	
Coarse Aggregate	1	1,921.0	lb/yd^3	
	2	0.00	lb/yd^3	
Admixture	1	0.48	lb/yd^3	
	2	0.00	lb/yd^3	
Water		260.0	lb/yd^3	31.30 gal/yd^3
Total Weight		4,149.0	lb/yd^3	

Physical Properties of Plastic Concrete

Slump in inches	0.5
Air Content, %	2.1
Unit wt, lb/ft^3	153.6

Batch Analysis

Water cement ratio	0.38	by wt	4.38	gal/yd^3
% of fine to total aggregate	40.2	by wt	40.6	abs vol
Voids/cement ratio, by absolute vol	1.38	press	1.41	unit wt

Additional Data

Specimen size:	6- by 12-in. cylinders, cast 16 per batch.
Cure:	continuous moist
Mixer:	6.0 ft^3 tilting drum
Mix cycle:	5 min all in

TABLE A-18. Batch Ingredients and Physical Properties
for Mix No. 4.5K2 (Date: April 5, 1975).

Materials
  Cement   Portland Cement Type II
  Fine Aggregate   1-S
                    2-None
  Coarse Aggregate 1-R
                    2-None
  Admixture   1-Darex, 1/3 nor-
                    mal strength
                    2-None

Batch Ingredients

Cement		673.0	lb/yd^3	7.16 bags/yd^3
Fine Aggregate	1	1,300.0	lb/yd^3	
	2	0.0	lb/yd^3	
Coarse Aggregate	1	1,927.0	lb/yd^3	
	2	0.00	lb/yd^3	
Admixture	1	0.48	lb/yd^3	
	2	0.00	lb/yd^3	
Water		261.0	lb/yd^3	31.40 gal/yd^3
Total Weight		4,163.59	lb/yd^3	

Physical Properties
of Plastic Concrete
  Slump in inches   1.0
  Air Content, %   2.1
  Unit wt, lb/ft^3 154.2

Batch Analysis

Water cement ratio	0.38 by wt	4.38 gal/yd^3
% of fine to total aggregate	40.2 by wt	40.6 abs vol
Voids/cement ratio, by absolute vol	1.38 press	1.39 unit wt

Additional Data
  Specimen size: 6- by 12-in. cylinders,
                  cast 16 per batch.
  Cure: continuous moist
  Mixer: 6.0 ft^3 tilting drum
  Mix cycle: 5 min all in

TABLE A-19. Batch Ingredients and Physical Properties
for Mix No. 4.5K-3 (Date: May 22, 1975).

Materials
 Cement   Lone Star Portland Cement Co Type II
 Fine Aggregate   1-S
  2-None
 Coarse Aggregate 1-R
  2-None
 Admixture   1-Darex, AEA
                   2-None

Batch Ingredients

Cement			652.0	lb/yd^3	6.94 bags/yd^3
Fine Aggregate	1		1,215.0	lb/yd^3	
	2		0.0	lb/yd^3	
Coarse Aggregate	1		1,864.0	lb/yd^3	
	2		0.00	lb/yd^3	
Admixture	1		0.59	lb/yd^3	
	2		0.00	lb/yd^3	
Water			278.00	lb/yd^3	33.38 gal/yd^3
Total Weight			4,010.96	lb/yd^3	

Physical Properties
of Plastic Concrete
 Slump in inches   3.00
 Air Content, %   5.0
 Unit wt, lb/ft^3 148.5

Batch Analysis

Water cement ratio	0.42 by. wt	4.80 gal/yd^3
% of fine to total aggregate	39.4 by wt	39.8 abs vol
Voids/cement ratio, by absolute vol	1.72 press	1.72 unit wt

Additional Data
 Specimen size: 6- by 12-in. cylinders,
                  cast 28 in summ.
 Cure: moist cure 70°F,
                  100% RH 90 days
 Mixer: 6.0 ft^3 tilting drum
 Mix cycle: 5 min all in

TABLE A-20. Batch Ingredients and Physical Properties
for Mix No. 4.5K-4 (Date: May 22, 1975).

Materials
  Cement   Lone Star Portland Cement Co Type II
  Fine Aggregate   1-S
                        2-None
  Coarse Aggregate   1-R
                        2-None
  Admixture   1-Darex, AEA
                        2-None

Batch Ingredients
  Cement   652.0   lb/yd^3 6.94 bags/yd^3
  Fine Aggregate   1   1,209.0   lb/yd^3
                      2   0.0   lb/yd^3
  Coarse Aggregate   1   1,860.0   lb/yd^3
                      2   0.00   lb/yd^3
  Admixture   1   0.63   lb/yd^3
                      2   0.00   lb/yd^3
  Water   289.0   lb/yd^3 34.72 gal/yd^3

  Total Weight   4,012.33   lb/yd^3

Physical Properties
of Plastic Concrete
  Slump in inches   3.00
  Air Content, %   4.6
  Unit wt, lb/ft^3 148.6

Batch Analysis
  Water cement ratio   0.44 by wt   5.00 gal/yd^3
  % of fine to total
    aggregate   39.3 by wt   39.7 abs vol
  Voids/cement ratio,
    by absolute vol   1.75 press   1.74 unit wt

Additional Data
  Specimen size: 6- by 12-in. cylinders,
                      cast 30 in summ.
  Cure: moist cure 70°F,
                      100% RH 90 days
  Mixer: 6.0 ft^3 tilting drum
  Mix cycle: 5 min all in

TABLE A-21. Batch Ingredients and Physical Properties
for Mix No. 4.5K-5 (Date: May 22, 1975).

Materials
Cement   Lone Star Portland Cement Co Type II
Fine Aggregate   1-S
                       2-None
Coarse Aggregate   1-R
                       2-None
Admixture   1-Darex, AEA
                       2-None

Batch Ingredients

Cement		651.0 lb/yd^3	6.93 bags/yd^3
Fine Aggregate	1	1,192.0 lb/yd^3	
	2	0.0 lb/yd^3	
Coarse Aggregate	1	1,855.0 lb/yd^3	
	2	0.00 lb/yd^3	
Admixture	1	0.63 lb/yd^3	
	2	0.00 lb/yd^3	
Water		309.0 lb/yd^3	37.20 gal/yd^3
Total Weight		4,009.58 lb/yd^3	

**Physical Properties
of Plastic Concrete**

Slump in inches	4.00
Air Content, %	4.5
Unit wt, lb/ft^3	148.5

Batch Analysis

Water cement ratio	0.47 by wt	5.36 gal/yd^3
% of fine to total aggregate	39.1 by wt	39.4 abs vol
Voids/cement ratio, by absolute vol	1.85 press	1.78 unit wt

Additional Data
Specimen size: 6- by 12-in. cylinders,
                       cast 28 in summ.
Cure: moist cure 70°F,
                       100% RH 90 days
Mixer: 6.0 ft^3 tilting drum
Mix cycle: 5 min all in

TABLE A-22. Batch Ingredients and Physical Properties
for Mix No. 4.5K-6 (Date: May 22, 1975).

Materials

Cement	Lone Star Portland Cement Co Type II
Fine Aggregate	1-S
	2-None
Coarse Aggregate	1-R
	2-None
Admixture	1-Darex, AEA
	2-None

Batch Ingredients

Cement		640.0 lb/yd^3	6.81 bags/yd^3
Fine Aggregate	1	1,190.0 lb/yd^3	
	2	0.0 lb/yd^3	
Coarse Aggregate	1	1,830.0 lb/yd^3	
	2	0.00 lb/yd^3	
Admixture	1	0.67 lb/yd^3	
	2	0.00 lb/yd^3	
Water		280.0 lb/yd^3	33.63 gal/yd^3
Total Weight		3,942.21 lb/yd^3	

**Physical Properties
of Plastic Concrete**

Slump in inches	4.50
Air Content, %	5.4
Unit wt, lb/ft^3	146.0

Batch Analysis

Water cement ratio	0.43 by wt		4.93 gal/yd^3
% of fine to total aggregate	39.4 by wt		39.7 abs vol
Voids/cement ratio, by absolute vol	1.79 press		1.88 unit wt

Additional Data

Specimen size:	6- by 12-in. cylinders, cast 30 in summ.
Cure:	moist cure 70°F, 100% RH 90 days
Mixer:	6.0 ft^3 tilting drum
Mix cycle:	5 min all in

TABLE A-23. Batch Ingredients and Physical Properties
for Mix No. 4.5K-7 (Date: May 22, 1975).

Materials

Cement	Lone Star Portland Cement Co Type II
Fine Aggregate	1-S
	2-None
Coarse Aggregate	1-R
	2-None
Admixture	1-Darex, AEA
	2-None

Batch Ingredients

Cement			643.0	lb/yd^3	6.84 bags/yd^3
Fine Aggregate	1		1,186.0	lb/yd^3	
	2		0.0	lb/yd^3	
Coarse Aggregate	1		1,832.0	lb/yd^3	
	2		0.00	lb/yd^3	
Admixture	1		0.67	lb/yd^3	
	2		0.00	lb/yd^3	
Water			294.0	lb/yd^3	35.34 gal/yd^3
Total Weight			3,957.33	lb/yd^3	

**Physical Properties
of Plastic Concrete**

Slump in inches	4.50
Air Content, %	5.7
Unit wt, lb/ft^3	146.5

Batch Analysis

Water cement ratio	0.45 by wt	5.16 gal/yd^3
% of fine to total aggregate	39.2 by wt	39.6 abs vol
Voids/cement ratio, by absolute vol	1.88 press	1.87 unit wt

Additional Data

Specimen size:	6- by 12-in. cylinders, cast 29 in summ.
Cure:	moist cure 70°F, 100% RH 90 days
Mixer:	6.0 ft^3 tilting drum
Mix cycle:	5 min all in

TABLE A-24. Batch Ingredients and Physical Properties
for Mix No. 4.5K-8 (Date: May 22, 1975).

Materials

Cement	Lone Star Portland Cement Co Type II
Fine Aggregate	1-S
	2-None
Coarse Aggregate	1-R
	2-None
Admixture	1-Darex, AEA
	2-None

Batch Ingredients

Cement		652.0	lb/yd^3	6.93 bags/yd^3
Fine Aggregate	1	1,207.0	lb/yd^3	
	2	0.0	lb/yd^3	
Coarse Aggregate	1	1,856.0	lb/yd^3	
	2	0.00	lb/yd^3	
Admixture	1	0.68	lb/yd^3	
	2	0.00	lb/yd^3	
Water		294.0	lb/yd^3	35.33 gal/yd^3
Total Weight		4,010.96	lb/yd^3	

**Physical Properties
of Plastic Concrete**

Slump in inches	3.0
Air Content, %	4.6
Unit wt, lb/ft^3	148.5

Batch Analysis

Water cement ratio	0.45 by wt	5.09 gal/yd^3
% of fine to total aggregate	39.4 by wt	39.7 abs vol
Voids/cement ratio, by absolute vol	1.78 press	1.75 unit wt

Additional Data

Specimen size:	6- by 12-in. cylinders, cast 30 in summ.
Cure:	moist cure 70°F, 100% RH 90 days
Mixer:	6.0 ft^3 tilting drum
Mix cycle:	5 min all in

TABLE A-25. Batch Ingredients and Physical Properties
for Mix No. 4.5K-9 (Date: May 23, 1975).

__Materials__
  Cement   Lone Star Portland Cement Co Type II
  Fine Aggregate   1-S
                    2-None
  Coarse Aggregate   1-R
                    2-None
  Admixture   1-Darex, AEA
                    2-None

__Batch Ingredients__

Cement			650.0	lb/yd^3	6.92 bags/yd^3
Fine Aggregate	1		1,240.0	lb/yd^3	
	2		0.0	lb/yd^3	
Coarse Aggregate	1		1,862.0	lb/yd^3	
	2		0.00	lb/yd^3	
Admixture	1		0.68	lb/yd^3	
	2		0.00	lb/yd^3	
Water			239.0	lb/yd^3	28.75 gal/yd^3
Total Weight			3,993.08	lb/yd^3	

__Physical Properties__
__of Plastic Concrete__

Slump in inches	3.50
Air Content, %	5.2
Unit wt, lb/ft^3	147.8

__Batch Analysis__

Water cement ratio		0.36 by wt		4.15 gal/yd^3
% of fine to total aggregate		39.9 by wt		40.3 abs vol
Voids/cement ratio, by absolute vol		1.55 press		1.69 unit wt

__Additional Data__
  Specimen size: 6- by 12-in. cylinders,
                   cast 29 in summ.
  Cure: moist cure 70°F,
                   100% RH 90 days
  Mixer: 6.0 ft^3 tilting drum
  Mix cycle: 5 min all in

TABLE A-26. Batch Ingredients and Physical Properties
for Mix No. 4.5K-10 (Date: Sept. 21, 1977).

Materials

Cement	Type II
Fine Aggregate	1-S
	2-None
Coarse Aggregate	1-R
	2-None
Admixture	1-Darex, 1/3 normal strength
	2-None
	3-None

Batch Ingredients

Cement		675.0	lb/yd^3	7.19 bags/yd^3
Fine Aggregate	1	1,286.0	lb/yd^3	
	2	0.0	lb/yd^3	
Coarse Aggregate	1	1,949.0	lb/yd^3	
	2	0.00	lb/yd^3	
Admixture	1	0.49	lb/yd^3	
	2	0.00	lb/yd^3	
	3	0.00	lb/yd^3	
Water		262.0	lb/yd^3	31.48 gal/yd^3
Total Weight		4,172.0	lb/yd^3	

Physical Properties of Plastic Concrete

Slump in inches	5.4
Air Content, %	2.0
Unit wt, lb/ft^3	154.5

Batch Analysis

Water cement ratio	0.39	by wt	4.38	gal/yd^3
% of fine to total aggregate	39.7	by wt	40.1	abs vol
Voids/cement ratio, by absolute vol	1.38	press	0.00	unit wt
Paste aggregate ratio	0.29	by wt	0.41	ABS vol
Mix ratio, by wt	1:1.90:2.89			

Additional Data

Specimen size:	6- by 12-in. cylinders,
Cure:	70°F, 100% RH
Mixer:	6.0 ft^3 tilting drum
Mix cycle:	5 min all in

TABLE A-27. Batch Ingredients and Physical Properties
for Mix No. 4.5K-10 (Date: Sept. 23, 1977).

Materials

Cement	Type II		
Fine Aggregate	1-S		
	2-None		
Coarse Aggregate	1-R		
	2-None		
Admixture	1-Darex, 1/3 normal strength		
	2-None		
	3-None		

Batch Ingredients

Cement		674.0	lb/yd^3	7.17	bags/yd^3
Fine Aggregate	1	1,283.0	lb/yd^3		
	2	0.0	lb/yd^3		
Coarse Aggregate	1	1,945.0	lb/yd^3		
	2	0.00	lb/yd^3		
Admixture	1	0.49	lb/yd^3		
	2	0.00	lb/yd^3		
	3	0.00	lb/yd^3		
Water		262.00	lb/yd^3	31.42	gal/yd^3
Total Weight		4,164.0	lb/yd^3		

Physical Properties
of Plastic Concrete

Slump in inches	3.75
Air Content, %	2.2
Unit wt, lb/ft^3	154.2

Batch Analysis

Water cement ratio	0.39	by wt	4.38	gal/yd^3
% of fine to total aggregate	39.7	by wt	40.1	abs vol
Voids/cement ratio, by absolute vol	1.40	press	0.00	unit wt
Paste/aggregate ratio	0.29	by wt	0.41	ABS vol
Mix ratio, by wt	1:1.90:2.89			

Additional Data

Specimen size:	6- by 12-in. cylinders,
Cure:	70oF, 100% RH
Mixer:	6.0 ft^3 tilting drum
Mix cycle:	5 min all in

TABLE A-28. Batch Ingredients and Physical Properties
for Mix No. 4.5K-12 (Date: Sept. 23, 1977).

Materials
Cement   Type II
Fine Aggregate   1-S
                        2-None
Coarse Aggregate   1-R
                        2-None
Admixture   1-Darex, 1/3 nor-
                        mal strength
                        2-None
                        3-None

Batch Ingredients

Cement		669.0	lb/yd^3	7.12 bags/yd^3
Fine Aggregate	1	1,280.0	lb/yd^3	
	2	0.0	lb/yd^3	
Coarse Aggregate	1	1,940.0	lb/yd^3	
	2	0.00	lb/yd^3	
Admixture	1	0.71	lb/yd^3	
	2	0.00	lb/yd^3	
	3	0.00	lb/yd^3	
Water		244.0	lb/yd^3	29.30 gal/yd^3
Total Weight		4,134.0	lb/yd^3	

Physical Properties
of Plastic Concrete
Slump in inches   4.8
Air Content, %   3.5
Unit wt, lb/ft^3 153.1

Batch Analysis

Water cement ratio	0.36 by wt	4.42 gal/yd^3
% of fine to total aggregate	39.7 by wt	40.1 abs vol
Voids/cement ratio, by absolute vol	1.43 press	0.00 unit wt
Paste/aggregate ratio	0.28 by wt	0.39 ABS vol
Mix ratio, by wt	1:1.91:2.90	

Additional Data
Specimen size: 6- by 12-in. cylinders,
Cure: 70°F, 100% RH
Mixer: 6.0 ft^3 tilting drum
Mix cycle: 5 min all in

TABLE A-29. Batch Ingredients and Physical Properties
for Mix No. 4.5K-13 (Date: Sept. 23, 1975).

Materials

Cement	Type II
Fine Aggregate	1-S
	2-None
Coarse Aggregate	1-R
	2-None
Admixture	1-Darex, 1/3 normal strength
	2-None
	3-None

Batch Ingredients

Cement		671.0 lb/yd^3	7.14 bags/yd^3
Fine Aggregate	1	1,284.0 lb/yd^3	
	2	0.0 lb/yd^3	
Coarse Aggregate	1	1,946.0 lb/yd^3	
	2	0.00 lb/yd^3	
Admixture	1	0.71 lb/yd^3	
	2	0.00 lb/yd^3	
	3	0.00 lb/yd^3	
Water		245.0 lb/yd^3	29.39 gal/yd^3
Total Weight		4,146.0 lb/yd^3	

Physical Properties
of Plastic Concrete

Slump in inches	3.5
Air Content, %	3.2
Unit wt, lb/ft^3	153.6

Batch Analysis

Water cement ratio	0.36 by wt	4.12 gal/yd^3
% of fine to total aggregate	39.7 by wt	40.1 abs vol
Voids/cement ratio, by absolute vol	1.40 press	0.00 unit wt
Paste/aggregate ratio	0.28 by wt	0.39 ABS vol
Mix ratio, by wt	1:1.91:2.90	

Additional Data

Specimen size:	6- by 12-in. cylinders,
Cure:	70°F, 100% RH
Mixer:	6.0 ft^3 tilting drum
Mix cycle:	5 min all in

APPENDIX B

SPECIMEN WEIGHT AND DIMENSIONS, AND STRENGTH AND
ELASTIC PROPERTIES USING THE STATIC METHOD

TABLE B-1. Dimensions and Weights of Cylinders
at Ambient Temperature.

Specimen Number	Diameter, in.	Height, in.	Weight, lb
3K3-1	6.00	11.99	30.15
3K3-3	6.02	12.00	30.24
3K3-5	5.98	11.95	30.32
3K3-7	5.99	12.15	30.56
3K3-8	6.01	11.97	30.40
3K3-9	6.03	12.15	30.40
3K3-10	6.01	11.99	30.31
3K3-11	6.01	11.94	30.22
3K3-12	6.00	12.02	30.29
3K3-13	6.01	12.15	30.48
3K3-14	6.01	12.05	30.35
3K3-17	6.02	11.95	30.21
3K3-20	6.02	11.93	30.18
3K3-23	5.99	11.98	30.16
3K3-25	6.01	11.99	29.33
3K3-26	6.03	11.96	30.39
3K3-27	6.01	12.00	30.00
3K4-1	6.04	12.00	29.60
3K4-2	6.04	12.11	29.74
3K4-3	6.05	11.98	29.60
3K4-4	6.02	12.12	29.75
3K4-5	6.01	11.98	29.54
3K4-7	5.99	11.99	29.65
3K4-8	6.03	11.96	29.50
3K4-9	6.02	11.97	29.64
3K4-10	6.00	12.05	29.71
3K4-11	6.02	11.95	29.65
3K4-14	6.02	11.98	29.65
3K4-15	6.00	11.97	29.58
3K4-16	6.03	11.96	29.43
3K4-17	5.99	11.97	29.55
3K4-18	6.00	12.12	29.70
3K4-19	6.03	11.99	29.51
3K4-20	6.06	12.00	29.62
3K4-23	6.06	12.01	29.66
3K4-24	6.03	11.99	29.55
3K4-25	5.98	12.10	29.65
3K4-26	6.01	12.05	29.72
3k4-27	6.02	12.05	29.93
3K4-28	5.98	12.06	29.68
3K4-29	6.01	12.08	29.70
3K4-30	6.01	12.08	29.63

TABLE B-1. Dimensions and Weights of Cylinders
at Ambient Temperature (Continued).

Specimen Number	Diameter, in.	Height, in.	Weight, lb
3K5-2	6.04	11.93	29.59
3K5-3	6.00	12.01	29.76
3K5-4	6.02	11.97	29.77
3K5-5	6.03	11.99	29.64
3K5-7	6.01	12.11	29.97
3K5-8	6.01	11.97	29.86
3K5-9	6.00	11.95	29.81
3K5-10			
3K5-11	5.98	11.93	29.82
3K5-12	6.01	12.11	29.88
3K5-13	6.02	12.13	30.16
3K5-14	6.01	11.97	29.87
3K5-17	6.01	12.00	29.94
3K5-20	5.99	11.97	29.84
3K5-23	5.99	11.96	29.76
3K5-25	6.01	12.00	29.70
3K5-27	6.00	12.00	29.74
3K5-28	6.01	12.00	29.69
3K6-1	6.03	11.99	29.59
3K6-3	6.03	11.98	29.50
3K6-4	6.03	12.12	29.58
3K6-5	6.01	12.00	29.61
3K6-6	6.01	12.15	29.62
3K6-8	6.01	11.99	29.57
3K6-10	6.00	12.13	29.95
3K6-11	6.02	11.94	29.51
3K6-14	6.00	11.98	29.55
3K6-16	6.00	12.10	29.77
3K6-17	6.00	11.99	29.53
3K6-19	6.03	11.98	29.66
3K6-23	6.04	12.00	29.53
3K6-24	6.01	12.15	29.64
3K6-25	6.01	11.97	29.55
3K6-26	6.00	12.10	29.74
3K6-27	5.98	12.01	29.64
3K6-28	5.99	11.99	29.63
3K6-30	6.02	11.98	29.62
3K7-1	6.00	12.01	29.13
3K7-2	6.01	11.95	28.94
3K7-3	6.08	12.01	29.11
3K7-4	6.00	12.07	29.16
3K7-5	6.03	11.97	28.95

TABLE B-1. Dimensions and Weights of Cylinders
at Ambient Temperature (Continued).

Specimen Number	Diameter, in.	Height, in.	Weight, lb
3K7-6	6.00	12.09	29.21
3K7-7	6.02	12.12	29.41
3K7-8	6.03	11.97	28.84
3K7-9	6.07	12.12	29.14
3K7-10	6.02	11.98	28.99
3K7-11	6.02	11.96	29.09
3K7-14	6.00	11.97	28.90
3K7-17	6.01	11.98	29.07
3K7-19	6.01	11.95	29.27
3K7-20	6.02	12.00	28.97
3K7-21	6.00	11.98	29.12
3K7-22	5.98	12.11	29.04
3K7-23	6.02	11.99	29.28
3K7-24	6.04	12.13	29.40
3K7-25	6.03	11.99	29.10
3K7-27	6.03	11.97	29.04
3K7-28	6.02	12.13	28.35
3K8-1	6.01	11.98	29.49
3K8-3	6.02	11.99	29.56
3K8-4	6.01	12.10	29.48
3K8-5	6.06	11.98	29.45
3K8-6	6.00	12.17	29.67
3K8-8	6.02	11.98	29.55
3K8-11	6.01	11.99	29.59
3K8-13	6.05	12.17	29.59
3K8-14	6.03	11.98	29.43
3K8-15	-	-	-
3K8-17	6.03	11.98	29.57
3K8-18	-	-	-
3K8-21	5.96	11.97	29.38
3K8-22	6.00	12.01	29.61
3K8-23	-	-	-
3K8-24	6.00	11.98	29.62
3K8-25	6.03	12.00	29.51
3K8-26	6.00	12.17	29.69
3K8-28	6.01	12.03	29.67
3K8-29	-	-	-
3K8-30	6.00	11.97	29.57
3K9-1	6.01	11.96	29.51
3K9-2	5.98	12.10	29.84
3K9-3	6.05	11.94	29.37
3K9-5	6.01	11.99	29.56

TABLE B-1. Dimensions and Weights of Cylinders
at Ambient Temperature (Continued).

Specimen Number	Diameter, in.	Height, in.	Weight, lb
3K9-8	5.99	11.99	29.61
3K9-9	6.04	12.13	29.72
3K9-10	5.99	12.11	29.72
3K9-11	6.03	11.97	29.62
3K9-12	5.99	12.09	29.76
3K9-14	6.01	11.97	29.63
3K9-17	6.01	11.99	29.64
3K9-20	6.00	11.96	29.46
3K9-23	6.03	11.98	29.62
3K9-25	6.00	11.97	29.54
3K9-28	6.03	11.98	29.54
3K9-29	5.99	12.10	29.64
4.5K3-1	6.01	12.01	29.45
4.5K3-2	6.02	12.06	29.63
4.5K3-3	6.00	12.02	29.46
4.5K3-5	6.00	12.01	29.37
4.5K3-7	6.02	12.11	29.75
4.5K3-8	5.99	11.97	29.37
4.5K3-11	6.01	12.01	29.42
4.5K3-14	5.98	11.98	29.36
4.5K3-15	6.03	12.11	29.57
4.5K3-17	6.01	12.01	29.43
4.5K3-18	6.01	12.08	29.57
4.5K3-19	6.03	11.99	29.40
4.5K3-21	6.01	11.99	29.32
4.5K3-22	6.00	11.95	29.36
4.5K3-23	6.02	11.99	29.45
4.5K3-25	6.05	11.98	29.44
4.5K3-27	5.98	12.01	29.31
4.5K4-1	6.00	11.97	29.45
4.5K4-3	6.02	11.92	29.41
4.5K4-4	5.98	12.01	29.58
4.5K4-6	6.05	12.11	29.64
4.5K4-7	6.03	11.99	29.63
4.5K4-8	6.02	11.95	29.43
4.5K4-10	6.01	12.15	29.48
4.5K4-11	6.07	11.97	29.44
4.5K4-12	6.00	12.00	29.52
4.5K4-13	5.99	12.04	29.60
4.5K4-14	6.00	11.97	29.72
4.5K4-15	6.02	12.02	29.82
4.5K4-17	6.03	12.00	29.73
4.5K4-19	6.05	12.13	29.70

TABLE B-1. Dimensions and Weights of Cylinders
at Ambient Temperature (Continued).

Specimen Number	Diameter, in.	Height, in.	Weight, lb
4.5K4-20	6.02	11.96	29.58
4.5K4-21	6.01	11.95	29.64
4.5K4-23	6.04	11.93	29.57
4.5K4-24	6.02	12.02	29.74
4.5K4-26	6.00	12.08	29.66
4.5K4-28	6.01	12.06	29.50
4.5K4-29	5.95	12.09	29.62
4.5K4-30	5.99	12.09	29.73
4.5K5-1	5.99	11.92	29.47
4.5K5-2	5.99	11.96	29.60
4.5K5-3	6.01	11.98	29.60
4.5K5-5	5.99	12.00	29.66
4.5K5-6	6.00	12.14	29.80
4.5K5-7	6.00	11.96	29.47
4.5K5-8	5.98	12.02	29.62
4.5K5-9	5.98	11.99	29.41
4.5K5-10	5.96	12.12	29.65
4.5K5-11	6.00	11.99	29.43
4.5K5-13	6.02	12.06	29.69
4.5K5-14	6.03	11.97	29.46
4.5K5-16	6.03	11.93	29.45
4.5K5-20	5.98	12.01	29.30
4.5K5-23	5.99	11.95	29.25
4.5K5-25	6.04	12.00	29.53
4.5K5-27	6.02	12.14	29.67
4.5K5-28	6.00	12.14	29.80
4.5K6-2	6.01	12.09	29.35
4.5K6-3	6.01	11.96	29.12
4.5K6-6	6.00	11.97	29.14
4.5K6-7	6.03	12.11	29.21
4.5K6-8	6.02	11.99	29.09
4.5K6-11	6.03	12.02	29.23
4.5K6-12	6.01	11.95	29.28
4.5K6-14	6.01	11.99	29.17
4.5K6-17	6.03	12.02	29.30
4.5K6-18	6.02	11.97	29.23
4.5K6-19	6.02	12.14	29.43
4.5K6-20	6.00	12.00	29.30
4.5K6-23	6.03	11.98	29.25
4.5K6-24	6.04	12.07	29.48
4.5K6-25	6.03	11.94	29.12
4.5K6-26	6.00	12.00	29.25
4.5K6-27	6.04	11.97	29.16

TABLE B-1. Dimensions and Weights of Cylinders
at Ambient Temperature (Continued).

Specimen Number	Diameter, in.	Height, in.	Weight, lb
4.5K6-28	6.02	11.99	29.29
4.5K6-29	6.01	12.12	29.39
4.5K7-1	5.94	11.97	29.01
4.5K7-2	6.01	12.09	29.37
4.5K7-3	5.96	11.98	29.11
4.5K7-4	6.01	12.01	29.05
4.5K7-5	5.99	12.09	29.24
4.5K7-8	5.98	11.97	28.97
4.5K7-9	6.05	12.13	29.35
4.5K7-10	6.03	11.98	29.16
4.5K7-12	6.02	12.12	29.25
4.5K7-15	6.01	12.00	29.06
4.5K7-17	6.02	11.95	29.07
4.5K7-18	5.99	11.97	29.05
4.5K7-19	6.01	12.12	29.21
4.5K7-20	6.02	11.96	28.98
4.5K7-21	5.99	11.96	28.99
4.5K7-22	5.98	11.99	28.95
4.5K7-23	6.02	11.98	29.10
4.5K7-24	6.03	11.97	29.09
4.5K7-25	6.02	11.98	29.19
4.5K7-27	5.98	11.99	29.01
4.5K7-28	6.01	12.13	29.36
4.5K7-29	6.02	12.13	29.19
4.5K8-1	6.07	11.98	29.50
4.5K8-2	-	-	-
4.5K8-3	-	12.01	29.55
4.5K8-5	-	-	-
4.5K8-6	6.01	11.97	29.42
4.5K8-8	5.99	11.97	29.53
4.5K8-10	6.02	11.93	29.43
4.5K8-11	6.02	11.96	29.46
4.5K8-12	6.02	12.16	29.72
4.5K8-13			
4.5K8-14	6.03	12.00	29.66
4.5K8-15	6.02	12.12	29.60
4.5K8-16	6.01	11.95	29.41
4.5K8-17	6.03	11.96	29.70
4.5K8-18	6.03	12.13	29.75
4.5K8-20	-	-	-
4.5K8-22	6.02	11.96	29.46
4.5K8-23	5.96	11.97	29.48

TABLE B-1. Dimensions and Weights of Cylinders
at Ambient Temperature (Continued).

Specimen Number	Diameter, in.	Height, in.	Weight, lb
4.5K8-24	-	-	-
4.5K8-25	6.00	12.00	29.51
4.5K8-26	6.02	12.16	29.71
4.5K8-27	6.00	11.98	29.50
4.5K8-28	6.00	11.97	29.43
4.5K8-29	6.01	11.99	29.54
4.5K8-30	6.01	12.00	29.66
4.5K9-1	6.01	11.94	29.29
4.5K9-2	6.02	12.14	29.46
4.5K9-3	6.05	11.97	29.40
4.5K9-5	5.99	11.98	29.46
4.5K9-8	6.03	12.03	29.54
4.5K9-11	5.98	11.99	29.38
4.5K9-14	6.05	11.94	29.34
4.5K9-15	6.02	12.15	29.60
4.5K9-17	6.00	11.99	29.49
4.5K9-24	6.01	12.17	29.68
4.5K9-25	6.04	11.98	29.31
4.5K9-29	6.03	12.13	29.65

TABLE B-2. Compressive Strength and Elastic Properties of Specimens
at Room and Elevated Temperatures Using the Static Method.

Specimen Number	Date of Test	Age at Test, Days	Days in Fog Room*	Temperature at Test, °F	Compressive Strength, psi	Modulus of Elasticity, psi	Poisson's Ratio
3K2-6	5-5-75	30	30	70	6,195	5.39	0.21
3K1-5	5-9-75	34	34	70	5,120	3.97	0.18
3K1-7	5-9-75	34	34	70	5,480	4.33	0.21
3K1-3	5-9-75	34	30	350	6,150	3.46	0.14
3K2-2	5-9-75	34	30	350	6,180	3.92	0.17
4.5K1-7	5-5-75	30	30	70	7,030	5.99	0.20
4.5K2-7	5-9-75	34	34	70	7,380	5.28	0.19
4.5K1-5	5-9-75	34	30	350	7,610	3.91	0.16
4.5K2-3	5-7-75	34	30	350	7,990	4.35	0.12
3K1-2	6-13-75	69	30	350	6,300	3.28	0.16
3K2-1	6-13-75	69	30	350	6,590	3.50	0.13
4.5K1-8	6-13-75	69	30	350	7,550	3.66	0.14
4.5K2-2	6-13-75	69	30	350	7,815	3.65	0.12
3K1-4	6-15-75	71	71	70	6,100	5.40	0.22
4.5K2-15	6-15-75	71	71	70	7,605	6.40	0.24
3K2-12	6-17-75	73	65	450	6,210	2.64	0.14
3K2-5	6-19-75	75	71	350	6,950	4.03	0.14
3K2-13	6-19-75	75	71	350	6,530	4.23	0.13
4.5K1-9	6-19-75	75	71	350	7,800	4.57	0.16
4.5K1-15	6-19-75	75	71	350	8,130	4.71	0.16

*Specimens in fog room at 100% RH and 70°F. Specimens tested at 350°F and 450°F removed from fog room at 30 days and heated in oven at 75°F/day to test temperature.

TABLE B-2. Compressive Strength and Elastic Properties of Using
the Static Method at Room and Elevated Temperatures (Continued).

Specimen Number	Date of Test	Age at Test, Days	Time in Fog Room,* Days[1]	Time in Oven, Days[2]	Temperature at test, °F	Weight at Test, lb	Compressive Strength, psi	Modulus of Elasticity, million psi	Poisson's Ratio
3K4-28	6-21-75	30	30	0	70	29.62	4,430	4.48	0.15
3K4-30	6-21-75	30	30	0	70	29.49	4,250	4.05	0.15
4.5K4-28	6-21-75	30	30	0	70	29.37	5,160	4.32	0.15
4.5K4-30	6-21-75	30	30	0	70	29.68	5,510	4.58	0.16
3K9-1	12-2-75	194	194	0	70	29.51	5,570	4.65	0.16
3K9-3	12-2-75	194	194	0	70	29.37	5,480	4.76	0.16
4.5K9-1	12-2-75	194	194	0	70	29.29	6,450	5.00	0.16
4.5K9-3	12-2-75	194	194	0	70	29.40	6,320	5.02	0.18
3K6-25	1-19-76	240	240	0	70	29.55	5,680	4.87	0.17
4.5K6-25	1-19-76	240	240	0	70	29.12	6,530	5.03	0.16
3K6-28	5-17-76	361	361	0	70	29.64	5,410	4.38	0.17
4.5K6-28	5-17-76	361	361	0	70	29.31	6,790	4.46	0.17
3K5-28	3-31-77	679	679	0	70	29.71	5,860	5.06	0.15
3K8-28	3-31-77	679	679	0	70	29.68	-[3]	4.92	0.16
4.5K5-9	3-31-77	679	679	0	70	29.43	6,640	5.64	0.18
4.5K8-29	3-31-77	679	679	0	70	29.56	-	5.44	0.18
3K4-9	11-18-77	880	880	0	70	29.64	5,750	4.61	0.15
3K4-15	11-18-77	880	880	0	70	29.58	-	4.83	0.17
4.5K4-7	11-18-77	880	880	0	70	29.63	5,950	5.71	0.18
4.5K4-12	11-18-77	880	880	.0	70	29.53	-	5.39	0.17
3K8-15	9-6-78	1,204	1,204	0	70		6,070	4.98	0.16
3K8-18	9-6-78	1,204	1,204	0	70		-	5.21	0.18
3K8-29	9-6-78	1,204	1,204	0	70		6,150	5.06	0.16
4.5K8-5	9-6-78	1,204	1,204	0	70		-	5.65	0.19
4.5K8-20	9-6-78	1,204	1,204	0	70		7,725	5.48	0.20
4.5K8-24	9-6-78	1,204	1,204	0	70		8,120	5.79	0.19

[1]Specimens in fog room at 100% RH and 70°F.

[2]Specimens tested at 250°, 350°, and 450°F heated in oven at 75°F/day to test temperature.

[3]Designates that specimen was used for splitting tensile test after elastic constants were determined.

TABLE B-2. Compressive Strength and Elastic Properties of Using the Static Method at Room and Elevated Temperatures (Continued).

Specimen Number	Date of Test	Age at Test, Days	Time in Fog Room,* Days[1]	Time in Oven, Days[2]	Temperature at test, ^{o}F	Weight at Test, lb	Compressive Strength, psi	Modulus of Elasticity, million psi	Poisson's Ratio
3K3-1	12-4-75	196	193	3	250	29.15	5,600	3.82	0.14
3K3-5	12-4-75	196	193	3	250	29.34	5,590	4.03	0.13
3K3-3	12-4-75	196	193	3	250	29.23	-[3]	3.80	0.13
4.5K3-3	12-4-75	196	193	3	250	28.58	5,320	3.82	0.12
4.5K3-5	12-4-75	196	193	3	250	28.54	5,230	4.04	0.14
4.5K3-1	12-4-75	196	193	3	250	28.70	-	3.91	0.12
3K8-3	12-11-75	203	193	10	250	27.81	5,665	3.66	0.15
3K8-5	12-11-75	203	193	10	250	27.74	5,420	3.71	0.14
3K8-1	12-11-75	203	193	10	250	27.74	-	3.71	0.11
4.5K8-1	12-11-75	203	193	10	250	27.79	6,920	4.36	0.14
4.5K8-6	12-11-75	203	193	10	250	27.72	6,780	4.04	0.14
4.5K8-3	12-11-75	203	193	10	250	27.94	-[3]	4.11	0.14
3K7-1	12-31-75	223	193	30	250	27.33	5,295	3.02	0.12
3K7-5	12-31-75	223	193	30	250	27.16	5,250	3.04	0.13
3K7-3	12-31-75	223	193	30	250	27.29	-	3.14	0.15
4.5K7-3	12-31-75	223	193	30	250	27.32	6,055	3.31	0.15
4.5K7-4	12-31-75	223	193	30	250	27.24	5,930	3.42	0.14
4.5K7-1	12-31-75	223	193	30	250	27.22	-	4.06	0.19
3K4-1	2-19-76	273	193	80	250	27.72	5,170	3.13	0.15
3K4-3	2-19-76	273	193	80	250	27.75	5,160	3.05	0.13
3K4-5	2-19-76	273	193	80	250	27.67	-	3.24	0.13
4.5K4-3	2-19-76	273	193	80	250	27.61	6,290	3.40	0.12
4.5K4-4	2-19-76	273	193	80	250	27.80	6,020	3.42	0.15
4.5K4-1	2-19-76	273	193	80	250	27.59	-	3.34	0.12
3K5-3	4-29-76	343	193	150	250	27.95	5,710	3.15	0.11
3K5-5	4-29-76	343	193	150	250	27.82	5,510	3.09	0.12

[1]Specimens in fog room at 100% RH and 70°F.

[2]Specimens tested at 250°, 350°, and 450°F heated in oven at 75°F/day to test temperature.

[3]Designates that specimen was used for splitting tensile test after elastic constants were determined.

TABLE B-2. Compressive Strength and Elastic Properties of Using
the Static Method at Room and Elevated Temperatures (Continued).

Specimen Number	Date of Test	Age at Test, Days	Time in Fog Room,* Days[1]	Time in Oven, Days[2]	Temperature at test, °F	Weight at Test, lb	Compressive Strength, psi	Modulus of Elasticity, million psi	Poisson's Ratio
3.K5-2	4-29-76	343	193	150	250	27.84	_[3]	3.13	0.12
4.5K5-3	4-29-76	343	193	150	250	27.72	6,160	3.41	0.14
4.5K5-5	4-29-76	343	193	150	250	27.76	6,180	3.18	0.11
4.5K5-1	4-29-76	343	193	150	250	27.64	-	3.12	0.12
3K6-3	8-27-76	463	193	270	250	27.71	5,250	3.09	0.14
3K6-5	8-27-76	463	193	270	250	27.84	5,080	3.00	0.12
3K6-1	8-27-76	463	193	270	250	27.80	-	2.84	0.14
4.5K6-3	8-27-76	463	193	270	250	27.11	6,020	3.16	0.12
4.5K6-6	8-27-76	463	193	270	250	27.14	5,990	3.07	0.13
4.5K6-8	8-27-76	463	193	270	250	27.04	-	3.68	0.14
3K9-14	4-1-77	679	283	396	250	27.77	5,190	3.17	0.13
3K9-20	4-1-77	679	283	396	250	27.59	4,990	3.08	0.13
3K9-17	4-1-77	679	283	396	250	27.78	-	3.15	0.13
4.5K8-25	4-1-77	679	283	396	250	27.64	6,470	3.36	0.13
4.5K8-28	4-1-77	679	283	396	250	27.49	7,020	3.48	0.12
4.5K8-16	4-1-77	679	283	396	250	27.50	-	3.41	0.11
3K9-25	9-29-77	861	283	578	250	27.69	5,300	3.07	0.14
3K9-28	9-29-77	861	283	578	250	27.68	5,080	3.03	0.14
3K9-23	9-29-77	861	283	578	250	27.76	-	2.99	0.18
4.5K8-10	9-29-77	861	283	578	250	27.54	6,620	3.32	0.12
4.5K8-27	9-29-77	861	283	578	250	27.64	6,425	3.21	0.12
4.5K8-22	9-29-77	861	283	578	250	27.57	-	3.21	0.12
3K8-21	9-1-78	1,198	276	922	250		4,530	2.43	0.11
3K8-25	9-1-78	1,198	276	922	250		4,625	2.60	0.13
3K8-30	9-1-78	1,198	276	922	250		-	2.71	0.14

[1]Specimens in fog room at 100% RH and 70°F.

[2]Specimens tested at 250°, 350°, and 450°F heated in oven at 75°F/day to test temperature.

[3]Designates that specimen was used for splitting tensile test after elastic constants were determined.

TABLE B-2. Compressive Strength and Elastic Properties of Using the Static Method at Room and Elevated Temperatures (Continued).

Specimen Number	Date of Test	Age at Test, Days	Time in Fog Room,* Days[1]	Time in Oven, Days[2]	Temperature at test, °F	Weight at Test, lb	Compressive Strength, psi	Modulus of Elasticity, million psi	Poisson's Ratio
4.5K9-5	9-1-78	1,198	270	928	250		-[3]	4.01	0.14
4.5K9-8	9-1-78	1,198	270	928	250		5,855	3.29	0.13
4.5K9-25	9-1-78	1,198	270	928	250		5,890	3.37	0.13
3K3-8	12-5-75	197	193	4	350	28.64	6,100	3.47	0.12
3K3-14	12-5-75	197	193	4	350	28.53	5,780	3.38	0.09
3K3-11	12-5-75	197	193	4	350	28.37	-	3.53	0.10
4.5K3-8	12-5-75	197	193	4	350	27.63	5,600	4.04	0.17
4.5K3-14	12-5-75	197	193	4	350	27.65	5,430	3.33	0.14
4.5K3-11	12-5-75	197	193	4	350	27.55	-	3.46	0.12
3K4-8	12-11-75	203	193	10	350	27.53	5,150	2.69	0.10
3K4-11	12-11-75	203	193	10	350	27.58	4,740	2.62	0.12
3K4-14	12-11-75	203	193	10	350	27.71	-	2.73	0.14
4.5K4-8	12-11-75	203	193	10	350	27.50	6,520	3.09	0.11
4.5K4-11	12-11-75	203	193	10	350	27.50	6,330	3.40	0.10
4.5K4-14	12-11-75	203	193	10	350	27.80	-	3.04	0.09
3K5-11	12-31-75	223	193	30	350	27.90	5,480	2.72	0.14
3K5-14	12-31-75	223	193	30	350	27.93	5,540	2.59	0.11
3K5-8	12-31-75	223	193	30	350	27.94	-	2.74	0.12
4.5K5-8	12-31-75	223	193	30	350	27.65	5,280	2.75	0.13
4.5K5-11	12-31-75	223	193	30	350	27.45	5,675	2.77	0.13
4.5K5-14	12-31-75	223	193	30	350	27.43	-	2.94	0.13
3K6-11	2-19-76	273	193	80	350	27.54	4,780	2.56	0.10
3K6-14	2-19-76	273	193	80	350	27.56	4,810	2.38	0.11
3K6-8	2-19-76	273	193	80	350	27.61	-	2.51	0.13
4.5K6-11	2-19-76	273	193	80	350	27.19	5,430	2.74	0.14

[1] Specimens in fog room at 100% RH and 70°F.

[2] Specimens tested at 250°, 350°, and 450°F heated in oven at 75°F/day to test temperature.

[3] Designates that specimen was used for splitting tensile test after elastic constants were determined.

TABLE B-2. Compressive Strength and Elastic Properties of Using
the Static Method at Room and Elevated Temperatures (Continued).

Specimen Number	Date of Test	Age at Test, Days	Time in Fog Room,* Days[1]	Time in Oven, Days[2]	Temperature at test, °F	Weight at Test, lb	Compressive Strength, psi	Modulus of Elasticity, million psi	Poisson's Ratio
4.5K6-14	2-19-76	273	193	80	350	27.13	5,275	2.72	0.14
4.5K6-12	2-19-76	273	193	80	350	27.24	-[3]	2.66	0.14
3K7-8	4-29-76	343	193	150	350	26.87	4,410	2.11	0.15
3K7-11	4-29-76	343	193	150	350	27.11	4,675	2.29	0.14
3K7-14	4-29-76	343	193	150	350	26.93	-	2.17	0.14
4.5K7-8	4-29-76	343	193	150	350	26.92	5,490	2.34	0.12
4.5K7-10	4-29-76	343	193	150	350	27.11	4,890	2.29	0.15
4.5K7-15	4-29-76	343	193	150	350	26.99	-	2.32	0.14
3K8-8	8-27-76	463	193	270	350	27.55	4,910	2.52	0.13
3K8-11	8-27-76	463	193	270	350	27.66	4,960	2.51	0.14
3K8-14	8-27-76	463	193	270	350	27.39	-	2.52	0.14
4.5K8-8	8-27-76	463	193	270	350	27.46	6,190	2.78	0.11
4.5K8-11	8-27-76	463	193	270	350	27.37	6,300	3.14	0.11
4.5K8-14	8-27-76	463	193	270	350	27.61	-	2.78	0.11
3K6-24	4-1-77	679	276	403	350	27.65	4,650	2.37	0.13
3K6-30	4-1-77	679	276	403	350	27.65	4,430	2.17	0.15
3K6-27	4-1-77	679	276	403	350	27.65	-	2.20	0.12
4.5K6-18	4-1-77	679	276	403	350	27.12	5,450	2.43	0.12
4.5K6-26	4-1-77	679	276	403	350	27.18	5,160	2.46	0.12
4.5K6-27	4-1-77	679	276	403	350	27.07	-	2.37	0.16
3K7-19	9-30-77	861	276	585	350	27.31	4,390	2.33	0.16
3K7-25	9-30-77	861	276	585	350	27.10	4,320	2.32	0.15
3K7-10	9-30-77	861	276	585	350	26.97	-	2.16	0.14
4.5K7-24	9-30-77	861	276	585	350	28.01	5,100	2.32	0.14
4.5K7-25	9-30-77	861	276	585	350	28.12	5,500	2.34	0.14

[1]Specimens in fog room at 100% RH and 70°F.

[2]Specimens tested at 250°, 350°, and 450°F heated in oven at 75°F/day to test temperature.

[3]Designates that specimen was used for splitting tensile test after elastic constants were determined.

TABLE B-2. Compressive Strength and Elastic Properties of Using the Static Method at Room and Elevated Temperatures (Continued).

Specimen Number	Date of Test	Age at Test, Days	Time in Fog Room,* Days[1]	Time in Oven, Days[2]	Temperature at test, °F	Weight at Test, lb	Compressive Strength, psi	Modulus of Elasticity, million psi	Poisson's Ratio
4.5K7-17	9-30-77	861	276	585	350	27.01	-[3]	2.41	0.09
3K7-2	9-1-78	1,198	276	922	350		4,525	2.46	0.12
3K7-21	9-1-78	1,198	276	922	350		4,350	2.47	0.13
3K7-27	9-1-78	1,198	276	922	350		-	2.53	0.13
4.5K7-21	9-1-78	1,198	276	922	350		4,680	2.58	0.13
4.5K7-22	9-1-78	1,198	276	922	350		4,770	2.62	0.11
4.5K7-27	9-1-78	1,198	276	922	350		-	2.56	0.10
3K4-20	12-11-75	203	197	6	450	27.59	4,540	2.39	0.15
3K4-23	12-11-75	203	197	6	450	27.60	4,930	2.26	0.14
3K4-17	12-11-75	203	197	6	450	27.52	-	2.41	0.14
4.5K4-17	12-11-75	203	197	6	450	27.70	5,760	2.75	0.12
4.5K4-20	12-11-75	203	197	6	450	27.57	5,820	2.69	0.08
4.5K4-23	12-11-75	203	197	6	450	27.56	-	2.82	0.13
3K5-20	12-15-75	207	197	10	450	27.85	4,995	2.26	0.13
3K5-23	12-15-75	207	197	10	450	27.74	4,830	2.33	0.13
3K5-17	12-15-75	207	197	10	450	27.86	-	2.16	0.09
4.5K5-16	12-15-75	207	197	10	450	27.29	5,990	2.60	0.12
4.5K5-20	12-15-75	207	197	10	450	27.38	5,150	2.26	0.13
4.5K5-23	12-15-75	207	197	10	450	27.37	-	2.67	0.13
3K6-17	12-23-75	215	197	18	450	27.47	4,540	2.13	0.13
3K6-23	12-23-75	215	197	18	450	27.43	4,320	2.23	0.14
3K6-19	12-23-75	215	197	18	450	27.65	-	2.09	0.12
4.5K6-17	12-23-75	215	197	18	450	27.06	5,255	2.13	0.10
4.5K6-23	12-23-75	215	197	18	450	27.00	5,430	2.24	0.11
4.5K6-20	12-23-75	215	197	18	450	27.15	-	2.35	0.14

[1]Specimens in fog room at 100% RH and 70°F.

[2]Specimens tested at 250°, 350°, and 450°F heated in oven at 75°F/day to test temperature.

[3]Designates that specimen was used for splitting tensile test after elastic constants were determined.

TABLE B-2. Compressive Strength and Elastic Properties of Using
the Static Method at Room and Elevated Temperatures (Continued).

Specimen Number	Date of Test	Age at Test, Days	Time in Fog Room,* Days[1]	Time in Oven, Days[2]	Temperature at test, °F	Weight at Test, lb	Compressive Strength, psi	Modulus of Elasticity, million psi	Poisson's Ratio
3K7-17	1-7-76	230	197	33	450	27.01	4,280	2.08	0.18
3K7-23	1-7-76	230	197	33	450	27.22	4,455	2.06	0.17
3k7-20	1-7-76	230	197	33	450	26.80	-[3]	2.06	0.16
4.5K7-18	1-7-76	230	197	33	450	26.89	5,165	2.18	0.14
4.5K7-20	1-7-76	230	197	33	450	26.84	5,110	2.20	0.14
4.5K7-23	1-7-76	230	197	33	450	26.73	-	2.28	0.09
3K8-17	2-3-76	257	197	60	450	27.44	4,780	2.29	0.15
3K8-22	2-3-76	257	197	60	450	27.35	4,630	2.34	0.16
3K8-24	2-3-76	257	197	60	450	27.37	-	2.17	0.14
4.5K8-17	2-3-76	257	197	60	450	27.51	5,560	2.37	0.13
4.5K8-30	2-3-76	257	197	60	450	27.50	5,130	2.27	0.09
4.5K8-23	2-3-76	257	197	60	450	27.30	-	2.28	0.14
3K9-5	3-15-76	297	197	100	450	27.54	4,350	1.93	0.16
3K9-8	3-15-76	297	197	100	450	27.47	4,415	2.08	0.15
3K9-11	3-15-76	297	197	100	450	27.53	-	2.04	0.21
4.5K9-11	3-15-76	297	197	100	450	27.26	5,270	2.14	0.10
4.5K9-17	3-15-76	297	197	100	450	27.41	5,210	2.08	0.10
4.5K9-14	3-15-76	297	197	100	450	27.28	-	2.12	0.15
3K3-25	5-24-76	367	197	170	450	27.25	5,140	2.06	0.09
3K5-25	5-24-76	367	197	170	450	27.52	4,560	1.91	0.14
3K4-24	5-24-76	367	197	170	450	27.52	-	1.84	0.16
4.5K3-25	5-24-76	367	197	170	450	27.43	4,880	1.73	0.12
4.5K4-24	5-24-76	367	197	170	450	27.60	5,340	1.70	0.13
4.5K5-25	5-24-76	367	197	170	450	27.40	-	1.84	0.12
3K3-20	9-30-76	497	197	300	450	28.09	5,920	1.94	0.10

[1]Specimens in fog room at 100% RH and 70°F.

[2]Specimens tested at 250°, 350°, and 450°F heated in oven at 75°F/day to test temperature.

[3]Designates that specimen was used for splitting tensile test after elastic constants were determined.

TABLE B-2. Compressive Strength and Elastic Properties of Using the Static Method at Room and Elevated Temperatures (Continued).

Specimen Number	Date of Test	Age at Test, Days	Time in Fog Room,* Days[1]	Time in Oven, Days[2]	Temperature at test, °F	Weight at Test, lb	Compressive Strength, psi	Modulus of Elasticity, million psi	Poisson's Ratio
3K3-23	9-30-76	497	197	300	450	28.04	5,150	2.14	0.12
3K3-17	9-30-76	497	197	300	450	28.11	-3	2.62	0.10
4.5K3-19	9-30-76	497	197	300	450	27.36	4,620	1.75	0.17
4.5K3-23	9-30-76	497	197	300	450	27.40	4,940	1.67	0.16
4.5K3-17	9-30-76	497	197	300	450	27.39	-	1.74	0.09
3K3-10	3-31-77	679	270	409	450	28.20	4,720	1.91	0.15
3K3-12	3-31-77	679	270	409	450	28.17	4,590	1.84	0.18
3K3-27	3-31-77	679	270	409	450	27.91	-	1.90	0.14
4.5K3-27	3-31-77	679	270	409	450	27.25	4,850	1.78	0.16
4.5K3-21	3-31-77	679	270	409	450	28.29	4,950	1.77	0.15
4.5K3-22	3-31-77	679	270	409	450	27.32	-	1.96	0.15
3K4-16	9-29-77	861	270	591	450	27.20	3,540	1.28	0.16
3K4-19	9-29-77	861	270	591	450	27.32	3,630	1.29	0.18
3K4-7	9-29-77	861	270	591	450	27.44	-	1.51	0.20
4.5K4-15	9-29-77	861	270	591	450	27.50	4,240	1.50	0.12
4.5K4-21	9-29-77	861	270	591	450	27.37	4,580	1.54	0.09
4.5K4-19	9-29-77	861	270	591	450	27.36	-	1.46	0.13
3K5-4	9-1-78	1,198	283	915	450	27.60	-	1.55	0.14
3K5-9	9-1-78	1,198	283	915	450		3,850	1.52	0.12
3K5-27	9-1-78	1,198	283	915	450		3,605	1.42	0.15
4.5K5-2	9-1-78	1,198	283	915	450	27.39	-	1.55	0.11
4.5K5-7	9-1-78	1,198	283	915	450		4,100	1.40	0.11
4.5K5-28	9-1-78	1,198	283	915	450		4,165	1.46	0.10

[1]Specimens in fog room at 100% RH and 70°F.

[2]Specimens tested at 250°, 350°, and 450°F heated in oven at 75°F/day to test temperature.

[3]Designates that specimen was used for splitting tensile test after elastic constants were determined.

TABLE B-3. Splitting Tensile Strength at
Room and Elevated Temperatures.

Specimen Number	Date of Test	Age at Test, Days	Time in Fog Room,* Days	Temperature at Test, $^\circ$F	Splitting Tensile Strength, psi
3K2-9	5-9-75	34	30	350	576
3K2-10	5-9-75	34	30	350	583
4.5K1-4	5-9-75	34	30	350	685
4.5K2-14	5-9-75	34	30	350	663
3K2-8	6-13-75	69	30	350	561
3K2-11	6-13-75	69	30	350	552
4.5K2-1	6-13-75	69	30	350	652
4.5K2-13	6-13-75	69	30	350	584
3K2-4	6-15-75	71	71	70	588
4.5K1-11	6-15-75	71	71	70	671
3K1-15	6-17-75	73	65	450	470
4.5K1-10	6-17-75	73	65	450	610
4.5K1-14	6-17-75	73	65	450	643
3K2-16	6-19-75	75	71	350	605
3K2-17	6-19-75	75	71	350	587
4.5K2-16	6-19-75	75	71	350	649
4.5K1-15	6-19-75	75	71	350	682

*Specimens in fog room at 100% RH and 70°F. Specimens tested at 350°F removed from fog room at 30 days and heated in oven at 75°F/day to test temperature. Specimens tested at 450°F removed from fog room at 65 days and heated in oven at 75°F/day to test temperature.

TABLE B-3. Splitting Tensile Strength at Room and Elevated Temperatures (Continued).

Specimen Number	Date of Test	Age at Test, Days	Time in Fog Room, Days[1]	Time in Oven, Days[2]	Temperature at Test, °F	Weight at Test, lb	Splitting Tensile Strength, psi
3K4-26	6-21-75	30	30	0	70	29.73	412
3K4-29	6-21-75	30	30	0	70	29.69	418
4.5K4-26	6-21-75	30	30	0	70	29.67	457
4.5K4-29	6-21-75	30	30	0	70	29.63	522
3K9-2	12-2-75	194	194	0	70	29.84	548
3K9-10	12-2-75	194	194	0	70	29.72	513
4.5K9-2	12-2-75	194	194	0	70	29.46	622
4.5K9-15	12-2-75	194	194	0	70	29.62	644
3K7-28	1-19-76	240	240	0	70	28.35	470
4.5K7-29	1-19-76	240	240	0	70	28.19	550
3K7-7	5-17-76	361	361	0	70	29.41	451
4.5K7-28	5-17-76	361	361	0	70	29.36	525
3K8-28	3-31-77	679	679	0	70	29.68	519
4.5K8-29	3-31-77	679	679	0	70	29.56	525
3K4-15	11-18-77	880	880	0	70	29.58	491
4.5K4-12	11-18-77	880	880	0	70	29.53	592
3K8-18	9-7-78	1,204	1,204	0	70		512
3K8-23	9-7-78	1,204	1,204	0	70		561
4.5K8-5	9-7-78	1,204	1,204	0	70		591
4.5K8-13	9-7-78	1,204	1,204	0	70		642
3K3-3	12-4-75	196	193	3	250	29.23	502
3K3-7	12-4-75	196	193	3	250	29.51	550
4.5K3-1	12-4-75	196	193	3	250	28.70	547
4.5K3-7	12-4-75	196	193	3	250	28.71	529
3K8-1	12-11-75	203	193	10	250	27.74	476
3K8-4	12-11-75	203	193	10	250	27.68	476
4.5K8-2	12-11-75	203	193	10	250	27.94	568
4.5K8-3	12-11-75	203	193	10	250	27.83	499
3K7-3	12-31-75	223	193	30	250	27.29	434

[1]Specimens in fog room at 100% RH and 70°F.

[2]Specimens tested at 250°, 350°, and 450°F heated in oven at 75°F/day to test temperature.

TABLE B-3.   Splitting Tensile Strength at Room and Elevated Temperatures (Continued).

Specimen Number	Date of Test	Age at Test, Days	Time in Fog Room, Days[1]	Time in Oven, Days[2]	Temperature at Test, °F	Weight at Test, lb	Splitting Tensile Strength, psi
3K7-4	12-31-75	223	193	30	250	27.37	453
4.5K7-1	12-31-75	223	193	30	250	27.22	496
4.5K7-9	12-31-75	223	193	30	250	27.55	478
3K4-2	2-19-76	273	193	80	250	27.84	441
3K4-5	2-19-76	273	193	80	250	27.67	423
4.5K4-1	2-19-76	273	193	80	250	27.59	497
4.5K4-6	2-19-76	273	193	80	250	27.82	498
3K5-2	4-29-76	343	193	150	250	27.84	441
3K5-7	4-29-76	343	193	150	250	28.17	498
4.5K5-1	4-29-76	343	193	150	250	27.64	497
4.5K5-6	4-29-76	343	193	150	250	27.93	506
3K6-1	8-27-76	463	193	270	250	27.80	412
3K6-4	8-27-76	463	193	270	250	27.77	395
4.5K6-2	8-27-76	463	193	270	250	27.31	471
4.5K6-8	8-27-76	463	193	270	250	27.04	430
3K9-17	4-1-77	679	283	396	250	27.78	451
3K9-29	4-1-77	679	283	396	250	27.73	417
4.5K8-16	4-1-77	679	283	396	250	27.50	460
4.5K8-26	4-1-77	679	283	396	250	27.80	477
3K9-9	9-29-77	861	283	578	250	27.87	484
3K9-23	9-29-77	861	283	578	250	27.76	396
4.5K8-12	9-29-77	861	283	578	250	27.82	504
4.5K8-22	9-29-77	861	283	578	250	27.57	464
3K8-26	9-1-78	1,198	276	922	250		408
3K8-30	9-1-78	1,198	276	922	250		400
4.5K9-5	9-1-78	1,198	270	928	250		373
4.5K9-29	9-1-78	1,198	270	928	250		491
3K3-9	12-5-75	197	193	4	350	28.58	495
3K3-11	12-5-75	197	193	4	350	28.37	546

[1]Specimens in fog room at 100% RH and 70°F.

[2]Specimens tested at 250°, 350°, and 450°F heated in oven at 75°F/day to test temperature.

TABLE B-3. Splitting Tensile Strength at Room and Elevated Temperatures (Continued).

Specimen Number	Date of Test	Age at Test, Days	Time in Fog Room, Days[1]	Time in Oven, Days[2]	Temperature at Test, °F	Weight at Test, lb	Splitting Tensile Strength, psi
3K7-4	12-31-75	223	193	30	250	27.37	453
4.5K7-1	12-31-75	223	193	30	250	27.22	496
4.5K7-9	12-31-75	223	193	30	250	27.55	478
3K4-2	2-19-76	273	193	80	250	27.84	441
3K4-5	2-19-76	273	193	80	250	27.67	423
4.5K4-1	2-19-76	273	193	80	250	27.59	497
4.5K4-6	2-19-76	273	193	80	250	27.82	498
3K5-2	4-29-76	343	193	150	250	27.84	441
3K5-7	4-29-76	343	193	150	250	28.17	498
4.5K5-1	4-29-76	343	193	150	250	27.64	497
4.5K5-6	4-29-76	343	193	150	250	27.93	506
3K6-1	8-27-76	463	193	270	250	27.80	412
3K6-4	8-27-76	463	193	270	250	27.77	395
4.5K6-2	8-27-76	463	193	270	250	27.31	471
4.5K6-8	8-27-76	463	193	270	250	27.04	430
3K9-17	4-1-77	679	283	396	250	27.78	451
3K9-29	4-1-77	679	283	396	250	27.73	417
4.5K8-16	4-1-77	679	283	396	250	27.50	460
4.5K8-26	4-1-77	679	283	396	250	27.80	477
3K9-9	9-29-77	861	283	578	250	27.87	484
3K9-23	9-29-77	861	283	578	250	27.76	396
4.5K8-12	9-29-77	861	283	578	250	27.82	504
4.5K8-22	9-29-77	861	283	578	250	27.57	464
3K8-26	9-1-78	1,198	276	922	250		408
3K8-30	9-1-78	1,198	276	922	250		400
4.5K9-5	9-1-78	1,198	270	928	250		373
4.5K9-29	9-1-78	1,198	270	928	250		491
3K3-9	12-5-75	197	193	4	350	28.58	495
3K3-11	12-5-75	197	193	4	350	28.37	546

[1]Specimens in fog room at 100% RH and 70°F.

[2]Specimens tested at 250°, 350°, and 450°F heated in oven at 75°F/day to test temperature.

TABLE B-3. Splitting Tensile Strength at Room and Elevated Temperatures (Continued).

Specimen Number	Date of Test	Age at Test, Days	Time in Fog Room, Days[1]	Time in Oven, Days[2]	Temperature at Test, °F	Weight at Test, lb	Splitting Tensile Strength, psi
4.5K7-17	9-30-77	861	276	585	350	27.01	441
3K7-6	9-5-78	1,202	276	926	350	27.19	424
3K7-27	9-5-78	1,202	276	926	350		424
4.5K7-2	9-5-78	1,202	276	926	350	27.31	394
4.5K7-27	9-5-78	1,202	276	926	350		378
3K4-17	12-11-75	203	197	6	450	27.52	393
3K4-18	12-11-75	203	197	6	450	27.64	392
4.5K4-19	12-11-75	203	197	6	450	27.69	469
4.5K4-23	12-11-75	203	197	6	450	27.56	477
3K5-13	12-15-75	207	197	10	450	28.14	425
3K5-17	12-15-75	207	197	10	450	27.86	387
4.5K5-23	12-15-75	207	197	10	450	27.37	424
4.5K5-27	12-15-75	207	197	10	450	27.53	463
3K6-10	12-23-75	215	197	18	450	27.92	392
3K6-19	12-23-75	215	197	18	450	27.47	399
4.5K6-19	12-23-75	215	197	18	450	27.29	440
4.5K6-20	12-23-75	215	197	18	450	27.15	407
3K7-20	1-7-76	230	197	33	450	26.80	387
3K7-22	1-7-76	230	197	33	450	27.03	407
4.5K7-19	1-7-76	230	197	33	450	26.92	436
4.5K7-23	1-7-76	230	197 ·	33	450	26.73	425
3K8-13	2-3-76	257	197	60	450	27.44	396
3K8-24	2-3-76	257	197	60	450	27.37	355
4.5K8-18	2-3-76	257	197	60	450	27.64	426
4.5K8-23	2-3-76	257	197	60	450	27.30	416
3K9-11	3-15-76	297	197	100	450	27.53	393
3K9-12	3-15-76	297	197	100	450	27.62	396
4.5K9-14	3-15-76	297	197	100	450	27.28	396
4.5K9-24	3-15-76	297	197	100	450	27.54	409

[1]Specimens in fog room at 100% RH and 70°F.

[2]Specimens tested at 250°, 350°, and 450°F heated in oven at 75°F/day to test temperature.

TABLE B-3. Splitting Tensile Strength at Room and Elevated Temperatures (Continued).

Specimen Number	Date of Test	Age at Test, Days	Time in Fog Room, Days[1]	Time in Oven, Days[2]	Temperature at Test, $^\circ$F	Weight at Test, lb	Splitting Tensile Strength, psi
3K4-24	5-24-76	367	197	170	450	27.60	349
3K6-16	5-24-76	367	197	170	450	27.61	391
4.5K5-25	5-24-76	367	197	170	450	27.40	410
4.5K6-29	5-24-76	367	197	170	450	27.18	390
3K3-13	9-30-76	497	197	300	450	28.41	433
3K3-17	9-30-76	497	197	300	450	28.11	424
4.5K3-17	9-30-76	497	197	300	450	27.39	425
4.5K3-18	9-30-76	497	197	300	450	27.54	451
3K3-26	3-31-77	679	270	409	450	28.27	357
3K3-27	3-31-77	679	270	409	450	27.25	391
4.5K3-2	3-31-77	679	270	409	450	27.59	424
4.5K3-22	3-31-77	679	270	409	450	27.91	407
3K4-7	9-29-77	861	270	591	450	27.44	285
3K4-10	9-29-77	861	270	591	450	27.51	264
4.5K4-13	9-29-77	861	270	591	450	27.40	355
4.5K4-19	9-29-77	861	270	591	450	27.36	347
3K5-4	9-6-78	1,203	283	920	450	27.60	261
3K5-10	9-6-78	1,203	283	920	450	27.73	324
4.5K5-2	9-6-78	1,203	283	920	450	27.39	341
4.5K5-13	9-6-78	1,203	283	920	450	27.44	366

[1]Specimens in fog room at 100% RH and 70°F.

[2]Specimens tested at 250°, 350°, and 450°F heated in oven at 75°F/day to test temperature.

APPENDIX C

ELASTIC PROPERTIES USING THE SONIC METHOD

TABLE C-1. Elastic Constants at Room Temperature Using the Sonic Method.

Date of Test	Age at Test, Days*	Modulus of Elasticity, million psi				Poisson's Ratio			
		3K1-8	3K1-9	4.5K1-16	4.5K2-8	3K1-8	3K1-9	4.5K1-16	4.5K2-8
4-16-75	11	5.72	5.81	5.97	6.01	0.20	0.20	0.21	0.20
4-25-74	20	5.94	6.02	6.08	6.22	0.21	0.20	0.20	0.20
5-5-75	30	6.06	6.16	6.24	6.30	0.21	0.20	0.20	0.19
5-20-75	45	6.12	6.25	6.28	6.38	0.20	0.21	0.20	0.19
6-4-75	60	6.20	6.32	6.34	6.51	0.21	0.21	0.20	0.20
6-15-75	71	6.27	6.40	6.46	6.59	0.21	0.21	0.21	0.22

*Specimens in fog room at 100% RH and 70°F.

TABLE C-1. Elastic Constants at Room Temperature Using the Sonic Method (Continued).

Specimen Number	Date of Test	Age at Test, Days[1]	Weight at Test, lb	Modulus of Elasticity, million psi	Poisson's Ratio
3K4-25	6-23-75	32	29.66	5.16	0.22
3K4-27	6-23-75	32	29.94	5.45	0.22
4.5K4-25	6-23-75	32	29.60	5.38	0.20
4.5K4-27	6-23-75	32	29.80	5.66	0.23
3K4-25	7-21-75	60	29.67	5.29	0.22
3K4-27	7-21-75	60	29.95	5.51	0.21
4.5K4-25	7-21-75	60	29.61	5.54	0.21
4.5K4-27	7-21-75	60	29.80	5.64	0.19
3K4-25	8-20-75	90	29.69	5.38	0.19
3K4-27	8-20-75	90	29.96	5.65	0.22
4.5K4-25	8-20-75	90	29.63	5.65	0.21
4.5K4-27	8-20-75	90	29.70	5.93	0.23
3K4-25	12-3-75	193	29.69	5.50	0.21
3K4-27	12-3-75	193	29.96	5.76	0.22
4.5K4-25	12-3-75	193	29.64	5.81	0.21
4.5K4-27	12-3-75	193	29.72	6.11	0.25
3K4-25	1-19-76	240	29.69	5.50	0.30
3K4-27	1-19-76	240	29.97	5.70	0.20
4.5K4-25	1-19-76	240 .	29.65	5.82	0.22
4.5K4-27	1-19-76	240	29.72	6.11	0.31
3K4-25	5-15-76	360	29.72	5.63	0.23
3K4-27	5-15-76	360	29.99	5.86	0.23
4.5K4-25	5-15-76	360	29.67	5.86	0.22
4.5K4-27	5-15-76	360	29.75	6.18	0.24

[1]Specimens in fog room at 100% RH and 70°F.

TABLE C-1. Elastic Constants at Room Temperature Using the Sonic Method (Continued).

Specimen Number	Date of Test	Age at Test, Days[1]	Weight at Test, lb	Modulus of Elasticity, million psi	Poisson's Ratio
3K4-25	10-5-76	502	29.73	5.64	0.22
3K4-27	10-5-76	502	29.99	5.87	0.23
4.5K4-25	10-5-76	502	29.70	5.89	0.21
4.5K4-27	10-5-76	502	29.76	6.23	0.25
3K4-25	3-30-77	678	29.74	5.74	0.23
3K4-27	3-30-77	678	30.00	5.92	0.22
4.5K4-25	3-30-77	678	29.72	5.99	0.22
4.5K4-27	3-30-77	678	29.78	6.30	0.25
3K4-25	11-11-77	873	29.73	5.66	0.20
3K4-27	11-11-77	873	29.99	5.91	0.22
4.5K4-25	11-11-77	873	29.71	5.99	0.22
4.5K4-27	11-11-77	873	29.77	6.30	0.24
3K4-25	5-9-78	1,083	29.75	5.71	0.20
3K4-27	5-9-78	1,083	30.03	5.97	0.22
4.5K4-25	5-9-78	1,083	29.73	6.11	0.23
4.5K4-27	5-9-78	1,083	29.82	6.33	0.22
3K4-25	9-6-78	1,204	29.73	5.69	0.21
3K4-27	9-6-78	1,204	30.00	5.93	0.20
4.5K4-25	9-6-78	1,204	29.71	6.02	0.20
4.5K4-27	9-6-78	1,204	29.79	6.33	0.24

[1]Specimens in fog room at 100% RH and 70°F.

TABLE C-2. Elastic Constants at Elevated Temperatures Using the Sonic Method.

Date of Test	Age at Test, Days*	Time in Oven, Days	Temperature, °F**	Modulus of Elasticity, million psi				Poisson's Ratio			
				3K1-10	3K2-7	4.5K1-1	4.5K2-16	3K1-10	3K2-7	4.5K1-1	4.5K2-16
5-5-75	30	0	70	6.05	6.10	6.26	6.27	0.20	0.20	0.21	0.21
5-6-75	31	1	150	5.75	5.62	5.50	5.45	0.19	0.17	0.22	0.14
5-7-75	32	2	250	4.93	4.60	4.32	4.78	0.16	0.11	0.17	0.14
5-9-75	34	4	350	3.93	3.81	3.83	4.14	0.12	0.06	0.06	0.10
5-21-75+	46	16	350	3.40	3.37	3.56*	3.62	0.11	0.05	0.06	0.08
6-2-75	58	28	350	3.27	3.08	3.56	3.42	0.09	0.01	0.08	0.08
6-13-75	69	39	350	3.17	3.08	3.32	3.32	0.09	0.03	0.04	0.06
				3K1-8	3K1-9	4.5K1-16	4.5K2-8	3K1-8	3K1-9	4.5K1-16	4.5K2-8
6-15-75	71	0	70	6.27	6.40	6.46	6.59	0.21	0.21	0.21	0.22
6-16-75	72	1	150	5.85	6.01	6.05	6.07	0.20	0.21	0.21	0.19
6-17-75	73	2	250	4.63	4.63	5.19	5.28	0.11	0.11	0.18	0.16
6-19-75	75	4	350	3.96	3.73	4.25	4.32	0.10	0.05	0.12	0.08

*All specimens in fog room at 100% RH and 70°F for 30 days prior to heating in oven.

**Temperature of oven increased 75°F/day to 350°F and held constant at this temperature.

+A large crack was observed in Specimen Number 4.5K1-1 on 5-21-75. Elastic constant values for that date and subsequent dates were obtained on Specimen Number 4.5K1-3.

TABLE C-2. Elastic Constants at Elevated Temperatures Using the Sonic Method. (Continued)

Date of Test	Age at Test, Days*	Time in Oven, Days	Temperature, °F**	Modulus of Elasticity, million psi				Poisson's Ratio			
				3K1-15	3K2-12	4.5K1-10	4.5K1-14	3K1-15	3K2-12	4.5K1-10	4.5K1-14
6-9-75	65	0	70	6.28	6.50	6.53	6.58	0.22	0.22	0.22	0.22
6-10-75	66	1	150	5.81	6.04	5.95	5.60	0.20	0.20	0.19	0.17
6-11-75	67	2	250	4.51	4.87	4.88	4.80	0.11	0.12	0.09	0.15
6-12-75	68	3	350	3.87	4.31	4.49	4.36	0.07	0.09	0.12	0.12
6-14-75[+]	70	5	450	2.55	3.06	2.99	3.21	0.03	0.04	0.01	0.07
6-14-75[++]	70	5	450	2.40	2.89	2.82	3.05	-0.04	0.04	-0.01	0.07
6-15-75[+]	71	6	450	2.27	2.80	2.75	2.93	-0.05	0.04	-0.02	0.05
6-15-75[++]	71	6	450	2.22	2.67	2.64	2.87	-0.06	0.01	-0.05	0.05
6-16-75	72	7	450	2.19	2.60	2.57	2.81	-0.06	0.01	-0.05	0.05
6-17-75	73	8	450	2.13	2.50	2.53	2.74	-0.07	-0.01	-0.05	-0.04

*All specimens in fog room at 100% RH and 70°F for 65 days prior to heating in oven.

**Temperature of oven increased 75°F/day to 450°F and held constant at this temperature.

+Tested at 8:00 A.M.

++Tested at 4:00 P.M.

APPENDIX D

DATA ON SIZE EFFECTS ON TEST SPECIMENS
AND PROPERITIES

TABLE D-1. Dimensions and Weights of CTL/PCA
Cast 6- by 12-In. Cylinders at 70°F.

Specimen Number	Diameter, in.	Length, in.	Weight, lb
3K5-18	6.02	12.00	29.34
3K5-19	5.95	12.00	29.57
3K5-21	5.95	11.98	29.28
3K5-22	5.93	12.00	29.37
3K9-6	5.96	11.97	28.88
3K9-13	5.98	11.98	29.07
3K9-16	6.00	12.01	28.88
3K9-22	6.00	12.00	29.10

TABLE D-2. Dimensions and Weights of
3- by 6-In. Cylinders at 70°F.

Specimen Number	Diameter, in.	Length, in.	Weight, lb
3K9-7-1	2.78	5.66	2.864
3K9-7-2	2.78	5.61	2.836
3K5-15-3	2.78	5.60	2.860
3K5-15-4	2.78	5.63 .	2.866
3K5-24-5	2.78	5.33	2.752
3K5-24-6	2.78	5.40	2.803
3K9-4-7	2.78	5.63	2.882
3K9-4-8	2.78	5.62	2.774

TABLE D-3. Dimensions and Weights of 3-In. Cubes at 70°F.

Specimen Number	Height, in.	Width, in.	Depth, in.	Weight, lb
3K9-18-1	2.92	3.02	2.98	2.385
3K8-7-2	2.96	2.99	2.91	2.187
3K9-18-3	3.04	2.96	2.95	2.394
3K9-18-4	2.91	2.94	2.96	2.181

TABLE D-4. Compressive Strength and Elastic Properties of 6- by 12-In.
Cylinders at Room and Elevated Temperatures.

Specimen Number	Date of Test	Time in Oven, Days	Temp. at Test, ^{o}F	Weight at Test, lb	Compressive Strength, psi	Modulus of Elasticity, million psi	Poisson's Ratio
3K5-21	8-9-77	0	70	29.28	5,600	4.66	0.16
3K9-6	8-9-77	0	70	28.88	6,000	4.44	0.17
3K5-19	9-7-77	30	250	28.28	5,490	3.35	0.13
3K9-22	9-7-77	30	250	27.85	5,260	3.21	0.13

TABLE D-5. Compressive Strength and Elastic Properties of 3- by 6-In.
Cylinders at Room and Elevated Temperatures.

Specimen Number	Date of Test	Time in Oven, Days	Temp. at Test, ^{o}F	Weight at Test, lb	Compressive Strength, psi	Modulus of Elasticity, million psi	Poisson's Ratio
3K9-7-2	5-25-77	0	70	2.836	5,190	3.78	0.19
3K5-15-4	5-25-77	0	70	2.866	5,025	4.07	0.19
3K5-24-5	8-24-77	30	250	2.752	5,245	2.96	0.14
3K9-4-8	8-24-77	30	250	2.774	3,870	2.59	0.12

TABLE D-6. Compressive Strength and Elastic Properties of
3 In. Cubes at Room and Elevated Temperatures.

Specimen Number	Date of Test	Time in Oven, Days	Temp. at Test, $^\circ$F	Weight at Test, lb	Compressive Strength, psi	Modulus of Elasticity, million psi	Poisson's Ratio
3K9-18-1	4-13-78	0	70	2.385	6,970	4.16	-
3K8-7-2	4-13-78	0	70	2.187	5,230	3.70	0.16
3K9-18-3	4-13-78	30	250	2.307	7,190	4.61	-
3K9-18-4	4-13-78	30	250	2.114	6,740	3.89	0.17

TABLE D-7. Tensile Splitting Strength of 6- by 12-In.
Cylinders at Room and Elevated Temperatures.

Specimen Number	Date of Test	Time in Oven, Days	Temp. at Test, °F	Weight at Test, lb	Tensile Splitting Strength, psi
3K5-22	8-9-77	0	70	29.37	522
3K9-16	8-9-77	0	70	28.88	516
3K5-18	9-7-77	30	250	28.08	492
3K9-13	9-7-77	30	250	27.83	496

TABLE D-8. Tensile Splitting Strength of 3- by 6-In.
Cylinders at Room and Elevated Temperatures.

Specimen Number	Date of Test	Time in Oven, Days	Temp. at Test, °F	Weight at Test, lb	Tensile Splitting Strength, psi
3K9-7-1	5-25-77	0	70	2.864	850
3K5-15-3	5-25-77	0	70	2.860	769
3K5-24-6	8-24-77	30	250	2.743	721
3K9-4-7	8-24-77	30	250	2.825	538

APPENDIX E

CREEP-STRAIN READINGS

TABLE E-1. Deformation of Test Cylinders.

Time at Test Temperature	Frame No. 1 1,500 psi/$250°F$		Frame No. 2 500 psi/$350°F$		Frame No. 3 1,500 psi/$350°F$	
	4.5K11-17	4.5K11-18	4.5K11-22	4.5K11-24	4.5K11-14	4.5K11-15
0 hr (Unloaded, $68°$)	0	0	0	0	0	0
0 hr (Loaded, $68°$)	-20*	-60	-50	-180	-220	-210
6 hr Heat to Test Temperature	490	260	700	550	-230	860
Day 1	320	190	450	340	-400	-270
Day 2	180	120	410	270	-460	-440
Day 3	110	100	-**	-	-580	-550
Day 5	-	-	300	120	-	-
Day 6	10	0	320	130	-590	-570
Day 7	0	0	350	120	-	-
Day 8	30	-10	260	70	-	-
Day 9	-80	-60	290	70	-700	-710
Day 10	-80	-100	-	-	-	-
Day 12	-	-	200	0	-	-
Day 13	-100	-120	270	50	-	-
Day 14	-	-	-	-	-720	-790
Day 16	-180	-210	200	-10	-	-

*Negative strain values imply net contraction of the speciman.

**No readings taken.

E-1

RHO-C-54

TABLE E-1. Deformation of Test Cylinders (Continued).

Time at Test Temperature	Strain in millionths					
	Frame No. 1 1,500 psi/250°F		Frame No. 2 500 psi/350°F		Frame No. 3 1,500 psi/350°F	
	4.5K11-17	4.5K11-18	4.5K11-22	4.5K11-24	4.5K11-14	4.5K11-15
Day 21	-180	-220	-	-	-790	-820
Day 22	-	-	120	-110	-	-
Day 27	-	-	230	-50	-	-
Day 28	-250	-330	-	-	-800	-880
Day 34	-	-	60	-150	-	-
Day 35	-270	-350	-	-	-	-
Day 36	-	-	-	-	-750	-880
Day 41	-	-	160	-150	-	-
Day 42	-	-	-	-	-850	-890
Day 43	-260	-360	-	-	-	-
Day 49	-310	-430	170	-100	-850	-910
Day 55	-	-	50	-170	-	-
Day 56	-280	-420	-	-	-1,020	-1,030
Day 62	-	-	170	-100	-	-
Day 63	-330	-370	-	-	-	-
Day 64	-	-	-	-	-1,020	-1,030
Day 69	-	-	-20	-190	-	-
Day 71	-310	-480	-	-	-	-

TABLE E-1. Deformation of Test Cylinders (Continued).

Time at Test Temperature	Frame No. 1 1,500 psi/250°F		Frame No. 2 500 psi/350°F		Frame No. 3 1,500 psi/350°F	
	4.5K11-17	4.5K11-18	4.5K11-22	4.5K11-24	4.5K11-14	4.5K11-15
Day 77	-	-	-70	-150	-	-
Day 98	-	-	-	-	-970	-980
Day 105	-300	-440	-	-	-	-
Day 111	-	-	-90	-180	-	-
Day 126	-	-	-	-	-1,020	-1,010
Day 133	-300	-470	-	-	-	-
Day 139	-	-	-50	-180	-	-
Day 160	-	-	-	-	-1,020	-1,010
Day 167	-300	-460	-	-	-	-
Day 173	-	-	-50	-150	-	-
Day 196	-	-	-	-	-1,060	-1,080
Day 203	-360	-500	-	-	-	-
Day 209	-	-	-110	-200	-	-
Day 224	-	-	-	-	-1,050	-1,060
Day 231	-370	-500	-	-	-	-
Day 237	-	-	-130	-220	-	-
Day 318		-	-	-	-1,130	-1,140

TABLE E-1. Deformation of Test Cylinders (Continued).

Time at Test Temperature	Frame No. 1 1,500 psi/250°F		Frame No. 2 500 psi/350°F		Frame No. 3 1,500 psi/350°F	
	4.5K11-17	4.5K11-18	4.5K11-22	4.5K11-24	4.5K11-14	4.5K11-15
Day 325	-410	-510	-	-	-	-
Day 331	-	-	-240	-320	-	-
Day 559	-	-	-	-	***	-1,090
Day 566	-410	-540	-	-	-	-
Day 572	-	-	***	-290	-	-
Day 640	-	-	-	-	***	-1,170
Day 647	-420	-580	-	-	-	-
Day 653	-	-	***	-350	-	-
Day 640 (Unloaded 68°F)	-	-	-	-	***	-1,710
Day 647 (Unloaded 68°F)	-1,100	-880	-	-	-	-
Day 653 (Unloaded 68°F)	-	-	***	-1,030	-	-

***Brass gage points on specimen dislodged, no readings taken.

APPENDIX F

THERMAL EXPANSION SPECIMENS
AND PROPERTIES DATA

TABLE F-1. Weights and Dimensions of Dilatometer Specimens.

Specimen Number	Test Number	Date of Test	Weight at Test, lb	Length, in	Diameter, in	Weight after Test, lb	Weight loss, percent
3K8-7	1	8-24-78	0.0483	3.016	0.502	0.0447	7.42
3K9-18	2	8-30-78	0.0470	3.010	0.495	0.0435	7.54
4.5K8-19	3	8-31-78	0.0475	2.878	0.494	0.0441	7.16
4.5K9-10	4	9-01-78	0.0479	3.015	0.495	0.0444	7.36
3K14-12	5	9-13-78	0.0512	3.019	0.494	0.0473	7.47
3K14-12	6	9-14-78	0.0479	2.958	0.497	0.0433	9.57
4.5K12-12	7	9-15-78	0.0512	2.985	0.497	0.0476	6.99
4.5K12-12	8	9-20-78	0.0513	3.000	0.496	0.0474	7.66

TABLE F-2. Average Coefficient of Thermal
Expansion,$\bar{\alpha}$, From 70° To 1,000°F.

Specimen Number	Test Number	Date of Test	$10^{-6}/°F$
3K8-7	1	8-24-78	3.79
3K9-18	2	8-30-78	3.60
4.5K8-19	3	8-31-78	3.84
4.5K9-10	4	9-01-78	2.63
3K14-12	5	9-13-78	3.25
3K14-12	6	9-14-78	3.91
4.5K12-12	7	9-15-78	3.18
4.5K12-12	8	9-20-78	2.12

APPENDIX G

THERMAL CYCLING SPECIMENS AND PROPERTIES DATA

TABLE G-1. Weight and Dimensions of Test Cylinders at 70°F.

Specimen Number	Length in.	Diameter in.	Moist Weight lb	Weight at Test lb
3K10-17	12.08	5.98	30.85	30.85
3K10-18	12.08	5.98	30.80	30.80
4.5K10-17	12.07	5.98	30.39	30.39
4.5K10-18	12.10	6.01	30.42	30.42
3K10-1	12.05	5.98	30.71	28.75
3K10-2	11.98	6.03	31.30	29.40
4.5K10-1	12.08	5.99	30.38	28.40
4.5K10-2	12.09	5.99	30.52	28.52
3K10-3	12.07	5.99	30.81	29.45
3K10-5	12.08	5.97	30.74	29.34
4.5K10-3	12.06	6.01	30.36	28.95
4.5K10-5	12.07	6.00	30.43	28.98
3K10-6	12.08	5.99	30.63	28.60
3K10-7	12.07	6.00	30.73	28.76
4.5K10-6	12.09	5.97	30.53	28.54
4.5K10-7	12.10	5.97	30.50	28.45
3K10-9	12.04	6.00	30.70 ·	28.71
3K10-10	12.07	5.98	30.87	28.96
4.5K10-9	12.13	5.98	30.62	28.61
4.5K10-10	12.12	6.00	30.54	28.55
3K10-11	12.07	6.01	30.73	28.70
3K10-13	12.07	5.97	30.73	28.77
4.5K10-11	12.08	6.00	30.38	28.30
4.5K10-13	12.11	5.99	30.45	28.38
3K10-14	12.03	5.96	30.64	28.70
3K10-15	12.08	5.99	30.75	28.76
4.5K10-14	12.10	5.98	30.48	28.44
4.5K10-15	12.12	5.97	30.53	28.45

TABLE G-1. Weight and Dimensions of Test Cylinders at 70°F (Continued).

Specimen Number	Length, in.	Diameter, in.	Moist Weight, lb	Weight at Test, lb
3K14-9	12.14	5.97	30.70	30.70
3K14-10	12.12	6.00	30.66	30.66
3K14-11	12.06	5.98	30.47	28.46
3K14-13	12.04	5.97	30.47	28.49
3K14-14	12.01	6.02	30.98	29.00
3K14-15	12.07	6.02	30.48	28.48
3K14-17	12.00	6.01	30.90	28.90
3K14-18	12.11	5.96	30.55	28.57
3K14-19	12.03	5.99	30.39	28.37
3K14-21	12.05	5.99	30.36	28.35
3K14-22	12.14	5.96	30.56	28.55
3K14-23	12.08	5.96	30.50	28.51
3K14-24	12.08	5.96	30.48	28.43
3K14-25	12.06	5.98	30.45	28.40
4.5K12-1	12.07	5.98	30.37	28.40
4.5K12-2	12.12	5.97	30.44	28.46
4.5K12-3	12.10	5.96	30.30	28.29
4.5K12-5	12.11	6.00	30.35	28.38
4.5K12-6	12.09	5.98	30.31	28.37
4.5K12-7	12.12	6.00	30.41	28.45
4.5K12-9	12.09	5.98	30.27	28.30
4.5K12-10	12.11	5.98	30.39	28.42
4.5K12-11	12.12	5.99	30.37	28.36
4.5K12-13	12.14	5.99	30.34	28.30
4.5K12-14	12.11	5.99	30.38	28.38
4.5K12-15	12.00	6.01	30.50	28.42
4.5K12-17	12.15	5.95	30.44	30.44
4.5K12-18	12.10	6.00	30.26	30.26

TABLE G-2. Compressive Strength and Elastic Properties
Using the Static Method at 70°F as a Function of
Temperature Cycles to 350°F.

Specimen Number	Date of Test	Number of Cycles	Length of Cycles, Days	Compressive Strength, psi	Modulus of Elasticity, million psi	Poisson's Ratio
3K14-9	5-8-78	0	-	6,230	-	-
3K14-10	5-8-78	0	-	6,160	4.90	0.17
4.5K12-17	5-8-78	0	-	7,250	5.44	0.17
4.5K12-18	5-8-78	0	-	7,760	5.80	0.18
3K14-11	5-3-78	1	14	7,090	5.60	0.14
3K14-13	5-3-78	1	14	6,370	5.05	0.15
4.5K12-1	5-3-78	1	14	7,165	5.90	0.16
4.5K12-2	5-3-78	1	14	7,760	6.10	0.16
3K14-14	5-31-78	3	14	6,270	4.53	0.14
3K14-15	5-31-78	3	14	5,800	4.48	0.13
4.5K12-3	5-31-78	3	14	7,140	4.41	0.13
4.5K12-5	5-31-78	3	14	6,300	5.88	0.13
3K14-17	6-28-78	5	14	6,110	4.86	0.14
3K14-18	6-28-78	5	14	6,010	4.60	0.15
4.5K12-6	6-28-78	5	14	7,460	4.83	0.15
4.5K12-7	6-28-78	5	14	6,690	4.90	0.15
3K14-19	8-9-78	8	14	6,050	3.69	0.17
3K14-21	8-9-78	8	14	5,540	3.47	0.16
4.5K12-9	8-9-78	8	14	6,940	3.80	0.15
4.5K12-10	8-9-78	8	14	6,930	3.79	0.17
3K14-22	10-6-78	12	14	5,160	3.32	0.14
3K14-23	10-6-78	12	14	5,600	3.38	0.15
4.5K12-11	10-6-78	12	14	6,480	3.62	0.16
4.5K12-13	10-6-78	12	14	6,500	3.51	0.14
3K14-24	12-13-78	17	14	5,775	3.34	0.15
3K14-25	12-13-78	17	14	5,735	3.43	0.18
4.5K12-14	12-13-78	17	14	6,640	3.45	0.16
4.5K12-15	12-13-78	17	14	6,910	3.36	0.15

TABLE G-2. Compressive Strength and Elastic Properties (Static Method)
of Unheated and Thermal Cycled Concrete at 70°F.

Specimen Number	Date of Test	Number of Cycles	Length of Cycles, Days	Compressive Strength, psi	Modulus of Elasticity, million psi	Poisson's Ratio
3K10-17	2-15-79	0	-	7,920	6.08	0.17
3K10-18	2-15-79	0	-	7,915	6.18	0.18
4.5K10-17	2-15-79	0	-	8,320	6.24	0.17
4.5K10-18	2-15-79	0	-	8,460	6.41	0.20
3K10-1	2-8-79	1	28	7,630	3.47	0.11
3K10-2	2-8-79	1	28	7,670	3.61	0.11
4.5K10-1	2-8-79	1	28	8,060	3.62	0.13
4.5K10-2	2-8-79	1	28	7,800	3.88	0.12
3K10-3	4-4-79	3	28	6,940	3.43	0.14
3K10-5	4-4-79	3	28	7,110	3.38	0.15
4.5K10-3	4-4-79	3	28	7,440	3.76	0.14
4.5K10-5	4-4-79	3	28	7,835	3.64	0.16
3K10-6	6-7-79	5	28	6,550	3.32	0.17
3K10-7	6-7-79	5	28	6,925	3.54	0.14
4.5K10-6	6-7-79	5	28	7,040	3.76	0.15
4.5K10-7	6-7-79	5	28	7,065	3.71	0.14
3K10-9	9-13-79	8	28	6,570	3.28	0.13
3K10-10	9-13-79	8	28	6,490	3.32	0.14
4.5K10-9	9-13-79	8	28	7,490	3.49	0.14
4.5K10-10	9-13-79	8	28	7,530	3.55	0.13
3K10-11	2-6-80	13	28	7,000	3.12	0.13
3K10-13	2-6-80	13	28	6,525	3.11	0.16
4.5K10-11	2-6-80	13	28	7,450	3.35	0.14
4.5K10-13	2-6-80	13	28	7,155	3.21	0.15
3K10-14	7-2-80	18	28	6,500	3.13	0.18
3K10-15	7-2-80	18	28	6,160	--*	--*
4.5K10-14	7-2-80	18	28	7,190	--*	--*
4.5K10-15	7-2-80	18	28	6,720	--*	--*

*Equipment malfunction prevented determination of these properties.

TABLE G-3. Coefficient of Thermal Expansion Determined
From Cyclically Heated Concrete.

Cylinder Number	Specimen Number	Coefficient of Thermal Expansion, Millionths/$^{\circ}$F	
		α_o	$\bar{\alpha}$
3K8-7	1	2.25	3.44
3K9-18	2	2.43	3.79
4.5K8-9	3	2.59	3.90
4.5K9-10	4	2.31	3.83
3K14-12	5	2.71	3.80
3K14-12	6	3.43	4.41
4.5K12-12	7	3.39	3.76
4.5K12-12	8	2.78	4.40

APPENDIX H

STEAM CURING COMPRESSIVE STRENGTH DATA

TABLE H-1. Atmospheric Pressure Steam Curing at
137°F Compressive Strength Tests.

Specimen Number	Test Date	Time in Steam Box, Days	Age of Test, Days	Compressive Strength, psi
3K16-1	10-18-77	0	1	1,300
3K16-2	10-20-77	0	1	1,300
3K16-3	10-20-77	0	3	2,410
3K16-4	10-20-77	0	3	2,410
3K16-5	11-14-77	0	28	5,870
3K16-6	11-14-77	0	28	5,850
3K16-7	10-18-77	1	1	2,780
3K16-8	10-18-77	1	1	2,790
3K16-9	10-18-77	1	1	2,700
3K16-10	11-14-77	1	28	5,320
3K16-11	11-14-77	1	28	4,980
3K16-12	11-14-77	1	28	5,400
3K16-13	10-19-77	2	2	3,650
3K16-14	10-19-77	2	2	3,600
3K16-15	10-19-77	2	2	3,680
3K16-16	11-14-77	2	28	5,270
3K16-17	11-14-77	2	28	4,980
3K16-18	11-14-77	2	28	5,320
3K16-19	10-20-77	3	3	4,110
3K16-20	10-20-77	3	3.	4,120
3K16-21	10-20-77	3	3	4,020
3K16-22	11-14-77	3	28	5,005
3K16-23	11-14-77	3	28	5,310
3K16-24	11-14-77	3	28	5,230

APPENDIX I

"VARIABLE-STATE METHODS OF MEASURING THE
THERMAL PROPERTIES OF SOLIDS" © * BY
T. C. HARMATHY; AND SUPPORTING
TEST DATA

VARIABLE-STATE METHODS OF MEASURING THE THERMAL PROPERTIES OF SOLIDS

BY

T. Z. HARMATHY

OTTAWA

Variable-State Methods of Measuring the Thermal Properties of Solids*

T. Z. HARMATHY

Fire Section, Division of Building Research, National Research Council, Ottawa 2, Canada

(Received 24 June 1963; in final form 27 December 1963)

Two variable-state methods have been developed which both offer the advantage of producing negligible thermal disturbance in a solid during measurement. The first is a curve-fitting method. It makes use of the fact that the initial temperature rise, due to a constant flux plane heat source, at points within a certain region of a finite solid is essentially the same as that in an infinite solid. Temperature records obtained from such points thus can be analyzed with the assumption of linear heat flow, and used for calculating all thermal properties of the solid.

The second is a pulse method. If a hot or cold pulse is applied to a plane surface of a specimen, the rise or drop of temperature at some distance from the surface will pass through a maximum; from the time of the maximum the thermal diffusivity can be calculated. The main advantage of this method is the ease of specimen preparation.

THE commonly used steady-state methods are not particularly well suited for measuring the thermal conductivity of solids that are liable to physicochemical changes as a result of heating. The prolonged maintenance of a significant temperature gradient across the test specimen may present several unresolvable problems to the experimenter. One of the most common problems is the migration and partial desorption of moisture when porous materials are tested in their natural condition. At higher temperatures the formation of structurally or chemically different layers perpendicular to the direction of heat flow causes difficulties in the interpretation of the test result. If the thermal conductivity is a markedly nonlinear function of the tem-

perature, and there is often good reason to assume this, correlating the measured value of the thermal conductivity with the average temperature of the specimen may be grossly erroneous.

This laboratory has long been concerned with the measurement of the thermal properties of building materials in the 20° to 1000°C range. As most building materials are subject to certain physicochemical changes (e.g., desorption of moisture, dehydration, and crystalline transformation) in this temperature interval, a minimum thermal disturbance from measurements seemed to be the most desirable feature of the technique to be adopted. Several known variable-state methods were scrutinized and discarded, partly because of their failure to yield the expected accuracy and partly because of the difficulty of specimen preparation.

The methods described in this paper were developed

---

* This is a contribution from the Division of Building Research of the National Research Council, and is published with the approval of the director of the division.

two years ago in this laboratory. The first is a curve-fitting method. It may seem to be somewhat similar to that recently published by Plummer, Campbell, and Comstock[1]; in fact, it is markedly different as regards the experimental technique and the evaluation of the measurements.[2] The second method is a pulse technique that yields a very simple way of determining thermal diffusivity at elevated temperatures.

1. NOTATION

a = thickness (dimension along x), cm

b = width (dimension along y), cm

c = length (dimension along z), cm

c = specific heat, W sec/g°C

h = coefficient of heat transfer, W/cm^2°C

I = electric current, A

k = thermal conductivity, W/cm°C

l = distance between the hot junction of thermo-couples and the plane of heat supply, cm

$n = 1, 2, 3, \cdots \infty$

q = heat flux, W/cm^2

Q = heat, W sec/cm^2

Q' = heat, W sec

r = electric resistivity, Ω cm

t = time, sec

T = temperature above or below the initial level, °C

x = space coordinate, cm

y = space coordinate, cm

z = space coordinate, cm

$$\mathrm{erfc}\, x = \frac{2}{\pi^{\frac{1}{2}}} \int_x^\infty e^{-\xi^2} d\xi, \quad \mathrm{ierfc}\, x = \int_x^\infty \mathrm{erfc}\, \xi\, d\xi,$$

$$\mathrm{i}^2 \mathrm{erfc}\, x = \int_x^\infty \mathrm{ierfc}\, \xi\, d\xi.$$

Greek

α = dummy variable, 1/cm

β = root of Eq. (A2), dimensionless

ϵ = emissivity of surface, dimensionless

θ = absolute temperature, °K

κ = thermal diffusivity, cm^2/sec

λ = variable, defined by Eq. (19), dimensionless

μ = variable, defined by Eq. (20), dimensionless

ρ = density, g/cm^3

σ = Stefan–Boltzmann constant, 5.71×10^{-12} W/cm^2°K^4

τ = period of heat supply, sec

$\phi(x) = e^{x^2} \mathrm{erfc}\, x$.

[1] W. A. Plummer, D. E. Campbell, and A. A. Comstock, J Am. Ceram. Soc. 45, 310 (1962).

[2] W. A. Plummer et al. used their method for the evaluation of thermal diffusivity only. It will be shown later that thermal diffusivity can be evaluated from much simpler measurements.

Subscripts

a = of the ambient atmosphere

av = average

c = by natural convection

f = of the heating foil

i = initial

l = at $x = l$

m = maximum, at the maximum

$n = 1, 2, 3, \cdots \infty$

o = at $x = 0$

p = of the medium used for starting a heat pulse

r = recommended, by radiation

s = of the surface

τ = of the surface during $0 < t < \tau$.

2. CURVE-FITTING METHOD

Theoretical

The problem of heat flow in an infinite solid with constant heat flux in the $x = 0$ plane is presented by the following equations[3]:

$$\partial T / \partial t = \kappa (\partial^2 T / \partial x^2) \quad \begin{array}{l} \text{for } -\infty < x < 0 \\ \text{and } 0 < x < \infty, \end{array} \quad (1)$$

$$q/2 = -k(\partial T / \partial x) \quad \text{when } x = 0,\ t > 0, \quad (2)$$

$$T = 0 \quad \text{for } -\infty < x < \infty,\ t = 0. \quad (3)$$

The solution has been given by Carslaw and Jaeger.[4] For a point selected at $x = l$ the dimensionless form of solution is

$$k T_l / q l = (\kappa l / l^2)^{\frac{1}{2}}\, \mathrm{ierfc}\tfrac{1}{2} (l^2/\kappa t)^{\frac{1}{2}}. \quad (4)$$

At $x = 0$

$$T_0 = (q/k)(\kappa t / \pi)^{\frac{1}{2}}. \quad (5)$$

It also follows from Eq. (4) that

$$\frac{T_l(2t)}{T_l(t)} = \frac{\sqrt{2}\, \mathrm{ierfc}(1/2\sqrt{2})(l^2/\kappa t)^{\frac{1}{2}}}{\mathrm{ierfc}\tfrac{1}{2}(l^2/\kappa t)^{\frac{1}{2}}} \quad (6)$$

Equations (4) and (6) are plotted in Fig. 1. If the temperature history of a point at $x = l$ in an infinite solid is known, then these plots offer a convenient way of determining the thermal diffusivity and thermal conductivity, and hence (if the density is known), the specific heat of the material. A sample calculation, based on an experimental curve shown in Fig. 2, is given in Table I.

Because the condition of constant heat flux in the $x = 0$ plane is easily realizable by the use of an electrically heated metallic foil, and because recording the temperature at some $x = l$ point of the solid presents no experimental problem, a very simple method of measur-

[3] Symbols are listed above.

[4] H. S. Carslaw and J. C. Jaeger, Conduction of Heat in Solids (Oxford University Press, London, 1959), 2nd ed., pp. 63, 75, 76, 88, 112, 358, 373.
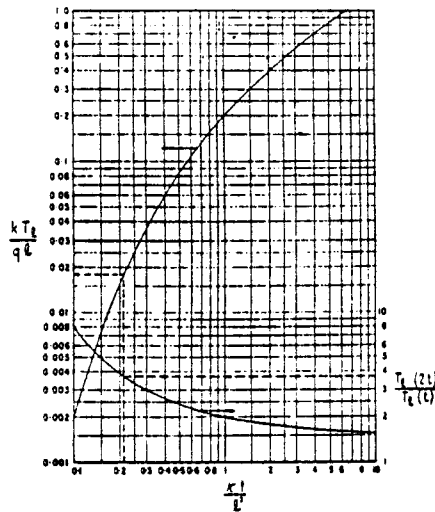
Fig. 1. Plot of Eqs. (4) and (6).

the technique to be adopted. A few preliminary experiments with the method outlined above indicated that the period of heat supply τ could be reduced to 420 sec and $T'(l,\tau)$ to 5° to 7°C without any loss in accuracy, provided that $\kappa\tau/l^2$ remained smaller than about 1.6. (An inspection of the $T_i(2l)/T_i(l)$ curve reveals that, owing to the flattening out of the curve, the evaluation of the $\kappa l/l^2$ group from experimental values of $T_i(2l)/T_i(l)$ is rather difficult if $\kappa\tau/2l^2 > 1.$[5]) Combining these observations, a criterion can be derived for the "recommended" value of l (i.e., for the recommended location of the hot junction of the thermocouples, whose signal is used for recording the temperature):

$$l_r = (420\kappa/1.6)^{\frac{1}{2}} = (262.5\kappa)^{\frac{1}{2}} \qquad (7)$$

as well as for the "recommended" heat flux in the $x=0$ plane [taking $T_i(\tau)=6°C$ as an average and using Eq. (4)]:

$$q_r = 6k/(262.5\kappa)^{\frac{1}{2}}(1.6)^{\frac{1}{2}} \text{ ierfc}\tfrac{1}{2}(1/1.6)^{\frac{1}{2}}$$

$$= 1.14887 \ (k\rho c)^{\frac{1}{2}}. \quad (8)$$

As it is not too difficult to estimate the values of k and c with a ±50% accuracy from ρ, or from data available from the literature, l_r and q_r can always be approximated within ±30%, most often within ±10%. These recommended values have, therefore, been chosen for calculating those numerical values through which the effect of the finite size of the specimen on the accuracy of the test result will be studied in the following paragraphs.

In practical cases the error in the value of $T(l,\tau)$ due to the finite thickness $2a$ of the specimen is obviously always less than it would be in that hypothetical case where the specimen is perfectly insulated in the $x=-a$ and $x=a$ planes. Calculations performed by means of the expression derived by Carslaw and Jaeger[4] indicated that during the standard test period (420 sec) this error is never larger than 0.006% if $a \geq 4l$.

As will be discussed later, fulfilling the $a \geq 4l$ condition seldom presents any practical problem. The selection of

ing the thermal properties of solids seems to be available. It is obvious, however, that since the sizes of an actual test specimen are finite, Eqs. (4) and (6) cannot be expected to hold true for any point inside the specimen or for any length of time. It has to be proven, therefore, that experimental conditions under which Eqs. (4) and (6) (or their plots in Fig. 1) can be used for the evaluation of the thermal properties do exist, and that the calculations are capable of yielding acceptable accuracy.

This laboratory has mainly been concerned with chemically unstable materials; thus the production of a minimum thermal disturbance in the solid during the measurements was regarded as an important feature of
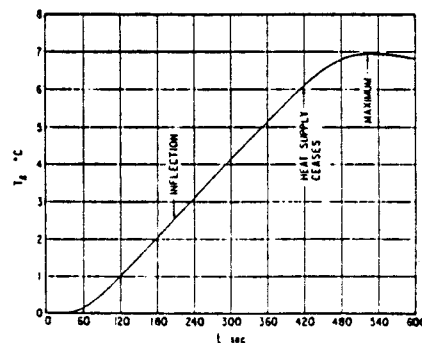

Fig. 2. Experimental curve for expanded shale concrete at room temperature.

Table I. Sample calculation, based on the curve in Fig. 2. Material: expanded shale concrete, oven-dry. Initial temperature $= 21.5°C$, $l = 1.369$ cm, $q = 0.1168$ W/cm², $\rho = 1.2747$ g/cm³.[a]

t sec	$T_i(2l)/T_i(l)$	$\kappa l/l^2$	κ cm²/sec	kT_i/ql	k W/cm°C
90	2.03/0.55 = 3.69	0.213	0.00444	0.0178	0.00518
120	3.10/1.01 = 3.07	0.290	0.00453	0.0337	0.00534
150	4.14/1.52 = 2.74	0.362 [b]	0.00452	0.0503 [b]	0.00530
180	5.14/2.03 = 2.53	0.435	0.00453	0.0670	0.00528
210	6.09/2.57 = 2.37	0.515	0.00460	0.0865	0.00538
Average			0.004524		0.005296

[a] $c = 0.005296/1.2747 \times 0.004524 = 0.9183$ W sec/g°C; average temperature of the $0 < x < l$ region $= 27.5°C$.
[b] Determined from Fig. 1.

[5] Note that, since the heat input is terminated at τ, the last value of $T_i(2l)/T_i(l)$ that can be used for the evaluation of $\kappa l/l^2$ is $T_i(\tau)/T_i(\tau/2)$.

the width b of the specimen, on the other hand, is rarely without restrictions. Many building materials (e.g., bricks, some concrete blocks) come in a standard maximum width, $3\frac{3}{4}$ in. (9.5 cm) as a rule. Obtaining metallic heating strips of satisfactory characteristics in widths larger than $3\frac{1}{2}$ in. is also very difficult. But even if wider strips are available, increasing their width significantly beyond $3\frac{1}{2}$ in. would cause considerable experimental difficulties. The heat flux, in terms of the electric current, is given by

$$q = I^2 r / b_f^2 a_f. \qquad (9)$$

If b_f is too great, inconveniently high current may be needed to satisfy Eq. (8).

From these considerations it appears that the practical range for b is from 8 to 10 cm. In the case of building materials and other materials of noncrystalline or highly disordered crystalline structure, this width corresponds roughly to $8l_r$.

The solution of the equation of heat conduction for a region bounded by two parallel planes at $y = 0$ and $y = b$ is given by Eq. (A6) in the Appendix. Calculations have been performed on the assumption that the coefficient of heat transfer h is infinite (more exactly, $hb/k \rightarrow \infty$) at $y = 0$ and $y = b$. It has been found that even in this not realizable limiting case $T(l,b/2,\tau)$ does not differ from the value calculable from Eq. (4) by more than 1.15%. Based on this finding it can also be concluded that the finite length c of the specimen will hardly affect the value of $T(l,b/2, c/2,\tau)$ if $c \gg b$. In this laboratory c is generally taken as $2b$.

The results of the above mentioned and some additional calculations are summarized in Table II. These values provide proof that if l, a, b, and c are properly chosen the temperatures at $\tau = l$, $y = b/2$, and $z = c/2$ do not depart significantly from the value yielded by Eq. (4) during a 420-sec period. This fact, in turn, supports the applicability of the plots in Fig. 1 to the evaluation of the thermal properties of specimens of finite sizes from the recorded temperature history of a point reasonably close to $x = l_r$, $y = b/2$, and $z = c/2$.

Figure 3 shows a correctly sized specimen assembled for test. In the case of good heat conductors, especially semiconductors and metals, l_r may become comparable with or even larger than the recommended width.
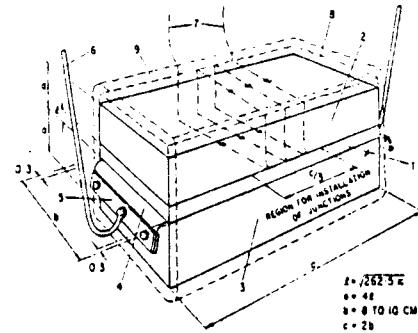

Fig. 3. Specimen assembled for high-temperature test. 1, measuring piece; 2, top piece; 3, bottom piece; 4, palladium foil; 5, Inconel clamps; 6, Alumel lead wire for foil heating; 7, thermocouple wires; 8, Fiberfrax cover; 9, over-all Fiberfrax wrapping; —·—·— Chromel; —··—··— Alumel; X, thermocouple junctions.

Although the author has little experience with such materials, he thinks that a relatively high l/b ratio does not necessarily spoil the test result. According to Eq. (A6) it is primarily the hb/k group that determines the component of heat flux in the y direction. If, at the same value of h and b, k is large, the value of the hb/k group is small; consequently, the fact that the condition of perfect insulation at the planes $y = 0$ and $y = b$ is better approximated may counteract the adverse effect of the large l/b ratio. Of course, in the case of good conductors q_r is also very large; thus the high current requirement (50 to 130 A with the heating foils used in this laboratory) may cause some experimental difficulties.

By wrapping a $\frac{1}{4}$-in.-thick Fiberfrax blanket around the specimen the error due to the finite width can further be reduced. The use of such insulating wrapping is especially important when elevated temperature measurements are contemplated. At 700°C the coefficient of heat transfer between the specimen and the surroundings is about 30 times higher than that at room temperature; thus, without insulation the condition $hb/k \rightarrow \infty$ may arise.

Figure 3 shows an additional layer of Fiberfrax on the top of the specimen. The reason for using this extra insulating layer is to provide a convenient location for the cold junctions of the thermocouples. Since for the evaluation of the thermal properties of the material the rise of T_i above the initial level is of interest, the cold junctions have to be located where the temperature remains constant during measurement. Table II shows that the rise of temperature at $x = a$ may be rather significant, so that the cold junctions must not be put in contact with the upper surface of the specimen.

However thin the heating foil, it has finite thermal conductance and finite heat capacity. If the sides of the specimen are not insulated, the effect of finite conductance is a slight flow of heat within the foil toward the

TABLE II. Temperature distribution in the specimen at $t = 420$ sec, for various boundary conditions. Case A: infinite solid, constant heat flux $q = q_r$ at $x = 0$, $T_i = 0$; Case B: infinite slab, $-a < x < a$, $a = 8l_r$, constant heat flux $q = q_r$ at $x = 0$, $T_i = 0$; Case C: region bounded by two parallel planes, $-\infty < x < \infty$, $0 < y < b$, $b = 8l_r$, constant heat flux $q = q_r$ at $x = 0$, $hb/k \rightarrow \infty$, $T_i = 0$

Location of point	Temperature, °C		
	Case A	Case B	Case C in plane $y = b/2$
at $x = 0$	13.2837°	13.2838°	13.2008°
at $x = l_r$	6.0000°	6.0003°	5.9319°
at $x = 4l_r$	0.1468°	0.2935°	0.1426°

edges where significant temperature gradient may exist. Though Fiberfrax wrapping is the best defence against this undesirable phenomenon, it seems good practice to have the specimen extend slightly beyond the width of the foil.

The effect of the finite heat capacity is that the Joule heat generated in the foil is partly absorbed by the foil itself. The average heat absorption of a 0.001-in.-(0.025-mm) thick foil during a 420-sec test is about 0.0003 W/cm², and can thus be disregarded in most practical cases. Nevertheless, if good insulators are tested, the heat absorption may amount to 5% to 10% of q_r during the first 10 sec, and to an average of about 1% for the duration of the test.

The average temperature of the region $0 < x < l$, i.e., the temperature to which the measured values of the thermal properties shall be related, can be calculated from Eq. (A11), or can be taken roughly as $T_1(r)$. When $l = l_r$ and $q = q_r$, $T_{av} = 5.3652°C$.

The average temperature of the heating foil will also be of interest. From Eq. (5) it follows immediately that

$$(T_f)_{av} = \tfrac{2}{3}(q/k)(\kappa r/\pi)^{\frac{1}{2}} = \tfrac{2}{3}T_0(r). \qquad (10)$$

If $q = q_r$, $(T_f)_{av} = 8.8558°C$.

Experimental

The combination of heating foils and thermocouples used for various temperature ranges in this laboratory is given in Table III.

The resistivity [more exactly, the r/a_f ratio which appears in equation (9)] of the heating foils has been determined in this laboratory by measuring the potential drop through a specimen 3 cm wide and about 30 cm long, due to a current of about 100 mA. The variation of the r/a_f ratio with temperature is shown in Fig. 4. The resistivity of the palladium proved somewhat higher than the values reported in the literature,[4] probably

TABLE III. Heating foils and thermocouples used for various temperature ranges.

Temperature range, °C	Heating foil	Thermocouples
0°–300°	Constantan 0.001 in. thick,[a] 3.5 in. wide	Chromel-Constantan double differential B and S gauge 36
0°–700°	Palladium[b] 0.001 in. thick,[a] 3 to 4 in. wide	Chromel-Alumel triple differential B and S gauge 36
0°–1000°	Palladium[b] 0.001 in. thick,[a] 3 to 4 in. wide	Pt–Pt 13% Rh triple differential B and S gauge 36

[a] Nominal; 0.001 in. = 25 μ.
[b] Commercially pure.

[a] *Handbook of Thermophysical Properties of Solid Materials: Elements* (Pergamon Press, Inc., New York, 1961), Vol. I, Sec. I, p. 487.

because of the presence of some alloying material. It showed an excellent stability and practically no change after prolonged exposure to 1000°C. The resistivity of Constantan was found to be close to the generally accepted values.[7] There was a slight spread in the results, and the values obtained during the heating and cooling cycles followed different courses. It seems possible that this problem could be eliminated by stabilizing the material at about 320°C. probably the highest temperature that Constantan can be exposed to for longer periods. The curve given in Fig. 4 for Constantan represents the average of several measurements.

In spite of its stable properties palladium is a very poor choice for tests at room-temperature and moderately elevated temperatures. At room temperature the increase in its resistivity during a test may be as high as 5%; if the current is kept constant this corresponds to a 5% increase in the heat flux. Of course when a series of tests covering a range larger than 0° to 300°C is con-
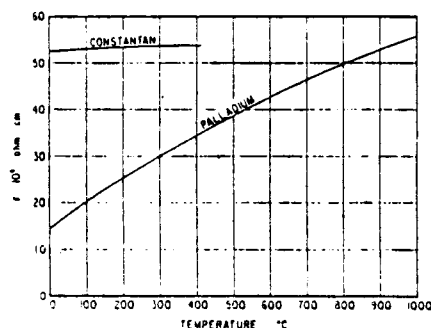

Fig. 4. Electric resistance of heating foils.

templated, there are practical reasons for using palladium throughout the whole range. In such cases, however, a slight drop in the current, corresponding to half the estimated percentage increase in the resistivity, should be allowed during the test.

When testing electrical conductors, the foil has to be sandwiched between thin sheets of paper or mica, and the potential difference between the foil and specimen should be kept at a minimum value.

If $l \approx l_r$ and $q \approx q_r$, the output from double Chromel-Constantan or triple Chromel-Alumel differential thermocouples connected in series (see Fig. 3) can be recorded directly on a 1-mV recorder. To keep the signal-to-noise ratio as high as possible, installation of a dc amplifier in the thermocouple circuit should be avoided. In the case of noble metal thermocouples, however, over 20 junctions would be required to produce a signal large enough to record directly. As it is rather difficult to install more

[7] *International Critical Tables* (McGraw-Hill Book Company, Inc., New York, 1929), Vol. 6, p. 170.

than six junctions in the specimen, a slight amplification of the signal has to be tolerated.

The use of very light bare thermocouple wires is recommended for two reasons: to reduce the flow of heat away from the hot junctions to a negligible value, and to allow a practically gap-free contact between the "measuring piece" and the "top piece" (see Fig. 3) without making grooves in their surfaces.

In the case of electrical conductors the thermocouple wires must be coated with insulation. If a single differential thermocouple is used, the hot junction can be in direct contact with the specimen and may be introduced into the specimen through a hole drilled in the $x=l$ plane.

In this laboratory a masonry saw is used to cut the three pieces that generally make up the specimen. If the cutting is done carefully, it is rarely necessary to grind the surfaces.

It often happens that the maximum available thickness of the material is less than the recommended thickness, $4l_i$. In such cases the specimen can be composed of several well-fitting thinner slabs.

The block diagram of an experimental setup for elevated temperature measurements is shown in Fig. 5. To reduce the possibility of stray signal pickup by the thermocouple circuit the metal foil is heated by direct current. For the same reason the furnace heating is also switched to direct current a few minutes before the beginning of test. The batteries are charged between tests.

A special furnace has been built for thermal conductivity tests; it is heated from all six sides, and the current to each can be adjusted separately. In this way a very uniform temperature distribution in the specimen can be attained. It has been found, however, that the uniformity of the initial temperature of the specimen is not absolutely necessary. Many successful tests have been performed on specimens of nonuniform temperature distribution in steady-state or even in quasisteady-state condition. A constant output from the differential thermocouples during a 420-sec period seems to be the only prerequisite of the test.

For materials which are regarded as electrical insulators at room temperature, there are generally no experimental problems up to about 700°C. Above this temperature serious difficulties may arise, which are associated partly with a gradual increase in the electrical conductivity of such materials, and partly with a slow charge buildup on the metal foil and thermocouple wires following the switching on of the foil heating. This last phenomenon is caused mainly by space-charge polarization,[*] and is less serious when alternating current is used for foil heating.

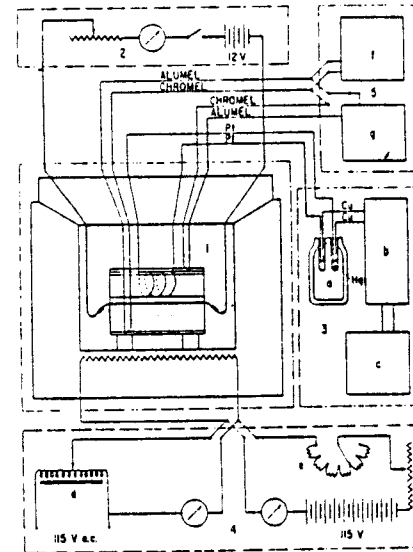The $0 < t < 90$-sec portion of the temperature record is

FIG. 5. Experimental setup for high-temperature measurements with curve-fitting method. 1, furnace and specimen; 2, foil heating; 3, measuring of output from thermocouples [(a), Dewar flask for keeping constant temperature at copper connections; (b), dc amplifier; (c), 1-mV recorder]; 4, furnace heating [(d), variable transformer; (e), resistor switch with globar resistors]; 5, furnace temperature measurement [(f), temperature recorder, (g), potentiometer for checking the difference of temperature at top and bottom of specimen).

generally not suitable for the evaluation of the thermal properties of the material. In this interval, as Fig. 2 shows, T_i is very small; thus the value of the $T_i(2t)/T_i(t)$ ratio is somewhat uncertain. In addition, as mentioned before, the effect of the finite heat capacity of the heating foil is sometimes very noticeable at early stages of the test.

In Fig. 6 the result of a series of tests performed on insulating fire brick, group 23, is plotted. The agreement with data reported in the literature[*] seems to be satisfactory.

J. HEAT PULSE METHOD

Theoretical

As Fig. 2 shows, T_i continues rising for a short time, even after the heat supply is switched off at $t=\tau$. An analytical expression for the temperature history of an infinite solid for $t>\tau$ has been derived by Carslaw and Jaeger.[*] For $x=l$ this expression can be given in the

[*] W. D. Kingery, *Introduction to Ceramics* (John Wiley & Sons, Inc., New York, 1960), pp. 695, 725.

[*] C. L. Mantell, *Engineering Materials Handbook* (McGraw-Hill Book Company, Inc., New York, 1958), 1st ed., Sec. 25, p. 72.

• CONSTANTAN HEATING FOIL, $l=0.87$ cm, $\rho=0.736$ g/cm^3
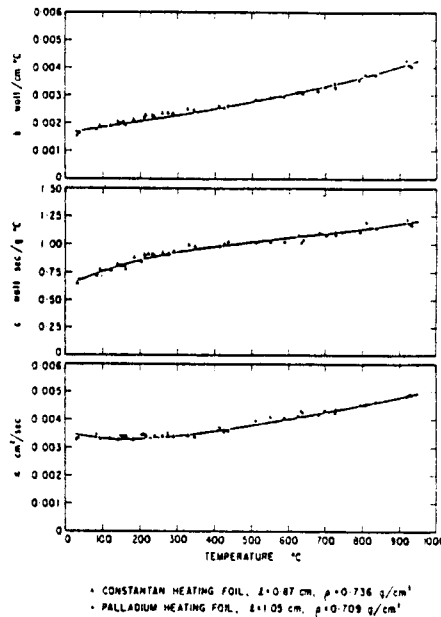• PALLADIUM HEATING FOIL, $l=1.05$ cm, $\rho=0.709$ g/cm^3

Fig. 6. Thermal properties of insulating fire brick, group 23.

following dimensionless form:

$$\frac{kT_l}{ql} = \left(\frac{\kappa t}{l^2}\right)^{\frac{1}{2}} \left\{ \mathrm{ierfc}\frac{1}{2}\left(\frac{l^2}{\kappa t}\right)^{\frac{1}{2}} \right.$$
$$\left. -\left(1-\frac{\tau}{t}\right)^{\frac{1}{2}} \mathrm{ierfc}\frac{1}{2}\left(\frac{l^2}{\kappa(t-\tau)}\right)^{\frac{1}{2}} \right\} \quad (11)$$

After differentiating with respect to t, and making the right side of the resulting equation equal to zero, the following expression is obtained for the time coordinate of the maximum, t_m:

$$\frac{\kappa t_m}{l^2} = \frac{1}{2}\frac{\tau/t_m}{[1-(\tau/t_m)]\ln[1-(\tau/t_m)]^{-1}} \quad (12)$$

This equation provides a simple way of evaluating κ from measured value of t_m. If, in addition, $(T_l)_m$ is also known, k can be computed from Eq. (11).

If $\tau = 420$ sec, τ/t_m is close to 1, and this method of determining κ is not very accurate. The accuracy can greatly be improved by making $\tau \to 0$.

As the period of heat supply, τ, is gradually decreased, the expression on the right side of Eq. (12) tends to $\frac{1}{2}$. Thus, if a momentary heat pulse is supplied through the metal foil, the thermal diffusivity κ can be calculated from the following simple expression:

$$(\kappa t_m/l^2)_{h=0} = \frac{1}{2}. \quad (13)$$

The subscript $h=0$ is used to indicate that there is no heat flux through the $x=0$ plane, because the same condition would arise in the case of a $0<x<\infty$ region if the heat transfer coefficient at the $x=0$ plane (which is also the plane of heat supply during $0<t<\tau$) was zero.

If $h\neq 0$, only part of the heat applied to the surface (not necessarily through a metal foil) of a semi-infinite solid penetrates the solid after the removal of the heat source; part of it is transferred to the ambient atmosphere by convection and radiation. It is obvious, therefore, that t_m must be a function of h as well as of κ and l.

The fact that h does affect the time coordinate of the maximum can easily be proven by examining the case of $h \to \infty$. This condition is obviously fulfilled by assuming that the temperature at $x=0$, after being kept at T_τ for $0<t<\tau$, becomes equal to that of the ambient atmosphere (which is taken here as zero) for $t>\tau$. The solution of this problem for $x=l$ is as follows[4]:

$$T_l/T_\tau = \mathrm{erfc}\frac{1}{2}(l^2/\kappa t)^{\frac{1}{2}} - \mathrm{erfc}\frac{1}{2}[l^2/\kappa(t-\tau)]^{\frac{1}{2}}. \quad (14)$$

With the usual procedure it can be shown that in this case

$$\frac{\kappa t_m}{l^2} = \frac{1}{6}\frac{\tau/t_m}{[1-(\tau/t_m)]\ln[1-(\tau/t_m)]^{-1}} \quad (15)$$

or if $\tau/t_m \to 0$ (momentary heat supply),

$$(\kappa t_m/l^2)_{h\to\infty} = \frac{1}{6}. \quad (16)$$

By comparing Eqs. (12) and (15) or Eqs. (13) and (16), one can see that as h increases from 0 to ∞, t_m decreases by a factor of 3. It is reasonable to assume that if τ/t_m is very small, the value of the $\kappa t_m/l^2$ group is somewhere between $\frac{1}{6}$ and $\frac{1}{2}$ for finite values of h. The calculations that have been performed to find the correlation between the $\kappa t_m/l^2$ group and h are outlined below.

If at $t=0$ an instantaneous plane source of strength $Q/\rho c$ is applied to the $x=0$ surface of an $x>0$ semi-infinite region, the variation of the temperature in the $x=l$ plane is described by the following expression[4]:

$$T_l = \frac{Q}{\rho c l}e^{-(l^2/4\kappa t)}\left\{\frac{1}{\pi^{\frac{1}{2}}}\left(\frac{l^2}{\kappa t}\right)^{\frac{1}{2}} - \frac{hl}{k}\phi\left[\frac{1}{2}\left(\frac{l^2}{\kappa t}\right)^{\frac{1}{2}} + \frac{h}{k}(\kappa t)^{\frac{1}{2}}\right]\right\}. \quad (17)$$

After differentiating with respect to t and making the right side of the resulting equation equal to zero, the following equation is obtained:

$$\lambda^2 - \lambda\mu + \mu^2 - \pi^{\frac{1}{2}}\mu^3\phi(\lambda+\mu) - \frac{1}{2} = 0, \quad (18)$$
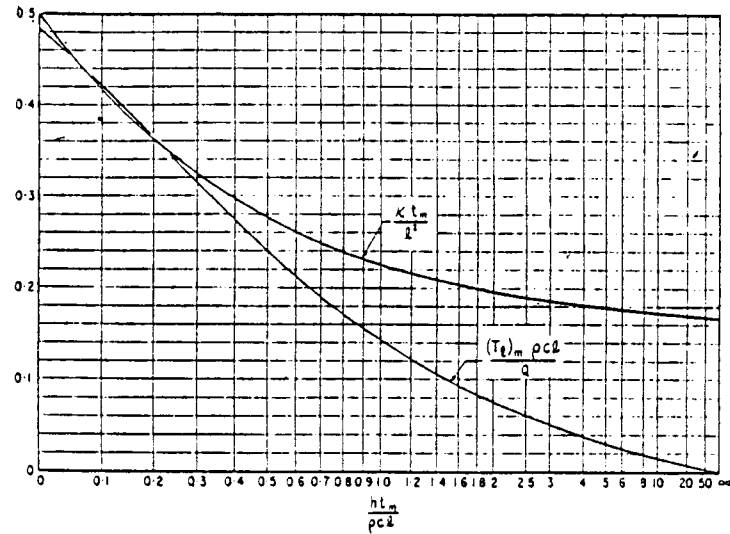
where

$$\lambda = \frac{1}{2}(l^2/\kappa t_m)^{\frac{1}{2}}, \quad (19)$$

and

$$\mu = (h/k)(\kappa t_m)^{\frac{1}{2}}, \quad (20)$$

Fig. 7. Dimensionless plot of the solution of Eq. (17) (at the maximum) and of Eq. (18).

since Eq. (18) is obviously the one defining the time coordinate of the maximum of T_l.

The solution of Eq. (18) is presented graphically in Fig. 7. When plotting the curve the

$$\kappa t_m/l^2 \equiv 1/4\lambda^2$$

and

$$h t_m/\rho c l \equiv \tfrac{1}{2}(\lambda/\mu)$$

dimensionless groups have been chosen instead of λ and μ for convenience. It may be seen that if $h = 0$, $\kappa t_m/l^2 = \tfrac{1}{6}$, and if $h \longrightarrow \infty$, $\kappa t_m/l^2 = \tfrac{1}{6}$, in agreement with Eqs. (13) and (16).

Figure 7 offers a simple means of calculating the thermal diffusivity from experimental value of t_m, provided the heat transfer coefficient at the $x = 0$ surface is known. Unfortunately, it is not always possible to estimate h with sufficient accuracy, especially at room temperature. The main difficulty lies in the fact that h is not a true constant but a function of the surface temperature.

It may be useful to review briefly the way of estimating h. The coefficient of heat transfer by natural convection between a surface facing upward and the ambient air can be calculated from the following empirical formula[19]:

$$h_c = 0.00025 |T_s - T_a|^{\tfrac{1}{4}}. \qquad (21)$$

The coefficient of radiant heat transfer from a surface of emissivity ϵ to nonreflecting surroundings can be de-

[19] W. H. McAdams, *Heat Transmission* (McGraw-Hill Book Company, Inc., New York, 1942), p. 240.

rived from the Stefan–Boltzmann law and is given by

$$h_r = \sigma \epsilon [(\theta_s{}^4 - \theta_a{}^4)/(\theta_s - \theta_a)] \qquad (22)$$

which, if $\theta_s \longrightarrow \theta_a$, becomes

$$h_r = 4\sigma \epsilon \theta_a{}^3. \qquad (23)$$

The coefficient of heat transfer by a combined convection–radiation mechanism can be taken as the sum of the coefficients for the two individual mechanisms, i.e.,

$$h = h_c + h_r. \qquad (24)$$

Because of the variation of T_s during the $0 < t < t_m$ period, the effective value of h depends not only on the strength of heat pulse but also on l. From temperature records obtained following a short heat pulse, from two thermocouples installed in an insulating fire brick at 1- and 2-cm distances from the $x = 0$ plane, respectively, the following effective values have been calculated:

for $l = 1$ cm $\quad h = 0.00077$ W/cm²°C,

for $l = 2$ cm $\quad h = 0.00057$ W/cm²°C.

The first value indicates an average temperature difference of about 1°C between the surface and the surroundings. The second value is approximately equal to that which can be obtained from Eq. (23) alone, i.e., on the assumption that $\theta_s \longrightarrow \theta_a$; thus $h_c \approx 0$.

If the intensity of the heat pulse is not too high, calculating h from Eq. (23) is often permissible, even at room temperature. It is always permissible at higher temperatures for two reasons: first, the heat transfer by convection is negligible in comparison with that by

radiation, and secondly, the coefficient of heat transfer by radiation is not significantly affected by slight changes in θ_s.

As Fig. 7 shows, at high values of $ht_m/\rho c l$ the variation of the $\kappa t_m/l^2$ group is very slow; at higher temperatures, therefore, only a rough estimate of h is needed. In the case of good conductors, on the other hand, the high-temperature range is more critical. At room temperature the $ht_m/\rho c l$ group is so small that taking $\kappa t_m/l^2$ as equal to $\frac{1}{4}$ is often permissible.

There is, of course, no need to estimate h, if not the thermal diffusivity proper, but the effect of some slowly developing physicochemical changes (e.g., desorption of moisture, dehydration, and crystalline transformation) at a given temperature level on the thermal diffusivity is of primary interest.

When selecting the distance l the following facts should be considered. When l is small, $(T_l)_m$ is high, and the T_l vs t curve exhibits a sharp maximum from which t_m can be determined fairly accurately. Nevertheless, the value obtained for κ may be grossly inaccurate for three reasons. First, because τ is always finite, the t/τ_m ratio may become large enough to invalidate the assumption of instantaneous heat supply. Secondly, the variation of the surface temperature is very significant immediately after the application of the heat pulse, so that estimating the effective value of h for a short t_m is rather difficult. Thirdly, the error increases as the distance to be measured is decreased, and any error in l causes twice as large an error in the value of κ.

By selecting l large, all these difficulties can be eliminated; nevertheless, $(T_l)_m$ becomes much lower and the peak much flatter.

It has been found that selecting l corresponding roughly to l_r defined by Eq. (7) is probably the best compromise. With this selection t_m is of the order of 60 sec.

The $(T_l)_m \rho c l/Q$ vs $ht_m/\rho c l$ plot, which is also presented in Fig. 7, can be used to estimate the value of Q that will yield a certain $(T_l)_m$. The actual value of $(T_l)_m$ is, of course, immaterial in these tests, but it should be high enough to produce a sufficiently large emf in the hot junction, located at l, of a differential thermocouple. Taking $(T_l)_m \approx 2°C$, selecting an average value of 0.33 for the $(T_l)_m \rho c l/Q$ group, and assuming that $l \approx l_r$, the following equation is obtained:

$$Q \approx 100(k\rho c)^{\frac{1}{2}}. \qquad (25)$$

At room temperature the most convenient means of producing a heat pulse is to bring a piece of hot metal into contact with the upper surface of the specimen. From the solution of the equation of heat conduction when a material of k_p, c_p, ρ_p properties and of T_p temperature is brought into contact with another material of k, c, ρ properties and zero temperature along the $x=0$ plane,[4] the following expression can be derived for the heat absorbed by unit area of the latter material in a time τ:

$$Q = (2T_p/\pi^{\frac{1}{2}}) \left\{ \frac{\tau^{\frac{1}{2}}}{(1/k_p\rho_p c_p)^{\frac{1}{2}} + (1/k\rho c)^{\frac{1}{2}}} \right\}. \qquad (26)$$

If the first material is metal, and the second a non-metallic specimen, then because $k_p\rho_p c_p \gg k\rho c$, the above equation reduces to

$$Q \approx 2T_p(k\rho c\tau/\pi)^{\frac{1}{2}}. \qquad (27)$$

By combining Eqs. (25) and (27) one gets

$$\tau \approx 7850/T_p^2, \qquad (28)$$

which is an expression for the time of application of a metal object of T_p temperature to the surface of a non-metallic specimen, to produce about 2°C temperature rise at l, from the surface.

At elevated temperatures it is more convenient to use a "cold pulse" by applying a momentary jet of cool air to the surface of the specimen. Assuming that the coefficient of heat transfer between the jet and the surface is of the order of 0.06 W/cm²°C, and that the temperature of the jet is T_p below that of the initial surface temperature, the time of application to produce a 2-C° drop at l, is obtained as

$$\tau \approx 1670[(k\rho c)^{\frac{1}{2}}/T_p]. \qquad (29)$$

The effect of the finite thickness (the dimension in the x direction) of the specimen on t_m was investigated by numerical analyses. It has been found that if $a > 2.5l$ this effect is insignificant.

In a further series of numerical analyses the effect of the frequency of the pulses was studied. It has been established that an interval of not less than $10 t_m$ should be left between two subsequent pulses. As the interval is reduced some reduction in t_m is experienced.

The effect of the finite values of b and c on t_m has not been investigated analytically. In this laboratory square or round specimens are most often used for these tests. The l/b ratio has ranged from 0.75 to 10. The specimens are always surrounded by insulation.

It may be mentioned that in 1961 two pulse methods were described.[11,12] Both are applicable only to metals and neither is comparable in simplicity to the present method.

Experimental

As the output from the differential thermocouple in these tests serves only for evaluating t_m, any two dissimilar metals can be used for thermocouple wires. When metallic specimens are tested the specimen itself can be chosen as one leg of the differential thermocouple.

The perfect smoothness of the emf vs t curve is now not so essential as it was with the curve-fitting method.

[11] E. L. Woisand, J. Appl. Phys. 32, 40 (1961).
[12] W. J. Parker, R. J. Jenkins, C. P. Butler, and G. L. Abbott, J. Appl. Phys. 32, 1679 (1961).
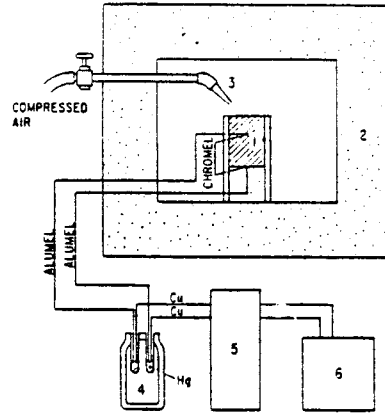
FIG. 8. Experimental setup for high-temperature measurements with pulse method. 1, specimen; 2, furnace; 3, fan-shaped horn; 4, Dewar flask for keeping constant temperature at copper connections; 5, dc amplifier; 6, 1-mV recorder.

FIG. 9. Experimental curve for insulating fire brick at 470°C.

Thus as higher amplification of the signal is tolerable, it is not necessary to use multiple differential thermocouples. The hot junction of the thermocouple is generally introduced into the specimen through a hole drilled in the $x=l$ plane. The cold junction can be in contact with the specimen, but should be insulated from the furnace.

The block diagram of an experimental setup for high-temperature measurements is shown in Fig. 8. In this laboratory a fan-shaped horn made from Inconel is used for the introduction of cool air. It is advisable here, too, to switch to dc furnace heating for the period during

which the maximum of the emf vs time curve is passed, or to take other measures to minimize the pickup of stray signals by the thermocouple wires.

An experimentally obtained emf vs t curve is shown in Fig. 9. The test was carried out at 470°C on a specimen of insulating fire brick, group 23. Assuming $\epsilon=0.9$, according to Eq. (23), $h\approx0.0084$ at this temperature. With $l=1$ cm and $t_m=62.5$ sec the value of the $hl_m/\rho cl$ group is about 0.94. Figure 7 shows that in this regime the variation of $\kappa l_m/l^2$ is rather slow; thus even a rough value of the $hl_m/\rho cl$ group will yield acceptable accuracy. From Fig. 7 $\kappa l_m/l^2=0.229$, and, therefore, $\kappa=0.00366$ cm²/sec. This value is in good agreement with that obtained with the curve fitting method (see Fig. 6).

ACKNOWLEDGMENT

APPENDIX

The temperature of a solid region $-\infty<x<\infty$, $0<y<b$, $-\infty<z<\infty$ ($T_s=0$) due to an instantaneous point source of strength $Q'/\rho c$ at $x=0$, $y=y'$, $z=z'$ when $t=0$, and to linear heat transfer (characterized by a heat transfer coefficient h) at the $y=0$ and $y=b$ surfaces into a medium at $T_a=0$, is given by[1]

$$T=\frac{Q'}{\rho cb}\frac{e^{-[z^2-(x-x')^2]/4\kappa t}}{2\pi\kappa t}\sum_{n=1}^{\infty}\frac{[\beta_n\cos\beta_n(y/b)+(hb/k)\sin\beta_n(y/b)][\beta_n\cos\beta_n(y'/b)+(hb/k)\sin\beta_n(y'/b)]}{\beta_n^2+2(hb/k)+(hb/k)^2}e^{-\beta_n^2(\kappa t/b^2)},\quad(A1)$$

where the β are positive roots of

$$\tan\beta=2\beta(hb/k)/[\beta^2-(hb/k)^2].\quad(A2)$$

In the case of a continuous heat source of $q/\rho c$ strength in the plane $x=0$, $0<y<b$, the following equation results:

$$T=\frac{q}{\rho cb}\int_{-\infty}^{\infty}dz'\int_0^b dy'\int_0^t dt'\left\{\frac{e^{-[z^2-(x-x')^2]/4\kappa(t-t')}}{2\pi\kappa(t-t')}\sum_{n=1}^{\infty}e^{-\beta_n^2[\kappa(t-t')/b^2]}\frac{[\beta_n\cos\beta_n(y/b)+(hb/k)\sin\beta_n(y/b)][\beta_n\cos\beta_n(y'/b)+(hb/k)\sin\beta_n(y'/b)]}{\beta_n^2+2(hb/k)+(hb/k)^2}\right\}.\quad(A3)$$

The first two integrals present no problem. After performing these integrations one gets

$$T = \frac{q}{\rho c}\sum_{n=1}^{\infty}\frac{[(hb/k)(1-\cos\beta_n)+\beta_n\sin\beta_n][\beta_n\cos\beta_n(y/b)+(hb/k)\sin\beta_n(y/b)]}{\beta_n[\beta_n^2+2(hb/k)+(hb/k)^2]}\int_0^t\frac{e^{-[x^2/4\kappa(t-t')]}}{[\pi\kappa(t-t')]^{\frac{1}{2}}}e^{-\beta^2[\kappa(t-t')/b^2]}dt'. \quad (A4)$$

The simplest way of evaluating this integral is by making use of the following Fourier cosine transformation[13]:

$$e^{-[x^2/4\kappa(t-t')]} = \frac{2}{\pi^{\frac{1}{2}}}[\kappa(t-t')]^{\frac{1}{2}}\int_0^{\infty}e^{-\alpha^2\kappa(t-t')}\cos\alpha x\, d\alpha. \quad (A5)$$

After substituting and performing the integration with respect to t' one gets

$$\frac{2}{\pi}\int_0^{\infty}\frac{\cos\alpha x}{[\alpha^2+(\beta_n/b)^2]\kappa}(1-e^{-[\alpha^2+(\beta_n/b)^2]\kappa t})d\alpha.$$

The solution of this integral is available in tables of Fourier cosine transforms. Finally the following expression is obtained:

$$T = \frac{qb}{k}\sum_{n=1}^{\infty}\frac{1}{\beta_n^2}\frac{[(hb/k)(1-\cos\beta_n)+\beta_n\sin\beta_n][\beta_n\cos\beta_n(y/b)+(hb/k)\sin\beta_n(y/b)]}{\beta_n^2+2(hb/k)+(hb/k)^2}$$
$$\cdot\left(e^{-\beta_n(x/b)}-\frac{1}{2}\left\{e^{-\beta_n(x/b)}\mathrm{erfc}\left[\beta_n\left(\frac{\kappa t}{b^2}\right)^{\frac{1}{2}}-\frac{1}{2}\left(\frac{x^2}{\kappa t}\right)^{\frac{1}{2}}\right]+e^{\beta_n(x/b)}\mathrm{erfc}\left[\beta_n\left(\frac{\kappa t}{b^2}\right)^{\frac{1}{2}}+\frac{1}{2}\left(\frac{x^2}{\kappa t}\right)^{\frac{1}{2}}\right]\right\}\right). \quad (A6)$$

If $hb/k \to \infty$, $\beta_n = n\pi$, then

$$T = \frac{qb}{k}\frac{2}{\pi^2}\sum_{n=1}^{\infty}\frac{[\sin(n\pi/2)]^2\sin(n\pi y/b)}{n^2}$$
$$\cdot\left(e^{-n\pi x/b}-\frac{1}{2}\left\{e^{-n\pi x/b}\mathrm{erfc}\left[n\pi\left(\frac{\kappa t}{b^2}\right)^{\frac{1}{2}}-\frac{1}{2}\left(\frac{x^2}{\kappa t}\right)^{\frac{1}{2}}\right]+e^{n\pi x/b}\mathrm{erfc}\left[n\pi\left(\frac{\kappa t}{b^2}\right)^{\frac{1}{2}}+\frac{1}{2}\left(\frac{x^2}{\kappa t}\right)^{\frac{1}{2}}\right]\right\}\right), \quad (A7)$$

and if, in addition, $x = 0$ and $y = b/2$,

$$T\left(0,\frac{b}{2}\right) = \frac{qb}{k}\frac{2}{\pi^2}\left\{G-\sum_{n=1}^{\infty}\frac{\sin(n\pi/2)}{n^2}\mathrm{erfc}\,n\pi\left(\frac{\kappa t}{b^2}\right)^{\frac{1}{2}}\right\}, \quad (A8)$$

where G is Catalan's constant, 0.9159656.

The average temperature of the $0 < x < l$ region in an infinite solid with constant heat flux in the plane $x = 0$ can be calculated from Eq. (4) in the following way:

$$T_{av} = \frac{q}{k}\frac{1}{l\tau}\int_0^{\tau}\int_0^l(\kappa t)^{\frac{1}{2}}\mathrm{ierfc}\frac{x}{2(\kappa t)^{\frac{1}{2}}}dx\,dt. \quad (A9)$$

The integration with respect to x is straightforward, and gives

$$T_{av} = \frac{2q\kappa}{kl}\frac{1}{\tau}\int_0^{\tau}\left(\frac{t}{4}-t\,i^2\mathrm{erfc}\frac{l}{2(\kappa t)^{\frac{1}{2}}}\right)dt. \quad (A10)$$

A series of integrations by parts will finally result in the following expression:

$$T_{av} = \frac{1}{4}\frac{ql}{k}\left\{\frac{\kappa\tau}{l^2}+\frac{1}{6\pi^{\frac{1}{2}}}\left[10\left(\frac{\kappa\tau}{l^2}\right)^{\frac{1}{2}}+\left(\frac{l^2}{\kappa\tau}\right)^{\frac{1}{2}}\right]e^{-(l^2/4\kappa\tau)}-\left(\frac{\kappa\tau}{l^2}+\frac{l^2}{12\kappa\tau}+1\right)\mathrm{erfc}\frac{1}{2}\left(\frac{l^2}{\kappa\tau}\right)^{\frac{1}{2}}\right\}. \quad (A11)$$

This is obviously the temperature to which the measured values of k and c shall be related.

[13] F. Oberhettinger, *Tabellen zur Fourier Transformation* (Springer-Verlag, Berlin, 1957), pp. 3, 11, 12.

APR 2 1 1981

In reply, refer to Letter R81-1263

Mr. T. Z. Harmathy
Fire Section, Division of
 Building Research
National Research Council
Ottawa 2, CANADA

Dear Mr. Harmathy

VARIABLE-STATE METHODS OF MEASURING THE THERMAL PROPERTIES OF SOLIDS

Ref: Journal of Applied Physics, Volume 35, No. 4, Page 1190 - 1200,
       April 1964, T. Z. Harmathy, same subject

Rockwell Hanford Operations is preparing a detailed report on
the effects of long-term exposure to elevated temperature on
the mechanical properties of Hanford concrete. Most of the work
to be reported was conducted by the Construction Technology
Division, Portland Cement Association, Skokie, IL. The report,
which is funded by the Department of Energy's Long-Term High-Level
Waste Management Program, will not be issued for profit but
would be available at printing cost to anyone who requests it
through the Technical Information Center, Oak Ridge, Tennessee.

As part of Appendix 9 of the report, we request permission to
reprint the Reference article. The report is scheduled
for issuance in July 1981 so we would appreciate a timely
response to our request.

Sincerely,

C. DeFigh-Price, Team Leader
Waste Processing
 Engineering Mechanics

CDP/lka

OUTGOING LTR NO

R81-1263

INCOMING LTR NO

ACTION

REPLY DUE

DIST	LTR.	ENCL	APR
Bartholomew, O.C.			
Bellefotto, M.			
Brazeal, R.K.			
Carey, J.M.			
Cockeram, O.L.			
Dew, R.A.			
Deuchman, J.L.			
Donahoe, J.W.			
Freeman, R.A.			
Fritch, P.J.			
Gimera, R.J.			
Gruhn, R.S.			
Hammond, R.D.			
Horneman, R.E.			
Kinzer, J.E.			
Lorenzini, P.G.			
Oglesre, L.R.			
Pitn, G.B.			
Roecker, J.H.			
Salino, C.M.			
Shaw, H.P.			
Wod, V.R.			
Wodrich, D.D.			
Contract Administrator			
Central Files	X		
M Hanigan	X		
DE Braden	X	X	
C. DeFigh-Price	X	X	

DATE
APR 2 1 1981

54-6000-117

National Research Council
Canada

Conseil national de recherches
Canada

Division of Building
Research

Division des recherches sur le
bâtiment

File Reference M43-3-146

May 8, 1981.

Mr. C. DeFigh-Price,
Team Leader,
Waste Processing
 Engineering Mechanics,
Rockwell Hanford Operations,
Energy Systems Group,
P.O. Box 800,
Richland, WA 99352,
U.S.A.

Dear Mr. DeFigh-Price:

Re: Your Letter R81-1263, dated April 21, 1981

Thank you for your interest in my paper
"Variable-State Methods of Measuring the Thermal
Properties of Solids". I have no objection what-
ever to your plan to reprint that article as part
of Appendix 9 of your report. Since I am not fami-
liar with the copyright situation, I suggest that
you also contact the Editor of the Journal of Applied
Physics in an effort to secure his permission.

Yours sincerely,

T. Z. Harmathy, Head,
Fire Research Section.

TZH:bb
81-F-94

Ottawa, Canada
K1A 0R6

TABLE I-1. Thermal Properties Tests of Hanford Concrete.

Specimen Number	Temperature, °F	Density, lb/ft³	Thermal Diffusivity ft²/Hr	Thermal Conductivity, Btu/ft/hr/°F	Specific Heat, Btu/lb/°F
4.5K12-4	79	139.8	0.0240	0.8138	0.2419
	320		0.0218	0.8283	0.2715
	590		0.0184	0.7456	0.2904
	887		0.0176	0.6913	0.2811
	1,175		0.0147	0.6092	0.2957
	968		0.0157	0.6005	0.2737
	869		0.0159	0.6086	0.2739
	626		0.0147	0.5387	0.2614
	356		0.0154	0.5208	0.2422
	79		0.0171	0.4965	0.2154
3K14-20	79	141.0	0.0322	0.9549	0.2105
	320		0.0252	0.8861	0.2486
	626		0.0220	0.7138	0.2297
	1,166		0.0174	0.6514	0.2654
	1,040		0.0165	0.5959	0.2564
	752		0.0181	0.6133	0.2404
	383		0.0185	0.5595	0.2138
	79		0.0246	0.5977	0.1779

APPENDIX J

PETROGRAPHIC AND FRACTOGRAPHIC ANALYSES

PETROGRAPHIC ANALYSIS OF HEATED TEST HANFORD
CONCRETE MIX TEST SPECIMENS

Samples of 28 cylinders of lab-prepared concrete, stored at various temperatures for different lengths of time, have been studied with a polarized-light microscope and stereomicroscope to determine the microstructural effects on the paste and the paste-aggregate bond. An attempt was made to discern the progressive changes in microcrystalline texture of the pastes as functions of duration and temperature of storage. Duration of storage ranged from 3 to 270 days (after a 193-day initial cure at 70°F and 100% RH). Temperatures were 250°, 350°, and 450°F.

METHODS

Cylinders representing specified time and temperature combinations were withdrawn from storage ovens and, after a few hours of cooling in the lab atmosphere, a 2.5-cm-thick slice was cut transversely on a water cooled saw. A small block, cut from the interior of the slice with an oil cooled saw, was leveled and dried at 50°C (112°F), and mounted on standard petrographic glass slides with epoxy. Thin sections were ground to a thickness of approximately 10 to 20 microns and protected with cover glass, loose mounted in epoxy. The thin sections were labeled and most were numerically coded so that they could be described without prior bias as to duration of storage and temperature.

Optical properties of any solid material are functions of chemical composition and conditions of formation (temperature and pressure). After genesis, some phases are thermodynamically sensitive to changes in these conditions, with consequent changes in some optical properties. Calcium hydroxide, one of the principal hydration products of portland cement, normally occurs in crystal sizes large enough for optical examination in polarized light and determination of birefringence.

Birefringence is the numerical difference between the maximum and minimum indices of refraction of an anisotropic crystalline solid and can be related to the crystal thickness (thin section thickness) in the following equation:

$$t = \frac{\lambda\theta}{180}/B$$

where

λ = wavelength of transmitted light in millimicrons (540)

θ = degrees of analyzer rotation on the microscope

B = birefringence of the crystalline solid

t = thickness.

Assuming a quartz birefringence of 0.009, thickness of the concrete thin section was determined by averaging several measurements of θ on 6 to 8 grains of quartz. Using this calculated value of thickness, the average birefringence of calcium hydroxide in the same thin section was determined by examination of 8 to 10 crystals in the portland cement paste of the concrete. Birefringence data are given in Table J-1.

Data groups in terms of temperature and duration of storage are presented in Table J-2.

DESCRIPTION OF THE CONCRETE

Coarse aggregates in the concrete are principally basalt, dolerite, and gabbro, with lesser amounts of quartz, plagioclase, and biotite gneiss. Fine aggregates are fragments of the above-mentioned rocks; and in addition, metasandstones of various types, metaquartzite, quartz diorite, and argillite. No reaction products of potentially reactive aggregates were noted.

The paste, which is formed by the combination of water and cement, contains, in addition to hydration products, unhydrated portland cement grains (UPCs) and air voids. Hydration products are primarily calcium

TABLE J-1. Thin Section List and Birefringence
of Calcium Hydroxide.

Code No.	Concrete	Temperature, °F	Time, Days	Average Birefringence
1	4.5K	450	100	0.0125
2	3K	Control Specimen		0.0202
3	3K	450	100	0.0108
4	4.5K	450	6	0.0208
5	3K	450	6	0.0159
6	3K	350	4	0.0120
7	4.5K	350	4	0.0197
8	3K	350	150	0.0113
9	3K	250	150	0.0142
10	4.5K	250	3	0.0173
11	3K	450	10	0.0091
12	3K	250	3	0.0178
13	3K	450	170	0.0179
14	4.5K	450	10	0.0117
15	4.5K	350	150	0.0203
16	3K	250	100	0.0187
17	4.5K	450	170	0.0187
18	4.5K	450	60	0.0117
19	3K	450	60	0.0090
20	4.5K	250	150	0.0087
21	3K	250	3	0.0186
22	4.5K	250	100	0.0123
23	3K	350	270	0.0160
24	4.5K	250	270	0.0182
25	3K	250	270	0.0176
26	4.5K	350	270	0.0198
27	4.5K	450	270	0.0202
28	3K	450	270	0.0123

TABLE J-2. Average Birefringence Versus Temperature Values for
Various Samples at Given Temperatures and Time Periods.

250°F for 4 days	350°F for 4 days	450°F for 6 days
0.0142	0.0120	0.0125
0.0173	0.0197	0.0108
0.0178	0.0113	0.0208
0.0187	0.0203	0.0159
0.0087	0.0160	0.0091
0.0186	0.0198	0.0179
0.0123	n = 6	0.0117
0.0182	σ = 0.0041	0.0187
0.0176	$\bar{X}$ = 0.0165	0.0117
n = 9		0.0090
σ = 0.0035		0.0202
$\bar{X}$ = 0.0159		0.0123
		n = 12
		σ = 0.0043
		$\bar{X}$ = 0.0142

Ambient Temperature for 1-10 days	Ambient Temperature for 60-100 days	Ambient Temperature for 150-170 days	Ambient Temperature for 270 days
0.0208	0.0125	0.0113	0.0160
0.0159	0.0108	0.0142	0.0182
0.0120	0.0187	0.0179	0.0176
0.0197	0.0117	0.0203	0.0198
0.0173	0.0090	0.0187	0.0202
0.0091	0.0123	0.0087	0.0123
0.0178	n = 6	n = 6	n = 6
0.0117	σ = 0.0032	σ = 0.0046	σ = 0.0029
0.0186	$\bar{X}$ = 0.0125	$\bar{X}$ = 0.0152	$\bar{X}$ = 0.0174
n = 9			
σ = 0.0040			
$\bar{X}$ = 0.0159			

silicate hydrates and calcium hydroxide, the latter having crystals large enough in normal concrete for determination of optical properties.

Calcium hydroxide occurs in pastes as:

- Aggregate fringes
- Concentrations in the paste
- Finely dispersed amidst other hydration products
- Air void fillings.

Only the first two occurrences are considered in this report. Calcium hydroxide, in pure form, is assumed to have the properties listed in Taylor* (1964), p. 352:

- Hexagonal system
- Refractive indices of 1.573 and 1.545
- Birefringence of 0.028.

It is clear that the birefringence determined for calcium hydroxide in the present report does not equal that stated by Taylor, even for the "control" specimen (thin section No. 2).

The products of hydration are aggregated in paste to form a micro-crystalline mosaic, an intimate intergrowth of principally calcium silicate hydrate and calcium hydroxide, the amounts of which are determined largely by the quantities of cement and water. Individual crystals comprising the microscrystalline mosaic are normally in the range of 0.1 to 100.0 microns, with a submicron average. The average size is beyond resolution in a polarized-light microscope; thus all of the calcium hydroxide birefringence measurements in the present study were made on relatively large, probably impure crystals or groups of crystals.

It is thought that the modal crystal sizes of calcium silicate hydrate and calcium hydroxide would show progressive changes with temperature and duration of storage. However, because of the small crystal

---

*H. F. W. Taylor, Chemistry of Cements, Academic Press, New York (1976).

size and optically indefinite crystal boundaries, measurements could not
be made reliably. Perhaps, examination of a polished and etched surface
with a scanning electron microscope (SEM) would show progressive changes
in crystal size. The SEM allows only observation of size and morphology
(form) to the exclusion of other optical properties; thus the method has
some limitations.

During sample preparation for thin sectioning, slight differences in
tenacity of paste/aggregate bond were noted. Using the categories given
below, on hand specimens (slices 2.5 to 3.0 in. thick) were broken with a
small hammer and the relative differences of paste/aggregate tenacity
were determined. The ranks are outlined below:

- 1.0 - all coarse aggregates sheared
- 2.0 - most sheared, a few not broken
- 3.0 - approximately equal proportions of sheared and nonbroken
  aggregates
- 4.0 - most aggregates not sheared (pullouts common), but a few
  aggregates broken
- 5.0 - all coarse aggregates remain unbroken (pullouts abundant).

Of 40 samples examined (Table J-3), tenacity of the paste/aggregate
bond averages 4.6 (standard deviation equals 0.52); thus, in almost all
of the samples, pullouts and unbroken aggregates characterize the hammer
fractured surface. Samples giving relatively low values are:

- 4.5K/350°F/4 days - 3.0
- 3K Control - 3.2 (no heat treatment)
- 3K/450°F/6 days - 3.5.

It appears that significant reduction of the strength of the paste/
aggregate bond occurs after cooling and returning to room temperature
conditions.

Air contents, estimated on broken surfaces of 40 cylinder samples,
have an average of 2.8% (standard deviation equals 0.86%). Comparatively
high tenacity values generally correlate with relatively high air
contents.

TABLE J-3. Air Content and Tenacity.

Specimen Number	Temperature, °F	Days	Estimated Air Content by percent σ = 0.86 x̄ = 2.8	Rating of Fracture Surface* σ = .52 x̄ = 4.6
4.5K	350	4	2	3.0
3K	Control	–	1	3.2
3K	450	6	3	3.5
4.5K	350	80	3	5.0
4.5K	250	3	3	4.5
3K	350	4	3	4.5
4.5K	450	6	2.5	4.5
3K	250	150	1	5.0
4.5K	250	6	3.5	5.0 bubbles around aggregates)
3K	450	18	3.5	5.0
4.5K	450	18	3	5.0
3K	350	10	3	4.75
4.5K	450	10	3	5.0
4.5K	450	100	2.5	4.75
3K	450	101	2	4.75 (bubble clusters)
4.5K	250	150	2.5	4.75 (bubbles around aggregates)
4.5K	350	150	2	4.75
3K	450	33	2	4.0
3K	450	–	3.5	5.0
4.5K	450	60	2.5	4.75
4.5K	350	30	2.5	5.0
3K	250	6	2	4.0
3K	250	80	2	5.0
4.5K	350	10	3.5	5.0
3K	350	30	3	5.0
4.5K	250	30	3.5	4.5 (leveled)
3K	250	30	3	4.5 (leveled)
3K	350	150	4	5.0
4.5K	450	170	4	5.0
3K	450	60	4.5	5.0
4.5K	250	80	4	5.0 (bubbles around aggregates)

TABLE J-3. Air Content and Tenacity (Continued).

Specimen Number	Temperature, ^{0}F	Days	Estimated Air Content by percent $\sigma = 0.86$ $\bar{x} = 2.8$	Rating of Fracture Surface* $\sigma = .52$ $\bar{x} = 4.6$
3K	350	80	3.0	5.0
4.5K	450	33	3.5	4.75
3K	450	10	3.0	5.0
4.5K	250	270	2.5	3.8
4.5K	350	270	2.5	4.0
3K	250	270	1.5	4.5
3K	350	270	3.0	4.5
4.5K	450	270	3.2	4.75
3K	450	270	2.8	4.75

*Based on rating table on page J-6.

CONCLUSIONS

Calcium hydroxide birefringences show no clearly defined correlation with temperature of storage, judging from the averages given in Table J-2. A Student's t-Distribution Test for a significant difference between the 250^0 and 350^0F versus the 450^0F data gives a value of 1.28, which suggests the possibility that a real difference exists, but implies the necessity for additional data. In terms of storage times, samples stored for 270 days revealed relatively high birefringence. A Student's t-Distribution Test for significant difference in the birefringences of the 1 to 100 day versus 150 to 270 day samples results in a value of 1.37. This again suggests a poorly defined relationship and the need for additional data. Both Student's t-Distribution Tests show correlation at 90% probability level, but better relationships are usually required.

Examination of the fracture surfaces of samples broken with a hammer reveal an obvious weakening of the paste/aggregate bond. Apparently, desiccation of the concrete during storage for appreciable lengths of time at moderately high temperatures dehydrates the cement hydration products, resulting in submicroscopic contraction of the paste and

consequently weakening its bond with aggregate after cooling. An additional factor contributing to rupture of the bond may be related to relaxation of thermally induced stresses arising from differential expansion of various aggregate minerals at the paste contact.

FRACTOGRAPHIC ANALYSIS OF BROKEN TEST SPECIMENS

Fracture surfaces on 202 concrete cylinders, broken by compressive or split tensile methods, have been examined. The cylinders represent concrete stored for various lengths of time at tempertures of 70°, 250°, 350°, and $450^\circ F$. Each fracture surface was categorized with the following numerical scale:

- 1.0 - Aggregates sheared, very few pullouts
- 2.0 - Most aggregates broken, some not
- 3.0 - Sheared and unbroken aggregates about equal
- 4.0 - Some aggregates broken, pullouts abundant
- 5.0 - Very few aggregates broken, pullouts very abundant.

Observational data are given in Table J-4. Photo samples are shown in Figures J-1 through J-6.

RELATIONSHIP OF FRACTURE SURFACE TO TEMPERATURE

Comparison of types of fracture surfaces produced in compression and split tensile tests, using Student's t-Distribution Tests on average values, indicate significant differences between compressive test surfaces at $70^\circ F$ and those at $450^\circ F$ (95% level).

Insignificant differences, determined in the same way, are indicated for surfaces produced by the split tensile test ($70^\circ F$ and $450^\circ F$).

Inspection of the data in Table J-4 suggests obvious differences in compressive versus split tensile surfaces. The typical surface produced in compressive shows a relatively large number of pullouts and few broken aggregates (average is 4.60). In contrast, the surface produced by the split tensile test reveals comparatively fewer pullouts and more broken

aggregates (average is 3.63). Average standard deviations for compressive and tensile test data are 0.17 and 0.05, respectively; indicating relative uniformity in the tensile test data.

RELATIONSHIP OF FRACTURE SURFACE TO DURATION OF STORAGE

Data presented in Table J-1 were grouped into two storage categories: 4 to 101 days of storage and 150 to 679 days of storage. Fracture surfaces produced by compression tests are not significantly different at the 95% probability level, using Student's t-Distribution Test for concrete in both storage categories.

Average compression test values are 4.58 and 4.63 for the 4 to 101 day and 150 to 679 day categories, respectively.

Fracture surfaces formed in the split tensile test are significantly different at the 95% level, using the same categories and statistical tests. Average values are 3.57 and 3.76 for the 4 to 101 day and 150 to 679 day categories, respectively.

CONCLUSIONS

These data suggest the possibility of major effects of both temperature and time on the type of fracture produced in compression and split tensile tests. However, all the tests were conducted after the cylinder had cooled to room temperature; possibly producing a poorly understood "relaxation" effect in the paste/aggregate bond and weakening the concrete. Partial elimination of cement water of hydration and subsequent paste recrystallization may account for strength decrease with time and temperature. Recrystallization normally involves an increase in crystal size, but this was not observed by thin section microscopy. Use of a scanning electron microscope may yield conclusive data.

FIGURE J-1. Compression Test Cylinder 4.5K4-28, stored at 70°F for 30 days, with a fracture surface rating of 4.6. Note Numerous sockets (pullouts) and relatively few broken aggregates.

FIGURE J-2. Split Tensile Test Cylinder 4.5K4-29, stored at 70°F for 30 days, with a fracture surface rating of 3.5 (2 cm scale).

FIGURE J-3. Compression Test Cylinder 4.5K3-21, stored at 450°F for 487 days, ranking 4.7 on the relative scale and showing mostly pullouts and very few broken aggregates. (2 cm scale).
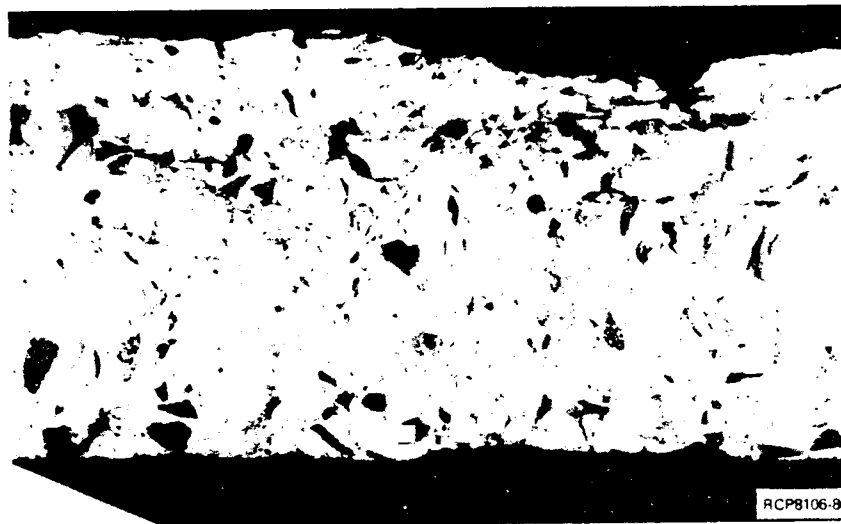
FIGURE J-4. Split Tensile Test Cylinder 4.5K3-22, stored at 450°F for 487 days, which ranks 3.7 on the fracture surface scale and shows abundant pullouts.

FIGURE J-5. Compression Test Cylinder, 4.5K5-9, moist cured for 679 days, with a fracture surface ranking of 3.6. Note relatively numerous broken aggregates.

FIGURE J-6. Split Tensile-Test Cylinder, 4.5K8-29, moist cured for 679 days. Fracture surface has relatively few pullouts and many broken aggregates, with a ranking of 3.5 on the relative scale.

TABLE J-4. Fracture Surfaces on Tested Cylinders.

Cylinder Number	Temperature, °F	Days	Rating Based on Scale*	
			Compression Test	Split Tensile Test
4.5K4-29	70	30	-	3.5
4.5K4-26	70	30	-	3.5
3K4-28	70	30	4.6	-
3K1-4	70	71	4.0	-
3K4-26	70	30	-	3.5
3K4-30	70	30	4.8	-
4.5K6-28	70	361	4.7	-
4.5K4-29	70	30	-	3.7
4.5K1-11	70	71	-	3.5
4.5K2-15	70	71	-	3.7
3K6-28	70	361	4.5	-
3K7-7	70	361	-	3.7
4.5K9-1	70	194	4.5	-
3K9-1	70	194	4.0	-
3K9-3	70	194	4.8	-
4.5K9-3	70	194	4.8	-
4.5K9-15	70	194	-	3.3
4.5K9-2	70	194	-	3.5
3K9-2	70	194	-	4.2
3K9-10	70	194	-	4.5
3K1-5	70	34	4.5	-
4.5K2-7	70	34	4.0	-
3K1-7	70	34	4.0	-
3K6-25	70	240	4.6	-
3K7-28	70	240	-	4.0
4.5K6-25	70	240	4.0	-
4.5K7-29	70	240	-	3.4
3K5-5	250	150	4.7	-
3K5-2	250	150	-	4.0
3K5-3	250	150	4.8	-
3K5-7	250	150	-	4.0
4.5K5-5	250	150	4.7	-
4.5K5-1	250	150	-	3.8
4.5K5-6	250	150	-	3.8
4.5K5-3	250	150	4.8	-
4.5K8-1	250	10	4.5	-
4.5K8-6	250	10	4.5	-
4.5K8-3	250	10	-	3.5
4.5K8-2	250	10	-	3.3

TABLE J-4. Fracture Surfaces on Tested Cylinders.(Continued)

Cylinder Number	Temperature, °F	Days	Rating Based on Scale*	
			Compression Test	Split Tensile Test
3K8-3	250	10	4.7	-
3K8-4	250	10	-	3.5
3K8-1	250	10	-	3.7
3K8-5	250	10	4.5	-
3K4-3	250	80	4.5	-
3K4-2	250	80	-	3.8
3K4-1	250	80	4.7	-
3K4-5	250	80	-	3.6
3K6-4	250	270	-	3.8
3K6-1	250	270	-	4.0
3K6-3	250	270	4.5	-
3K6-5	250	270	4.3	-
4.5K6-6	250	270	4.7	-
4.5K6-3	250	270	4.7	-
4.5K6-2	250	270	-	3.5
4.5K6-8	250	270	-	3.5
4.5K7-4	250	30	4.6	-
4.5K7-1	250	30	-	3.5
3K7-3	250	30	-	3.6
4.5K7-3	250	30	4.8	-
4.5K7-9	250	30	-	3.6
3K7-4	250	3	-	3.5
4.5K3-5	250	3	4.6	-
4.5K3-3	250	3	4.7	-
4.5K3-1	250	3	-	3.6
4.5K3-7	250	3	-	3.5
3K3-3	250	3	-	3.4
3K3-5	250	3	4.6	-
3K3-7	250	3	-	3.5
3K3-1	250	3	4.6	-
3K4-8	350	10	4.5	-
3K7-14	350	10	-	3.6
3K4-11	350	10	4.7	-
3K4-4	350	10	-	3.5
4.5K4-11	350	10	4.3	-
4.5K4-10	350	10	-	3.3
4.5K4-14	350	10	-	3.0
4.5K4-8	350	10	4.3	-
3K3-11	350	4	-	3.5
3K3-14	350	4	4.7	-
3K3-8	350	4	4.7	-

TABLE J-4. Fracture Surfaces on Tested Cylinders.(Continued)

Cylinder Number	Temperature, °F	Days	Rating Based on Scale*	
			Compression Test	Split Tensile Test
3K3-9	350	4	-	3.5 .
4.5K3-11	350	4	-	3.4
4.5K3-8	350	4	4.7	-
4.5K3-14	350	4	4.7	-
4.5K3-15	350	4	-	3.4
3K6-6	350	80	-	3.6
3K6-8	350	80	-	3.6
3K6-11	350	80	4.7	-
3K6-14	350	80	4.8	-
4.5K6-7	350	80	-	3.5
4.5K6-12	350	80	-	3.5
4.5K6-11	350	80	4.6	-
4.5K6-14	350	80	4.8	-
4.5K5-10	350	30	-	3.6
4.5K5-8	350	30	4.5	-
4.5K5-14	350	30	-	3.6
4.5K5-11	350	30	4.6	-
3K5-8	350	30	-	3.6
3K5-11	350	30	4.4	-
3K5-14	350	30	4.2	-
3K5-12	350	30	-	3.5
3K7-14	350	150	-	3.7
3K7-8	350	150	4.6	-
3K7-9	350	150	-	3.7
3K7-11	350	150	4.8	-
4.5K7-8	350	150	4.5	-
4.5K7-12	350	150	-	3.7
4.5K7-15	350	150	-	3.5
4.5K7-10	350	150	4.7	-
4.5K8-15	350	270	-	3.5
4.5K8-11	350	270	4.7	-
4.5K8-8	350	270	4.7	-
4.5K8-14	350	270	-	3.7
3K8-14	350	270	-	3.7
3K8-11	350	270	4.7	-
3K8-8	350	270	4.8	-
3K8-6	350	270	-	4.0
4.5K6-23	450	18	4.8	-
4.5K6-19	450	18	-	3.7
4.5K6-17	450	18	4.5	-
4.5K6-20	450	18	-	3.7

TABLE J-4. Fracture Surfaces on Tested Cylinders.(Continued)

Cylinder Number	Temperature, °F	Days	Rating Based on Scale*	
			Compression Test	Split Tensile Test
3K6-19	450	18	-	3.6
3K6-23	450	18	4.7	-
3K6-10	450	18	-	4.0
3K6-17	450	18	4.7	-
3K7-23	450	33	4.7	-
3K7-20	450	33	-	3.6
3K7-17	450	33	4.5	-
4.5K7-20	450	33	4.5	-
4.5K7-23	450	33	-	3.5
4.5K7-18	450	33	4.5	-
4.5K7-19	450	33	-	3.6
4.5K6-29	450	170	-	3.7
4.5K5-25	450	170	-	3.8
4.5K4-24	450	170	4.7	-
4.5K3-25	450	170	4.7	-
3K3-25	450	170	4.8	-
3K5-25	450	170	4.8	-
3K4-24	450	170	-	3.8
3K6-16	450	170	-	3.6
4.5K4-19	450	6	-	3.5
4.5K4-20	450	6	4.8	-
4.5K4-23	450	6	-	3.5
4.5K4-17	450	6	4.8	-
3K4-20	450	6	4.6	-
3K4-17	450	6	-	3.6
3K4-23	450	6	4.8	-
3K4-18	450	6	-	3.6
3K8-17	450	60	4.8	-
3K8-13	450	60	-	3.6
3K8-22	450	60	4.8	-
3K8-24	450	60	-	3.7
4.5K8-23	450	60	-	3.5
4.5K8-30	450	60	4.6	-
4.5K8-18	450	60	-	3.5
4.5K8-17	450	60	4.7	-
4.5K9-14	450	100	-	3.4
4.5K9-24	450	100	-	3.6
3K9-11	450	100	-	3.8
3K9-12	450	100	-	3.8
3K5-20	450	10	4.6	-
3K5-13	450	10	-	3.7
3K5-17	450	10	-	3.7

TABLE J-4. Fracture Surfaces on Tested Cylinders.(Continued)

Cylinder Number	Temperature, °F	Days	Rating Based on Scale*	
			Compression Test	Split Tensile Test
4.5K5-16	450	10	4.6	-
4.5K5-27	450	10	-	3.5
4.5K5-23	450	10	-	3.6
4.5K5-20	450	10	4.6	-
4.5K3-23	450	300	4.8	-
4.5K3-19	450	300	4.8	-
4.5K3-28	450	300	-	3.6
4.5K3-17	450	300	-	3.7
3K3-20	450	300	4.5	-
3K3-23	450	300	4.7	-
3K3-17	450	300	-	3.6
3K3-13	450	300	-	3.5
4.5K6-20	350	487	4.8	-
3K6-24	350	487	4.8	-
3K6-30	350	487	4.9	-
4.5K6-26	350	487	4.8	-
4.5K8-28	250	487	4.7	-
4.5K8-25	250	487	4.7	-
3K9-20	250	487	4.8	-
3K9-14	250	487	4.7	-
4.5K8-29	70	679	-	3.5
3K8-28	70	679	-	3.6
4.5K5-9	70	679	3.6	-
3K5-28	70	679	4.0	-
4.5K3-21	450	487	4.7	-
4.5K3-27	450	487	4.8	-
3K3-12	450	487	4.8	-
3K3-10	450	487	4.8	-
4.5K3-22	450	487	-	3.7
3K3-26	450	487	-	3.9
4.5K3-2	450	487	-	4.0
3K3-27	450	487	-	4.0
4.5K8-26	250	487	-	3.8
3K9-29	250	487	-	3.6
3K9-17	250	487	-	4.0
4.5K8-16	250	487	-	3.7
4.5K6-27	350	487	-	3.9
3K6-27	350	487	-	4.0
4.5K6-24	350	487	-	4.0
3K6-26	350	487	-	3.8

DISTRIBUTION LIST

Number of
Copies

1	Colorado State Univeristy
	F. W. Whicker
4	Construction Technology Laboratories Of The Portland Cement Association Skokie, Illinois 60076
	M. S. Abrams (3)
	M. Gillen
1	Cornell University
	J. C. Smith
4	E. I. du Pont Nemours and Company
	Savannah River Laboratory
	J. L. Crandall
	P. L. Gray
3	Oak Ridge National Laboratory
	T. H. Rowe
1	Office of Nuclear Waste Isolation Battelle Memorial Institute - Columbus
	W. Carbeiner
1	Pennsylvania State University
	R. Roy
1	Stanford University
	I. Remson

Number of
Copies

1   Vanderbilt University

                     F. L. Parker

1   27071-B Calle Caballero
                     San Juan Capistrano, California

                     D. C. Van Dine

Onsite

4   U. S. Department of Energy
                     Richland Operations Office

                     P. F. X. Dunigan
                     R. E. Gerton
                     J. J. Schreiber
                     M. W. Shupe

14   Pacific Northwest Laboratory

                     W. E. Anderson (10)
                     M. C. C. Bampton
                     R. D. Nelson
                     A. M. Platt

2   Westinghouse Hanford

                     L. D. Blackburn
                     J. D. McCormack

34   Rockwell Hanford Operations

                     M. R. Adams
                     B. N. Anderson
                     H.   Babad
                     D. E. Braden
                     C.   DeFigh-Price (5)
                     J. L. Deichman
                     G. T. Dukelow
                     G. D. Forehand
                     S. A. Gallagher
                     K. A. Gasper
                     W. E. Heine

Number of
Copies

1 Onsite

Rockwell Hanford Operations (continued)

R. L. Koontz
M. J. Kupfer
H. E. McGuire
I. E. Reep
R. C. Roal
J. H. Roecker
W. W. Schulz
H. A. Wallskog
J. R. Wetch
D. E. Wood
Document Control (5)
RCP Department (3)
TIC

Number of
Copies

Onsite

Rockwell Hanford Operations (continued)

R. L. Koontz
M. J. Kupfer
H. E. McGuire
I. E. Reep
R. C. Roal
J. H. Roecker
W. W. Schulz
H. A. Wallskog
J. R. Wetch
D. E. Wood
Document Control (5)
RCP Department (3)
TIC